

NOTE TO USERS

This reproduction is the best copy available.

UMI[®]

©Copyright 2006

Regine M. Schoenherr

CE-Microreactor-CE-MS-MS for Protein Analysis

Regine M. Schoenherr

A dissertation submitted in partial fulfillment of the
requirements for the degree of

Doctor of Philosophy

University of Washington

2006

Program Authorized to Offer Degree:
Department of Chemistry

UMI Number: 3205879

Copyright 2006 by
Schoenherr, Regine M.

All rights reserved.

INFORMATION TO USERS

The quality of this reproduction is dependent upon the quality of the copy submitted. Broken or indistinct print, colored or poor quality illustrations and photographs, print bleed-through, substandard margins, and improper alignment can adversely affect reproduction.

In the unlikely event that the author did not send a complete manuscript and there are missing pages, these will be noted. Also, if unauthorized copyright material had to be removed, a note will indicate the deletion.

UMI[®]

UMI Microform 3205879

Copyright 2006 by ProQuest Information and Learning Company.

All rights reserved. This microform edition is protected against
unauthorized copying under Title 17, United States Code.

ProQuest Information and Learning Company
300 North Zeeb Road
P.O. Box 1346
Ann Arbor, MI 48106-1346

University of Washington
Graduate School

This is to certify that I have examined this copy of a doctoral dissertation by

Regine M. Schoenherr

and have found that it is complete and satisfactory in all respects,
and that any and all revisions required by the final
examining committee have been made.

Chair of the Supervisory Committee:



Norman J. Dovichi

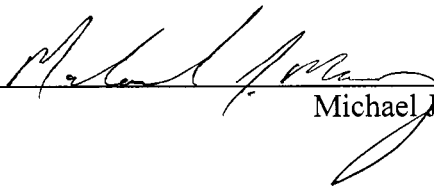
Reading Committee:



Norman J. Dovichi



František Tureček



Michael J. MacCoss

Date: 3/2/06

In presenting this dissertation in partial fulfillment of the requirements for the doctoral degree at the University of Washington, I agree that the Library shall make its copies freely available for inspection. I further agree that extensive copying of the dissertation is allowable only for scholarly purposes, consistent with "fair use" as prescribed in the U.S. Copyright Law. Requests for copying or reproduction of this dissertation may be referred to ProQuest Information and Learning, 300 North Zeeb Road, Ann Arbor, MI 48106-1346, 1-800-521-0600, to whom the author has granted "the right to reproduce and sell (a) copies of the manuscript in microform and/or (b) printed copies of the manuscript made from microform."

Signature Regina M. Schwartz

Date 3/2/06

University of Washington

Abstract

CE-Microreactor-CE-MS-MS for Protein Analysis

Regine M. Schoenherr

Chair of the Supervisory Committee:
Endowed Professor Norman J. Dovichi
Department of Chemistry

Capillary electrophoresis-mass spectrometry (CE-MS) provides a powerful system that combines the speed and automation capabilities of CE with the detection and identification capabilities of MS. Integrating on-line enzymatic microreactor digestion with a CE-MS system reduces sample handling and allows fast digestions of small protein samples.

In this thesis work, an on-line CE-microreactor-CE-MS-MS instrument is developed that can separate proteins in a first dimension, digest them inside a pepsin-immobilized microreactor, separate peptides in a second dimension, and detect the peptides with MS. The development begins from the MS end by coupling capillary free zone electrophoresis (CZE) to a linear ion trap mass spectrometer with a sheath flow interface, and works its way forward to the protein separation.

Two CE-MS interfaces are tested and a sheath flow configuration is chosen for further instrument development because it provides robust electrosprays and does not cause band broadening. The CZE separation is optimized using bulk solution digested cytochrome *C*. Peptide-capillary wall interactions are reduced by coating capillaries with poly(vinyl alcohol) and by using high ionic strength buffers. The information dependent

acquisition (IDA) capability of the mass spectrometer is used to obtain peptide fragment mass spectra that are submitted to a protein database search engine to identify cytochrome *C*.

Pepsin-immobilized monolithic capillary microreactors are prepared and their homogeneity and digestion efficiency are investigated in both off-line and on-line experiments with CZE-ESI-MS. On-line coupling is achieved with a Plexiglas-glass interface. The microreactors are rather heterogeneous, yet cytochrome *C* was still successfully digested within 2 min. Hydroquinone (and *p*-benzoquinone) is added to buffers to alleviate CE current instabilities due to the electrolysis of water.

The instrument is modified to a 2D CE-UV-microreactor-CE-ESI-MS-MS system by adding a protein separation capillary in front of the peptide separation. The protein separation capillary end that is coupled to the peptide separation dimension has an ~ 1 cm microreactor integrated in it. A cytochrome *C* and myoglobin mixture is separated and identified using this 2D system. Only myoglobin is detected in a 6 protein sample, possibly because the other proteins contain disulfide bonds and/or are pepsin-resistant.

TABLE OF CONTENTS

	Page
List of Figures	viii
List of Tables	xii
Glossary	xiii
 Chapter 1 – Introduction	 1
1.I. Background of Capillary Electrophoresis (CE).....	2
1.I.A. Brief History of CE.....	2
1.I.B. CZE Theory	3
1.II. Protein and Peptide Separations by CE.....	10
1.II.A. Various CE Modes and 1D Separations	10
1.II.A.1. Capillary Zone Electrophoresis (CZE).....	10
1.II.A.2. Micellar Electrokinetic Capillary Chromatography (MECC)	12
1.II.A.3. Capillary Isoelectric Focusing (CIEF)	13
1.II.A.4. Capillary Sieving Electrophoresis (CSE)	14
1.II.A.5. Capillary Electrochromatography (CEC).....	15
1.II.B. 2D Separations.....	16
1.II.C. Detection Methods for Protein and Peptide CE.....	19
1.II.C.1. Sample Preconcentration	20
1.II.C.2. UV Absorbance	21
1.II.C.3. Fluorescence	22

1.III. Protein and Peptide Analysis by Mass Spectrometry	23
1.III.A. Database Identification of Proteins and Peptides.....	24
1.III.B. Top-Down Analysis	25
1.III.C. Bottom-Up Analysis.....	26
1.IV. Capillary Electrophoresis Coupled to Mass Spectrometry	30
1.IV.A. CE-MS Interfaces	30
1.IV.B. Protein and Peptide Analysis by CE-MS	33
1.V. Immobilized Enzyme Microreactors.....	34
1.V.A. Open Tubular Microreactors	35
1.V.B. Particle-based Microreactors	37
1.V.C. Membrane Microreactors	38
1.V.D. Monolithic Column Microreactors.....	38
1.VI. Notes to Chapter 1	43
Chapter 2 – 1D CE-MS.....	54
2.I. Introduction	54
2.II. Experimental	57
2.II.A. Chemicals and Miscellaneous Materials	57
2.II.B. Instrumental Set-up.....	58
2.II.B.1. CE-UV-ESI-MS Instrument with a Sheathless CE-MS Interface	58
2.II.B.2. CE-UV-ESI-MS and CE-ESI-MS Instrument with a Sheath Flow CE-MS Interface	60

2.II.C. Coating Capillaries with Poly(vinyl alcohol)	64
2.II.D. Bulk Digestion of Cytochrome <i>C</i>	66
2.II.D.1. Bulk Digestion with Trypsin	66
2.II.D.2. Bulk Digestion with Pepsin	66
2.II.E. CE-ESI-MS Separations	67
2.II.E.1. CE-UV-ESI-MS Experiments with the Sheathless CE-MS Interface	67
2.II.E.2. CE-UV-ESI-MS and CE-ESI-MS Experiments with the Sheath Flow CE-MS Interface	67
2.II.F. Data Analysis	69
2.III. Results and Discussion	71
2.III.A. Experiments Using a Sheathless CE-ESI-MS Interface	71
2.III.B. Experiments Using a Sheath Flow CE-ESI-MS Interface	74
2.III.B.1. CE-UV-ESI-MS with Dimethylsulfoxide as a Neutral Marker	74
2.III.B.2. CE-UV-ESI-MS of Trypsin Bulk-digested Cytochrome <i>C</i>	76
2.III.B.3. CE-ESI-MS of Trypsin Bulk-digested Cytochrome <i>C</i>	77
2.III.B.4. CE-ESI-MS of Pepsin Bulk-digested Cytochrome <i>C</i>	79
2.III.B.5. Batch Acquisition Using the Q TRAP Analyst Software	80
2.III.B.6. CE-ESI-MS-MS	83
2.IV. Conclusions	85
2.V. Notes to Chapter 2	112
Chapter 3 – Microreactor Experiments Off- and On-line with CE-MS	113

3.I. Introduction	113
3.II. Experimental	114
3.II.A. Chemicals and Materials	114
3.II.B. Microreactor Preparation	116
3.II.B.1. Whole Capillary Microreactors	116
3.II.B.1.a. 48 μm ID, 142 μm OD	116
3.II.B.1.b. 523 μm ID, 695 μm OD	120
3.II.B.2. Integrated Capillary Microreactors	120
3.II.C. Instrumental Set-up	122
3.II.C.1. Off-line Microreactor Experiments	122
3.II.C.2. On-line Microreactor Experiments	122
3.II.C.2.a. Plexiglas-glass Interface Cross	122
3.II.C.2.b. Plexiglas Injection Block	125
3.II.C.2.c. 4-way Valve	126
3.II.D. Off-line Microreactor Digestion and CE-ESI-MS Separations	127
3.II.D.1. Off-line Microreactor Digestion Using a 48 μm ID Microreactor and CE-ESI-MS Separation Conditions	127
3.II.D.2. Off-line Microreactor Digestion Using 523 μm ID Microreactors and CE-ESI-MS Separation Conditions	129
3.II.E. On-line Microreactor Digestion and Microreactor-CE-ESI-MS Separations	130
3.II.E.1. Protein Sample Preparation	130
3.II.E.2. Experimental Procedure	131

3.II.E.2.a. General Procedure.....	131
3.II.E.2.b. Preliminary Purging Experiments to Determine the Time Needed to Purge Sample to the Interface.....	132
3.III. Results and Discussion	133
3.III.A. Off-line Microreactor Digestion	133
3.III.A.1. Validation of the Pepsin Microreactor's Digestion Capability	133
3.III.A.2. Repeatability of Injection Using the 1D CE-ESI-MS Set-up	134
3.III.A.3. Microreactor Homogeneity	134
3.III.A.4. Concentration Limit of Microreactor Digestion Detectable with the 1D CE-ESI-MS Instrument.....	135
3.III.B. On-line Microreactor Digestion	136
3.III.B.1. Instrumental Set-up and Experiment-related.....	136
3.III.B.2. Repeatability of Digestion and Injection Using the Microreactor-CE-MS Set-up.....	138
3.III.B.3. Digestion Efficiency.....	138
3.III.B.4. Use of Hydroquinone and <i>p</i> -benzoquinone as Buffer Additives ...	141
3.III.B.4.a. Obtaining Stable CE Currents with Hydroquinone and <i>p</i> - benzoquinone as Buffer Additives.....	141
3.III.B.4.b. Optimizing Experimental Conditions when Using Hydroquinone (and <i>p</i> -benzoquinone) as Buffer Additives...	144
3.III.B.5. On-line Microreactor Digestion Using Myoglobin.....	146
3.IV. Conclusions.....	146
3.V. Notes to Chapter 3.....	164
Chapter 4 – 2D CE-UV-microreactor-CE-MS-MS	165

4.I. Introduction	165
4.II. Experimental	166
4.II.A. Chemicals	166
4.II.B. Sample Preparation.....	167
4.II.C. Instrumental Set-up.....	168
4.II.C.1. UV Detection System	168
4.II.C.2. Second Power Supply and Related Electronics Modifications	170
4.II.D. Experimental Procedures.....	170
4.II.D.1. CE-UV-microreactor-CE-MS Analyses.....	170
4.II.D.2. Preliminary 1D CE-UV Separations of Proteins.....	173
4.II.D.3. CE-UV-microreactor-CE-MS-MS Analyses.....	173
4.II.E. 2D Data Analysis	174
4.II.E.1. 2D Data Analysis with Analyst	174
4.II.E.2. 2D Data Analysis with Matlab.....	174
4.III. Results and Discussion	175
4.III.A. Sample Preparation	175
4.III.B. Determination of Prerun Times with Preliminary 1D CE-UV Experiments	176
4.III.C. Stability of First Dimension Contents During Second Dimension Separation Times	177
4.III.D. 2D Experiments with a Cytochrome <i>C</i> and Myoglobin Mixture.....	178
4.III.D.1. CE-UV-microreactor-CE-MS	178

4.III.D.2. CE-UV-microreactor-CE-MS-MS	181
4.III.E. 2D Experiments with a 6 Protein Mixture.....	182
4.III.F. Periodic MS Signal Dropouts	184
4.IV. Conclusions.....	186
4.V. Notes to Chapter 4.....	213
Chapter 5 – Conclusions and Future Directions	214
5.I. Conclusions	214
5.I.A. CE-ESI-MS Interface.....	214
5.I.B. 1D CE-ESI-MS and CE-ESI-MS-MS Experiments Using Bulk- digested Cytochrome <i>C</i>	215
5.I.C. Protein Digestion with a Pepsin Microreactor and 1D On-line Microreactor-CE-ESI-MS Experiments.....	215
5.I.D. 2D CE-UV-microreactor-CE-MS and -MS-MS	216
5.II. Future Directions.....	217
5.II.A. Improving Sensitivity and Detection Limits	217
5.II.B. Analyzing More Complex Samples.....	218
5.III. Notes to Chapter 5	219
Bibliography	220
Pocket Material: “Wiff to Matlab” script for Analyst software, LabView programs for 1D and 2D CE experiments	

LIST OF FIGURES

Figure Number	Page
1-1. Basic CE instrumentation	41
1-2. Electroosmotic flow in capillary electrophoresis	42
2-1. Schematic diagram of the 1D CE-UV-MS instrument.....	87
2-2. Head-on view of a UV fiber that has been cut square	88
2-3. Schematic diagram of the CE-UV Teflon detection cross	89
2-4. Schematic diagram and picture of the nanospray sheathless CE-ESI-MS interface	90
2-5. Schematic of the MicroIonSpray head for sheath flow CE-ESI-MS experiments	91
2-6. Schematic diagram of the MicroIonSpray head tip and picture of the MicroIonSpray head.....	92
2-7. Picture showing the CE instrument in the Plexiglas box raised on aluminum rods and a jack	93
2-8. Diagram illustrating how CE-MS data were analyzed with the Analyst software	94
2-9. Effect of capillary inner diameters of non-tapered fused silica capillaries on the average observed flow rate using the sheathless CE-ESI-MS interface	95
2-10. UV and MS electropherograms of 2% DMSO obtained using the sheathless CE-ESI-MS interface	96
2-11. UV and MS electropherograms of 4% DMSO obtained using the sheath flow CE-ESI-MS interface	97
2-12. Electropherograms of a CE-UV-ESI-MS experiment with trypsin bulk-digested cytochrome <i>C</i> using an uncoated fused silica capillary	98
2-13. Two extracted ion electropherograms of the experiment shown in Figure 2-12	99

2-14. Electropherograms of a CE-UV-ESI-MS experiment with trypsin bulk-digested cytochrome <i>C</i> using a poly(vinyl alcohol) (PVA)-coated capillary.....	100
2-15. Electropherograms of two consecutive CE-MS experiments with trypsin bulk-digested cytochrome <i>C</i> using a PVA-coated capillary	101
2-16. Extracted ion electropherograms of experiments using an uncoated and a PVA-coated capillary	102
2-17. Electropherograms of two consecutive CE-MS experiments with pepsin bulk-digested cytochrome <i>C</i>	103
2-18. Baselines obtained with running buffer before and after stopping and starting data acquisition in the MS Analyst software	104
2-19. Electropherograms of two consecutive blank experiments using batch acquisition in the Analyst software	105
2-20. Screen capture of Mascot Search Results identifying trypsin bulk-digested cytochrome <i>C</i>	106
2-21. Screen capture of Mascot Search Results listing the protein identifications and the peptides upon which the identifications were made	107
2-22. Screen capture of an individual fragment mass spectrum of a peptide of cytochrome <i>C</i> identified with Mascot.....	108
2-23. Extracted ion electropherogram of a cytochrome <i>C</i> peptide peak illustrating that fragmentation of a selected mass might occur at the back of that mass's peak.....	109
3-1. Pictures of the Plexiglas syringe purging device and the 1 mL flushing syringe.....	148
3-2. Reaction scheme for pepsin immobilization	149
3-3. Schematic diagram of the modified CE-MS set-up for on-line microreactor-CE-ESI-MS experiments and close-up picture center of the Plexiglas-glass interface ...	150
3-4. Picture and schematic diagram of the Plexiglas-glass interface	151
3-5. Side and top view pictures of the Plexiglas injection block	152
3-6. Schematic diagram of the two configurations of the 4-way valve	153

3-7. CE current of a preliminary purging experiment to determine the time needed to purge buffer (or sample) to the interface	154
3-8. Electropherograms of pepsin bulk-solution digested and microreactor-digested cytochrome <i>C</i> , and two controls	155
3-9. Electropherograms of microreactor homogeneity experiments.....	156
3-10. Electropherograms of different concentrations of cytochrome <i>C</i> digested off-line with the same microreactor	157
3-11. Mass spectra of a solution of UV glue soaked in ammonium acetate buffer and a control.....	158
3-12. Excel plots of peak areas and heights of selected XIEs vs. varying digestion times.....	159
3-13. Electropherograms of cytochrome <i>C</i> separations using various buffers and electric fields, and either bulk solution digested or microreactor digested sample	160
3-14. Electropherograms of on-line microreactor digested myoglobin.....	161
4-1. Schematic diagram of the 2D CE-UV-microreactor-CE-MS-MS instrument.....	188
4-2. Picture of the 2D instrumentation.....	189
4-3. Diagram illustrating the experimental procedure for 2D experiments.....	190
4-4. Screen capture of the front panel of the 2D LabView program	191
4-5. UV detection traces of a preliminary 1D CE-UV experiment with cytochrome <i>C</i> and myoglobin.....	192
4-6. UV traces of the optimization of applied voltages during protein digestion and peptide separation times in 2D cycles.....	193
4-7. Total ion electropherogram and selected mass spectra of a 2D experiment with cytochrome <i>C</i> and myoglobin.....	194
4-8. Reconstructed ion electropherograms of a 2D experiment with cytochrome <i>C</i> and myoglobin	195

4-9. Two-dimensional gel image representation of a 2D experiment with cytochrome <i>C</i> and myoglobin.....	196
4-10. Three-dimensional Matlab representation of selected XIEs of a 2D experiment with cytochrome <i>C</i> and myoglobin.....	197
4-11. Reconstructed ion electropherograms of a 2D experiment with cytochrome <i>C</i> and myoglobin	198
4-12. Two-dimensional gel image representation of a 2D experiment with cytochrome <i>C</i> and myoglobin.....	199
4-13. Three-dimensional Matlab representation of selected XIEs of a 2D experiment with cytochrome <i>C</i> and myoglobin.....	200
4-14. Screen capture of Mascot Search Results identifying cytochrome <i>C</i> based on a 2D experiment.....	201
4-15. Screen captures of Mascot Search Results showing the protein and peptide identifications for cytochrome <i>C</i> and an individual fragment mass spectrum of a peptide.....	202
4-16. Screen capture of Mascot Search Results identifying myoglobin based on a 2D experiment.....	203
4-17. Screen captures of Mascot Search Results showing the protein and peptide identifications for myoglobin and an individual fragment mass spectrum of a peptide..	204
4-18. UV electropherogram of a preliminary 1D CE-UV experiment using a 6 protein mixture.....	205
4-19. Two-dimensional gel image representation of a 2D experiment with a 6 protein mixture.....	206
4-20. Electropherograms of a 2D experiment with a 6 protein mixture	207
4-21. Three-dimensional Matlab representation of selected XIEs of a 2D experiment with a 6 protein mixture.....	208
4-22. Total ion electropherogram of a 2D experiment using 90% MeOH + 5% ACN + 5% ddH ₂ O illustrating the periodic MS signal dropouts	209

LIST OF TABLES

Table Number	Page
2-1. Pin assignments for the 50-pin ribbon cable for 1D CE-UV-MS experiments	110
2-2. 19 and 20 extracted ion electropherogram (XIE) masses that yielded most intense peaks for the trypsin- and pepsin-digested cytochrome <i>C</i> peptides	111
3-1. Percent relative standard deviations (%RSDs) for three extracted ion electropherogram (XIE) masses of four consecutive on-line microreactor-CE-ESI-MS experiments with cytochrome <i>C</i>	162
3-2. 20 extracted ion electropherogram (XIE) masses that yielded the most intense peaks for the myoglobin peptides	163
4-1. Pin assignments for the 50-pin ribbon cable for 2D CE-UV-microreactor-CE-MS experiments	210
4-2. 13 and 10 extracted ion electropherogram (XIE) masses that yielded peaks for myoglobin and cytochrome <i>C</i> peptides in 2D experiments, respectively.....	211
4-3. Voltage programs for 2D experiments	212

GLOSSARY

1D:	one-dimensional
2D:	two-dimensional
2DE:	two-dimensional gel electrophoresis
ACN:	acetonitrile
AIBN:	2,2'-azobisisobutyronitrile
AMT:	accurate mass tag
CE:	capillary electrophoresis
CEC:	capillary electrochromatography
CGE:	capillary gel electrophoresis
CIEF:	capillary isoelectric focusing
CSE:	capillary sieving electrophoresis
CTAB:	cetyltrimethylammonium bromide
CUR:	curtain gas
CZE:	capillary (free) zone electrophoresis
DAQ:	data acquisition
DMSO:	dimethylsulfoxide
EDMA:	ethylene glycol dimethacrylate
EOF:	electroosmotic flow
ESI:	electrospray ionization
EtOH:	ethanol

FQ:	3-(2-furoyl)quinoline-2-carboxaldehyde
FTICR:	Fourier transform ion cyclotron resonance
γ -MAPS:	3-(trimethoxysilyl)propylmethacrylate or γ -methacryloxypropyltrimethoxysilane
GMA:	glycidyl methacrylate
GS1:	nebulizer gas
HPLC:	high performance liquid chromatography
HQ:	hydroquinone
ICAT:	isotope-coded affinity tag
ID:	inner diameter
IDA:	information dependent acquisition
IEC:	ion exchange chromatography
IEF:	isoelectric focusing
IS:	ion spray
ITP:	isotachopheresis
LIF:	laser induced fluorescence
LIT:	linear ion trap
MALDI:	matrix assisted laser desorption ionization
MECC:	micellar electrokinetic capillary chromatography
MeOH:	methanol
mRNA:	messenger ribonucleic acid
MS:	mass spectrometry

MS/MS:	tandem mass spectrometry
MudPIT:	multidimensional protein identification technology
m/z:	mass-to-charge
NFM:	nanofluidic module
OD:	outer diameter
OTCEC:	open tubular capillary electrochromatography
PMT:	photomultiplier tube
PTM:	post-translational modification
PVA:	poly(vinyl alcohol)
Q:	quadrupole
RIE:	reconstructed ion electropherogram
RP:	reversed phase
RSD:	relative standard deviation
SCX:	strong cation exchange chromatography
SDS-PAGE:	sodium-dodecyl-sulfate polyacrylamide gel electrophoresis
SEC:	size-exclusion chromatography
SHE:	standard hydrogen electrode
TFA:	trifluoroacetic acid
TIE:	total ion electropherogram
T-jct:	Tee-junction
TOF:	time of flight
UV:	ultraviolet

XIE: extracted ion electropherogram

ACKNOWLEDGEMENTS

I would like to most gratefully acknowledge my supervisor, Prof. Norman J. Dovichi, for his support, guidance, and for giving me the opportunity to work on the CE-MS project. With his help I was able to further develop my scientific and professional knowledge and skills tremendously.

I would like to thank Dr. Mingliang Ye, a former post-doc of the Dovichi group, for his help with the pepsin microreactor and for providing the LabView programs that were used in this work. I would also like to acknowledge Dr. Chun-Sheng (Charles) Liu, also a former Dovichi group member, now at Applied Biosystems, for providing the MicroIonSpray head for the Q TRAP NanoSpray ion source, for his suggestions regarding its use, and for his help with CE-ESI-MS in general. I appreciate Dr. Darren Lewis's help (also a former Dovichi group member) in setting up the nanofluidic module (NFM) in our lab. Thanks also to Michael Vannatta for his assistance with the mass spectral data analysis, and to the University of Washington's electronics and machine shops for their aid in constructing the CE-UV instrumentation.

I also thank Dr. Martin Sadilek very much for his time and assistance, especially with regards to mass spectrometry. I appreciate the support from all the current and former Dovichi group members, with special thanks to Dr. Amy Dambrowitz, Dr. Danqian (Maggie) Mao, and Dr. Md. Abul Fazal for their friendship and direction throughout my years as a graduate student. In addition, I would like to thank Dr. Hidong Kim for his mentorship and time.

I gratefully acknowledge MDS Sciex and Applied Biosystems for their financial support and for providing the Q TRAP mass spectrometer. I also thank Scivex, Inc. for providing the nanofluidic module (NFM) that was used for the sheath flow.

Last, but certainly not least, I would like to thank my family, especially my parents, my brother, and my husband and his parents, for their love, encouragement, and support. Without you, I would not be where and who I am now.

DEDICATION

To my parents, brother, husband, and parents-in-law.

Chapter 1 – Introduction

A broader understanding of diseases such as cancer or Alzheimer's can be gained by examining the contents of diseased cells. A major contribution to this understanding was provided when the human genome was sequenced.^{1, 2} The genome, while providing a parts list for an organism, provides little guidance on the function and interaction of these parts. It was thought at one point that an analysis of the messenger ribonucleic acid (mRNA) would provide an accurate representation of the physiological state of cells. However, proteins that are translated from the mRNA can be post-translationally modified, and studies have shown that a direct correlation between mRNA and protein expression in cells is not always possible.³ Since it is at the protein level at which cellular functions and structures are actually controlled, various methods have been developed to probe the protein content of cells directly.

The most mature method for the separation of proteins is two-dimensional gel electrophoresis (2DE), which separates proteins based on their isoelectric points with isoelectric focusing (IEF) in one dimension, and based on their molecular weights with sodium-dodecyl-sulfate polyacrylamide gel electrophoresis (SDS-PAGE) in a second dimension. The proteins are visualized by staining and can be in-gel digested and identified by mass spectrometry (MS). Over 10,000 protein spots have been resolved in one 2DE analysis, which represents the highest peak capacity of any of the protein analysis methods thus far.^{4, 5} The method is unfortunately laborious, time-consuming, not easily automated, and often fails to detect low-abundance proteins when very complex

samples are analyzed.^{6, 7} Separations are thus increasingly carried out on columns and in capillaries, which have proven to be less labor intensive, more easily automated, and can be coupled on-line to MS. Capillary electrophoresis (CE) is especially suited for protein and peptide analyses because of its speed, high peak efficiencies, small sample requirements, and low solution consumption.

1.I. Background of Capillary Electrophoresis (CE)

1.I.A. Brief History of CE

The beginnings of capillary electrophoresis can be traced back to work done by Tiselius.⁸ He separated proteins from algae and human serum (albumin and globulins) with a U-shaped glass apparatus that had inner diameters (IDs) of a few mm. Relatively low electric fields were applied to avoid excessive Joule heating and convection that would degrade the separation. In the 1960s and 70s, Hjertén,⁹ Virtanen,¹⁰ and Mikkers¹¹ used smaller tubes to avoid convective forces and to separate a variety of analytes including inorganic ions, nucleotides, and proteins.

Then in 1981, Jorgenson and Lukacs¹² published breakthrough work that demonstrated the potential of CE for highly efficient separations. They used 75 μm ID open-tubular glass capillaries that allowed applied voltages of up to 30 kV across 80-100 cm long capillaries. The small IDs enabled less current generation and fast dissipation of the generated heat due to the small surface-to-volume ratios. Separation efficiencies up to 400,000 theoretical plates were demonstrated for amino acids, amines, and a human urine sample within 30 min separation times.

Research in capillary electrophoresis has expanded since then. A major factor has been the ready availability of polyimide-coated fused silica capillaries with very small IDs, usually below 100 μm . The polyimide coating makes the otherwise fragile capillaries very flexible, and hence makes their use very practical. In addition, advances in coupling various detection methods to CE, such as fluorescence^{13, 14} and mass spectrometry,¹⁵ have made the detection of minute volumes of analytes in the small capillaries possible, since only nL amounts of sample are usually introduced into the capillary.

Many different modes of capillary electrophoresis have been developed that separate analytes based on different physical and chemical properties, among them capillary (free) zone electrophoresis (CZE), micellar electrokinetic capillary chromatography (MECC),¹⁶ capillary isoelectric focusing (CIEF),¹⁷ capillary sieving electrophoresis (CSE),¹⁸ and capillary electrochromatography (CEC).¹⁹ These advances have made capillary electrophoresis available for a wide range of analytes, from inorganic ions to whole cells.

1.I.B. CZE Theory

The instrumentation for basic CE analyses is fairly simple, see **Figure 1-1**. Both ends of a capillary are suspended in electrolyte solution reservoirs, along with electrodes. One electrode is held at high voltage, the other is usually connected to ground. The reservoir with the high voltage electrode can be exchanged with a sample reservoir, and injection can be done electrokinetically by applying a voltage, or hydrodynamically by either raising the sample reservoir, by applying gas pressure, or by applying a negative

pressure at the outlet of the capillary. The buffer reservoir is replaced, and a high voltage is applied to commence the separation. Optical detection is most often done on-capillary by removing part of the polyimide, but can also be done post-column.

Electrophoresis is defined as the migration of a charged analyte under the influence of an electric field.^{20, 21} The electrophoretic velocity, v_{el} , of an analyte depends on the analyte's characteristic electrophoretic mobility, μ_{el} , and the applied electric field, E

$$v_{el} = \mu_{el} E \quad (1-1).$$

The electric field is given by the applied high voltage, V , divided by the total capillary length, L

$$E = V / L \quad (1-2).$$

In capillary free zone electrophoresis (CZE), the simplest form of CE, an analyte migrates based on its charge and hydrodynamic size. Two forces act on the charged analyte: an electrical force, F_{el} , and a frictional force, F_{fr} . The electrical force is defined by the analyte's charge, q , and the applied electric field

$$F_{el} = q E \quad (1-3).$$

The frictional force, which is directed opposite to the electrical force, and hence is negative in equation 1-4, depends on the analyte's Stokes' radius, r , (if one assumes a spherical, charged analyte), the viscosity of the buffer, η , and the analyte's electrophoretic velocity, v_{el}

$$F_{fr} = -6 \pi \eta r v_{el} \quad (1-4).$$

When an equilibrium of the two forces is attained during electrophoresis, the two forces are equal, but opposite, to each other

$$q E = 6 \pi \eta r v_{el} \quad (1-5).$$

A rearrangement of equation 1-5 yields an expression for the electrophoretic mobility, μ_{el} , of the charged analyte

$$\mu_{el} = v_{el} / E = q / 6 \pi \eta r \quad (1-6),$$

which is another form of equation 1-1. The electrophoretic mobility is a fundamental parameter in electrophoresis, because it is the basis for the separation of analytes. As equation 1-6 indicates, an analyte's electrophoretic mobility is dependent only on its size and charge, because a change in viscosity of the buffer affects all analytes to the same extent. The smaller and more highly charged an analyte, the greater its electrophoretic mobility.

An analyte's apparent velocity, v_{app} , is also affected by the electroosmotic, or endoosmotic, flow (EOF) that is associated with the bulk solution flow in fused silica capillaries. The EOF is based on the negative charges that deprotonated silanol (SiO^-) groups on the surface of the capillary wall exhibit. The exact pK_a of these groups is not known, but is estimated to range between 2 and 4. Positively charged buffer constituents associate very closely with the negatively charged capillary wall in a double layer. The double layer is composed of a static Stern layer closest to the wall, and a more diffuse, or mobile, layer further from the wall; the latter is also termed the outer Helmholtz plane.²⁰ The potential drop across the double layer is called the zeta potential, ζ . When an electric field is applied, the cations in the diffuse layer start to migrate towards the cathode of the

system. Because the cations are hydrated, and because the polar water molecules in the buffer interact with each other *via* hydrogen bonding, all of the liquid inside the capillary starts to move towards the cathode with a plug-like flow profile. The velocity of that electroosmotic flow, v_{EOF} , is defined as its electroosmotic mobility, μ_{EOF} , multiplied by the applied electric field

$$v_{EOF} = \mu_{EOF} E \quad (1-7).$$

The electroosmotic mobility, in turn, depends on the permittivity, ϵ , and the viscosity of a solution, and on the zeta potential, ζ

$$\mu_{EOF} = \epsilon \zeta / \eta \quad (1-8).$$

The zeta potential can vary with the extent of silanol deprotonation and the ionic strength of the buffer. At a high pH, the capillary wall is more highly charged since more silanol groups are deprotonated, which increases the zeta potential and the EOF. With high buffer ionic strength the double layer is said to be compressed, which results in a lower zeta potential and hence a decreased EOF.²¹ The EOF can also be modified by coating the capillary wall, which will be discussed in section 1.II.A.1..

One advantage of EOF is its plug-like flow profile, see **Figure 1-2**. This profile arises since the only opposing force to the EOF is at the surface of shear in the double layer, whose extent is minimal compared to the total inner diameter of the capillary. Unlike in pressure-driven separation systems, where the flow is parabolic and contributes to band broadening, the plug-like EOF profile eliminates this source of band broadening. The presence of a high EOF also enables the detection of both negatively and positively charged species in one electrophoretic experiment, because the bulk buffer flow sweeps

the negatively charged analytes to the cathode as well, see **Figure 1-2**. Neutral analytes, such as dimethylsulfoxide (DMSO), travel in one zone at the speed of the EOF. By using such neutral analytes, the electroosmotic velocity and mobility can be experimentally determined.

Having defined both an analyte's electrophoretic velocity, v_{el} , and a buffer's electroosmotic velocity, v_{EOF} , the apparent velocity, v_{app} , of an analyte is given by the sum of the velocities

$$v_{app} = v_{el} + v_{EOF} = (\mu_{el} + \mu_{EOF}) E \quad (1-9).$$

It is important to note that even though the electric field depends on the voltage applied across the whole capillary length, L , the calculation of the apparent velocity often involves the length from the capillary inlet to the detector, sometimes called the effective length, L_{eff} . This is the case with on-capillary detection. The apparent velocity can be calculated by dividing L_{eff} by the observed migration time, t

$$v_{app} = L_{eff} / t \quad (1-10).$$

Analogous to chromatography, efficiency and resolution are two main measures of the quality of a capillary electrophoresis separation. Both efficiency, given by the number of theoretical plates, N , and resolution, R , are influenced by the dispersion, or broadening, of solute zones in the capillary. Dispersion can be defined as the baseline peak width, w_b , of a Gaussian peak, and the peak width in turn is defined by its standard deviation, σ

$$w_b = 4 \sigma \quad (1-11).$$

The standard deviation is related to molecular diffusion, D , in chromatography, which can be extended to capillary electrophoresis if longitudinal diffusion is assumed to be the only contributing factor to zone broadening

$$\sigma^2 = 2 D t = \frac{2 D L_{\text{eff}} L}{\mu_{\text{app}} V} \quad (1-12).$$

Efficiency can be expressed in terms of the standard deviation and the effective length as

$$N = \left(\frac{L_{\text{eff}}}{\sigma} \right)^2 \quad (1-13).$$

Substituting equation 1-12 into equation 1-13 and rearranging with equation 1-2 yields

$$N = \frac{\mu_{\text{app}} V L_{\text{eff}}}{2 D L} = \frac{\mu_{\text{app}} E L_{\text{eff}}}{2 D} = \frac{(\mu_{\text{el}} + \mu_{\text{EOF}}) E L_{\text{eff}}}{2 D} \quad (1-14).$$

Importantly, this equation indicates that greater peak efficiencies can be obtained by applying higher electric fields. A more practical equation for calculating efficiency is given in equation 1-15, where $w_{1/2}$ is the peak width at half height

$$N = 5.54 (t / w_{1/2})^2 \quad (1-15).$$

The resolution of two peaks is often expressed as their difference in migration times divided by their average base peak width, in units of time

$$R = \frac{(t_2 - t_1)}{\frac{1}{2}(w_1 + w_2)} = \frac{(t_2 - t_1)}{4 \sigma} \quad (1-16).$$

Resolution can also be related to efficiency

$$R = \frac{1}{4} \sqrt{N} \left(\frac{\Delta \mu_{\text{app}}}{\mu_{\text{avg}}} \right) \quad (1-17),$$

where $\Delta \mu_{\text{app}}$ is the difference in the analytes' apparent mobilities, and μ_{avg} is the average of their mobilities. As Oda and Landers state,²⁰ equation 1-17 allows resolution to be

analyzed based on both a separation's selectivity, given by the analytes' mobilities, and by its efficiency. Equation 1-17 also shows that resolution does not improve to the same extent as efficiency does. Hence, by increasing the applied voltage, see equation 1-14, efficiency might be improved, but the gain in resolution will be less pronounced.

In the equations above for efficiency and resolution, an ideal case was assumed in which longitudinal diffusion was the only source of zone broadening. However, zone broadening can also occur because of, for instance, electrostatic interactions between an analyte and the capillary wall, injection volume, and Joule heating. The analyte-wall interactions will be discussed in section 1.II.A.1.. Joule heating is generated by the current that is based on the flux of charged species through a capillary. Even though the small capillaries can dissipate heat very well, excessive heat generation can cause zone spreading. Joule heating can be alleviated by decreasing the electric field or the ionic strength of the buffer. To determine whether specific applied parameters cause Joule heating, the current can be plotted vs. applied electric field to generate an Ohm's plot. Joule heating begins to occur where the plot starts to deviate from linearity.

One last aspect of CE theory covers the quantity of injected sample. As mentioned, samples can be injected hydrodynamically or electrokinetically. In the former, the injected volume can be calculated using the Hagen-Poiseuille equation²¹

$$\text{Volume} = \frac{\Delta P d^4 \pi t}{128 \eta L} \quad (1-18),$$

where ΔP is the pressure difference across the capillary, d is the capillary inner diameter, t is the injection time, η is the sample solution's viscosity, and L is the total capillary length. The amount of specific analyte can then be calculated based on its concentration.

In electrokinetic injection, the injected amount of a specific analyte can be calculated by the following equation.²²

$$\text{Analyte injected amount} = \frac{C \text{ Vol}_{\text{cap}} t_{\text{inj}} V_{\text{inj}}}{t V} \quad (1-19),$$

where C is the analyte's concentration, Vol_{cap} is the capillary volume from injection end to the detector, t_{inj} is the injection time, V_{inj} is the injection voltage, t is the analyte's migration time to the detector, and V is the voltage applied during the experiment. t in equation 1-19 implies that an analyte's injected amount depends on its electrophoretic mobility, and hence electrokinetic injection is biased against analytes with lower mobilities. The same bias is not observed in hydrodynamic injection.

1.II. Protein and Peptide Separations by CE

1.II.A. Various CE Modes and 1D Separations

1.II.A.1. Capillary Zone Electrophoresis (CZE)

Among the capillary electrophoretic methods, the simplest and most frequently used mode is capillary (free) zone electrophoresis. CZE takes place in buffer in open capillaries, and the separation of peptides and proteins depends on their charge-to-size ratio, which causes them to have different mobilities in an applied electric field. The basic arginine and lysine amino acids of peptides and proteins can cause them to adhere to the negatively charged walls of fused silica capillaries. This effect is greater for proteins than peptides due to the larger sizes of proteins. Modifications of buffer pH or ionic strength can reduce some of these interactions. For example, Nielson *et al.*²³ were able to separate different forms of human growth hormone without retention on the walls

by using a buffer whose pH was greater than the pI of the analytes. Bushey and Jorgenson²⁴ showed that increasing the ionic strength of buffers with zwitterionic species improved protein separations because the zwitterions, instead of the proteins, interacted with the capillary wall.²⁵

Various other capillary wall modifications²⁶⁻²⁹ have been employed that lower peptide- and protein-wall interactions by masking the negatively charged silanol groups and leaving the wall hydrophilic or hydrophobic, depending on the coating. Some coatings, such as cetyltrimethylammonium bromide (CTAB), even reverse the EOF when positively charged groups of the coating molecules extend into the capillary. Capillary coatings can either be static, or permanent, meaning the coating compounds are covalently linked to the wall; or dynamic, such as with adsorbed polymers or surfactants. Different coatings can be used for different pH ranges.

Common permanent coatings include polyacrylamide, polyethylene glycol (PEG), (3-aminopropyl)-trimethoxysilane (APS), and poly(vinyl alcohol) (PVA). The latter was used in this work and the coating procedure for PVA was found to be quite facile.³⁰

Unfortunately, the procedures for static coatings can often be complex and time-consuming, and the coatings invariably deteriorate with prolonged use so that new coated capillaries are needed. This has made dynamic coatings desirable since one capillary can be used for a long time. Dynamic coatings can either be stripped from the capillaries after each run and then regenerated, or the coating agents can be present in the running buffer, such as the zwitterions used by Bushey and Jorgenson²⁴ mentioned earlier. More recently, Wei and Ju³¹ used the zwitterionic surfactant dodecyl sulfobetaine (DSB) in conjunction with anions such as ClO_4^- as additives to buffers. Peak efficiencies as high

as almost 900,000 were achieved for basic proteins. Other dynamic coatings, such as the proprietary compounds EOTrolTM and UltraTrolTM, have been introduced.³² Different forms of these compounds can alter the EOF to varying degrees, and both EOTrolTM and UltraTrolTM have been used by the Dovichi group in one- and two-dimensional CE separations of proteins. These dynamic coatings have been especially useful for modifying capillaries with IDs smaller than 50 μm , whereas using static coatings with small IDs has sometimes been unsuccessful.

1.II.A.2. Micellar Electrokinetic Capillary Chromatography (MECC)

Micellar electrokinetic capillary chromatography (MECC), also referred to as micellar electrokinetic chromatography (MEKC), was introduced by Terabe *et al.* in 1985.³³ MECC separates proteins and peptides depending on their hydrophobic interactions with micelles in the buffer, in addition to their charge-to-size ratio during electrophoresis. Beattie and Richards³⁴ used SDS as the micellar surfactant to analyze isoforms of metallothionein metal binding proteins. Liu *et al.*³⁵ investigated peptide analysis with MEKC using dodecyltrimethylammonium bromide and SDS. Swedberg³⁶ formed micelles with zwitter- and non-ionic surfactants to separate standard peptides. Recently, Popa *et al.*³⁷ compared CZE, MECC, and capillary electrochromatography (CEC) in the analysis of a series of synthetic peptide diastereomer pairs. MECC was best suited for separating peptides with hydrophobic or aromatic diastereomer residues, and peptides were separated faster than by CE or CEC. But, CEC showed better resolution for other diastereomer residues.

1.II.A.3. Capillary Isoelectric Focusing (CIEF)

Capillary isoelectric focusing (CIEF) was first demonstrated by Hjertén in 1985.¹⁷ CIEF separates analytes based on their specific isoelectric points (*pI*s), which are at *pH*s at which the analytes are neutral. Unlike in gel-based IEF, no gels are needed to reduce convection since the capillaries allow efficient heat dissipation from the system. In CIEF, the sample is mixed with a carrier ampholyte solution and the whole capillary can be filled with this mixture, allowing large sample volumes to be injected. The carrier ampholytes form a buffered *pH* gradient when an electric field is applied across the capillary, and the proteins and peptides migrate to the *pH*s that correspond to their *pI*s, thus concentrating and focusing them in short zones with high resolution. After focusing, the proteins and peptides are moved to the detector by gravity or chemical mobilization.³⁸

Proteins and peptides are detected using UV and MS. The latter has better detection limits and of course identification ability, but low ampholyte concentrations have to be used to avoid much too analyte ion suppression and contamination of the MS. Storms *et al.*³⁹ have investigated omitting carrier ampholytes in CIEF-MS when analyzing tryptic digests of proteins, but found that the peptides did not elute according to their *pI*s even though the peptides were still fairly well focused and resolved. They also tried a low (0.20%) concentration of carrier ampholytes, which resulted in better resolution and better identification with tandem mass spectrometry than without carrier ampholytes. The ion suppression and MS contamination was found acceptable at the 0.20% concentration. Fluorescence detection is not very useful for CIEF, because any derivatization of the analytes changes their *pI* values; a multitude of *pI* states for a particular protein results, which makes focusing the protein futile.³⁸

When comparing protein and peptide CIEF, CIEF is better suited for protein than peptide analysis since most peptides approach their pI s over a broader pH range than proteins do. This broader pH range causes the zones in which the peptides are focused to be wider than for proteins.^{40, 41} Still, Smith *et al.*⁴² were able to separate tryptic digest peptides from cytosolic fractions of yeast with peak widths at half heights of ~ 3 sec.

1.II.A.4. Capillary Sieving Electrophoresis (CSE)

Capillary sieving electrophoresis (CSE) is the capillary analog to slab gel sodium dodecyl sulfate-polyacrylamide gel electrophoresis (SDS-PAGE) and separates proteins based solely on size, yet CSE is less labor intensive and more easily automated than SDS-PAGE. CSE has been employed since the 1980s,^{43, 44} but was then called capillary gel electrophoresis (CGE) because gels were polymerized inside the capillaries. The use of non-cross-linked, replaceable polymers has proven to be more practical, and common polymers include linear polyacrylamide (LPA), dextran, pullulan, and poly(ethylene glycol) (PEG). The capillaries are coated to prevent protein adsorption and to reduce the EOF to keep the sieving polymer matrix from migrating. Protein samples are denatured by addition of SDS, and SDS-protein complexes are formed that have a constant charge-to-size ratio; their separation is therefore dependent on their sizes only, with smaller proteins moving faster through the sieving matrix than larger proteins. CSE is not very useful for the separation of peptides because their sizes are too small to be differentially retained by the sieving matrix.

A replaceable cross-linked polyacrylamide matrix has recently been reported that has shown higher resolutions of proteins (standard proteins and an *E. coli* cell extract)

than other matrices such as non-cross-linked ones.⁴⁵ The replaceable matrix differed from ones used in early CGE because it was cross-linked before filling capillaries with it. CSE has also been used in the biotechnology industry to evaluate the purity of recombinant proteins.⁴⁶

1.II.A.5. Capillary Electrochromatography (CEC)

CEC is a cross between CE and capillary high performance liquid chromatography (HPLC) and was first introduced in the 1970s and 80s.⁴⁷ The capillaries are filled or coated with a stationary phase that can have various functionalities, but instead of using hydrodynamic pressure as in HPLC, an electric field is applied to create an EOF that aids in moving analytes through the capillaries. This has the advantage of achieving higher separation efficiencies than in LC due to the plug-like profile of the EOF. CEC usually employs aqueous buffers with organic modifiers, and the analytes are separated based on their interactions with the stationary phase in addition to their electrophoretic mobility differences. This often yields better separations than CZE or HPLC alone can achieve.

Different stationary phases have been employed in CEC. Initially, capillaries were packed with small silica particles, but the frits that were needed to keep the particles in the capillaries often created bubbles. In recent years, monolithic stationary phases have been introduced that do not need frits because the monoliths are covalently linked *in situ* to the capillary wall, and their use is thus more practical.⁴⁸ Hilder *et al.*⁴⁹ have reported a monolith that was modified by two layers of polymer chains, the inner layer being ionizable to enable EOF, the outer layer being hydrophobic to shield charged

analytes from being retained by the ionizable layer. Proteins and peptides were separated within 3 minutes. Okanda and Rassi⁵⁰ have described a neutral, nonpolar monolithic stationary phase based on pentareythritol diacrylate monostearate (PEDAS). The EOF needed for analyte migration was produced by adsorption of charged electrolytes from the buffer, yet because no fixed charges were part of the stationary phase, charged analytes were not retained.

Another form of CEC that has shown better and faster separations than HPLC is open tubular CEC (OTCEC), in which only the capillary wall is modified. Low sample capacities have been a challenge for OTCEC because of the low surface-to-volume ratio of the stationary phase. This has been somewhat alleviated by etching the capillaries to increase the surface-to-volume ratio.⁵¹

1.II.B. 2D Separations

The goal of two-dimensional (2D) separation methods is to increase the number of analytes that can be resolved. To achieve the greatest peak capacity, that is the greatest number of peaks in a separation space, the two dimensions should operate under two uncorrelated, or orthogonal, separation mechanisms. According to Giddings,⁵² the peak capacity that can be obtained in orthogonal 2D separations is the product of the peak capacity of each of the separations. Based on this principle, many different combinations of separation mechanisms have been reported.

The most mature method for the 2D separation of proteins is 2D gel electrophoresis (2DE), which was mentioned at the beginning of this chapter along with its labor-intensiveness and lack of automation. A more automated, less labor-intensive,

and less time-consuming approach to 2D separations was introduced by Jorgenson *et al.*⁵³ in the 1990s. He and co-workers developed an on-line, comprehensive 2D fluid separation system using ion exchange chromatography (IEC) coupled to size-exclusion chromatography (SEC) for the separation of protein standards and serum proteins. The word comprehensive stresses that all of the first dimension effluent is transferred to the second dimension. Jorgenson *et al.*^{54, 55} also coupled reversed phase-high performance liquid chromatography (RP-HPLC) to CZE in an automated system with either fluorescence (1990) or on-line MS detection (1997). A drawback of these 2D systems was that they were not completely comprehensive because the effluent of the first dimension was diverted to waste when it was not injected onto the CE capillary.⁵⁵

Other 2D systems that couple LC to CE or *vice versa* have been reported. For example, Chen *et al.*⁵⁶ integrated CIEF on-line with RP-HPLC *via* a microinjector to separate tryptic protein digests from a *Drosophila* extract. Zhou and Johnston similarly coupled CIEF to RP-HPLC and on-line electrospray ionization-mass spectrometry (ESI-MS) to first analyze standard proteins,⁵⁷ and later a complex yeast enzyme concentrate.⁵⁸ Zhang *et al.*⁵⁹ coupled RP-HPLC to CZE with matrix assisted laser desorption/ionization-time of flight-time of flight-MS (MALDI-TOF-TOF-MS) detection to separate tryptic digest peptides of a liver cancer tissue sample. Over 300 proteins were identified.

Pure CE-CE-based 2D separation systems have only been reported in the last few years. Ramsey and co-workers⁶⁰ developed a microfabricated fluidic device that used a 69 mm long channel for MECC in the first dimension and a 10 mm long channel for CZE in the second dimension. Tryptic peptides were fluorescently labeled and detected with a photomultiplier tube (PMT) with a xenon lamp as the light source. A 2D separation of

two digested proteins was achieved within ten minutes with separations in the second dimension lasting only a few seconds. Although their 2D system was not truly comprehensive because only ~ 10% of the first dimension was sampled by the second dimension, they improved their system by shortening the separation in the second dimension to ~ 1 sec.⁶¹ A peak capacity of ~ 4,000 was achieved.

Mohan and Lee⁶² have reported the use of a microdialysis junction to connect CIEF to transient isotachopheresis (ITP)-CZE. Transient isotachopheresis is a specialized preconcentration mode of CE,⁶³ see section 1.II.C.1., that allowed the carrier ampholytes to be separated from the proteolytic peptide sample before UV detection. The method was not fully automated because mobilization of the CIEF dimension was performed hydrodynamically by elevating the inlet end, but peak capacities of ~ 1,600 were estimated.

Zhang and co-workers developed a system that connected CIEF to capillary gel electrophoresis (CGE)⁶⁴ and capillary sieving electrophoresis (CSE)⁶⁵ *via* a hollow fiber dialysis membrane. UV absorbance was used for detection. In their 2003 system, the sample containing hemoglobin variants was apparently continuously mobilized and injected onto the CGE capillary after the CIEF focusing step. The protein movement in the first dimension was slow enough so that all of one focused protein band was separated in the second dimension before another protein band migrated from the first dimension. In their 2005 system, the mobilization was apparently interrupted while the second dimension separation was performed. Even though the system was not fully automated, increased peak capacities were achieved with the 2D system than with each

separate CE mode. Zhang *et al.* also developed a 2D CIEF-CZE system with a porous junction interface.⁶⁶

The Dovichi group has developed fully automated 2D CE-CE systems for the analysis of a variety of protein samples with laser induced fluorescence (LIF) as the detection method.⁶⁷⁻⁶⁹ The separation capillaries were aligned tens of μm apart from each other inside various types of crosses whose cross-flow channels were connected to a buffer reservoir and a waste receptacle. The systems were comprehensive in that the flow in the first dimension could be stopped by appropriately applied voltages while the second dimension separation took place, and hence no, or only very little, sample was lost to waste. The system in the first report⁶⁷ did not use two orthogonal CE methods, but accomplished differential migration of the proteins from a human colon cancer cell line extract by choosing different buffer systems in the two CZE dimensions. In the later reports, CSE and MECC were used as the first and second dimensions, respectively, to separate protein homogenates of *Deinococcus radiodurans* bacteria⁶⁸ and the contents of single mouse osteoprecursor cells.⁶⁹ Spot capacities of ~ 375 were achieved for ~ 3.5 hour separations,⁶⁹ and peak efficiencies as high as 900,000 were observed.⁶⁸

1.II.C. Detection Methods for Protein and Peptide CE

This section focuses on sample preconcentration, UV, and fluorescence detection. MS detection will be discussed in section 1.IV..

1.II.C.1. Sample Preconcentration

One of the advantages of CE is that only very small sample amounts are needed because typical injection volumes are in the nL range. But this also makes detection challenging. To not overload the capillary, sample volumes of usually only ~ 1% of the capillary volumes are advised (disregarding CIEF, where the whole capillary can be filled with sample). Various electrophoresis- and chromatography-based preconcentration techniques have therefore been developed,⁷⁰ with the latter including solid-phase extraction and membrane-based preconcentration. For brevity, only electrophoresis-based preconcentration will be explained here.

Two common electrophoresis-based preconcentration methods are stacking and transient isotachopheresis (ITP). In stacking, the sample has a lower ionic strength than the separation buffer. When the sample is injected, the resistance and also the electric field across the sample plug are higher than in the rest of the capillary, which leads to the analyte ions traveling rapidly to the leading boundary of the sample plug, thus concentrating the analytes.⁷¹

One convenient form of transient ITP takes place in the same capillary in which CZE is performed. The sample is prepared in a solution containing a high-mobility electrolyte, which migrates to the front of the sample plug once it is injected and an electric field is applied. The capillary inlet is then placed back into the separation buffer, which contains a lower-mobility electrolyte than the sample, and the lower-mobility electrolyte forms the terminating electrolyte at the back of the sample plug. The analytes concentrate in discrete zones at the back of the sample plug according to their mobilities.

Once the fast leading electrolyte has dispersed into the separation buffer in front of the sample plug, the system behaves as a CZE system.⁶³

1.II.C.2. UV Absorbance

UV detection is commonly used in CE primarily because of its low cost, easy implementation, and universality. Detection is done on-capillary after removing a portion of the non-UV-transparent polyimide coating by, for instance, burning it off with a flame or shaving it off with a razor blade. The ~ 214 nm or 280 nm wavelengths are often used for peptides and proteins since the peptide bonds and the aromatic amino acids absorb at those wavelengths, respectively. The ~ 214 nm wavelength is better for peptides, since not all peptides contain aromatic side chains.

Unfortunately, the limits of detection that can be achieved with UV detection are in the μM range because of the short pathlengths of the capillaries. Several approaches have been implemented to increase the pathlength, such as enlarging the capillary ID to form a bubble through which UV light travels perpendicularly to the capillary axis, or bending the capillary into a Z or U form so that the light can travel on-axis for a few mm inside the capillary. This has improved detection limits by one order of magnitude.⁷²

Another improvement for UV detection, which was also implemented in this thesis work, has been the use of a spherical ball lens that is placed next to the capillary on the side from which the UV light enters. The ball lens focuses the light onto the capillary ID to make much more efficient use of the incoming light.^{72, 73}

Although UV detection's universality is an advantage because samples do not have to be derivatized to be detected, it is also a drawback because certain buffers or

buffer additives absorb light at the same wavelength as the sample and hence mask the sample's absorbance. Careful wavelength and buffer selection is therefore advised.

1.II.C.3. Fluorescence

Fluorescence detection with laser induced fluorescence (LIF) by far provides the lowest detection limits and greatest sensitivities of detection systems to date, having made single molecule detection possible.^{74, 75} LIF also has a wide dynamic range, which is especially advantageous for the analysis of biological samples since they include both low and high abundance proteins and peptides.

Although the aromatic amino acids exhibit native fluorescence, increased sensitivity can be achieved if proteins are derivatized with fluorescent dyes either pre-, on-, or post-column.⁷⁶ Both fluorescent and fluorogenic dyes are available, with the latter becoming fluorescent only upon binding to the analyte. This alleviates the high background fluorescence that is observed with fluorescent dyes.^{77, 78} The Dovichi group uses the fluorogenic dye 3-(2-furoyl)quinoline-2-carboxaldehyde (FQ) that attaches to the ϵ -amine of lysine residues and terminal amine groups.⁷⁹ Standard proteins or cell homogenates are labeled pre-column, and the contents of single cells are labeled on-column. Fluorescent labeling leads to multiple products of identical proteins since not all proteins are labeled to the same extent, which causes broad protein peaks. With FQ, this problem has been solved by using sub-micellar concentrations of SDS in the separation buffers. Apparently, SDS interacts with non-reacted ϵ -amines of lysine residues to form neutral products, just as FQ would. This allows the proteins to become chemically similar again and efficient separations are achieved.⁸⁰

Detection can be done on- or post-column. Post-column detection is superior since, for example, square sheath flow cuvettes can be used that avoid the light scattering observed with the curved capillary wall in on-column detection.⁸¹

1.III. Protein and Peptide Analysis by Mass Spectrometry

Mass spectrometric detection has the inherent advantage of providing information that can be used to identify proteins and peptides. Studying proteomes (the protein complements of genomes) with MS has become an extensive research area, especially since the genomes of many organisms have been sequenced in recent years. Easily searchable, computerized protein databases have made it possible to match experimental MS data to theoretical mass spectra that are based on genome sequences.

Analyzing the complete proteomes of organisms is the ultimate goal of proteomics, along with identifying proteins that play a role in diseases so that this knowledge can lead to the treatment or prevention of the diseases. This is a formidable challenge because the number of proteins in organisms range in the hundreds of thousands, and the dynamic range of protein expression in cells ($\sim 10^6$)⁸² often causes low-abundant proteins to be undetected. To meet this challenge, great progress has been made in advancing technologies that analyze many aspects of proteomes, whether aiming to identify as many proteins as possible, or to elucidate the specific characteristics of selected proteins. Many of these technologies are complementary.

Proteomics very often involves the separation of proteins by 2D gel electrophoresis (2DE), in-gel digestion of the proteins, and subsequent LC-MS of the resulting peptides. Based on the limitations of 2DE mentioned previously, especially its

labor-intensiveness and lack of automation, two other general and complementary strategies have become common in proteomics: top-down and bottom-up proteomics. In top-down proteomics, intact proteins are separated and then analyzed with MS directly, often using fragmentation inside the MS to gain more information. In bottom-up proteomics, used more commonly, the proteins are first digested and the subsequent peptides are separated and analyzed with MS. Some representative work of both approaches will be covered in the following sections. First, however, database searching will be explained to provide some background.

1.III.A. Database Identification of Proteins and Peptides

In the last few decades, on-line protein databases, including the Protein Information Resource (PIR)⁸³ and Swiss-Prot,⁸⁴ have been established whose protein sequences are mostly theoretical sequences based on genome sequences. Database search algorithms, such as SEQUEST⁸⁵ and Mascot,⁸⁶ can query protein databases using different types of mass spectral data. One such type is obtained in peptide sequencing, for which peptides are fragmented by tandem mass spectrometry (MS/MS) to produce many different pieces of peptides. Not only can proteins be identified based on these data, but the exact sequences of the peptides can be reconstructed since mass spectral peaks differ by the masses of only single amino acids. Another type is obtained *via* peptide mapping, for which peptides are left intact and proteins are identified based on the m/z values of the peptides. The peptides can either be produced by enzymatic digestion before MS analysis, or by fragmenting whole proteins inside the MS.^{87, 88}

1.III.B. Top-Down Analysis

Top-down proteomics seeks to separate intact proteins before analyzing them with MS and fragmenting them inside the MS. Exact protein molecular weights and high sequence coverages can be obtained, and various post-translational modifications (PTMs) can be localized and identified. The existence of certain protein degradation products with specific molecular weights, or specific PTMs of a protein, might be indicative of disease states, which makes top-down analysis attractive.⁸² Top-down analyses of large proteins (above ~ 50 kDa), however, is still challenging for technological reasons, and large-scale analyses are still quite time-consuming.

An early proteome study of intact proteins was reported by Smith and co-workers,⁸⁹ although no information on PTMs was obtained. The authors used CIEF coupled to Fourier transform ion cyclotron resonance (FTICR)-MS and -MS/MS to analyze whole proteins of *E. coli* cell lysates. To increase the mass accuracy of the FTICR-MS technique, which by itself is already capable of obtaining very high mass accuracies, the *E. coli* cell culture was grown under isotopically depleted conditions. Between 400 and 1000 putative protein identifications were made based on m/z information from MS and pI information from CIEF.

More recently, Kelleher and co-workers⁹⁰ analyzed *Saccharomyces cerevisiae* lysates and were able to identify 117 gene products and numerous PTMs of those proteins. The lysates were first fractionated by acid-labile surfactant (ALS)-continuous gel electrophoresis that allowed subsequent retrieval of whole proteins (which is difficult in conventional 2DE). Further fractionation was performed by RP-HPLC and the fractions, containing up to 10 proteins, were analyzed by electrospray ionization-

quadrupole Fourier transform MS (ESI-Q-FTMS). Proteins in such fractions (~ 10 μ L) could be analyzed in detail because ESI-MS could be performed on one fraction for ~ 50 min before the sample was depleted. Fragmentation of the proteins inside the MS was done by infrared multiphoton dissociation (IRMPD) with an IR laser. Up to 100% sequence coverage of the proteins was obtained, and proteins and PTMs were identified either by database searching or by deducing the PTMs and their locations by detailed MS analysis.

1.III.C. Bottom-Up Analysis

Bottom-up methods digest proteins prior to peptide separation and MS identification. Since peptide mass spectra are less complex than protein mass spectra, the formers' interpretation is easier. However, the digestion of proteins yields very complex peptide samples, and often the samples are simplified by fractionation before further separating them with HPLC or CE. Even with fractionation, separations cannot resolve all peptides, and many peptides are not identified because they coelute with other peptides. These factors restrict the number of peptides that are identified per protein, which can make the positive identification of proteins problematic. Still, the bottom-up technologies developed to date have identified an unprecedented number of proteins of very complex biological samples, and the relative quantification of protein expression levels from, for instance, two different cell states, has been achieved.

One significant technology, introduced by Tureček, Gelb, and Aebersold,⁷ allows a relative quantitative analysis of complex protein mixtures stemming from different cell states using isotope-coded affinity tag (ICAT) reagents. The tags cause identical

proteins, and subsequent peptides, of the two cell populations to differ only in their masses, whereas the chemistry of the proteins and peptides is changed to the same extent. In the method, proteins from two differentially treated cell populations are labeled with the cysteine-specific ICAT reagents. The proteins are combined and digested, and peptides containing the ICAT reagent(s) are isolated by avidin affinity chromatography since the tags also contain a biotin moiety. The labeled peptides are then separated by 1D or 2D LC and identified directly by ESI-MS/MS and database searching. Since the peptide pairs are almost chemically identical, they elute around the same time. The peptide pairs can be recognized because their mass spectral peaks are separated by a specific mass-to-charge (m/z) difference. Quantification is based on the respective mass spectral signal intensities.

Some challenges to the technique are that many sample-handling steps are involved, and some proteins are not analyzed because they do not contain cysteine amino acids. However, since its advent, several improvements have been reported. For example, different combinations of multi-dimensional separations have been used and tags have been developed that attach to amino acids other than cysteine.⁹¹ Most recently, a new version of the ICAT reagents has been introduced that uses ^{12}C and ^{13}C isotopes and that has an acid-cleavable linker.⁹² The ^{12}C and ^{13}C isotopes allow tagged peptide pairs to elute at exactly the same time, which in turn makes automated data-dependent MS/MS acquisition possible (which includes selection of precursor ions during a survey scan and subsequent fragmentation of the precursor ions by MS/MS). The acid-cleavable linker enables the biotin moiety to be removed, which improves the quality of MS/MS spectra. In addition, absolute quantification of selected proteins has been performed.⁹³

Yates, Wolters, and Washburn^{94, 95} also devised very significant technology, an automated technique called multidimensional protein identification technology (MudPIT). This method allows the analysis of complex protein samples on a large scale, although the original protein mixture might be simplified by fractionation before the different fractions are digested and analyzed. Peptides are separated by strong cation exchange chromatography (SCX) and RP-HPLC on the same column and directly analyzed with ESI-MS/MS. The mass spectra are submitted to database searching using the SEQUEST algorithm. Differential elution of peptides is achieved by cycling SCX- and RP-specific gradient solvents through the system, and the technology is fully automated once sample is loaded onto the column.

With this technology, 1,484 proteins were identified from *S. cerevisiae*, and proteins were identified that are usually missed by 2DE. For example, membrane proteins, very high (>180 kDa) and low (<10 kDa) molecular weight proteins, and proteins with pIs higher than 10 and lower than 4 were detected and identified.

Since its inception, Yates and co-workers have demonstrated that MudPIT can be used in quantification studies involving ¹⁴N/¹⁵N metabolic labeling of *S. cerevisiae*,^{96, 97} and that post-translational modifications can be identified.⁹⁸ The latter publication was significant in that it showed for the first time that multiple types of PTMs can be identified using bottom-up analysis without initially selecting for the specific PTMs. The authors digested three fractions of samples with three different enzymes whose site-specificity for protein cleavage varied. This led to peptides whose sequences overlapped, which increased the sequence coverage of the proteins, but also allowed PTMs to be detected based on the different peptides. The PTMs were identified by letting the search

algorithm probe the protein database multiple times, each time allowing for a different PTM mass difference.

Last, Smith *et al.* have reported a high throughput and quantitative protein identification strategy, termed accurate mass tag (AMT) strategy, that uses 1D capillary LC and on-line FTICR-MS.⁹⁹ In their approach, a library of m/z values is established that presumably correlates exactly one peptide with one m/z value (to within 1 ppm mass measurement accuracy) and with an approximate LC elution time (to within 20% at the time of publication).

The library can be created by initially using LC-ion trap (IT)-MS/MS or LC-FTICR-MS/MS and database searching to obtain peptide masses and identifications. These preliminary peptide identity- m/z correlations are taken up into the library only if a subsequent LC-FTICR-MS experiment can match the m/z values and LC elution times to within 1 ppm and 20%, respectively.

Once such a library exists for a particular organism, experiments using only MS, not MS/MS, would need to be carried out to identify peptides based on the very accurate masses obtainable with FTICR-MS. The time that would be saved by not having to run MS/MS scans could be used to identify very low-abundant peptides, and therefore proteins. Stable isotope labeling techniques afford quantification of differentially expressed proteins from differentially treated populations of organisms. Using AMTs, Smith *et al.* were able to identify ~ 61% of the predicted *Deinococcus radiodurans* proteome.¹⁰⁰

1.IV. Capillary Electrophoresis Coupled to Mass Spectrometry

In light of the advances in protein and peptide analysis discussed so far, CE-MS is a complementary technique to HPLC. As Wittke *et al.*¹⁰¹ point out, CE-MS has attributes of automation, high sensitivity, low cost, low sample consumption, and speed. In addition, multi-dimensional systems using CE have been devised, see section 1.II.B.. CE-MS, however, still needs to gain maturity when compared with HPLC-MS.

The following sections cover mostly CE-MS instrumentation that is coupled via electrospray ionization (ESI), since ESI is more commonly used than matrix assisted laser desorption/ionization (MALDI) and MALDI is mostly an off-line technique. First, the various interfaces for CE-ESI-MS are described. Second, examples of research are given that use various CE modes for CE-MS, with CZE by far outweighing other modes.

1.IV.A. CE-MS Interfaces

The earliest on-line CE-ESI-MS experiments were reported by Smith *et al.* in the late 1980's.^{15, 102} Various interfaces for CE-ESI-MS have been devised since then, and these can be categorized into sheath flow, sheathless-flow (or simply sheathless), and liquid junction designs.¹⁰³ The latter is sometimes considered a type of sheath flow design.¹⁰⁴ In CE-ESI-MS, unlike in LC-ESI-MS, electrical contact with the liquid at the interface not only serves to establish the potential difference between the ESI emitter and the mass spectrometer inlet, but it also serves to complete the CE circuit. This requirement has been a major consideration in the design of CE-MS interfaces.

In sheath flow interfaces, the separation capillary is positioned concentrically inside a spray needle and the capillary effluent mixes with the sheath liquid before being sprayed into the MS. The CE circuit is established through the sheath liquid by, for example, using a metal spray needle¹⁰² or by inserting a metal wire between a non-conducting needle and the capillary.¹⁰⁵

The sensitivity obtained with sheath flow interfaces is somewhat decreased compared to sheathless interfaces because of the extra volume of the sheath liquid. But the sheath liquid can be beneficial. To achieve a stable spray, the fluids should be volatile and should be acidic if the positive ion mode of the MS is used; if an optimized separation buffer lacks these characteristics, they can be added *via* the sheath liquid. The sheath liquid therefore allows more flexibility in the composition of the separation buffer,¹⁰² which can be important if a good separation of a complex analyte mixture is to be achieved.

The electrosprays obtained with sheath flow interfaces are also more robust than with sheathless ones.^{106, 107} Sheathless interfaces depend on the electroosmotic flow (EOF) of the CE separation, which usually is in the nL/min range. If the EOF is not fast enough, the spray may not be stable and continuous. The flow rate of a sheath liquid, however, can be easily adjusted to obtain a stable spray. Another consideration is that coated capillaries are desirable to reduce analyte-wall interactions, as was covered in section 1.II.A.1.. Many coatings reduce the EOF, which is detrimental for sheathless interface use, but not a problem for sheath flow configurations.¹⁰⁸

For most of the work of this thesis project, a sheath flow interface was used whose design was based on a former group member's^{109, 110} and other authors' designs.^{55,}

¹⁰⁵ This sheath flow interface was found to be more easily used than a sheathless interface that was initially tried.

Many different sheathless-flow designs have been reported. The introduction of micro-¹¹¹ and nanospray¹¹² sheathless configurations (initially for LC-MS) has increased CE-MS sensitivities because smaller spray needle orifices produce smaller fluid droplets than do larger orifices. Smaller droplets allow more efficient solvent evaporation and more efficient analyte ionization; hence the increased sensitivity.

Some sheathless designs use the end of the separation capillary directly as the spray needle for ESI. The electrical contact to complete the CE circuit is made by either coating the capillary end with a metal¹¹³ or by inserting a wire into the capillary end.¹¹⁴ In one design, a small hole drilled near the capillary end allows a small amount of buffer to escape and make contact with an external electrode.¹¹⁵

Other sheathless designs attach short electrospray needles to the separation capillaries. Electrical contact is made either by using needles made of metal,¹¹⁶ conductively coating the needle tips,^{113, 117, 118} or by placing a metal wire close to the gap between the needle and the capillary. The latter design has been used in some of my work.

As mentioned above, greater sensitivities can be achieved with sheathless than with sheath flow interfaces. But the buffer choices are limited for sheathless interfaces, and this can limit the separation quality. On the one hand, the buffer should be volatile to be easily sprayed, which can be accomplished by adding methanol, for instance. On the other hand, methanol usually degrades separation efficiency and slows the EOF. A stable spray may not be obtained if the EOF rate is not high enough.

Other aspects can make sheathless interfaces less robust than sheath flow interfaces. For example, the metal coating on capillary ends easily flakes off due to the applied electrospray voltage, and bubbles are often observed due to electrolysis at an inserted electrode, causing the electrospray to become unstable or disturbing the separation in the capillary.^{103, 104}

The third interface type is the liquid junction. Interfaces of this type have the separation capillaries and ESI emitters separated by a gap that is surrounded by liquid having a similar or a different composition than the separation buffer. In both cases, the electrode to complete the CE circuit is positioned in the liquid surrounding the gap, which usually avoids bubbles inside the gap. The surrounding liquid can serve to modify the separation capillary effluent to obtain a more stable ESI spray and enhance the ion formation of analytes, as is found with sheath flow configurations.¹¹⁹⁻¹²¹

1.IV.B. Protein and Peptide Analysis by CE-MS

Much research in CE-MS has used CZE because of its simplicity and compatibility with MS, but CIEF-MS and CEC-MS have also been reported. Early work that focused on interface design was done with protein and peptide standards. Recently, more complex samples have been analyzed.

Wittke *et al.*¹²² used sheath flow CZE-TOF-MS for comparing the peptide and protein contents in urine from healthy persons and persons having kidney disease. Differences were observed on contour plots of polypeptide molecular weight vs. migration time, and 27 unique polypeptides were found in samples from patients. The authors pointed out that uncoated capillaries yielded better reproducibilities than coated

capillaries for these complex samples even though polypeptide adsorption occurred. The capillaries were cleaned with NaOH between experiments.

Demelbauer *et al.*¹²³ established preliminary carbohydrate structures of different glycoprotein (antithrombin) isoforms using sheath flow CZE-ion trap-MS of the whole proteins. Moini and Huang¹²⁴ used sheathless CZE-ion trap-MS to detect potential methylation and acetylation PTMs of proteins from fractions of *E. coli* lysates.

As mentioned in section 1.III.B. on top-down analysis, CIEF has been coupled to MS by Smith and co-workers. Recently, Storms *et al.*^{39, 125} also reported CIEF-MS for analyzing *E. coli* proteins. A low concentration (0.20%) of carrier ampholytes was used to avoid contamination of the MS yet still obtain reliable CIEF results. Protein pI information from the CIEF separation facilitated the protein identification with SEQUEST.

Sheathless CEC-MS was used by Guček *et al.*¹²⁶ for the analysis of a standard peptide mixture. Wu *et al.*¹²⁷ used open tubular (OT)-CEC-MS to separate and identify peptide standards and peptides from a horse-heart myoglobin tryptic digest.

1.V. Immobilized Enzyme Microreactors

Enzymatic digestion of protein samples is conventionally done in bulk solution for up to 24 hours. The protein-to-enzyme ratio is quite high, for example between 20:1 to 100:1 for trypsin,¹²⁸ to avoid excessive auto-digestion of the enzyme. In 1989, Cobb and Novotny¹²⁹ published an early report that used an immobilized enzyme inside of small tubing for the digestion of proteins. They recognized that using immobilized enzymes had several advantages. First, the enzymes undergo minimal autodigestion

because they are immobilized, and this avoids contamination of the sample by enzyme autodigestion products. Second, enzymatic microreactors can be used repeatedly, which is not possible in bulk-solution digestions. Last, very small amounts of proteins can be digested because of the small sizes of the reactors (even though Cobb's and Novotny's reactor was still relatively large with the dimensions of the Pyrex tubing having been 30 cm x 1 mm ID). Their microreactor consisted of trypsin immobilized on an agarose gel, with which the Pyrex tubing was filled. β -casein was flushed through the column and the digest was collected and further analyzed with HPLC or CE, both with UV detection. As little as 50 ng of protein was needed for the digestion.

Since that publication, different types of microreactors have been developed based on different immobilization supports. The types include open tubular, particle-based, membrane, and monolithic microreactors.

1.V.A. Open Tubular Microreactors

Other early work with immobilized enzymes in microreactors was done by Kuhr and co-workers.¹³⁰⁻¹³⁴ They immobilized trypsin *via* a biotin-avidin-biotin linker on the wall of a 50 μ m ID capillary. β -casein was flushed through the capillary and was completely digested within a 25 min residence time. Initially,¹³⁰ the protein digest effluent was collected and then off-line analyzed with CE and fluorescence detection. Later,¹³¹ they devised an on-line microreactor-CE separation system by coupling the microreactor to a separation capillary *via* a fluid joint. Protein was loaded onto the microreactor capillary, and after \sim 2 hours of undisturbed digestion time, a plug of the

digest was electrokinetically injected into the separation capillary and the peptides were separated. The system was extended to use other enzymes, including pepsin,¹³² and was also coupled on-line *via* a sheath flow interface to ESI-MS.¹³³ Licklider and Kuhr¹³⁴ also studied the reaction dynamics in their microreactor by vibrating it on a piezoelectric surface.

Amankwa *et al.*¹³⁵ performed on-line microreactor-CE-MS similarly to Licklider's and Kuhr's method. The formers' microreactor contained immobilized human protein tyrosine phosphatase, with which phosphate was cleaved off a phosphopeptide. Instead of a fluid joint, they used a Teflon sleeve to connect the microreactor and separation capillary.

Recently, Guo *et al.*¹³⁶ achieved trypsin immobilization in an open tubular microreactor *via* a metal-ion chelator, iminodiacetic acid (IDA). No separation of the digestion products of a cytochrome *C* sample was performed, but the peptides were directly analyzed with MALDI-MS. The enzyme could be easily stripped with EDTA after 4-6 digestion experiments, and then the microreactor could be regenerated with fresh enzyme.

A trypsin microreactor incorporated into a poly(dimethylsiloxane) (PDMS) microfluidic chip was reported by Wu *et al.*¹³⁷ The authors joined a separation channel with stainless steel tubing and a tapered fused silica capillary tip to perform ESI-MS of cytochrome *C* and bovine serum albumin digests. The microreactor could be used for one week without a noticeable decrease in enzyme activity.

1.V.B. Particle-based Microreactors

Compared to open tubular microreactors, particle-based, membrane, and monolithic reactors have greater surface-to-volume ratios, and hence often provide more efficient digestions. For example, Rashkovetsky *et al.*¹³⁸ used magnetic beads as substrates for alkaline phosphatase immobilization. The magnetic beads were held stationary in 2-3 mm of a capillary by a magnet positioned next to the capillary. A new plug of beads could be used for each experiment.

Bonneil *et al.*¹³⁹ packed 530 μm ID capillaries with controlled pore glass beads onto which trypsin had been immobilized. Insulin chain B and β -casein were flushed through the microreactors and the effluents were off-line injected onto a CE-UV system. The performance and reproducibility of the microreactors were studied when changing the flow rate and the concentration of the protein solutions.

Slysz and Schriemer¹⁴⁰ digested myoglobin and human transferrin, the latter of which is relatively resistant to digestion, in a 150 μm ID capillary filled with commercially available POROSzyme immobilized trypsin beads. The protein samples that were flushed through the capillary partially contained organic solvents such as acetonitrile or methanol, and these were found to increase digestion efficiencies. Digestions were performed in seconds to minutes, and the digests were analyzed with MALDI-MS. In later work,¹⁴¹ the same authors developed on-line HPLC-microreactor-ESI-MS instrumentation using the same microreactor technology as before.

1.V.C. Membrane Microreactors

Other alternative substrates for immobilizing enzymes are membranes. Jiang *et al.*¹⁴² employed a cellulose membrane with immobilized trypsin when they presented a novel method, high performance frontal analysis, for analyzing the reaction kinetics and activity of an immobilized enzyme. Their type of frontal analysis not only measured the interactions of biomolecules, but also the conversion rate of one molecule by the other. The relative activity of immobilized trypsin was shown to be 55.6% of bulk-solution trypsin, but the apparent Michaelis-Menten constant (K_m) was lower than the one for bulk-solution trypsin.

Cooper *et al.*¹⁴³ sandwiched a trypsin-immobilized polyvinylidene fluoride (PVDF) membrane inside a zero dead volume union. A micro sample injector valve was used to inject microreactor effluent on-line onto either an RP-HPLC-ESI-MS or a transient ITP/CZE-ESI-MS systems. Cytochrome *C* and ovalbumin were separately digested within 30 sec to 5 min.

1.V.D. Monolithic Column Microreactors

As already mentioned when covering capillary electrochromatography (CEC) in section 1.II.A.5., monolithic stationary phases are convenient because they do not require the use of frits since the polymer is covalently bound to the capillary. Also, monoliths with different porosities can be prepared by changing the monomer reaction solution composition. The preparation of monolithic microreactors can be time-consuming, however. Numerous different polymers have been used as monoliths.

Zou and co-workers¹⁴⁴ prepared a poly(glycidyl methacrylate-co-ethylene dimethacrylate) monolith and immobilized papain. Two reaction schemes were used, one of which allowed more steric freedom of the papain by using an 11 carbon atom spacer between the papain and the monolithic support. The sterically less hindered enzyme was more effective at digesting human IgG protein.

Fréchet and co-workers¹⁴⁵ fabricated microchips that incorporated monoliths of various polymers. Producing monoliths in microchip channels was more facile than, for example, trying to pack particles into the channels. The digestion efficiencies when digesting myoglobin and casein were probed with MALDI-TOF-MS and fluorescence detection, and digestions lasting only seconds were accomplished.

Sakai-Kato *et al.*¹⁴⁶ developed a monolithic microreactor based on the sol-gel method, in which trypsin could be encapsulated inside the sol-gel matrix. In their initial publication, microreactor digestions were restricted to proteins that could fit through the pores that contained the encapsulated trypsin. This problem was later solved¹⁴⁷ by first preparing a methacryloxypropyltrimethoxysilane (MPTMS) monolith with relatively large through-pores, and then coating the monolith surface with a sol-gel that contained the enzyme pepsin. Only the inlet end of a capillary was modified with the monolith, and the rest of the capillary was used for separation of the digests of lysozyme and insulin. This system was on-line connected to ESI-MS. Pepsin was used because it is active at low pHs. Low pH buffers, in turn, enhance analyte protonation in the ESI process.

Our group recently reported the use of a trypsin-immobilized monolithic microreactor made from poly(glycidyl methacrylate-co-ethylene dimethacrylate).¹⁴⁸ Digests of α -lactalbumin, β -casein, and cytochrome *C* were analyzed both off-line and

on-line with CZE and laser induced fluorescence (LIF) detection. The digest was post-column labeled with the dye naphthalene-2,3-dicarbaldehyde (NDA). For on-line experiments, a short (2 cm, 50 μm ID) piece of fused silica capillary that contained the monolith was coupled to a 40 cm, 50 μm ID separation capillary *via* a liquid junction interface. Digestions could be as short as 9 sec, and experiments could be completed in ~ 16 min from digestion to detection.

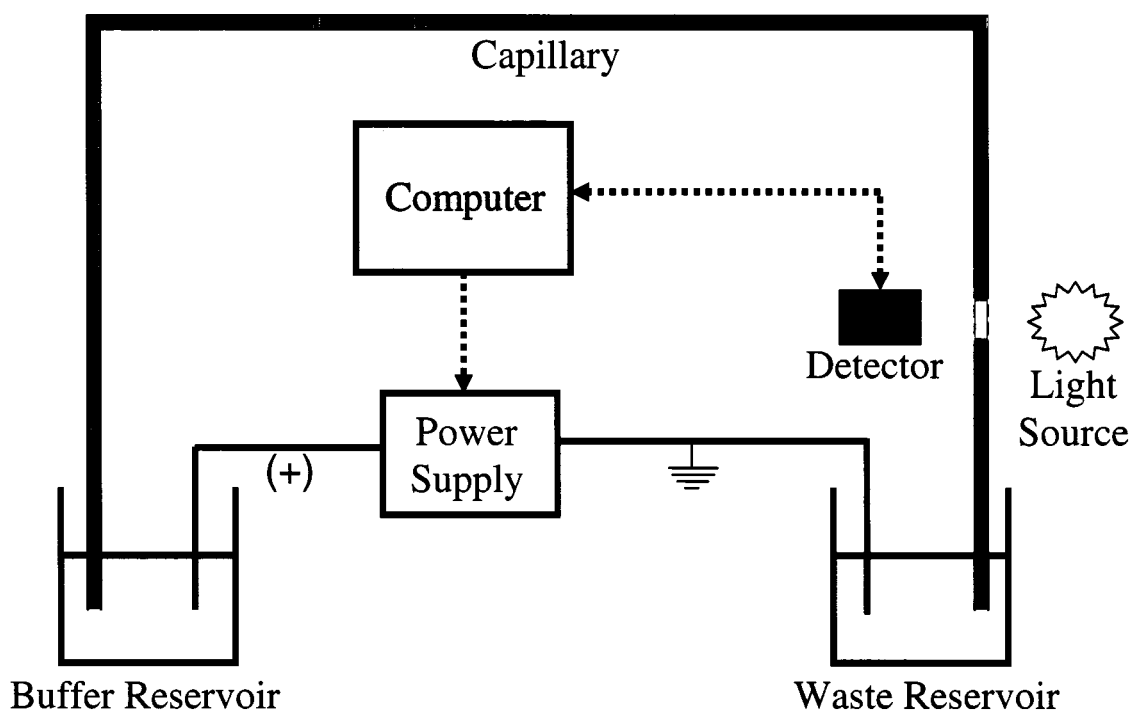


Figure 1-1. Basic CE instrumentation.

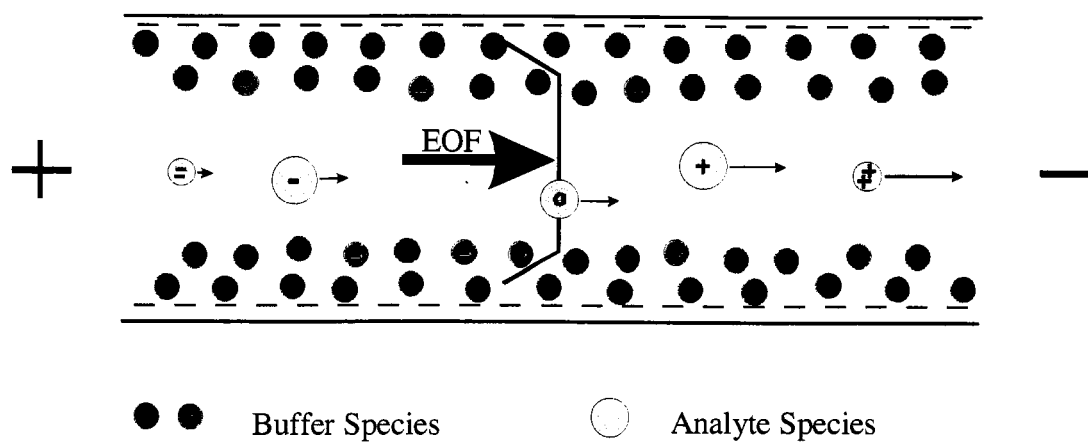


Figure 1-2. Illustration of the electroosmotic flow (EOF) in capillary electrophoresis. Negatively and positively charged analytes, along with neutral analytes, migrate toward the cathode if the EOF is large enough.

1.VI. Notes to Chapter 1

- (1) Lander, E. S.; Linton, L. M.; Birren, B.; Nusbaum, C.; Zody, M. C.; Baldwin, J.; Devon, K.; Dewar, K.; Doyle, M.; FitzHugh, W.; Funke, R.; Gage, D.; Harris, K.; Heaford, A.; Howland, J.; Kann, L.; Lehoczky, J.; LeVine, R.; McEwan, P.; McKernan, K.; Meldrim, J.; Mesirov, J. P.; Miranda, C.; Morris, W.; Naylor, J.; Raymond, C.; Rosetti, M.; Santos, R.; Sheridan, A.; Sougnez, C.; Stange-Thomann, N.; Stojanovic, N.; Subramanian, A.; Wyman, D.; Rogers, J.; Sulston, J.; Ainscough, R.; Beck, S.; Bentley, D.; Burton, J.; Clee, C.; Carter, N.; Coulson, A.; Deadman, R.; Deloukas, P.; Dunham, A.; Dunham, I.; Durbin, R.; French, L.; Grafham, D.; Gregory, S.; Hubbard, T.; Humphray, S.; Hunt, A.; Jones, M.; Lloyd, C.; McMurray, A.; Matthews, L.; Mercer, S.; Milne, S.; Mullikin, J. C.; Mungall, A.; Plumb, R.; Ross, M.; Shownkeen, R.; Sims, S.; Waterston, R. H.; Wilson, R. K.; Hillier, L. W.; McPherson, J. D.; Marra, M. A.; Mardis, E. R.; Fulton, L. A.; Chinwalla, A. T.; Pepin, K. H.; Gish, W. R.; Chissoe, S. L.; Wendl, M. C.; Delehaunty, K. D.; Miner, T. L.; Delehaunty, A.; Kramer, J. B.; Cook, L. L.; Fulton, R. S.; Johnson, D. L.; Minx, P. J.; Clifton, S. W.; Hawkins, T.; Branscomb, E.; Predki, P.; Richardson, P.; Wenning, S.; Slezak, T.; Doggett, N.; Cheng, J. F.; Olsen, A.; Lucas, S.; Elkin, C.; Uberbacher, E.; Frazier, M.; Gibbs, R. A.; Muzny, D. M.; Scherer, S. E.; Bouck, J. B.; Sodergren, E. J.; Worley, K. C.; Rives, C. M.; Gorrell, J. H.; Metzker, M. L.; Naylor, S. L.; Kucherlapati, R. S.; Nelson, D. L.; Weinstock, G. M.; Sakaki, Y.; Fujiyama, A.; Hattori, M.; Yada, T.; Toyoda, A.; Itoh, T.; Kawagoe, C.; Watanabe, H.; Totoki, Y.; Taylor, T.; Weissenbach, J.; Heilig, R.; Saurin, W.; Artiguenave, F.; Brottier, P.; Bruls, T.; Pelletier, E.; Robert, C.; Wincker, P.; Smith, D. R.; Doucette-Stamm, L.; Rubenfield, M.; Weinstock, K.; Lee, H. M.; Dubois, J.; Rosenthal, A.; Platzer, M.; Nyakatura, G.; Taudien, S.; Rump, A.; Yang, H.; Yu, J.; Wang, J.; Huang, G.; Gu, J.; Hood, L.; Rowen, L.; Madan, A.; Qin, S.; Davis, R. W.; Federspiel, N. A.; Abola, A. P.; Proctor, M. J.; Myers, R. M.; Schmutz, J.; Dickson, M.; Grimwood, J.; Cox, D. R.; Olson, M. V.; Kaul, R.; Shimizu, N.; Kawasaki, K.; Minoshima, S.; Evans, G. A.; Athanasiou, M.; Schultz, R.; Roe, B. A.; Chen, F.; Pan, H.; Ramser, J.; Lehrach, H.; Reinhardt, R.; McCombie, W. R.; de la Bastide, M.; Dedhia, N.; Blocker, H.; Hornischer, K.; Nordsiek, G.; Agarwala, R.; Aravind, L.; Bailey, J. A.; Bateman, A.; Batzoglou, S.; Birney, E.; Bork, P.; Brown, D. G.; Burge, C. B.; Cerutti, L.; Chen, H. C.; Church, D.; Clamp, M.; Copley, R. R.; Doerks, T.; Eddy, S. R.; Eichler, E. E.; Furey, T. S.; Galagan, J.; Gilbert, J. G.; Harmon, C.; Hayashizaki, Y.; Haussler, D.; Hermjakob, H.; Hokamp, K.; Jang, W.; Johnson, L. S.; Jones, T. A.; Kasif, S.; Kasprzyk, A.; Kennedy, S.; Kent, W. J.; Kitts, P.; Koonin, E. V.; Korf, I.; Kulp, D.; Lancet, D.; Lowe, T. M.; McLysaght, A.; Mikkelsen, T.; Moran, J. V.; Mulder, N.; Pollara, V. J.; Ponting, C. P.; Schuler, G.; Schultz, J.; Slater, G.; Smit, A. F.; Stupka, E.; Szustakowski, J.; Thierry-Mieg, D.; Thierry-Mieg, J.; Wagner, L.; Wallis, J.; Wheeler, R.; Williams, A.; Wolf, Y. I.; Wolfe, K. H.; Yang, S. P.; Yeh, R. F.; Collins, F.; Guyer, M. S.; Peterson, J.; Felsenfeld, A.; Wetterstrand, K. A.; Patrinos, A.;

Morgan, M. J.; de Jong, P.; Catanese, J. J.; Osoegawa, K.; Shizuya, H.; Choi, S.; Chen, Y. J. *Nature* **2001**, *409*, 860-921.

- (2) Venter, J. C.; Adams, M. D.; Myers, E. W.; Li, P. W.; Mural, R. J.; Sutton, G. G.; Smith, H. O.; Yandell, M.; Evans, C. A.; Holt, R. A.; Gocayne, J. D.; Amanatides, P.; Ballew, R. M.; Huson, D. H.; Wortman, J. R.; Zhang, Q.; Kodira, C. D.; Zheng, X. H.; Chen, L.; Skupski, M.; Subramanian, G.; Thomas, P. D.; Zhang, J.; Gabor Miklos, G. L.; Nelson, C.; Broder, S.; Clark, A. G.; Nadeau, J.; McKusick, V. A.; Zinder, N.; Levine, A. J.; Roberts, R. J.; Simon, M.; Slayman, C.; Hunkapiller, M.; Bolanos, R.; Delcher, A.; Dew, I.; Fasulo, D.; Flanigan, M.; Florea, L.; Halpern, A.; Hannenhalli, S.; Kravitz, S.; Levy, S.; Mobarry, C.; Reinert, K.; Remington, K.; Abu-Threideh, J.; Beasley, E.; Biddick, K.; Bonazzi, V.; Brandon, R.; Cargill, M.; Chandramouliswaran, I.; Charlab, R.; Chaturvedi, K.; Deng, Z.; Di Francesco, V.; Dunn, P.; Eilbeck, K.; Evangelista, C.; Gabrielian, A. E.; Gan, W.; Ge, W.; Gong, F.; Gu, Z.; Guan, P.; Heiman, T. J.; Higgins, M. E.; Ji, R. R.; Ke, Z.; Ketchum, K. A.; Lai, Z.; Lei, Y.; Li, Z.; Li, J.; Liang, Y.; Lin, X.; Lu, F.; Merkulov, G. V.; Milshina, N.; Moore, H. M.; Naik, A. K.; Narayan, V. A.; Neelam, B.; Nusskern, D.; Rusch, D. B.; Salzberg, S.; Shao, W.; Shue, B.; Sun, J.; Wang, Z.; Wang, A.; Wang, X.; Wang, J.; Wei, M.; Wides, R.; Xiao, C.; Yan, C.; Yao, A.; Ye, J.; Zhan, M.; Zhang, W.; Zhang, H.; Zhao, Q.; Zheng, L.; Zhong, F.; Zhong, W.; Zhu, S.; Zhao, S.; Gilbert, D.; Baumhueter, S.; Spier, G.; Carter, C.; Cravchik, A.; Woodage, T.; Ali, F.; An, H.; Awe, A.; Baldwin, D.; Baden, H.; Barnstead, M.; Barrow, I.; Beeson, K.; Busam, D.; Carver, A.; Center, A.; Cheng, M. L.; Curry, L.; Danaher, S.; Davenport, L.; Desilets, R.; Dietz, S.; Dodson, K.; Doup, L.; Ferriera, S.; Garg, N.; Gluecksmann, A.; Hart, B.; Haynes, J.; Haynes, C.; Heiner, C.; Hladun, S.; Hostin, D.; Houck, J.; Howland, T.; Ibegwam, C.; Johnson, J.; Kalush, F.; Kline, L.; Koduru, S.; Love, A.; Mann, F.; May, D.; McCawley, S.; McIntosh, T.; McMullen, I.; Moy, M.; Moy, L.; Murphy, B.; Nelson, K.; Pfannkoch, C.; Pratt, E.; Puri, V.; Qureshi, H.; Reardon, M.; Rodriguez, R.; Rogers, Y. H.; Romblad, D.; Ruhfel, B.; Scott, R.; Sitter, C.; Smallwood, M.; Stewart, E.; Strong, R.; Suh, E.; Thomas, R.; Tint, N. N.; Tse, S.; Vech, C.; Wang, G.; Wetter, J.; Williams, S.; Williams, M.; Windsor, S.; Winn-Deen, E.; Wolfe, K.; Zaveri, J.; Zaveri, K.; Abril, J. F.; Guigo, R.; Campbell, M. J.; Sjolander, K. V.; Karlak, B.; Kejariwal, A.; Mi, H.; Lazareva, B.; Hatton, T.; Narechania, A.; Diemer, K.; Muruganujan, A.; Guo, N.; Sato, S.; Bafna, V.; Istrail, S.; Lippert, R.; Schwartz, R.; Walenz, B.; Yooseph, S.; Allen, D.; Basu, A.; Baxendale, J.; Blick, L.; Caminha, M.; Carnes-Stine, J.; Caulk, P.; Chiang, Y. H.; Coyne, M.; Dahlke, C.; Mays, A.; Dombroski, M.; Donnelly, M.; Ely, D.; Esparham, S.; Fosler, C.; Gire, H.; Glanowski, S.; Glasser, K.; Glodek, A.; Gorokhov, M.; Graham, K.; Gropman, B.; Harris, M.; Heil, J.; Henderson, S.; Hoover, J.; Jennings, D.; Jordan, C.; Jordan, J.; Kasha, J.; Kagan, L.; Kraft, C.; Levitsky, A.; Lewis, M.; Liu, X.; Lopez, J.; Ma, D.; Majoros, W.; McDaniel, J.; Murphy, S.; Newman, M.; Nguyen, T.; Nguyen, N.; Nodell, M.; Pan, S.; Peck, J.; Peterson, M.; Rowe, W.; Sanders, R.; Scott, J.; Simpson, M.; Smith, T.; Sprague, A.; Stockwell, T.; Turner, R.; Venter, E.;

- Wang, M.; Wen, M.; Wu, D.; Wu, M.; Xia, A.; Zandieh, A.; Zhu, X. *Science* **2001**, *291*, 1304-1351.
- (3) Gygi, S. P.; Rochon, Y.; Franza, B. R.; Aebersold, R. *Mol Cell Biol* **1999**, *19*, 1720-1730.
 - (4) Klose, J.; Kobalz, U. *Electrophoresis* **1995**, *16*, 1034-1059.
 - (5) Link, A. J. *Trends Biotechnol* **2002**, *20*, S8-13.
 - (6) Rabilloud, T. *Proteomics* **2002**, *2*, 3-10.
 - (7) Gygi, S. P.; Rist, B.; Gerber, S. A.; Turecek, F.; Gelb, M. H.; Aebersold, R. *Nat Biotechnol* **1999**, *17*, 994-999.
 - (8) Tiselius, A. *Trans Faraday Soc* **1937**, *33*, 524-531.
 - (9) Hjertén, S. *Chromatogr Rev* **1967**, *9*, 122-219.
 - (10) Virtanen, R. *Acta Polytechnica Scand* **1974**, *123*, 1-67.
 - (11) Mikkers, F. E. P.; Everaerts, F. M.; Verheggen, T. P. E. M. *J Chromatogr* **1979**, *169*, 11-20.
 - (12) Jorgenson, J. W.; Lukacs, K. D. *Anal Chem* **1981**, *53*, 1298-1302.
 - (13) Gassmann, E.; Kuo, J. E.; Zare, R. N. *Science* **1985**, *230*, 813-814.
 - (14) Cheng, Y. F.; Dovichi, N. J. *Science* **1988**, *242*, 562-564.
 - (15) Olivares, J. A.; Nguyen, N. T.; Yonker, C. R.; Smith, R. D. *Anal Chem* **1987**, *59*, 1230-1232.
 - (16) Terabe, S.; Otsuka, K.; Ichikawa, K.; Tsuchiya, A.; Ando, T. *Anal Chem*, **1984**, *56*, 111-113.
 - (17) Hjertén, S.; Zhu, M. D. *J Chromatogr* **1985**, *346*, 265-270.
 - (18) Bruin, G. J.; Huisden, R.; Kraak, J. C.; Poppe, H. *J Chromatogr* **1989**, *480*, 339-349.
 - (19) Knox, J. H.; Grant, I. H. *Chromatographia* **1991**, *32*, 317-328.
 - (20) Oda, R. P.; Landers, J. P. In *Handbook of Capillary Electrophoresis*, Second ed.; Landers, J. P., Ed.; CRC Press: Boca Raton, 1997, pp 1-47.

- (21) Heiger, D. *High Performance Capillary Electrophoresis, An Introduction*; Agilent Technologies: Germany, 2000.
- (22) Smith, R. D.; Olivares, J. A.; Nguyen, N. T.; Udseth, H. R. *Anal Chem* **1988**, *60*, 436-441.
- (23) Nielsen, R. G.; Sittampalam, G. S.; Rickard, E. C. *Anal Biochem* **1989**, *177*, 20-26.
- (24) Bushey, M. M.; Jorgenson, J. W. *J Chromatogr* **1989**, *480*, 301-310.
- (25) Landers, J. P. *Handbook of Capillary Electrophoresis*, 2nd ed.; CRC Press: Boca Raton, 1997.
- (26) Hu, S.; Dovichi, N. J. *Anal Chem* **2002**, *74*, 2833-2850.
- (27) Quigley, W. W.; Dovichi, N. J. *Anal Chem* **2004**, *76*, 4645-4658.
- (28) Dougherty, A. M.; Cooke, N.; Shieh, P. In *Handbook of Capillary Electrophoresis*, Second ed.; Landers, J. P., Ed.; CRC Press: Boca Raton, 1997, pp 675-715.
- (29) Hernández-Borges, J.; Neustüß, C.; Cifuentes, A.; Pelzing, M. *Electrophoresis* **2004**, *25*, 2257-2281.
- (30) Belder, D.; Deege, A.; Husmann, H.; Koehler, F.; Ludwig, M. *Electrophoresis* **2001**, *22*, 3813-3818.
- (31) Wei, W.; Ju, H. *Electrophoresis* **2005**, *26*, 586-592.
- (32) Chang, W. W.; Hobson, C.; Bomberger, D. C.; Schneider, L. V. *Electrophoresis* **2005**, *26*, 2179-2186.
- (33) Terabe, S.; Otsuka, K.; Ando, T. *Anal Chem* **1985**, *57*, 834-841.
- (34) Beattie, J. H.; Richards, M. P. *J Chromatogr* **1994**, *664*, 129-134.
- (35) Liu, J.; Cobb, K. A.; Novotny, M. *J Chromatogr* **1990**, *519*, 189-197.
- (36) Swedberg, S. A. *J Chromatogr* **1993**, *503*, 449-452.
- (37) Popa, T. V.; Mant, C. T.; Hodges, R. S. *Electrophoresis* **2004**, *25*, 94-107.

- (38) Rodríguez-Díaz, R.; Wehr, T.; Zhu, M.; Levi, V. In *Handbook of Capillary Electrophoresis*, Second ed.; Landers, J. P., Ed.; CRC Press: Boca Raton, 1997, pp 101-138.
- (39) Storms, H. F.; van der Heijden, R.; Tjaden, U. R.; van der Greef, J. *Electrophoresis* **2004**, *25*, 3461-3467.
- (40) Shen, Y.; Smith, R. D. *Electrophoresis* **2002**, *23*, 3106-3124.
- (41) Kasicka, V. *Electrophoresis* **1999**, *20*, 3084-3105.
- (42) Shen, Y.; Berger, S. J.; Anderson, G. A.; Smith, R. D. *Anal Chem* **2000**, *72*, 2154-2159.
- (43) Hjertén, S. *J Chromatogr* **1983**, *270*, 1-6.
- (44) Cohen, A. S.; Karger, B. L. *J Chromatogr* **1987**, *397*, 409-417.
- (45) Lu, J. J.; Liu, S.; Pu, Q. *J Proteome Res* **2005**, *4*, 1012-1016.
- (46) Guttman, A. *LCGC North America* **2004**, *22*, 896-904.
- (47) Dittman, M. M.; Rozing, G. P. In *Handbook of Capillary Electrophoresis*, Second ed.; Landers, J. P., Ed.; CRC Press: Boca Raton, 1997, pp 139-153.
- (48) Zou, H.; Huang, X.; Ye, M.; Luo, Q. *J Chromatogr A* **2002**, *954*, 5-32.
- (49) Hilder, E. F.; Svec, F.; Frechet, J. M. *Anal Chem* **2004**, *76*, 3887-3892.
- (50) Okanda, F. M.; El Rassi, Z. *Electrophoresis* **2005**, *26*, 1988-1995.
- (51) Pesek, J. J.; Matyska, M. T.; Dawson, G. B.; Chen, J. I.; Boysen, R. I.; Hearn, M. T. *Anal Chem* **2004**, *76*, 23-30.
- (52) Giddings, J. C. *Unified Separation Science*; Wiley Interscience: New York, 1991.
- (53) Bushey, M. M.; Jorgenson, J. W. *Anal Chem* **1990**, *62*, 161-167.
- (54) Bushey, M. M.; Jorgenson, J. W. *Anal Chem* **1990**, *62*, 978-984.
- (55) Lewis, K. C.; Opiteck, G. J.; Jorgenson, J. W.; Sheeley, D. M. *J Am Soc Mass Spectrom* **1997**, *8*, 495-500.
- (56) Chen, J.; Lee, C. S.; Shen, Y.; Smith, R. D.; Baehrecke, E. H. *Electrophoresis* **2002**, *23*, 3143-3148.

- (57) Zhou, F.; Johnston, M. V. *Anal Chem* **2004**, *76*, 2734-2740.
- (58) Zhou, F.; Johnston Murray, V. *Electrophoresis* **2005**, *26*, 1383-1388.
- (59) Zhang, J.; Hu, H.; Gao, M.; Yang, P.; Zhang, X. *Electrophoresis* **2004**, *25*, 2374-2383.
- (60) Rocklin, R. D.; Ramsey, R. S.; Ramsey, J. M. *Anal Chem* **2000**, *72*, 5244-5249.
- (61) Ramsey, J. D.; Jacobson, S. C.; Culbertson, C. T.; Ramsey, J. M. *Anal Chem* **2003**, *75*, 3758-3764.
- (62) Mohan, D.; Lee, C. S. *Electrophoresis* **2002**, *23*, 3160-3167.
- (63) Burgi, D. S.; Chien, R.-L. In *Handbook of Capillary Electrophoresis*, Second ed.; Landers, J. P., Ed.; CRC Press: Boca Raton, 1997, pp 479-493.
- (64) Yang, C.; Liu, H.; Yang, Q.; Zhang, L.; Zhang, W.; Zhang, Y. *Anal Chem* **2003**, *75*, 215-218.
- (65) Liu, H.; Yang, C.; Yang, Q.; Zhang, W.; Zhang, Y. *J Chromatogr B Analyt Technol Biomed Life Sci* **2005**, *817*, 119-126.
- (66) Liu, H.; Zhang, L.; Zhu, G.; Zhang, W.; Zhang, Y. *Anal Chem* **2004**, *76*, 6506-6512.
- (67) Michels, D. A.; Hu, S.; Schoenherr, R. M.; Eggertson, M. J.; Dovichi, N. J. *Mol Cell Proteomics* **2002**, *1*, 69-74.
- (68) Michels, D. A.; Hu, S.; Dambrowitz, K. A.; Eggertson, M. J.; Lauterbach, K.; Dovichi, N. J. *Electrophoresis* **2004**, *25*, 3098-3105.
- (69) Hu, S.; Michels, D. A.; Fazal, M. A.; Ratisoontorn, C.; Cunningham, M. L.; Dovichi, N. J. *Anal Chem* **2004**, *76*, 4044-4049.
- (70) Stroink, T.; Paarlberg, E.; Waterval, J. C. M.; Bult, A.; Underberg, W. J. M. *Electrophoresis* **2001**, *22*, 2374-2383.
- (71) Shihabi, Z. K. In *Handbook of Capillary Electrophoresis*, Second ed.; Landers, J. P., Ed.; CRC Press: Boca Raton, 1997, pp 457-477.
- (72) Pentoney, S. L., Jr.; Sweedler, J. V. In *Handbook of Capillary Electrophoresis*, Second ed.; Landers, J. P., Ed.; CRC Press: Boca Raton, 1997, pp 379-423.

- (73) Wu, C. H.; Scampavia, L.; Ruzicka, J. *Analyst* **2002**, *127*, 898-905.
- (74) Lee, Y.-H.; Maus, R. G.; Smith, B. W.; Winefordner, J. D. *Anal Chem* **1994**, *66*, 4142-4149.
- (75) Chen, D.; Dovichi, N. J. *Anal Chem* **1996**, *68*, 690-696.
- (76) van de Goor, T.; Apffel, A.; Chakel, J.; Hancock, W. In *Handbook of Capillary Electrophoresis*, Second ed.; Landers, J. P., Ed.; CRC Press: Boca Raton, 1997, pp 213-258.
- (77) Pinto, D.; Arriaga, E.; Craig, D.; Angelova, J.; Sharma, N.; Ahmadzadeh, H.; Dovichi, N. J. *Anal Chem* **1997**, *69*, 3015-3021.
- (78) Albin, M.; Weinberger, R.; Sapp, E.; Moring, S. *Anal Chem* **1991**, *63*, 417-422.
- (79) Beale, S. C.; Savage, J. C.; Wiesler, D.; Wietstock, S. M.; Novotny, M. *Anal Chem* **1988**, *60*, 1765-1769.
- (80) Hu, S.; Zhang, L.; Cook, L. M.; Dovichi, N. J. *Electrophoresis* **2001**, *22*, 3677-3682.
- (81) Wu, S.; Dovichi, N. J. *J Chromatogr* **1989**, *480*, 141-155.
- (82) Kelleher, N. L. *Anal Chem* **2004**, *76*, 197A-203A.
- (83) www-nbrf.Georgetown.edu/.
- (84) www.ebi.ac.uk/swissprot/.
- (85) fields.scripps.edu/sequest/index.html.
- (86) www.matrixscience.com.
- (87) Kinter, M.; Sherman, N. E. *Protein Sequencing and Identification Using Tandem Mass Spectrometry*; Wiley Interscience: New York, 2000.
- (88) Yates, J. R., 3rd *Electrophoresis* **1998**, *19*, 893-900.
- (89) Jensen, P. K.; Pasa-Tolic, L.; Anderson, G. A.; Horner, J. A.; Lipton, M. S.; Bruce, J. E.; Smith, R. D. *Anal Chem* **1999**, *71*, 2076-2084.
- (90) Meng, F.; Du, Y.; Miller, L. M.; Patrie, S. M.; Robinson, D. E.; Kelleher, N. L. *Anal Chem* **2004**, *76*, 2852-2858.

- (91) Flory, M. R.; Griffin, T. J.; Martin, D.; Aebersold, R. *Trends Biotechnol* **2002**, *20*, S23-29.
- (92) Yi, E. C.; Li, X. J.; Cooke, K.; Lee, H.; Raught, B.; Page, A.; Aneliunas, V.; Hieter, P.; Goodlett, D. R.; Aebersold, R. *Proteomics* **2005**, *5*, 380-387.
- (93) Lu, Y.; Bottari, P.; Tureček, F.; Aebersold, R.; Gelb, M. H. *Anal Chem* **2004**, *76*, 4104-4111.
- (94) Wolters, D. A.; Washburn, M. P.; Yates, J. R., 3rd *Anal Chem* **2001**, *73*, 5683-5690.
- (95) Washburn, M. P.; Wolters, D.; Yates, J. R., 3rd *Nat Biotechnol* **2001**, *19*, 242-247.
- (96) Washburn, M. P.; Ulaszek, R.; Deciu, C.; Schieltz, D. M.; Yates, J. R., 3rd *Anal Chem* **2002**, *74*, 1650-1657.
- (97) Washburn, M. P.; Ulaszek, R. R.; Yates, J. R., 3rd *Anal Chem* **2003**, *75*, 5054-5061.
- (98) MacCoss, M. J.; McDonald, W. H.; Saraf, A.; Sadygov, R.; Clark, J. M.; Tasto, J. J.; Gould, K. L.; Wolters, D.; Washburn, M.; Weiss, A.; Clark, J. I.; Yates, J. R., 3rd *Proc Natl Acad Sci U S A* **2002**, *99*, 7900-7905.
- (99) Smith, R. D.; Anderson, G. A.; Lipton, M. S.; Pasa-Tolic, L.; Shen, Y.; Conrads, T. P.; Veenstra, T. D.; Udseth, H. R. *Proteomics* **2002**, *2*, 513-523.
- (100) Lipton, M. S.; Pasa-Tolic, L.; Anderson, G. A.; Anderson, D. J.; Auberry, D. L.; Battista, J. R.; Daly, M. J.; Fredrickson, J.; Hixson, K. K.; Kostandarithes, H.; Masselon, C.; Markillie, L. M.; Moore, R. J.; Romine, M. F.; Shen, Y.; Stritmatter, E.; Tolic, N.; Udseth, H. R.; Venkateswaran, A.; Wong, K. K.; Zhao, R.; Smith, R. D. *Proc Natl Acad Sci U S A* **2002**, *99*, 11049-11054.
- (101) Wittke, S.; Kaiser, T.; Mischak, H. *J Chromatogr B Analyt Technol Biomed Life Sci* **2004**, *803*, 17-26.
- (102) Smith, R. D.; Barinaga, C. J.; Udseth, H. R. *Anal Chem* **1988**, *60*, 1948-1952.
- (103) Gelpi, E. *J Mass Spectrom* **2002**, *37*, 241-253.
- (104) Moini, M. *Anal Bioanal Chem* **2002**, *373*, 466-480.
- (105) Hsieh, F.; Baronas, E.; Muir, C.; Martin, S. A. *Rapid Commun Mass Spectrom* **1999**, *13*, 67-72.

- (106) Neusüß, C.; Pelzing, M.; Macht, M. *Electrophoresis* **2002**, *23*, 3149-3159.
- (107) Liu, C. C.; Jong, R.; Covey, T. *J Chromatogr A* **2003**, *1013*, 9-18.
- (108) Simpson, D. C.; Smith, R. D. *Electrophoresis* **2005**, *26*, 1291-1305.
- (109) Liu, C. C.; Zhang, J.; Dovichi, N. J. *Rapid Commun Mass Spectrom* **2005**, *19*, 187-192.
- (110) Liu, C. C.; Alary, J.-F.; Vollmerhaus, P.; Kadkhodayan, M. *Electrophoresis* **2005**, *26*, 1366-1375.
- (111) Emmett, M. R.; Caprioli, R. M. *J Am Soc Mass Spectrom* **1994**, *5*, 605-613.
- (112) Wilm, M.; Mann, M. *Anal Chem* **1996**, *68*, 1-8.
- (113) Kriger, M. S.; Cook, K. D.; Ramsey, R. S. *Anal Chem* **1995**, *67*, 385-389.
- (114) Fang, L.; Zhang, R.; Williams, E. R.; Zare, R. N. *Anal Chem* **1994**, *66*, 3696-3701.
- (115) Moini, M. *Anal Chem* **2001**, *73*, 3497-3501.
- (116) Ishihama, Y.; Katayama, H.; Asakawa, N.; Oda, Y. *Rapid Commun Mass Spectrom* **2002**, *16*, 913-918.
- (117) Bateman, K. P.; White, R. L.; Thibault, P. *Rapid Commun Mass Spectrom* **1997**, *11*, 307-315.
- (118) Wetterhall, M.; Nilsson, S.; Markides, K. E.; Bergquist, J. *Anal Chem* **2002**, *74*, 239-245.
- (119) Settlage, R. E.; Russo, P. S.; Shabanowitz, J.; Hunt, D. F. *J Microcol Sep* **1998**, *10*, 281-285.
- (120) Severs, J. C.; Smith, R. D. *Anal Chem* **1997**, *69*, 2154-2158.
- (121) Wachs, T.; Henion, J. *Anal Chem* **2001**, *73*, 632-638.
- (122) Wittke, S.; Fliser, D.; Haubitz, M.; Bartel, S.; Krebs, R.; Hausadel, F.; Hillmann, M.; Golovko, I.; Koester, P.; Haller, H.; Kaiser, T.; Mischak, H.; Weissinger, E. M. *J Chromatogr A* **2003**, *1013*, 173-181.

- (123) Demelbauer, U. M.; Plematl, A.; Kremser, L.; Allmaier, G.; Josic, D.; Rizzi, A. *Electrophoresis* **2004**, *25*, 2026-2032.
- (124) Moini, M.; Huang, H. *Electrophoresis* **2004**, *25*, 1981-1987.
- (125) Storms, H. F.; van der Heijden, R.; Tjaden, U. R.; van der Greef, J. *J Chromatogr B Analyt Technol Biomed Life Sci* **2005**, *824*, 189-200.
- (126) Guček, M.; Gaspari, M.; Walhagen, K.; Vreeken, R. J.; Verheij, E. R.; van der Greef, J. *Rapid Commun Mass Spectrom* **2000**, *14*, 1448-1454.
- (127) Wu, J. T.; Huang, P.; Li, M. X.; Qian, M. G.; Lubman, D. M. *Anal Chem* **1997**, *69*, 320-326.
- (128) www.promega.com/tbs/9piv511/9piv511.pdf, (Promega product information sheet on trypsin).
- (129) Cobb, K. A.; Novotny, M. *Anal Chem* **1989**, *61*, 2226-2231.
- (130) Amankwa, L. N.; Kuhr, W. G. *Anal Chem* **1992**, *64*, 1610-1613.
- (131) Amankwa, L. N.; Kuhr, W. G. *Anal Chem* **1993**, *65*, 2693-2697.
- (132) Licklider, L.; Kuhr, W. G. *Anal Chem* **1994**, *66*, 4400-4407.
- (133) Licklider, L.; Kuhr, W. G.; Lacey, M. P.; Keough, T.; Purdon, M. P.; Takigiku, R. *Anal Chem* **1995**, *67*, 4170-4177.
- (134) Licklider, L.; Kuhr, W. G. *Anal Chem* **1998**, *70*, 1902-1908.
- (135) Amankwa, L. N.; Harder, K.; Jirik, F.; Aebersold, R. *Protein Sci* **1995**, *4*, 113-125.
- (136) Guo, Z.; Xu, S.; Lei, Z.; Zou, H.; Guo, B. *Electrophoresis* **2003**, *24*, 3633-3639.
- (137) Wu, H.; Zhai, J.; Tian, Y.; Lu, H.; Wang, X.; Jia, W.; Liu, B.; Yang, P.; Xu, Y.; Wang, H. *Lab Chip* **2004**, *4*, 588-597.
- (138) Rashkovetsky, L. G.; Lyubarskaya, Y. V.; Foret, F.; Hughes, D. E.; Karger, B. L. *J Chromatogr A* **1997**, *781*, 197-204.
- (139) Bonneil, E.; Mercier, M.; Waldron, K. C. *Anal Chim Acta* **2000**, *404*, 29-45.
- (140) Slys, G. W.; Schriemer, D. C. *Rapid Commun Mass Spectrom* **2003**, *17*, 1044-1050.

- (141) Slys, G. W.; Schriemer, D. C. *Anal Chem* **2005**, 77, 1572-1579.
- (142) Jiang, H.; Zou, H.; Wang, H.; Ni, J.; Zhang, Q.; Zhang, Y. *J Chromatogr A* **2000**, 903, 77-84.
- (143) Cooper, J. W.; Chen, J.; Li, Y.; Lee, C. S. *Anal Chem* **2003**, 75, 1067-1074.
- (144) Luo, Q.; Mao, X.; Kong, L.; Huang, X.; Zou, H. *J Chromatogr B Analyt Technol Biomed Life Sci* **2002**, 776, 139-147.
- (145) Peterson, D. S.; Rohr, T.; Svec, F.; Fréchet, J. M. J. *Anal Chem* **2002**, 74, 4081-4088.
- (146) Sakai-Kato, K.; Kato, M.; Toyo'oka, T. *Anal Chem* **2002**, 74, 2943-2949.
- (147) Kato, M.; Sakai-Kato, K.; Jin, H.; Kubota, K.; Miyano, H.; Toyo'oka, T.; Dulay Maria, T.; Zare Richard, N. *Anal Chem* **2004**, 76, 1896-1902.
- (148) Ye, M.; Hu, S.; Schoenherr, R. M.; Dovichi, N. J. *Electrophoresis* **2004**, 25, 1319-1326.

Chapter 2 – 1D CE-MS

2.I. Introduction

The coupling of capillary electrophoresis (CE) to mass spectrometry (MS) takes advantage of both the speed and efficiency of CE, and the identification power of MS. CE was first coupled to MS by Smith and co-workers in 1987,¹ and since then, the most widely used CE-MS interface has been based on electrospray ionization.

There are two types of electrospray interfaces used with CE, sheathless and sheath flow interfaces.^{2,3} Sheathless interfaces can provide high sensitivities and low detection limits, yet their operation is often difficult, especially when very small capillary outlet inner diameters (IDs) are used. Another disadvantage is that the choice of CE separation buffers is limited as the CE effluent has to be MS compatible and volatile enough to provide a stable spray. In contrast, sheath flow interfaces suffer from lower sensitivities and higher detection limits because the capillary effluent is diluted by the sheath liquid. Their operation is more robust than that of sheathless interfaces, however, because the sheath liquid can provide a more stable electrospray. More CE separation buffer choices are available with the sheath flow configuration, as the sheath liquid can add volatility to a rather non-volatile CE separation buffer. With both interfaces, one is still limited to relatively volatile buffers such as ammonium acetate or formate, or simply acetic or formic acid. The use of phosphate, chloride, sodium, or potassium containing buffers should be avoided to decrease the occurrence of adducts of these species with the analytes of interest, and to avoid analyte ion suppression.

As far as the CE method that might be coupled to MS is concerned, capillary zone electrophoresis (CZE) was chosen for this work because it is the simplest CE method. When optimizing CZE separations of proteins and peptides for CE-MS, several aspects have to be considered to achieve well-resolved and efficient separations, such as buffer identity, buffer pH, buffer ionic strength, capillary wall coatings, and additives including organic modifiers or surfactants. The use of surfactants, such as sodium dodecyl sulfate, is precluded from consideration because of their incompatibility with MS. Organic modifiers such as MeOH can sometimes lead to better selectivity, but also often increase the separation time.⁴ Capillary wall coatings can be very useful in peptide and protein separations with CE to alleviate electrostatic protein-wall interactions that can lead to tailed peaks. On the other hand, coating procedures can sometimes be complex and time consuming. Increasing the buffer ionic strength can decrease analyte-wall interactions as well, although the separation times become longer because the increased ionic strength increases the ionic double layer of the capillary wall, and hence the EOF is decreased.⁴ Non-ionic capillary coatings usually increase separation times as well, as the negatively charged silanol groups are shielded. Because of the relatively limited buffer choices in CE-MS, the buffer pH ranges are also rather limited. Fortunately, the volatile ammonium acetate and formate buffers have low pK_a s, which are compatible with MS because low pHs aid in the protonation of analytes, and this enhances analyte detection by MS.

It turns out that achieving very high separation efficiencies is not a very crucial aspect of separation condition optimization, especially when the identification of peptides and proteins is the goal. In this work, an automated fragmentation method was used to collect tandem mass spectral data that can be submitted to protein database search

engines. The time it takes to first select parent peptide ions in a survey MS scan, and then to perform fragmentation on the peptides, can be rather long (sec), and hence it is actually not advantageous to achieve very high peak efficiencies. A peak with high efficiency, whose parent ion mass has been selected for fragmentation, might already have passed completely out of the capillary by the time the fragmentation is commenced.

The previous points have been considered while working on this chapter's experiments. To arrive at the ultimate goal of developing a multi-dimensional CE-microreactor-CE-MS instrument, work was started from the MS end and continued forward to the first CE (protein separation) dimension. This chapter describes the coupling of the second CE (peptide separation) dimension to the mass spectrometer and the improvement of that peptide separation. One sheathless and one sheath flow CE-MS interface were tried. Based on UV detection in front of the interfaces and MS detection after the interfaces, the soundness of the interfaces was determined. Once the use of a sheath flow interface had been decided, the peptide separation was improved in the second dimension by coating the capillary wall and by varying the buffer conditions. In addition, an automated feature, Information Dependent Acquisition, of the MS software was used to acquire data that could be submitted to a protein database search engine, which could in turn provide protein identification.

2.II. Experimental

2.II.A. Chemicals and Miscellaneous Materials

Cytochrome *C* from bovine heart (C-3131), pepsin from porcine stomach mucosa (P-6887), ammonium bicarbonate solid (99%), dimethylsulfoxide solution (99.9%), 50% glutaraldehyde in water (G-7651), poly(vinyl alcohol) (PVA) (341584, avg. MW 89,000-98,000 Da), sodium hydroxide solid (98%), and trifluoroacetic acid solution (99%) were from Sigma (St. Louis, MO). Trypsin from porcine (V511A) was from Promega (Madison, WI). Acetonitrile (HPLC grade) and formic acid solutions (88%) were from Fisher Scientific (Fair Lawn, NJ). Ammonium acetate solid (puriss. p.a. for mass spectroscopy) was from Fluka (Buchs, Germany). Methanol solution (HPLC grade) was from EMD Chemicals (Gibbstown, NJ), hydrochloric acid solution (38%) was from J.T. Baker (Phillipsburg, NJ), and helium gas (99.99%) was from Airgas (Radnor, PA). Water was distilled and deionized by a Nanopure (Barnstead, Dubuque, IA) system. Buffers and sheath liquids were filtered with 0.22 μ m Stericup ExpressTM PLUS filters (Millipore, Billerica, MA) until no particles were seen in the liquids in their glass storage flasks when observed against a dark background. The liquids were not stored in plastic flasks to avoid contamination by plasticizers that might be detected in mass spectra. Buffers and sheath liquids were either sonicated or He sparged. 0.6 and 1.6 mL Eppendorf tubes were from Island Scientific (Bainbridge Island, WA).

2.II.B. Instrumental Set-up

2.II.B.1. CE-UV-ESI-MS Instrument with a Sheathless CE-MS Interface

A schematic of the CE-UV-ESI-MS system is shown in **Figure 2-1**. The CE-UV parts of the system were on a cart since the Bruker Esquire mass spectrometer to which the CE system was connected was shared by many users. A 0-30 kV positive dc power supply (UltraVolt, Ronkonkoma, NY) provided the high voltage at the inlet reservoir for CE. As a safety feature, the injection part of the CE system that contains the high voltage electrode was enclosed in a Plexiglas box, and the power supply was enclosed in a separate but adjoining Plexiglas box (not shown in **Figure 2-1**). A door with a safety interlock allowed access to the CE injection compartment. The liquid levels of the samples and buffers were adjusted to the height of the inlet orifice of the MS to avoid siphoning. A 50 μm ID, 138 μm outer diameter (OD), 51 cm long uncoated fused silica capillary (Polymicro Technologies, Phoenix, AZ) was used for these experiments with the sheathless interface. One centimeter of the polyimide coating was burned off ~ 34 cm from the inlet end of the capillary to create a window for UV detection.

A ~ 200 -400 nm deuterium light source (Oceanoptics, Dunedin, FL) generated the UV light. 200 μm ID, 240 μm OD UV-compatible optical fibers (Polymicro Technologies, Phoenix, AZ) were used for UV light propagation. The UV fibers were cut with a GC capillary column cutter (Part No. S0010, SGT Middelburg B.V., Holland) that worked well for capillaries with ODs greater than 150 μm . Cuts were checked both from the side and head-on (**Figure 2-2**) with a microscope, and only cleanly cut fibers were used to get the best light transmission.

Figure 2-3 illustrates the Teflon cross that enclosed the capillary detection window. The design was based on a detection chamber developed by Wu *et al.*⁵ The cross was machined by the UW chemistry department's machine shop and had dimensions of 2.54 cm x 2.54 cm x 1.27 cm, with two 1.58 mm diameter, perpendicular, and centered channels drilled into the cross. The capillary and optical fibers were held in place by PEEK tubing, ferrules, and nuts (Upchurch Scientific, Oak Harbor, WA). Light coming out of one optical fiber was approximately collimated with a 1.58 mm diameter sapphire ball lens (Edmund Industrial Optics, Barrington, NJ). The light went through the capillary detection window and was captured by a second optical fiber on the other side of the capillary. The optimal positioning of the components was determined by observing the UV signal with a LabView (National Instruments) program (written by one of the Dovichi group members) to achieve a high signal intensity. Unfortunately, since the Teflon cross was opaque, the width of the light beam crossing the capillary could only be approximated and is estimated at $\sim 200\ \mu\text{m}$. A 214 nm bandpass filter (full width half max of 10 nm, Omega Optical, Brattleboro, VT) restricted the light before it was detected by a photomultiplier tube (1P28, Hamamatsu, Bridgewater, NJ). UV data collection was performed with a PCI-6035E data acquisition (DAQ) board (National Instruments, Austin, TX) and visualized with a LabView (National Instruments) program written by one of the Dovichi group members (see Pocket Material). The DAQ board was connected to the hardware *via* a 50 pin ribbon cable (E57891, National Instruments) through lab-built wiring in an aluminum box. The pin assignments of the 50 pin cable are shown in **Table 2-1**. Since the program was written for laser induced fluorescence detection, graphs are composed of direct light intensity data in Volts.

The end of the separation capillary was connected to a nanospray ESI needle (New Objective, Woburn, MA) inside a Tee-junction (T-jct) (Uncoated Tip Module, New Objective), described below, which was part of a PicoViewTM nanospray source platform (New Objective). The platform was attached to the front of a Bruker Esquire ion trap-MS. MS data collection and analysis were performed with the programs associated with the Bruker Esquire MS.

The CE-MS T-jct interface is depicted in **Figure 2-4**. A 29 nL dead volume separated the separation capillary end from the electrospray needle. The T-jct was part of a metal holder (the Uncoated Tip Module) that connected the platinum electrode *via* the metal nut to ground and back to the UltraVolt power supply to complete the CE circuit. The separation capillary and nanospray needle were held in place by Teflon sleeves, ferrules, and nuts. Various nanospray needles (New Objective) with different inner diameters (20, 50, and 75 μm) and different orifice diameters at the tapered ends of the needles (5, 10, and 15 μm) were tried. Short (~ 2 cm), non-tapered fused silica capillaries (Polymicro Technologies, Phoenix, AZ), with inner diameters ranging from 9 to 73 μm , were also used in place of the ESI needles in some experiments.

2.II.B.2. CE-UV-ESI-MS and CE-ESI-MS Instrument with a Sheath Flow CE-MS Interface

The same general schematic set-up as for the sheathless CE-UV-ESI-MS instrument applies for the CE-UV-ESI-MS experiments using a sheath flow interface, see **Figure 2-1**. The mass spectrometer (2000 Q TRAP, MDS Sciex, Toronto, Canada) used for these experiments was a hybrid instrument with a triple quadrupole whose third quadrupole could also function as a linear ion trap. The Q TRAP was operated, and the

MS data analyzed, using the Q TRAP's Analyst software version 1.3, which was later upgraded to version 1.4. The electrospray ion source used for sheath flow CE-MS experiments was a NanoSpray ion source with an x-y-z translational stage for electrospray tip positioning. The Q TRAP was equipped with two cameras and monitors when used with the NanoSpray ion source, which allowed a view of the electrospray needle in front of the Q TRAP orifice inlet.

The sheath flow interface consisted of a stainless steel MicroIonSpray head (see **Figures 2-5** and **2-6**), which was provided by Dr. Chun-Sheng (Charles) Liu from Applied Biosystems (Foster City, CA), a former Dovichi group member. Whereas the sheathless T-jct interface was held at ground, the MicroIonSpray head had an electrospray (ion spray (IS)) voltage applied to it. The inner diameter (ID) of the through holes of the stainless steel tee used in the MicroIonSpray head was of the largest size provided, 750 μm , to permit easier insertion of a capillary into the head than when using tees with smaller IDs. Both uncoated and coated fused silica capillaries were used as separation capillaries, and their specific sizes and lengths will be given in the figure captions. The capillaries were inserted into a 5.4 cm stainless steel electrode, or needle, with a tapered tip that had a 150 μm ID outlet, see **Figures 2-5** and **2-6**. The capillary end that was inserted into the electrode was cut square, and ~ 1 mm of the polyimide was shaved off the end with a razor blade. The capillary was positioned so that the capillary end was very close to the outlet of the tip, yet did not protrude. Initially, the capillary was gently pushed toward the tip until it would move no further. Then, the optimum capillary position inside the tip was achieved by very slightly pulling the capillary back from the tip, tightening the nut that held the separation capillary in place, and observing

the liquid flow at the tip with a magnifying glass. Separately, sheath liquid flow *via* the sheath liquid capillary, and ddH₂O flow through the separation capillary, were used to judge how smooth the flow out of the tip was. The capillary position was adjusted (while loosening and tightening the nut each time an adjustment was made) to get the smoothest flow, rather than periodic spurts of liquid.

If the tip was found to be clogged, the MicroIonSpray head was disassembled and the electrode was inserted tip-first into a yellow Teflon sleeve (685 μm ID, 1/16" OD, F-246x, Upchurch Scientific, Oak Harbor, WA). Care was taken not to let the tip protrude from the sleeve to not damage the tip when the electrode and sleeve were subsequently inserted into a PEEK union (P-704, Upchurch Scientific). A 1 mL syringe with ddH₂O, or sometimes ACN, depending on the suspected cause of the plug, was attached to the other end of the union with a PEEK sleeve (762 μm ID, 1/16" OD, 1533, Upchurch Scientific) and thus the tip was vigorously and repeatedly back-flushed with about 5-10 mL total volume.

A 250 μL -capacity nanofluidic module (NFM) pump (Scivex, Inc., Oak Harbor, WA) was used to deliver the sheath flow. A 20 μm ID, 360 μm OD fused silica capillary (Polymicro Technologies, Phoenix, AZ) was used between the MicroIonSpray head and the NFM. The sheath flow rate ranged between 700 and 1300 nL/min, depending on the specific experiment. A few different sheath flow compositions were tried, which are noted in the figure captions.

Several other changes to the CE-UV-MS instrument were made. In preparation for two-dimensional experiments, the electronics shop of the University of Washington

chemistry department had built two power supply housings that contained both one negative and one positive 0-30 kV UltraVolt power supply (UltraVolt, Ronkonkoma, NY). (These housings were located on the bottom shelf of the cart, not on top of the Plexiglas box any more.) For both one- or two-dimensional experiments, the ground returns for the power supplies were connected to the screws of the power outlet at the back of the Q TRAP, since the Q TRAP provided a common ground for both the MS and CE electronics.

To avoid siphoning, all liquid levels had to be at the same height as the outlet of the electrospray tip, which was very close to the inlet orifice of the Q TRAP. To accomplish this, a giant jack (Fisher Scientific, Hampton, NH) with a platform of 30 x 30 cm and a 48 cm maximum height, was secured to the movable cart with four 19 cm long aluminum rods to give the jack additional height, see **Figure 2-6**. A Plexiglas board was screwed on top of the jack to be able to place the components of the CE system on top of it since the jack's platform was not big enough. To avoid having the jack lean to one side or also inadvertently change its height, a tapped aluminum rod was screwed on one side of the jack into holes in both the lower and upper jack platforms. Metal nuts secured the rod in position once a particular jack height had been chosen. To align the CE liquid levels with the MS orifice, the jack height was roughly adjusted first. Then, a 50 x 1 x 4 cm aluminum stick was placed between the Plexiglas platform and the front platform of the Q TRAP (the NanoSpray ion source was taken off the Q TRAP for this purpose). A level was put on top of the stick and small pieces of paper were placed under one end of the stick until the stick was horizontal. By using the top of the aluminum stick as a

common basis for a ruler, the liquid level in the buffer reservoir could be adjusted to coincide with the Q TRAP orifice level.

2.II.C. Coating Capillaries with Poly(vinyl alcohol)

The coating procedure was adapted from Belder⁶ and Fogarty⁷. Four capillaries (182 μm outer diameter (OD), 50 μm inner diameter (ID)) could be coated at one time in a He gas purging device (for later experiments that used 142 μm OD capillaries, six capillaries could be fit).

First, a poly(vinyl alcohol) (PVA) suspension was prepared. PVA was ground with a mortar and pestle for ~ 5 min. An initial 2.5% (w/w) PVA suspension was prepared by adding 37.5 mg of the ground PVA, 1.312 mL of ddH₂O, and 150 μL of 50% (v/v) ddH₂O-concentrated HCl to a 1.6 mL Eppendorf tube. The tube was shaken and vortexed for 3 min, then sonicated for 15 min. The PVA did not completely dissolve, so the suspension was allowed to stand for 1 min, and then 300 μL of the supernatant was transferred into a 0.6 mL Eppendorf tube. The concentration of the final PVA suspension is unknown, but the grinding of PVA and settling of the PVA in the solution for 1 min were performed to reduce the chances of clogging the capillaries when filling them with the PVA suspension. Some capillaries still became clogged, however; hence it was convenient to coat four or six capillaries at one time.

Second, the capillaries were cleaned. 1 M NaOH and ddH₂O were successively flushed through the capillaries for 30 min at 4 psi, then the capillaries were dried by flowing He gas through them for another 30 min at 4 psi.

Third, a glutaraldehyde-HCl solution was prepared. Since glutaraldehyde is sensitive to air, this was done while the capillaries were being cleaned. 100 μL of a 50% glutaraldehyde solution from Sigma was added to 150 μL of 10% (v/v) concentrated HCl in ddH₂O.

Fourth, the capillaries were flushed with the glutaraldehyde-HCl solution and PVA suspension. As Belder *et al.*⁶ point out, it is important to perform the coating steps in quick succession and in the sequence specified. Since the PVA settles after a while, the PVA suspension was briefly vortexed 10 min before starting the glutaraldehyde-HCl flush. After the capillaries had been dried with He for 30 min, the glutaraldehyde solution was flushed through the capillaries at 20 psi until the solution came out at the capillary ends. Immediately afterwards, the PVA suspension was flushed through the capillaries at 60 psi for 1 min, which was followed by He gas at 60 psi for 10 min. A foam could be observed at the capillary ends once the He pushed the PVA suspension out of the capillaries if they were not clogged. After the 10 min, the gas pressure was reduced to 5 psi and the flushing continued for 5 hours.

Last, ddH₂O was flushed through the capillaries. If a capillary was blocked, no, or relatively little (compared to other capillaries), ddH₂O would come out at its end. Such a capillary was discarded. The capillaries were stored with their ends in ddH₂O. Shortly before use, the capillaries were cut to the desired length, with the ends cut square. Care was taken to not let the capillaries dry out because a deterioration of separations was observed if the coating was exposed to air.

2.II.D. Bulk Digestion of Cytochrome *C*

2.II.D.1. Bulk Digestion with Trypsin

The procedure for digesting cytochrome *C* with trypsin was adapted from a Q TRAP manual's recipe that digests α -casein with trypsin.⁸ For initial experiments, the ratio of cytochrome *C* to trypsin was 34:1 (w/w). 20 μ L of freshly prepared ammonium bicarbonate (pH \sim 8.0) was added to 20 μ g of trypsin in the original trypsin glass vial from Promega. The vial was heated for 15 min in a 37°C incubator. Then, 30 μ L of a 1.8 mM solution of cytochrome *C* in 25 mM ammonium bicarbonate and 2.5 μ L of acetonitrile were added to the trypsin vial, and the digestion was allowed to proceed for 4 h. The reaction was quenched by adding 847.5 μ L of a freshly made 2% (v/v) acetonitrile-0.1% (v/v) trifluoroacetic acid solution to yield a final cytochrome *C* concentration of \sim 60 μ M. 100 μ L aliquots of the digest in 0.6 mL Eppendorf tubes were frozen at -80°C until use, at which time they were thawed in the refrigerator and kept at 4°C between injections. For later digestions, a 50:1 cytochrome *C* to trypsin (w/w) ratio was used, and the digestion allowed for 24 h to maybe obtain a more complete cytochrome *C* digestion. The final concentration of cytochrome *C* of the later digest was still 60 μ M.

2.II.D.2. Bulk Digestion with Pepsin

Based on an assay for pepsin activity that is used by Sigma (St. Louis, MO, based on ⁹), a pepsin-to-protein (w/w) ratio of \sim 1:570 was chosen for a cytochrome *C* pepsin bulk digest. 20.4 μ L of a 50 mg/mL (4.1×10^{-3} M) cytochrome *C* solution was added to

1.8 μL of a 1 mg/mL (2.9×10^{-5} M) pepsin solution, along with 37.5 μL of formic acid (pH 2.5). The digestion was allowed to proceed for 60 min at 37°C. The digestion solution was lyophilized and 840 μL of 50% acetonitrile-0.1% trifluoroacetic acid was added to yield a final cytochrome *C* concentration of 1×10^{-4} M. Aliquots of this sample solution were frozen in 0.6 mL Eppendorf tubes at -80°C until use. Shortly before use, an aliquot was lyophilized and resuspended in freshly prepared 2% acetonitrile-0.1% trifluoroacetic acid to yield a final concentration of ~ 60 μM cytochrome *C*.

2.II.E. CE-ESI-MS Separations

2.II.E.1. CE-UV-ESI-MS Experiments with the Sheathless CE-MS Interface

The instrumental set-up was described in section 2.II.B.1.. 1.6 mM (ammonium) acetate in 25%-75% MeOH-ddH₂O (pH 5.0) was used as the running buffer. Samples were injected with 20 kV (392 V/cm) for 3 sec, and the separation voltage was 20 kV (392 V/cm), with an electrical current of 2-4 μA . The PMT bias was 0.5 kV. Because it was unpractical to wipe liquid droplets from the electrospray capillary outlet once a position had been obtained that yielded a fairly stable spray, no buffer was flushed through the capillary between runs.

2.II.E.2. CE-UV-ESI-MS and CE-ESI-MS Experiments with the Sheath Flow CE-MS Interface

The general procedure for running experiments with and without UV detection was essentially the same; the only difference was that with UV detection, longer capillaries were used to accommodate the Teflon cross. Both uncoated and poly(vinyl

alcohol) (PVA)-coated fused silica capillaries of varying dimensions and lengths were used. The NanoSpray ion source had a rail along which the MicroIonSpray head could be moved back from the MS orifice. This made it convenient to wipe liquid off the stainless steel electrospray tip when flushing the capillaries with buffer between runs. Stable sprays were obtained with the electrode tip positioned ~ 5 mm from the orifice, ~ 1 mm below, and ~ 1 mm to the left. Also, based on a suggestion by Charles Liu, a former Dovichi group member, the MicroIonSpray head was tilted at a $\sim 15^\circ$ angle upward toward the MS orifice to achieve a more stable spray. In addition, buffers were sonicated before use in early experiments. In later experiments, sparging the buffers with He gas for 5-10 min proved even more effective than sonication to avoid frequent drops in the MS current signal due to liquid outgassing that caused small air bubbles. After a stable electrospray was obtained with a set of MS parameter values, the electrode tip position with respect to the orifice was marked with a permanent marker on one of the camera monitors. This allowed easy repositioning of the electrode tip after inserting a new capillary into the MicroIonSpray head, especially because the MS parameter values were not changed much in later experiments.

During sample injection, the ion spray (IS) voltage and Q TRAP gases were turned off (the Q TRAP was in standby mode). The capillary was dipped in ddH₂O before and after sample injection. In between experiments, the NFM flow rate was kept at 250 nL/min to keep the MicroIonSpray head space around the capillary filled with sheath liquid.

When using PVA-coated capillaries, care needed to be taken not to let the capillary become dry so the coating would not deteriorate. For this purpose, the time

between runs was kept as short as possible, and either the inlet buffer reservoir liquid level was kept above the MS orifice level to induce siphoning, or the capillary was flushed with buffer or water. To avoid drying of the PVA-coated capillary overnight, the NFM continuously pumped ddH₂O at 100 nL/min to the tip and around the capillary, and the capillary inlet was put into an Eppendorf tube with ddH₂O whose level was above the MS orifice.

There were three different ways in which data were acquired with the Analyst software: using the manual tune mode, batch acquisition, or information dependent acquisition (IDA). The specific applications of the different acquisition modes and their experimental parameter values are explained in the Results and Discussion section of this chapter (2.III.B.5. and 2.III.B.6.) and will be given in the figure captions. For experiments that did not utilize the Q TRAP's Information Dependent Acquisition (IDA) mode, the Q TRAP was run in either Q3 mode where the third quadrupole was the mass analyzer, or in linear ion trap (LIT) mode, where the third quadrupole was used as a linear ion trap. For all experiments, the Q TRAP was run in positive ion mode and the ion detector was set to 2300 V. The exact CE, MS, and NFM parameter values will be included in the figure captions.

2.II.F. Data Analysis

UV data were acquired with LabView as IGOR text files and were analyzed with IGOR Pro, version 3.16 (Wavemetrics, Inc., Lake Oswego, OR). UV data were smoothed binomially with a smoothing value of 3. CE current data were also acquired with LabView, but stored as text files that were analyzed with Excel.

Mass spectrometry data were acquired and analyzed with Analyst software versions 1.3 and 1.4 (Applied Biosystems, Foster City, CA, and MDS Sciex, Toronto, ON, Canada). Analyst collects data as total ion electropherograms (TIEs) that show the ion current of the whole mass-to-charge (m/z) range that is used for an experiment. If the masses of specific analytes are known, ion current data can be generated that correspond to only those masses; the graphs of such specific masses are called extracted ion electropherograms (XIEs). XIEs can also be overlaid and then their intensities summed, which results in reconstructed ion electropherograms (RIEs).

XIEs with a m/z range of 1 amu were chosen for this work, since the mass spectral peak widths of the Q TRAP in linear ion trap mode at a scan rate of 1000 amu/sec were comparable to this range. Data were usually collected at this scan rate, although scan rates of 250 and 4000 amu/sec were also available with the LIT. The faster the scan rate, the lower the resolution. Hence, choosing 1000 amu/sec was a compromise between speed and resolution.

Initially, it was not known which XIE peptide masses to choose for cytochrome *C* that had been digested with trypsin or pepsin. To obtain a list of XIE masses, the following procedure, which is illustrated in **Figure 2-8**, was followed: first, a background mass spectrum (**Figure 2-8 B**) that corresponded to a ~ 0.5 min region of a TIE (early highlighted region in **Figure 2-8 A**) was compared to the mass spectrum (**Figure 2-8 C**) of a later occurring 0.5 min region in the TIE (later highlighted region in **Figure 2-8 A**). Alternatively (not shown), the background mass spectrum could be subtracted from the other spectrum. Masses that distinguished the later spectrum from the background spectrum were noted (e.g. mass 510.4 amu in **Figure 2-8 C**). XIEs were generated with

the potential masses to determine whether the masses were due to noise spikes or were part of actual peaks, see **Figure 2-8 E**. The whole time period (in 0.5 min increments) of a TIE was thus analyzed. Once a list had been compiled and its XIEs generated, the XIEs were overlaid (**Figure 2-8 F**) and then summed to yield an RIE (**Figure 2-8 G**).

Other XIE masses were later obtained with information dependent acquisition (IDA) experiments. Two lists of 19 and 20 XIEs that showed the most intense peaks were compiled for data of trypsin- and pepsin-digested cytochrome *C*, respectively, see **Table 2-2**.

For comparison purposes, the RIEs that will be shown in later figures are based on these lists even though not all masses were observed in all experiments. TIEs and RIEs will be illustrated after having been 1 times Gaussian smoothed in Analyst. For practical reasons, figures that show overlaid XIEs will not be shown smoothed, unless noted otherwise.

2.III. Results and Discussion

2.III.A. Experiments Using a Sheathless CE-ESI-MS Interface

A 1D CE instrument was built that included UV as well as MS detection. A Bruker Esquire ion trap mass spectrometer was used that was located in the MS facility of the University of Washington's (UW's) chemistry department. Since the mass spectrometer was shared by many users, the CE instrument had to have a mobile design and be able to be easily connected and disconnected from the mass spectrometer. The CE and UV parts of the system were therefore on a cart. UV detection was included to be

able to perform CE experiments without having to rely on mass spectrometric detection. In addition, UV detection made it possible to observe analyte peaks before the CE-MS interface. Comparisons of UV electropherograms with MS ion current electropherograms allowed a characterization of the interface and made it easier to determine whether the interface was working properly.

Upon an initial literature search covering CE-MS interfaces (see section 1.IV.A.), sheathless interfaces seemed to be most promising since the greatest sensitivities had been reported with these, especially with nanospray set-ups. The MS facility of the chemistry department had a PicoViewTM nanospray source consisting of a small breadboard on x-y-z translational stages for positioning the ESI needle in front of the Bruker Esquire MS inlet orifice. A camera with magnifying objectives and an on-line TV monitor allowed the needle and orifice to be viewed while optimizing the needle's position. A part of the source was a union or tee-junction (T-jct) that coupled separation columns for either HPLC or CE to ESI needles. The platinum wire that was part of the T-jct provided the ground for the CE circuit and the ESI potential difference. Since the ion trap's voltages could be set as negative potentials, the flow of analyte occurred from CE inlet to T-jct to the ion trap. Ammonium acetate was chosen as the buffer because of its volatility and because it does not as readily form adducts with analytes as, for instance, sodium, potassium, or chloride do.

Initial experiments using tapered ESI needles with needle outlet IDs of 5, 10, or 15 μm were difficult because the needles often became clogged and it was difficult to establish a stable electrospray. Hence, non-tapered, 2 cm pieces of capillaries with IDs of 15 to 73 μm were tried in place of the tapered needles. However, based on flow rate

experiments using only a CE-UV set-up and the electrophoresis neutral marker dimethylsulfoxide (DMSO), it was found that the electroosmotic flow was hampered dramatically when using capillary pieces that had a smaller inner diameter than the separation capillary, see **Figure 2-9**. This decrease in apparent flow rate presumably caused the instability of the electrospray since not enough liquid was supplied to the end of the capillary, or needle orifice, to establish a stable, continuous spray.

In addition, bubbles were observed in the separation capillary with a magnifying glass, which pointed towards electrolysis at the interface, specifically at the platinum electrode. Even when using low buffer concentrations such as 1.6 mM (ammonium) acetate in 25%-75% MeOH-ddH₂O (pH 5.0), bubbles could not be eliminated.

In a subsequent CE-MS experiment that used a non-tapered 29 μ m ID capillary as the ESI needle, DMSO was successfully transferred from the capillary to the MS. The buffer used was 1.6 mM (ammonium) acetate in 25%-75% MeOH-ddH₂O (pH 5.0). However, peak tailing was observed in the MS electropherogram that was not present in the UV electropherograms, see **Figure 2-10**. This peak tailing was attributed to the dead volume of the T-jct. The negative effect of bubbles is also illustrated in **Figure 2-10**.

During the experiments with the T-jct interface and upon further consideration of the interface literature, several points became clear: first, although greatest sensitivities might be obtained with sheathless interfaces, the ESI spray was often unstable. Although more stability might be achieved by choosing different buffers, the number of choices of buffers would be decreased. If complex protein and peptide samples were to be analyzed, having greater flexibility in the choice of buffers might prove more important than

sensitivity. Second, it was shown that bubbles were detrimental to CE separations as they caused instability and irreproducibility. For 2D CE experiments, this was not acceptable. Third, the dead volume in the T-jet apparently caused considerable peak distortion.

Based on these points, a sheath flow interface seemed to be a good alternative. The use of a sheath liquid could aid in the stability of the ESI spray by adding to the overall flow rate and volatility of the liquid being sprayed. This could provide greater flexibility in the choices of separation buffers. Dr. Chun-Sheng (Charles) Liu, a former Dovichi group member, had devised a sheath flow interface while part of the group, and a commercial CE-MS sheath flow interface that was very similar to his interface had become available from Applied Biosystems. Dr. Liu, now employed by Applied Biosystems, kindly provided such an interface for us.

2.III.B. Experiments Using a Sheath Flow CE-ESI-MS Interface

2.III.B.1. CE-UV-ESI-MS with Dimethylsulfoxide as a Neutral Marker

For work with the sheath flow interface, the Q TRAP was dedicated to this project, which was very convenient since the CE instrument did not have to be constantly connected and disconnected to and from the MS, which saved considerable time. Initial experiments focused on establishing a stable electrospray and investigating whether the sheath flow interface would cause less tailing of peaks than the sheathless interface.

Although there was still some dead volume at the tip of the sheath flow interface because the capillary was positioned in the back of the electrospray tip and did not protrude from the tip (**Figure 2-6**), less peak tailing was expected with the sheathless interface based on Dr. Chun-Sheng Liu's thesis work with this type of sheath flow interface.¹⁰ Parameters

such as tip position, applied voltages, sheath liquid composition, and sheath flow rate, had to be brought into alignment. These parameters have been further optimized throughout the experiments that will be described in this dissertation, hence the specific CE, NFM, and MS parameter values will be given in the figure captions.

Initially, syringe pumps were used to deliver the sheath flow. However, pulsing of the syringe pumps caused an unstable electrospray. We were fortunate to then be provided with a Nanofluidic Module (NFM) pump by Dr. Darren Lewis, a former Dovichi group member who had developed the NFM while working for Scivex, Inc. (Oak Harbor, WA). The pump featured a thermal feedback sensor that minimized flow rate fluctuations. The flow rate could also be monitored on the display of a computer program. The flow rate fluctuations were typically within 1-2% of the flow rate when a 20 μm ID (360 μm OD) fused silica capillary was used between the NFM and the MicroIonSpray head. Use of larger IDs caused less backpressure, which increased the flow rate fluctuations.

Even though the Q TRAP features the linear ion trap that provides lower detection limits than when it is run in quadrupole mode,¹¹ more stable sprays were initially obtained when the Q TRAP was run in Q3+ mode. In this mode, only the third quadrupole acted as a mass analyzer.

Based on experiments with the sheathless CE-MS interface, a buffer of 1.6 mM ammonium acetate in 25%-75% MeOH-ddH₂O (pH 5.0) was chosen in experiments with 4% DMSO as the sample. In two consecutive experiments, hardly-tailed DMSO peaks were observed with UV and with MS detection using the sheath flow CE-MS interface, see **Figure 2-11**. Therefore, it was concluded that the dead volume at the tip of the

sheath flow interface did not cause peak tailing as had been seen with the sheathless interface.

It should be noted that the electric field strengths that are given in the figure captions for experiments with the Q TRAP were calculated by taking into account the IS voltage that was applied at the MicroIonSpray head. That is, the electric field strengths across the CE separation capillary were lower than what would be expected based on the applied CE voltages.

2.III.B.2. CE-UV-ESI-MS of Trypsin Bulk-digested Cytochrome *C*

The next step was to obtain a good separation of peptides in the second dimension of the CE-microreactor-CE-MS-MS system. The separation and MS conditions were improved by trying different separation buffers, coating the capillary wall, changing the sheath flow liquid, and changing the parameters in the Analyst software.

Cytochrome *C* was chosen as a model protein because the protein has been well characterized¹² and because cytochrome *C* has been used as a model protein in earlier work of the group¹³. First experiments used trypsin as the digestion enzyme. The optimum pH for trypsin digestion is around pH 8.¹⁴

Based on the DMSO experiments in section 2.III.B.1., a 1.6 mM (ammonium) acetate in 25%-75% MeOH-ddH₂O (pH 5.0) buffer was tried with an uncoated fused silica capillary. Many sheath flow liquid compositions have been reported in the literature,¹⁵ and an initial composition of 75%-24.9%-0.1% isopropanol-ddH₂O-formic acid was chosen for volatility and good electrical contact. The UV signal, total ion electropherogram (TIE), and reconstructed ion electropherogram (RIE) are shown in

Figure 2-12. In addition, two XIEs are shown in **Figure 2-13**. One XIE shows a fairly Gaussian shaped peak, the other a tailed peak. As will be shown shortly, the tailing of peaks was mostly due to interactions between the capillary wall and the peptides.

When comparing the UV graph with the RIE, it became evident that the limit of detection of the UV system was not adequate to provide very valuable information. Therefore, UV detection was omitted for further one-dimensional CE-ESI-MS experiments. This also had the advantage of being able to use shorter capillaries because the Teflon cross that was used for UV detection was not part of the set-up. In addition, the TIE was not very informative. Thus, TIE graphs will not be shown in the rest of this chapter. It should also be noted that from this point forward, data were acquired exclusively with the linear ion trap (LIT) mode of the Q TRAP. This provided lower detection limits than the Q3+ mode because ions can be stored in the LIT, and then scanned out over a given m/z range, whereas in the quadrupole mode, ions are lost if the quadrupole is not set to transmit their particular m/z values.

2.III.B.3. CE-ESI-MS of Trypsin Bulk-digested Cytochrome C

To improve the separation, Dr. Charles Liu suggested the use of poly(vinyl alcohol) (PVA)-coated capillaries and increased buffer ionic strengths. Both changes would alleviate electrostatic interactions between peptides and the capillary wall, but also decrease the electroosmotic flow. PVA-coated capillaries decrease these interactions and the EOF because the negatively charged silanol groups (SiO^-) (the extent of ionization depends on buffer pH) have been masked by PVA and the capillary wall is left with a hydrophilic PVA layer.⁶ An increased buffer ionic strength has the same effects because

the peptides are shielded from the wall by the increased amount of buffer ions that are associated with the wall.⁴ In addition, Dr. Liu suggested the use of MeOH as the sheath flow liquid based on his experience. It was found in my work that 90% MeOH worked well with the NFM and with the CE-MS interface. Since the separation capillary end was inside the electrospray needle, the buffer coming out of the capillary could mix with the 90% MeOH and electrical contact was established even though no buffer was in the sheath flow liquid.

Figure 2-14 illustrates the RIE of the separation of a trypsin bulk-digest of cytochrome *C* with the different conditions. Also shown are two XIEs of the same masses as in **Figure 2-13**. The reduced tailing indicated that the interactions between peptides and the capillary wall were clearly decreased.

Figure 2-15 shows two electropherograms that were run on the same day. The parameter values were slightly different than for **Figure 2-14**, but **Figure 2-15** illustrates the repeatability of the experiments. Based on the experiments above, PVA-coated capillaries and high ionic strength buffers were used from this point forward.

It was further investigated whether the high ammonium acetate concentration of 100 mM itself might be sufficient to improve peak shapes. For these experiments, a cytochrome *C* trypsin bulk-digest was separated in an uncoated capillary using 100 mM ammonium acetate (pH 4.0). **Figure 2-16** compares three XIEs of experiments that used a PVA-coated capillary vs. an uncoated capillary. The XIEs were once Gaussian smoothed for this figure. Unfortunately, the injection voltage had inadvertently not been the same for the two experiments. The differences in migration times are most likely due to the reduced EOF that is expected with PVA-coated capillaries. As can be seen, the

differences are not pronounced. Some peaks show very little difference, as in the 535-536 amu XIE. The tailing in the 729-730 amu XIE was not greatly reduced, indicating that analyte-capillary wall interactions other than ionic interactions might be the cause of the tailing for this particular peak. Still, a slight improvement was seen with the PVA-coated capillary for this peak. It is not clear what caused the fronting of the 1007-1008 amu peak when using an uncoated capillary, but the PVA-coated capillary was able to improve the peak shape. Therefore, even though the improvements with the PVA-coated capillary were not dramatic, a slight improvement of peak shapes was observed, and hence PVA-coated capillaries were used from this point forward for the peptide separation dimension.

2.III.B.4. CE-ESI-MS of Pepsin Bulk-digested Cytochrome C

Most researchers that analyze peptides with CE-MS use acidic conditions because the protonation of analytes is increased at acidic pHs, which leads to better detection limits. Trypsin is most active at \sim pH 8,¹⁴ which makes its use problematic with on-line microreactor digestion that is coupled to CE-MS. On the other hand, pepsin is most active at \sim pH 1-3.5.^{16, 17} In addition, Dr. Mingliang Ye, a former post-doc of the Dovichi group, had previously immobilized pepsin in microreactors, and thus pepsin was chosen for further studies. To establish a list of XIEs that would yield peaks, cytochrome C was bulk-digested with pepsin, see section 2.II.D.2., and the data were analyzed using the method described in section 2.II.F.. The XIE list is given in **Table 2-2**.

These experiments were performed using 50 mM ammonium acetate (pH 4.0) to decrease the migration times,⁴ since the migration times with the trypsin bulk-digested

cytochrome *C* sample were quite long, see **Figures 2-14** and **2-15**. For future two-dimensional experiments, the time window in which peaks are detected in the second dimension separation should be quite short to be able to decrease the overall experiment time (see section 4.II.D.1.).

Figure 2-17 shows RIEs of two experiments that were conducted on the same day. Not all components were separated, but the peak shapes are Gaussian and the separation window in which peaks are detected is ~ 3 min. The next steps, which are described in Chapter 3, were to make the microreactor and connect it on-line to the second dimension peptide separation. Before that, however, some aspects of the Analyst software will be discussed.

2.III.B.5. Batch Acquisition Using the Q TRAP Analyst Software

There were two different ways in which the Analyst software was used to acquire data for non-IDA runs (IDA experiments will be explained in section 2.III.B.6.): using the manual tune mode or batch acquisition. Analyst employs user-configured methods for data acquisition. In a method, specific MS parameter values are defined, including the m/z range, IS voltage, CUR gas, and GS1 gas, as well as whether the Q TRAP is to be run in LIT mode or in Q3+ mode. A method can also let an experiment run for a specified time, but the time can be expanded once the experiment is started. The same methods can be used in either manual or batch acquisitions.

When using the manual tune mode, the Q TRAP was in Tune mode and runs and data acquisitions were started manually. When using batch acquisition, the Q TRAP was in Acquire mode and it could automatically start and stop a series of runs, whose methods

had previously been defined, once the start of a series had been initiated. When a batch of experiments (i.e. one or more) is submitted in the Analyst software, the experiments are executed in the order they were submitted, with only a brief pause in between experiments.

For initial experiments that have been described in this chapter, data were acquired using the manual tune mode. However, it was observed that the MS signal could fluctuate considerably at the beginning of a run. On a day when the MS parameter values were adjusted to obtain a stable spray before beginning the day's experiments-and it had been difficult to obtain a stable spray-I had forgotten to extend the time the method would run, and data collection stopped after the pre-set 10 min of the method.

Afterwards, I immediately started another run in Analyst without having stopped the CE voltages or the NFM sheath flow. Surprisingly, the baseline and spray that were observed with this new Analyst acquisition were immediately very stable without any other adjustments, see **Figure 2-18**. The arrows in the figure indicate that the runs were stopped and started right after one another. It was not clear what caused the baseline to be suddenly stable, especially because the IS voltage and gases were not automatically shut off when data acquisition was stopped; for the voltages and gases to be turned off, the Q TRAP has to be put into standby mode. Simply starting, stopping, and starting a run in Analyst enabled the baseline to be stable (fortuitously, the optimal parameter values and tip position etc. had been chosen).

Additionally, it was observed that a liquid drop could sometimes form at the electrospray tip when the NFM liquid flow, the CE voltages, and the Q TRAP voltages and gases were started at the beginning of a run. When using the manual tune mode (in

which MS parameter values could be adjusted on-the-fly) this droplet could be blown off the tip by briefly applying a nebulizer gas flow setting (GS1) of e.g. 10.

When using batch acquisition, such on-the-fly GS1 setting changes were not possible, but by submitting two experiments in a batch, one could incorporate both the start-stop-start sequence and an initial GS1 setting of 10. It was found that the Q TRAP was not put into standby mode between different experiments that had been submitted as a batch to Analyst; hence, the use of these batches would enable a start-stop-start sequence mentioned above. Batches that were used from this point forward consisted of two experiments: a 0.2 min prerun, and a longer run that collected data of the peptide separations. The prerun method had the same Analyst parameter values as the subsequent run, except that the nebulizer gas flow was set to 10, whereas a GS1 setting of 0 gave a stable spray for the following run. Also, because Analyst went automatically from one run to the next, the timing of applying an initial GS1 setting of 10 for liquid droplets to be blown off the spray tip was more reproducible than applying such a gas flow manually. Two blank runs that show Analyst data for both the preruns and the subsequent runs are shown in **Figure 2-19**. Note that even though the preruns look quite differently and the signal intensity at the end of the preruns is at a different level, the subsequent runs are quite stable and have about the same baseline level. In addition, IDA experiments, which are explained in the next section, could not be run using the manual tune mode but had to be started in acquisition mode using batches. Hence, the use of the two runs in the batches was very convenient.

2.III.B.6. CE-ESI-MS-MS

The Q TRAP is capable of running tandem (MS-MS or MS²) mass spectrometry experiments. This means that the peptides that enter the MS from the CE capillary can be further fragmented inside the MS and mass spectra can be collected that show the masses of these fragments. These mass spectral data, along with the masses and charge states of the peptides that constituted the so-called parent ions of the fragments, can be submitted to database search engines, such as Mascot, to provide a list of possible peptide and protein identifications. The method that the Q TRAP uses for MS-MS experiments is called Information Dependent Acquisition (IDA).

IDA experiments are cyclic in nature. The general workflow of one cycle of an IDA experiment that was used for this work consisted of a survey scan, an enhanced resolution scan, a check of pre-defined criteria that restricted the subsequent fragmentation of peptides, and product ion scans of the fragmentation products. This workflow was repeated throughout an experiment. The survey scan was done with the linear ion trap (LIT) that scanned a wide, user defined, m/z range. For this work, the m/z range was 400 to 1200 m/z. The m/z range was not set below 400 m/z to exclude a region that usually showed intense background signals. This survey scan was done using a fast scan rate of 4000 amu/sec. The IDA method had been set up to automatically choose the two most intense m/z peaks of the survey scan to perform an enhanced resolution scan on those masses. The enhanced resolution scan scanned ~ 30 amu ranges around the chosen m/zs at a slower rate of 250 amu/sec to achieve greater resolution of the ions of interest. This allowed the charge states (e.g. 1+, 2+, etc., or unknown) of the analytes to be determined. Next, this information was automatically submitted to the pre-

defined IDA selection criteria. The criteria could be set to, for example, perform MS-MS fragmentation only on analytes that showed charge states of 2+ ions or higher (apparently, noise peaks often have a 1+ charge state; hence, time is not wasted on noise peaks). In addition, a particular m/z could be excluded from being fragmented for a time of e.g. 60 sec if it had been fragmented in e.g. two cycles already. This allowed less intense ions to be chosen for fragmentation as well. Next, product ion scans were performed on the m/z s that had passed the IDA criteria. The analytes to be fragmented were selected in the first quadrupole, then they were fragmented in the second quadrupole, and the fragment ions were collected in the third quadrupole that acted as an ion trap. The fragments were then scanned out of the LIT and detected. The scan rate was chosen as 1000 amu/sec to enable fast, yet still reasonably resolved mass spectral acquisition. Fragmentation in the second quadrupole occurred because the gas pressure in that quadrupole was set to a higher value than in the first or third quadrupoles. The collision of the analyte ions with the gas molecules caused the analytes to fragment. The energy with which the analytes were propelled into the second quadrupole (by differentially applied voltages on the MS ion optics) was calculated by the Analyst software based on their charge states and their m/z values; hence the previous enhanced resolution scans. Better fragmentation of analytes could be obtained if their charge states and masses were known.

IDA experiments were performed with the pepsin bulk-digested cytochrome *C*. Bovine cytochrome *C* was identified, see **Figures 2-20 to 2-22**, after trying several different combinations of IDA criteria. One part of the Mascot report, **Figure 2-20**, lists significant hits, or identifications, of proteins, of which bovine cytochrome *C* was one.

Rabbit cytochrome *C* was also identified, probably based on homology between the two species. **Figure 2-20** also includes a histogram generated by Mascot that illustrates the overall probability-based scores for peptides and whether their identifications are random or not. Scores that lie to the right of the greenly-shaded area are not considered random, and therefore significant. **Figure 2-21** shows a more detailed part of the Mascot report, which gives the sequences of the identified peptides and their masses. If one clicks on the underlined numbers (e.g. 19, circled red in **Figure 2-21**), a presentation as in **Figure 2-22** is shown, which illustrates the theoretical fragment ion mass spectrum of the peptide, and indicates how many experimental fragment ion masses were matched to theoretical masses.

Earlier, it was mentioned that high CE peak efficiency is not crucial in CE-MS. This is illustrated in **Figure 2-23**, where the black lines in the XIEs for a mass ~ 672 amu indicate at which times the enhanced resolution scan (**A**), and the product ion scan (**B**) were recorded. The line in **B** indicates that most of the ions of this m/z had already migrated from the capillary. The product ion mass spectra can thus be of rather poor quality because of low ion intensities. This can hinder the matching of experimental product ion spectra to theoretical spectra of the databases (illustrated in **Figure 2-22**), and hence can make identification difficult.

2.IV. Conclusions

A one-dimensional instrument was developed that coupled CE separations to MS detection. The use of UV detection in front of the CE-MS interfaces, and MS detection after the interfaces, established that less band broadening was observed when using a

sheath flow CE-MS interface than a sheathless interface. To optimize the CE separation of peptides in what will later be the **second dimension** in 2D CE-microreactor-CE-MS experiments, cytochrome *C* samples were used that had been bulk solution-digested with either trypsin or pepsin. Initial experiments used uncoated fused silica capillaries and low ionic strength buffers. Peaks observed with these conditions were tailed and not very well resolved. Coating the capillaries with poly(vinyl alcohol) and using higher ionic strength buffers improved the peak shapes and resolution.

In addition, the use of batch acquisitions with the Q TRAP's Analyst software resulted in more stable baselines, and batch acquisitions were also used to obtain information dependent acquisition (IDA) data. IDA data were submitted to the protein database search engine Mascot, and bovine cytochrome *C* was identified.

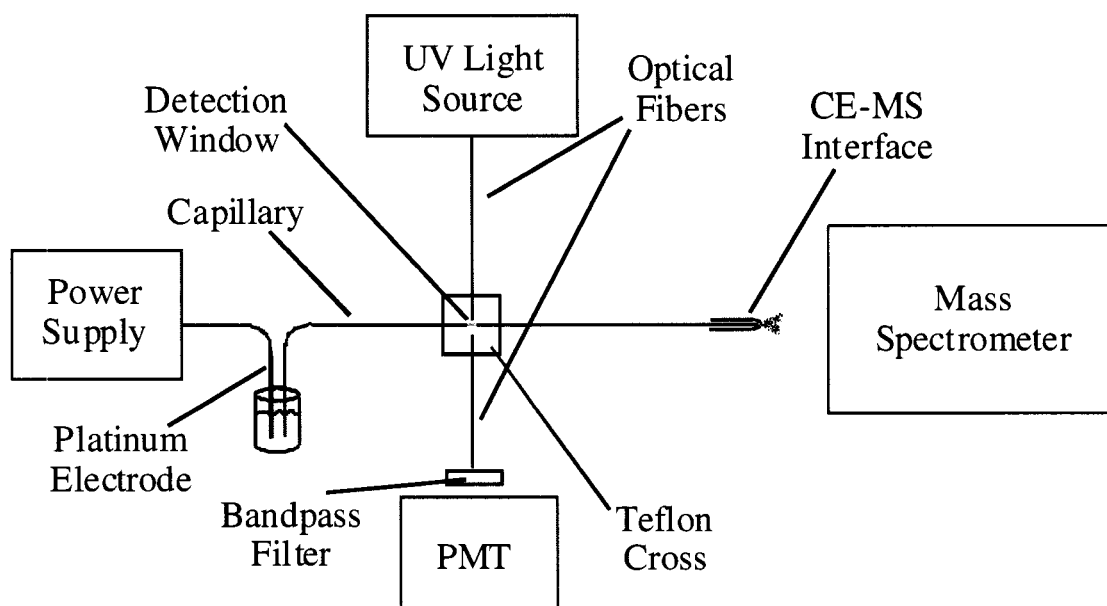


Figure 2-1. Schematic diagram of the 1D CE-UV-MS instrument with which the work with both the sheathless and sheath flow CE-MS interfaces was conducted. For a description, please see sections 2.II.B.1. and 2.II.B.2..

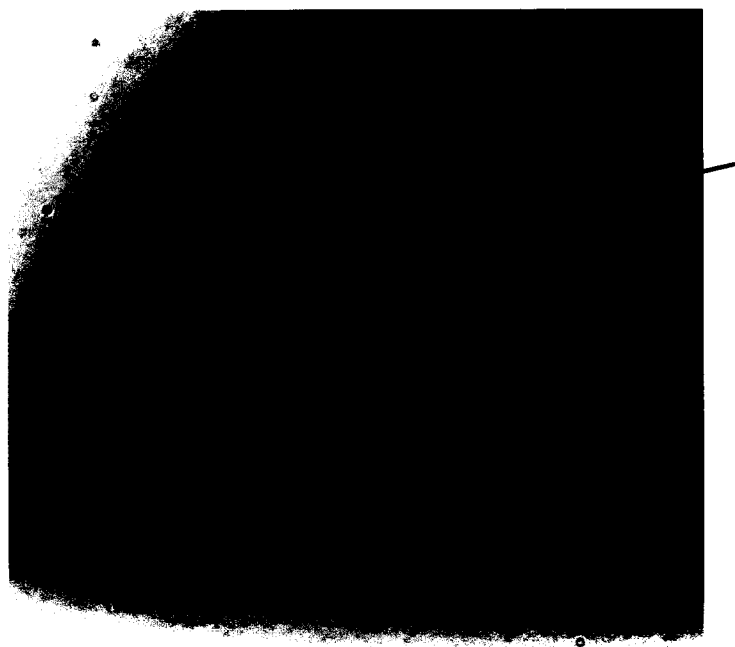


Figure 2-2. Head-on view of a UV fiber that has been cut square. The dark ring around the lighted fiber shows the polyimide coating of the fiber. The arrow points toward a dark line on the face of the fiber that indicates an unevenness. However, the rest of the surface seems smooth without defects.

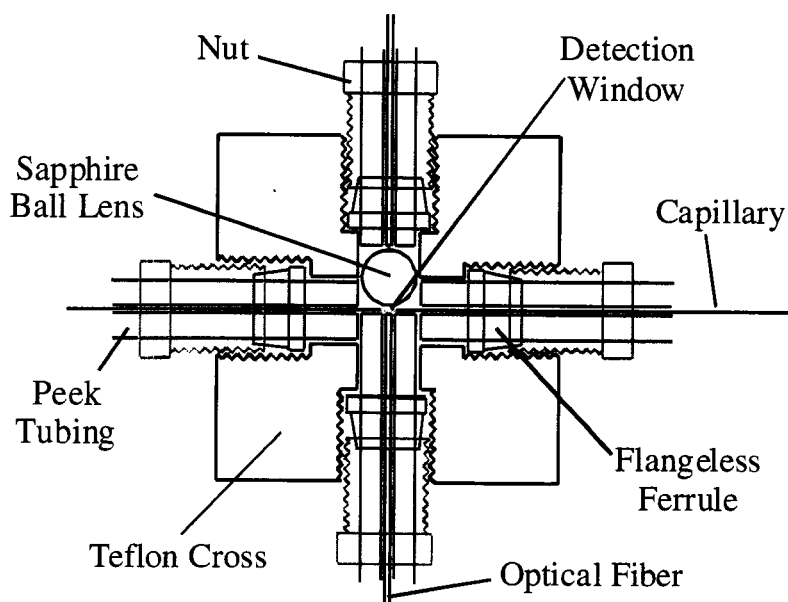


Figure 2-3. Schematic diagram of the CE-UV Teflon detection cross, based on a design by Wu *et al.*⁵ UV light comes through the optical fiber at the top and is directed onto the detection window of the separation capillary by a sapphire ball lens. The polyimide coating of the capillary has been partially burned off, or shaved off with a razor blade, to create the detection window. The light is collected on the opposite side of the capillary by another optical fiber that directs the light to the photomultiplier tube.

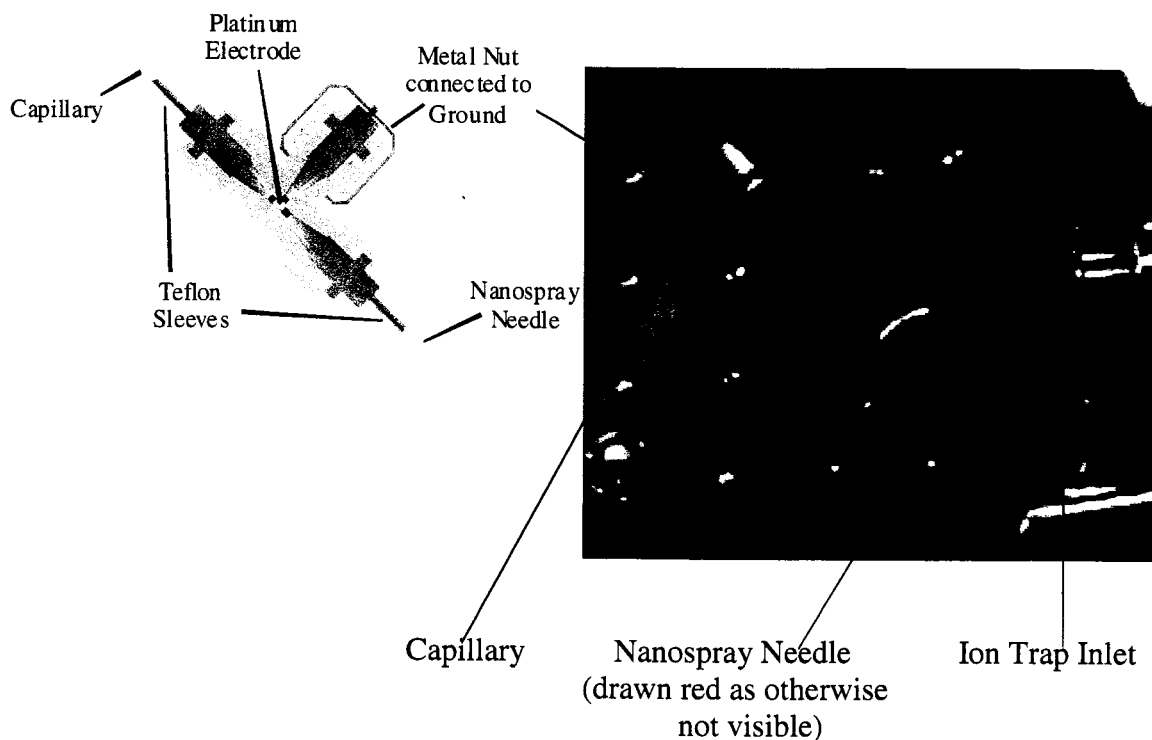
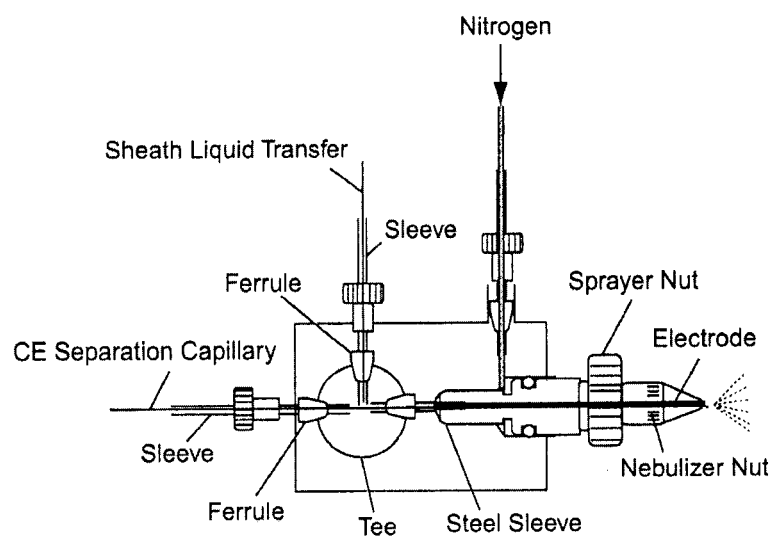


Figure 2-4. Schematic diagram and picture of the nanospray sheathless CE-MS interface. Adapted from a figure in *Upchurch Scientific 2002 Catalog of Chromatography & Fluid Transfer Components*, p.27, Micro Tee Model # P-775. The Micro Tee has been modified by New Objective, Inc. to include a platinum electrode. The digital picture shows the interface attached to the mini breadboard of the PicoViewTM nanospray platform. The ion trap inlet has a small orifice (not visible) into which the analyte is sprayed.



MicroIonSpray head configured for CE-MS

Figure 2-5. Schematic of the MicroIonSpray head that was used in the sheath flow CE-ESI-MS experiments. (Adapted from Applied Biosystems' *CE-MS Upgrade Kit Installation Guide*, 2003, p. 27)

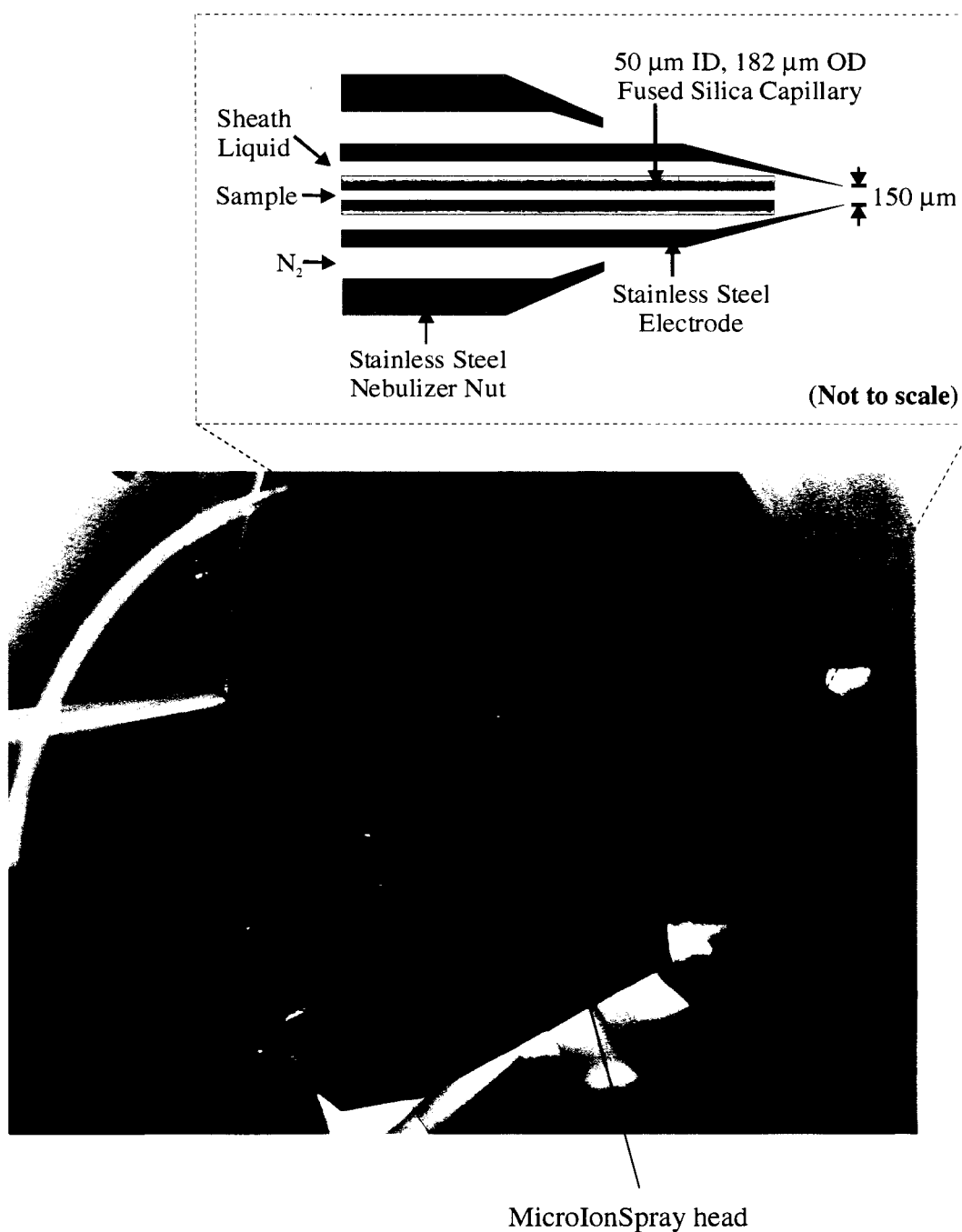


Figure 2-6. The photo shows the MicroIonSpray head in front of the MS orifice. The diagram shows the specifics of the front of the MicroIonSpray head (adapted from ¹⁰, pp. 174-5). See also **Figure 2-5** for specifics of the MicroIonSpray head.

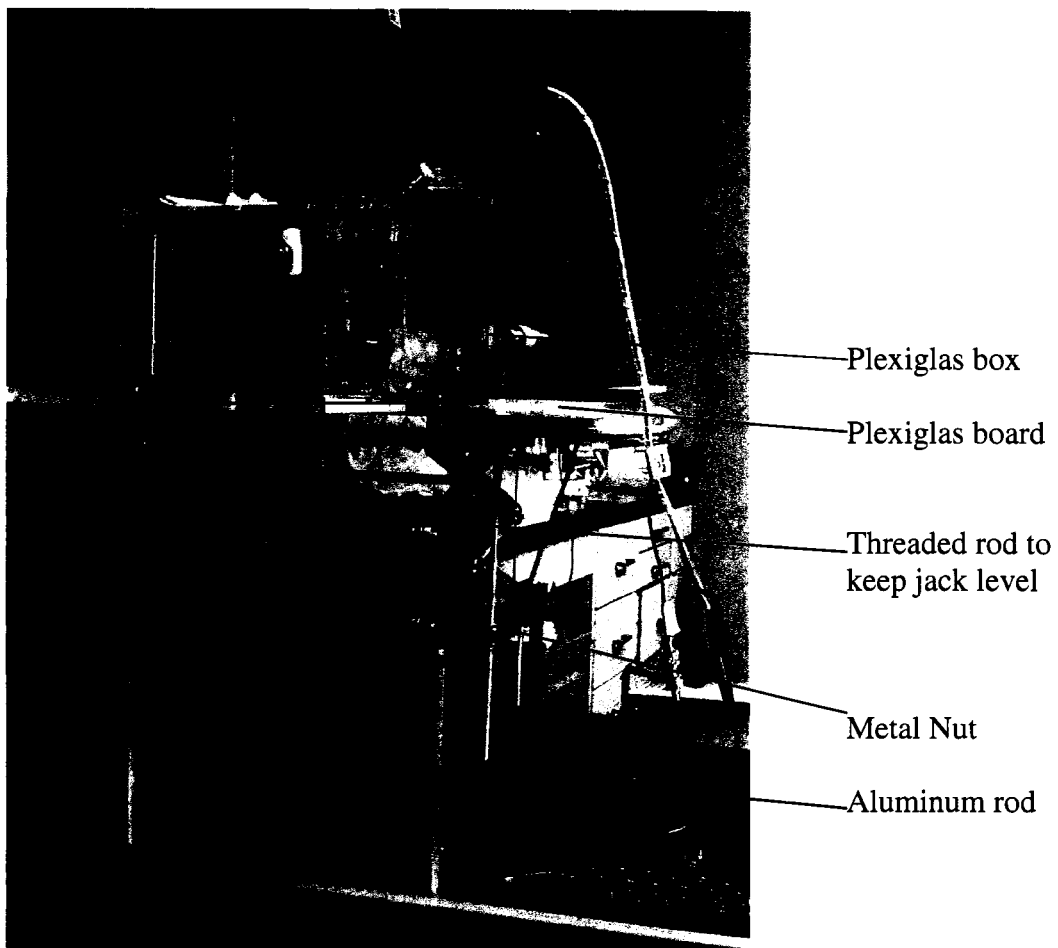


Figure 2-7. Picture showing the CE instrument in the Plexiglas box raised on aluminum rods and a jack. The liquid levels of the CE instrumentation needed to be the same as the inlet of the Q TRAP once the two systems were connected; hence, the CE instrumentation needed to be raised.

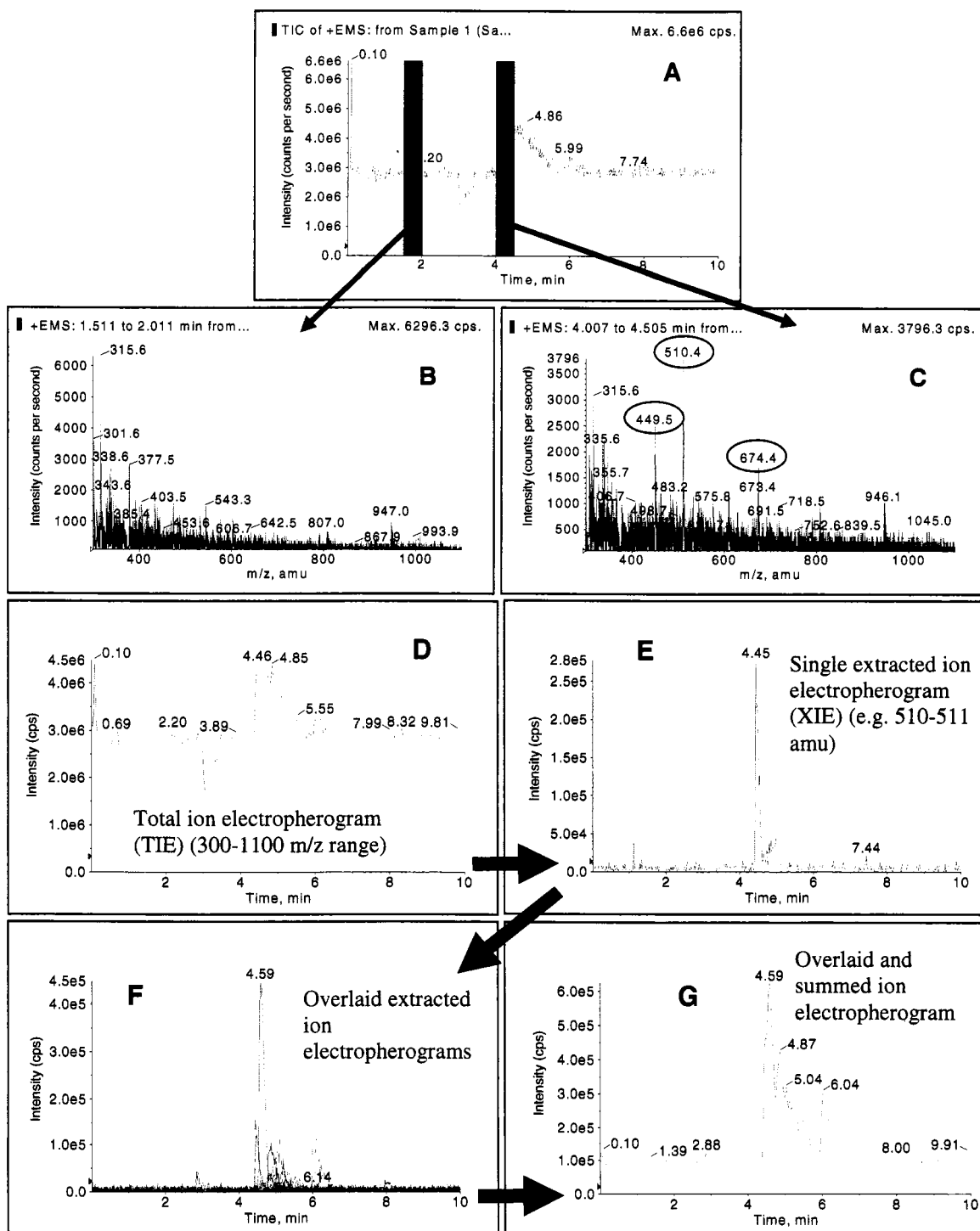


Figure 2-8. Diagram illustrating how CE-MS data were analyzed with the Analyst software. See section 2.II.F. for explanation.

Effect of Capillary Inner Diameters of Non-Tapered Capillaries in Place of ESI Needles

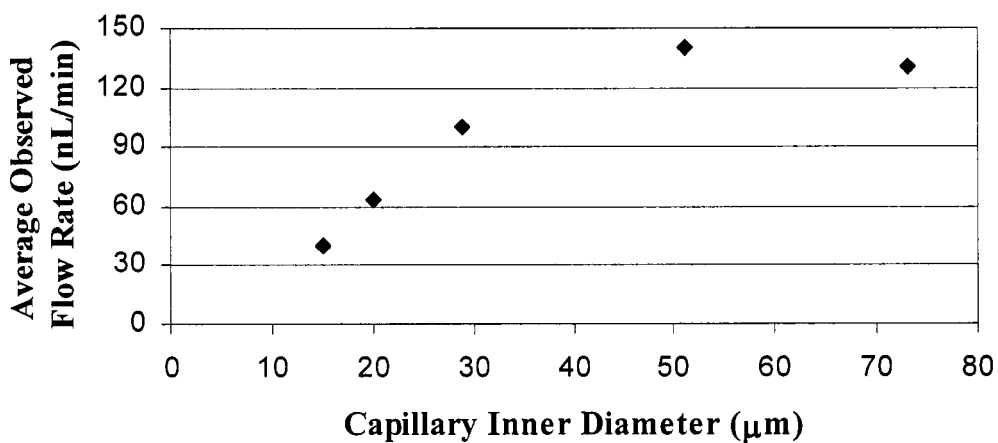


Figure 2-9. Effect of different inner diameters of short (~ 2 cm), non-tapered fused silica capillaries at the sheathless CE-MS interface in place of ESI needles. The inner diameter of the separation capillary was 50 μm. Experiments were carried out without the ion trap MS attached. As the inner diameter of the non-tapered capillaries decreased, the apparent flow rate decreased as well. This decrease in apparent flow rate presumably caused the instability of the electrospray since not enough liquid was supplied to the end of the capillary, or needle orifice, to establish a stable, continuous spray.

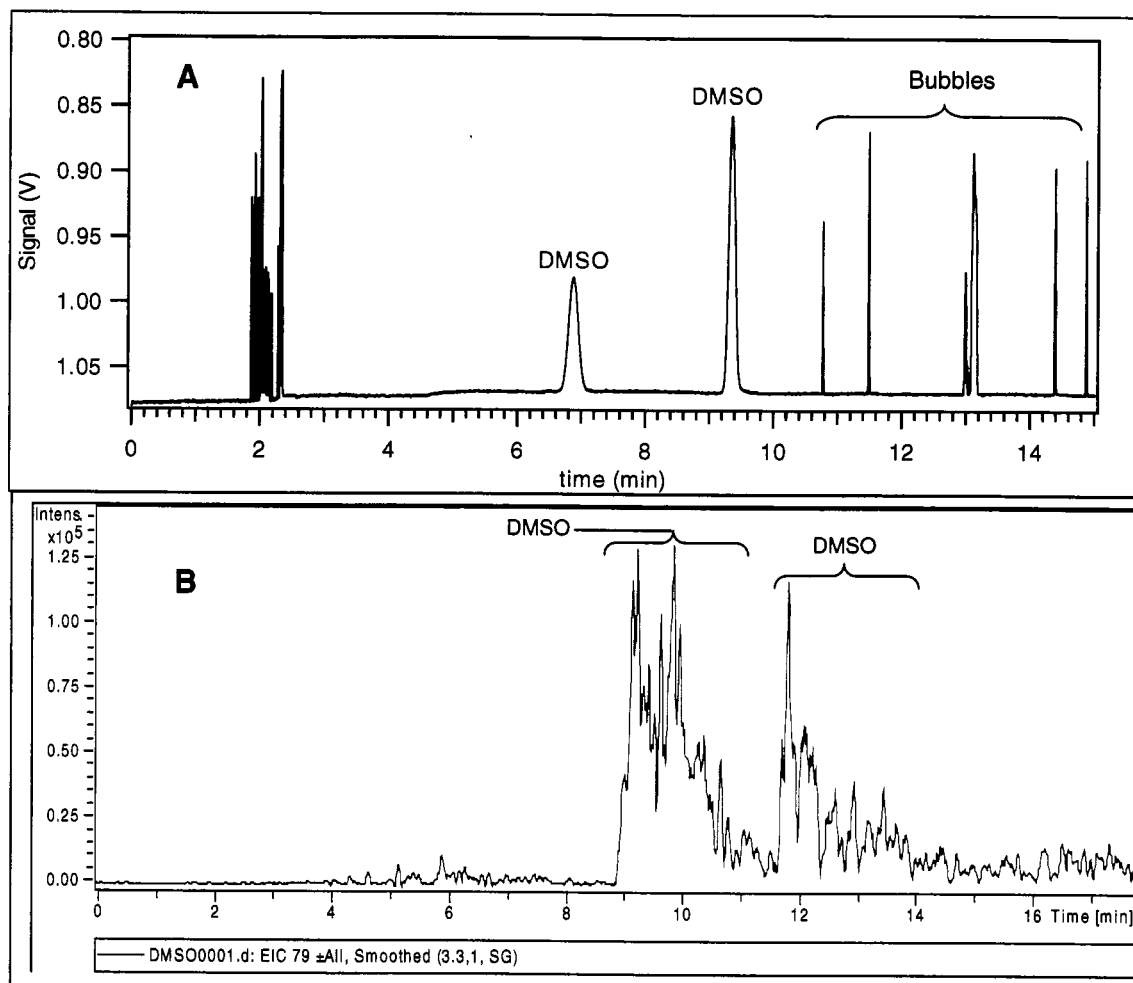


Figure 2-10. UV and MS electropherograms of 2% (v/v) dimethylsulfoxide (DMSO) (in running buffer) obtained with the sheathless CE-MS interface. Two DMSO peaks are observed because no DMSO eluted during a first, 10 min, run, and DMSO was then injected a second time. Hence, the effect of bubbles on the migration times can be seen. The peak tailing in **B** was most likely due to the dead volume of the sheathless CE-MS interface.

A) UV detection electropherogram. Capillary: 138 μm OD, 50 μm ID, 51 cm; length from capillary inlet to UV detector: 37 cm; buffer: 1.6 mM (ammonium) acetate in 25%-75% MeOH-ddH₂O (pH 5.0); injection voltage: 20 kV (392 V/cm) (3 sec); separation voltage: 20 kV (392 V/cm). Nanospray needle dimensions: 141 μm OD, 29 μm ID, 1.9 cm non-tapered fused silica capillary.

B) MS extracted ion electropherogram (79-80 amu) of the two DMSO peaks shown in **A**. MS: Three-dimensional ion trap (Bruker EsquireTM). Nanospray needle at ground. MS orifice voltage: 2500 V.

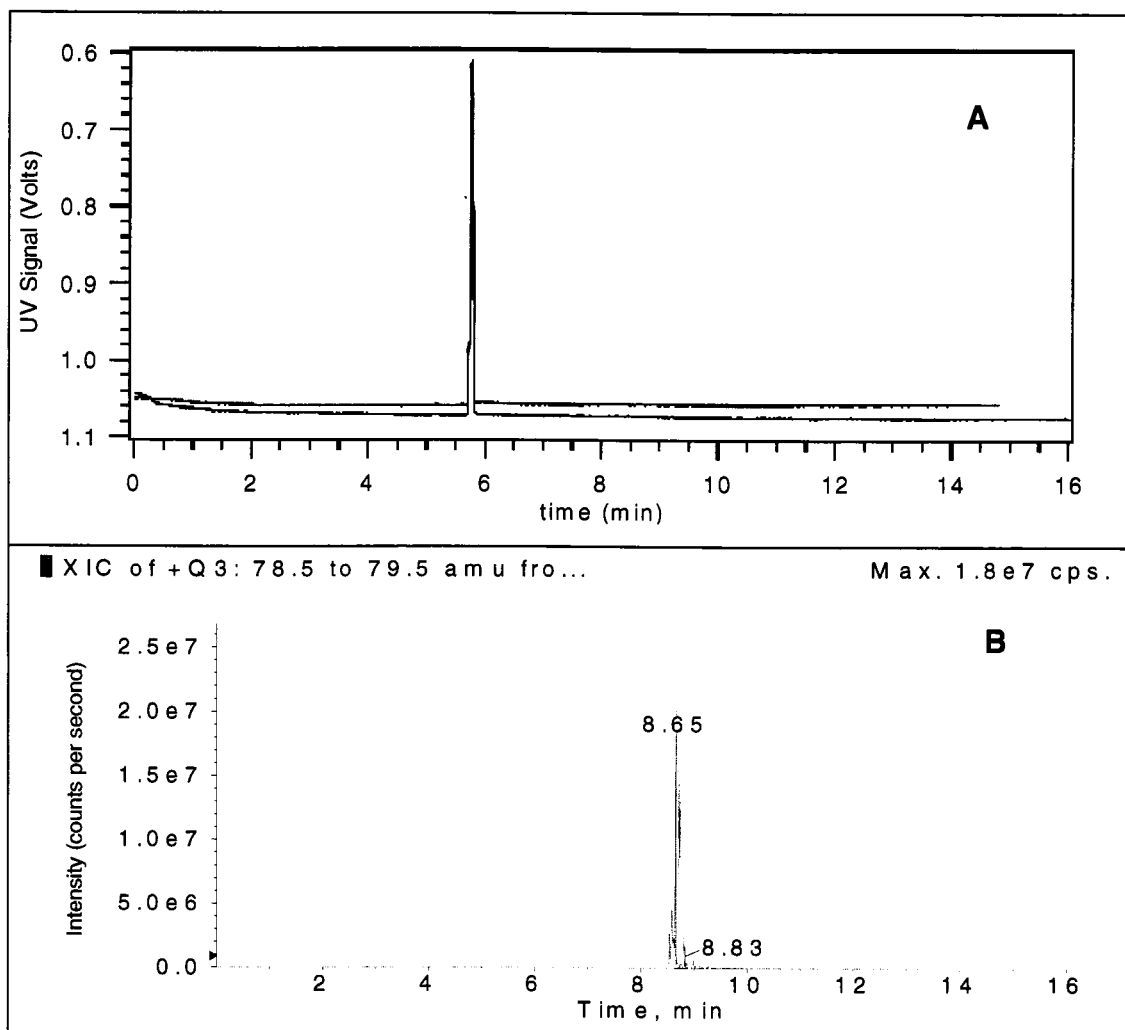


Figure 2-11. UV and MS electropherograms of 4% (v/v) DMSO (in running buffer) obtained using the sheath flow CE-MS interface. Two electropherograms were overlaid to show repeatability.

A) Two UV detection electropherograms overlaid. Capillary: 182 μm OD, 50 μm ID, 60 cm; length from capillary inlet to UV detector: 40 cm; buffer: 1.6 mM (ammonium) acetate in 25%-75% MeOH-ddH₂O (pH 5.0); injection voltage: 10 kV (167 V/cm) (3 sec); the IS voltage was off during injection; separation voltage: 23 kV (338 V/cm).

B) Two MS extracted ion electropherograms (78.5-79.5 amu) overlaid. MS: Q3+ mode of the triple quadrupole-linear ion trap (Q TRAP). IS voltage: 2750 V. Sheath liquid: 50%-50%-0.1% MeOH-ddH₂O-formic acid. Sheath flow rate: 700 nL/min.

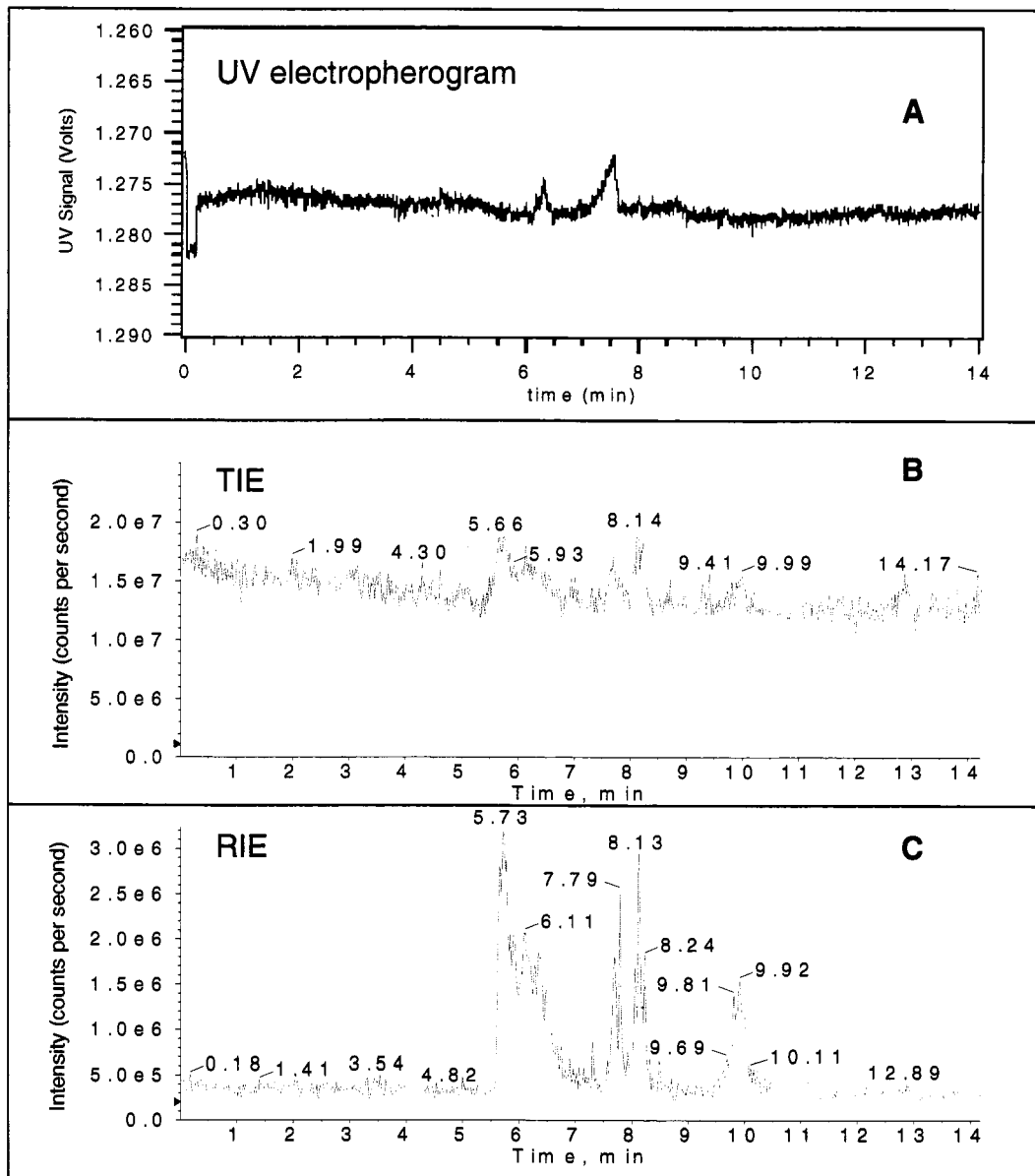


Figure 2-12. CE-UV-ESI-MS experiment with trypsin bulk-digested cytochrome C (60 μ M in 2% ACN-0.1% TFA) using an uncoated fused silica capillary.

Capillary: 182 μ m OD, 50 μ m ID, 60 cm length; length from capillary inlet to UV detector: 40 cm; **buffer:** 1.6 mM (ammonium) acetate in 25%-75% MeOH-ddH₂O (pH 5.0); **sheath liquid:** 75%-24.9%-0.1% isopropanol-ddH₂O-formic acid (900 nL/min); Injection voltage: +15.0 kV (250 V/cm) (3 sec); the IS voltage was off during injection; separation voltage: +23.0 kV (340 V/cm); **MS parameters:** Q3+ scan mode; IS voltage: 2575 V; CUR: 20.0; GS1: 0.0; m/z range: 150-1300 amu (scanned over 0.7 sec); step size: 0.1 amu; declustering potential: 50 V; entrance potential: 10 V.

A) UV detection. **B)** Total ion electropherogram (TIE). **C)** Reconstructed ion electropherogram (RIE).

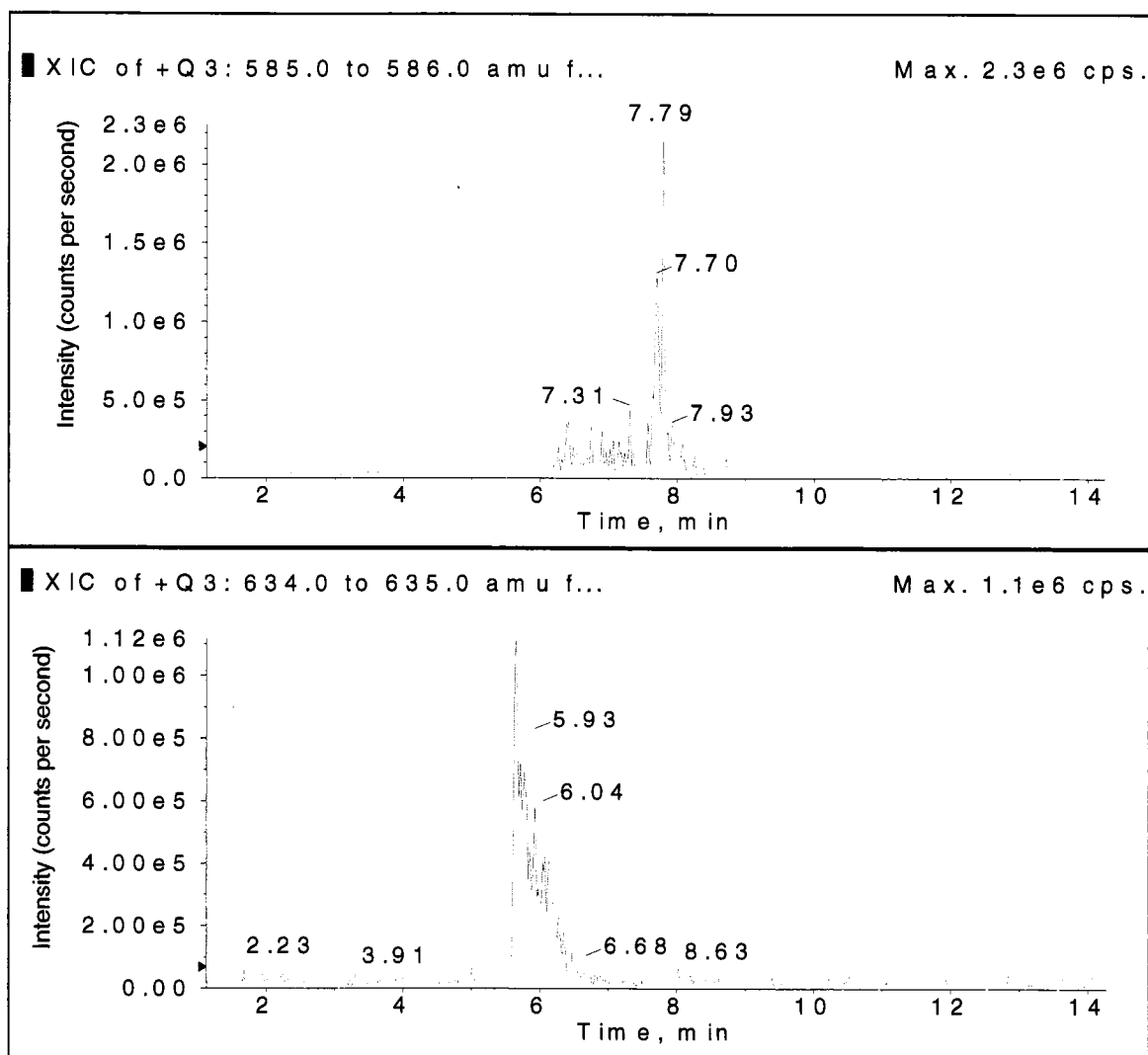
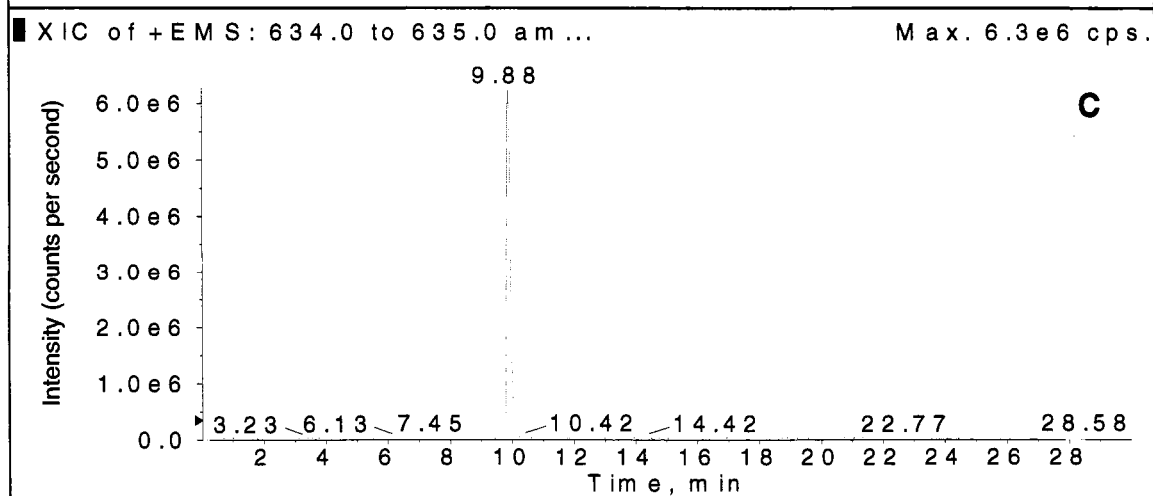
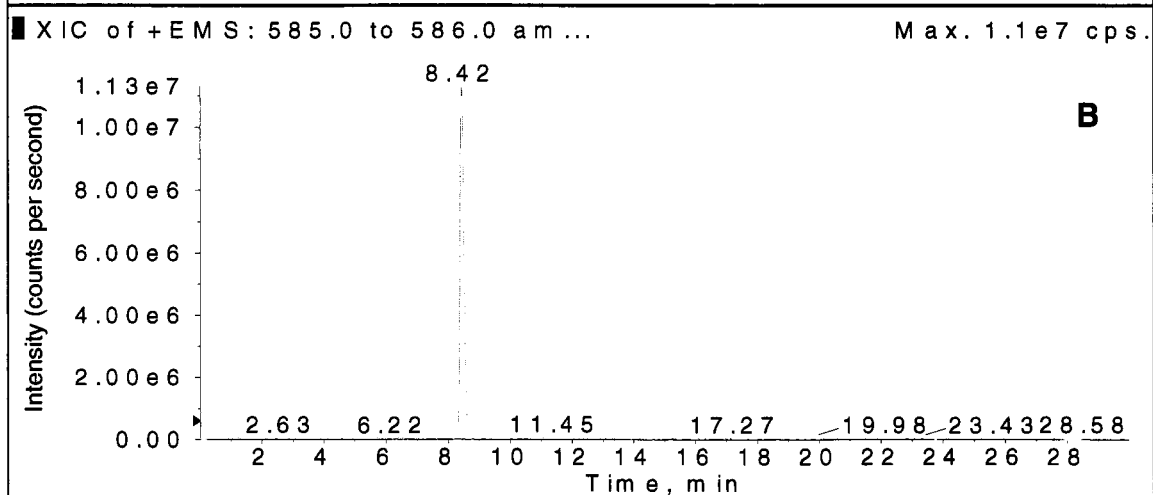
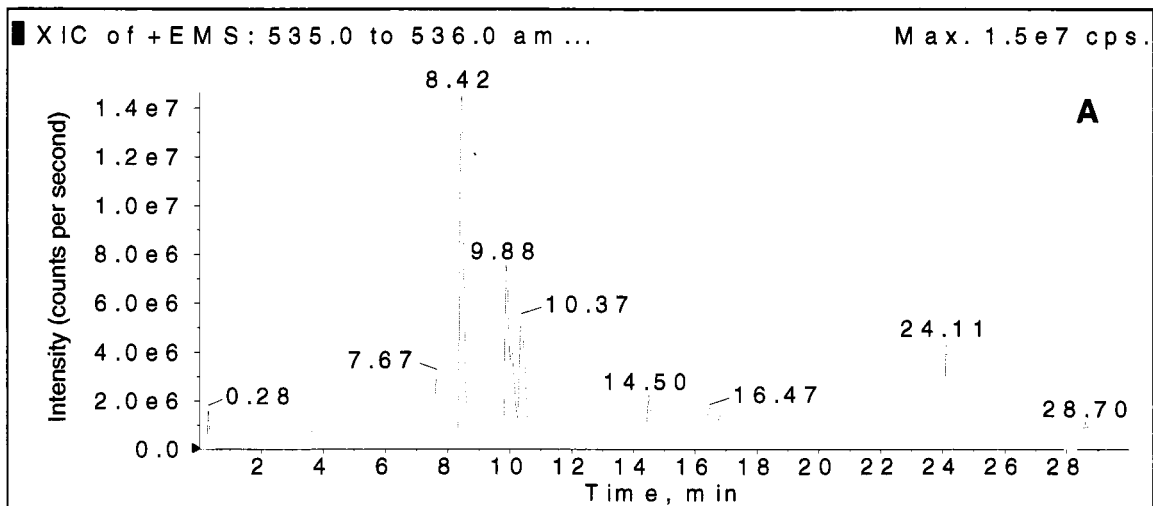


Figure 2-13. 2 XIEs from electropherogram in **Figure 2-12**. Compare to the 2 XIEs given in **Figure 2-14**.

Figure 2-14. Separation of trypsin bulk-digested cytochrome *C* using a PVA-coated capillary and 100 mM (ammonium) acetate (pH 4.0). Compare to **Figures 2-12** and **2-13**.

A) Total ion electropherogram. **B)** and **C)** Extracted ion electropherograms (1x Gaussian smoothed)

Capillary: 182 μm OD, 50 μm ID, 41.5 cm length; **buffer:** 100 mM (ammonium) acetate (pH 4.0); **sheath liquid:** 90% MeOH (1000 nL/min); **CE parameters:** Injection voltage: +15.0 kV (361 V/cm) (5 sec); the IS voltage was off during injection; separation voltage: +13.5 kV (277 V/cm); **MS parameters:** LIT scan mode; IS voltage: 2275 V; CUR: 15.0; GS1: 0.0; m/z range: 300-1100 amu; scan rate: 1000 amu/sec; declustering potential: 30 V; entrance potential: 10 V. **Sample:** 60 μM cytochrome *C* (bulk-digested with trypsin) in 2% ACN-0.1% TFA.



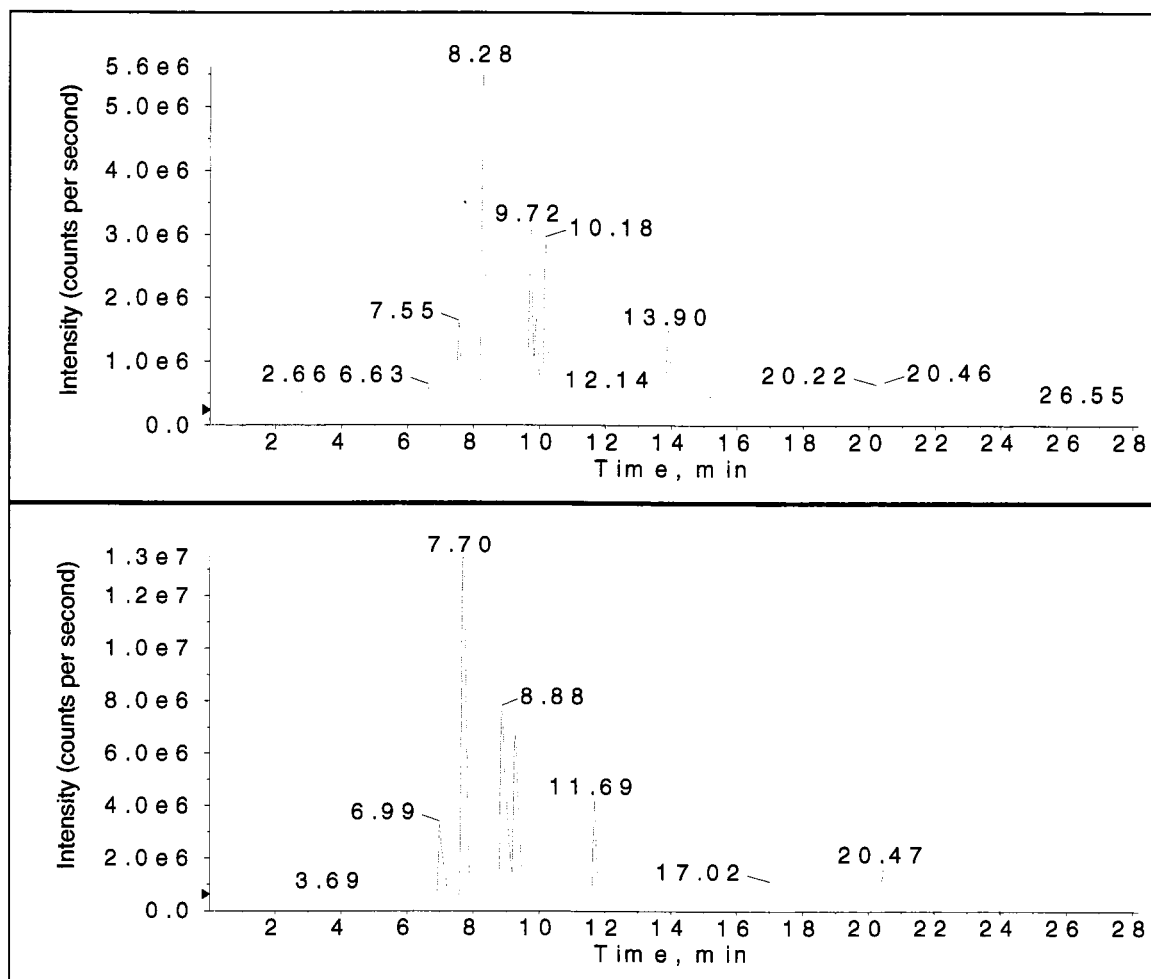


Figure 2-15. Two electropherograms of experiments run on the same day.

Capillary: 182 μm OD, 50 μm ID, 41.5 cm length; **buffer:** 100 mM (ammonium) acetate (pH 4.0); **sheath liquid:** 90% MeOH (1000 nL/min); **CE parameters:** Injection voltage: +5.0 kV (120 V/cm) (5 sec); the IS voltage was off during injection; separation voltage: +13.8 kV (278 V/cm); **MS parameters:** LIT scan mode; IS voltage: 2275 V; CUR: 15.0; GS1: 0.0; m/z range: 300-1100 amu; scan rate: 1000 amu/sec; declustering potential: 30 V; entrance potential: 10 V. **Sample:** 60 μM cytochrome C (bulk-digested with trypsin) in 2% ACN-0.1% TFA.

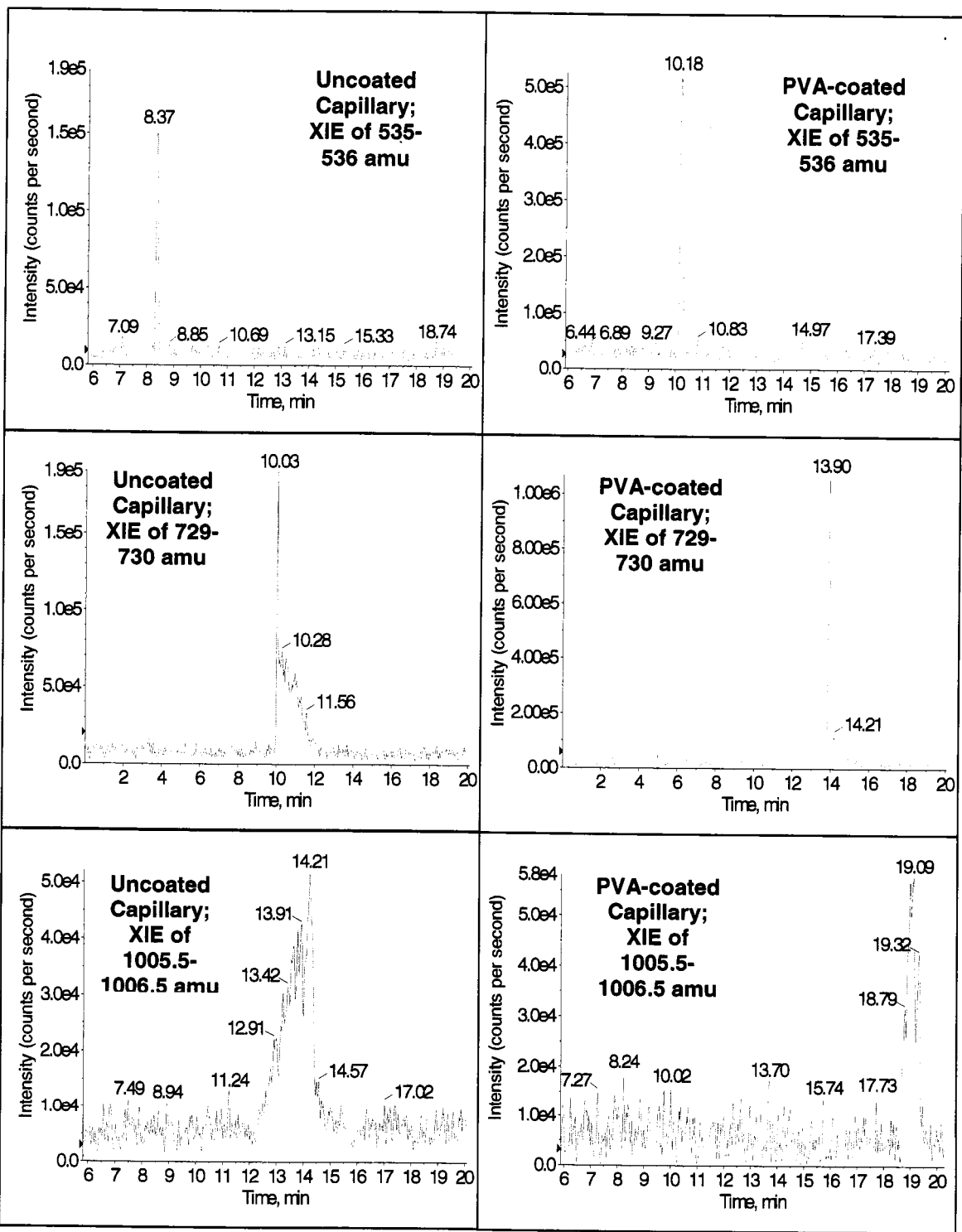
Figure 2-16. On the right, three XIEs from an experiment that used a PVA-coated capillary. On the left, three XIEs from an experiment that used an uncoated capillary. All XIEs were 1x Gaussian smoothed.

PVA-coated capillary experiment:

Capillary: 182 μm OD, 50 μm ID, 41.5 cm length; **buffer:** 100 mM (ammonium) acetate (pH 4.0); **sheath liquid:** 90% MeOH (1000 nL/min); **CE parameters:** Injection voltage: +5.0 kV (120 V/cm) (3 sec); the IS voltage was off during injection; separation voltage: +13.8 kV (278 V/cm); **MS parameters:** LIT scan mode; IS voltage: 2275 V; CUR: 15.0; GS1: 0.0; m/z range: 300-1100 amu; scan rate: 1000 amu/sec; declustering potential: 30 V; entrance potential: 10 V. **Sample:** 60 μM cytochrome *C* (bulk-digested with trypsin) in 2% ACN-0.1% TFA.

Uncoated capillary experiment:

Capillary: 182 μm OD, 50 μm ID, 41.7 cm length; **buffer:** 100 mM (ammonium) acetate (pH 4.0); **sheath liquid:** 90% MeOH (1000 nL/min); **CE parameters:** Injection voltage: +10.0 kV (240 V/cm) (3 sec); the IS voltage was off during injection; separation voltage: +13.8 kV (277 V/cm); **MS parameters:** LIT scan mode; IS voltage: 2250 V; CUR: 15.0; GS1: 0.0; m/z range: 300-1100 amu; scan rate: 1000 amu/sec; declustering potential: 30 V; entrance potential: 10 V. **Sample:** 60 μM cytochrome *C* (bulk-digested with trypsin) in 2% ACN-0.1% TFA.



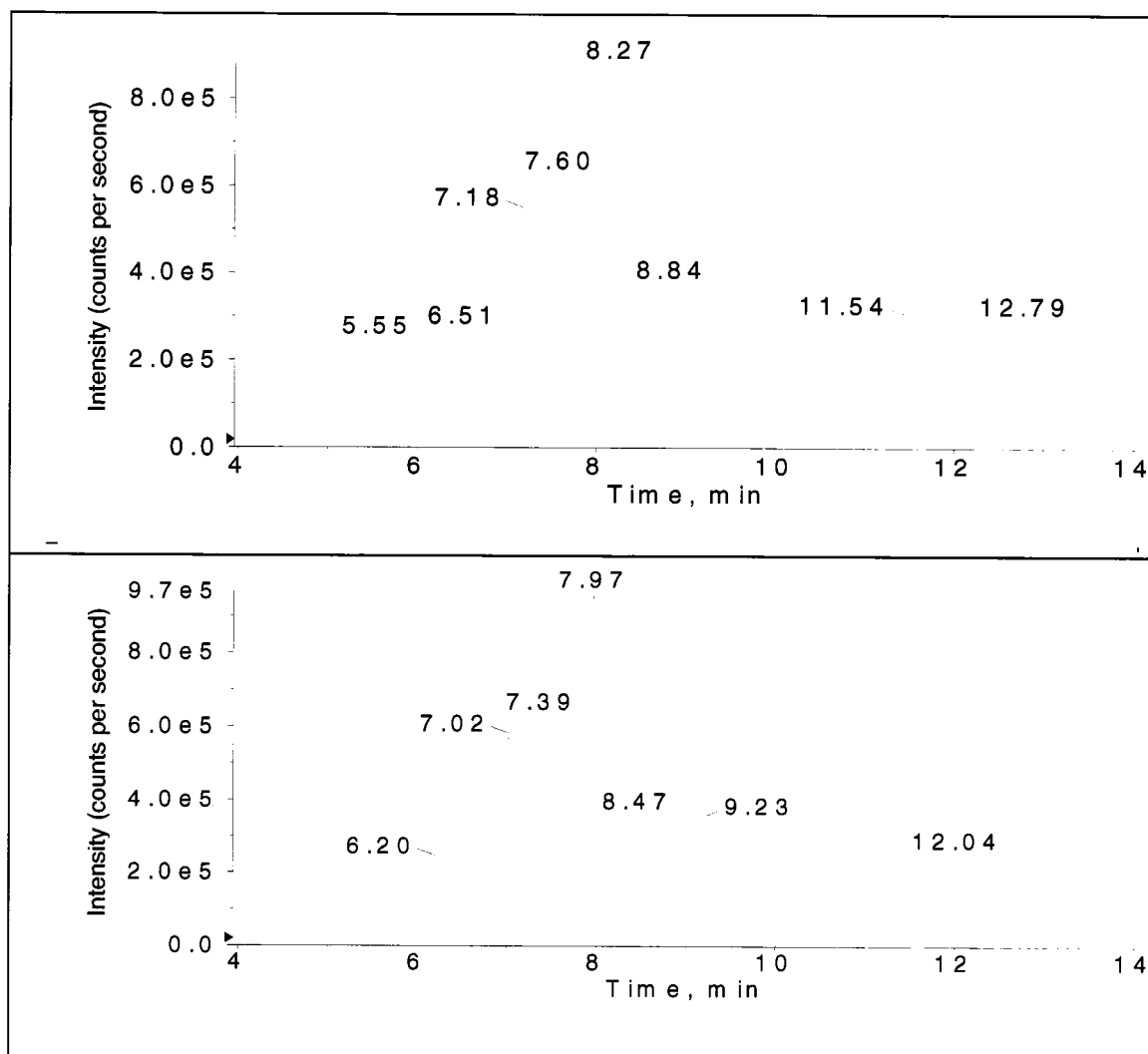


Figure 2-17. Two consecutive separations of a cytochrome *C* sample that was pepsin bulk-digested.

Capillary: 182 μm OD, 50 μm ID, 41.7 cm length; **buffer:** 50 mM (ammonium) acetate (pH 4.0); **sheath liquid:** 90% MeOH (1000 nL/min); **CE parameters:** Injection voltage: +10.0 kV (240 V/cm) (5 sec); the IS voltage was off during injection; separation voltage: +13.8 kV (278 V/cm); **MS parameters:** LIT scan mode; IS voltage: 2200 V; CUR: 15.0; GS1: 0.0; m/z range: 300-1100 amu; scan rate: 1000 amu/sec; declustering potential: 30 V; entrance potential: 10 V. **Sample:** 60 μM cytochrome *C* (bulk-digested with pepsin) in 2% ACN-0.1% TFA.

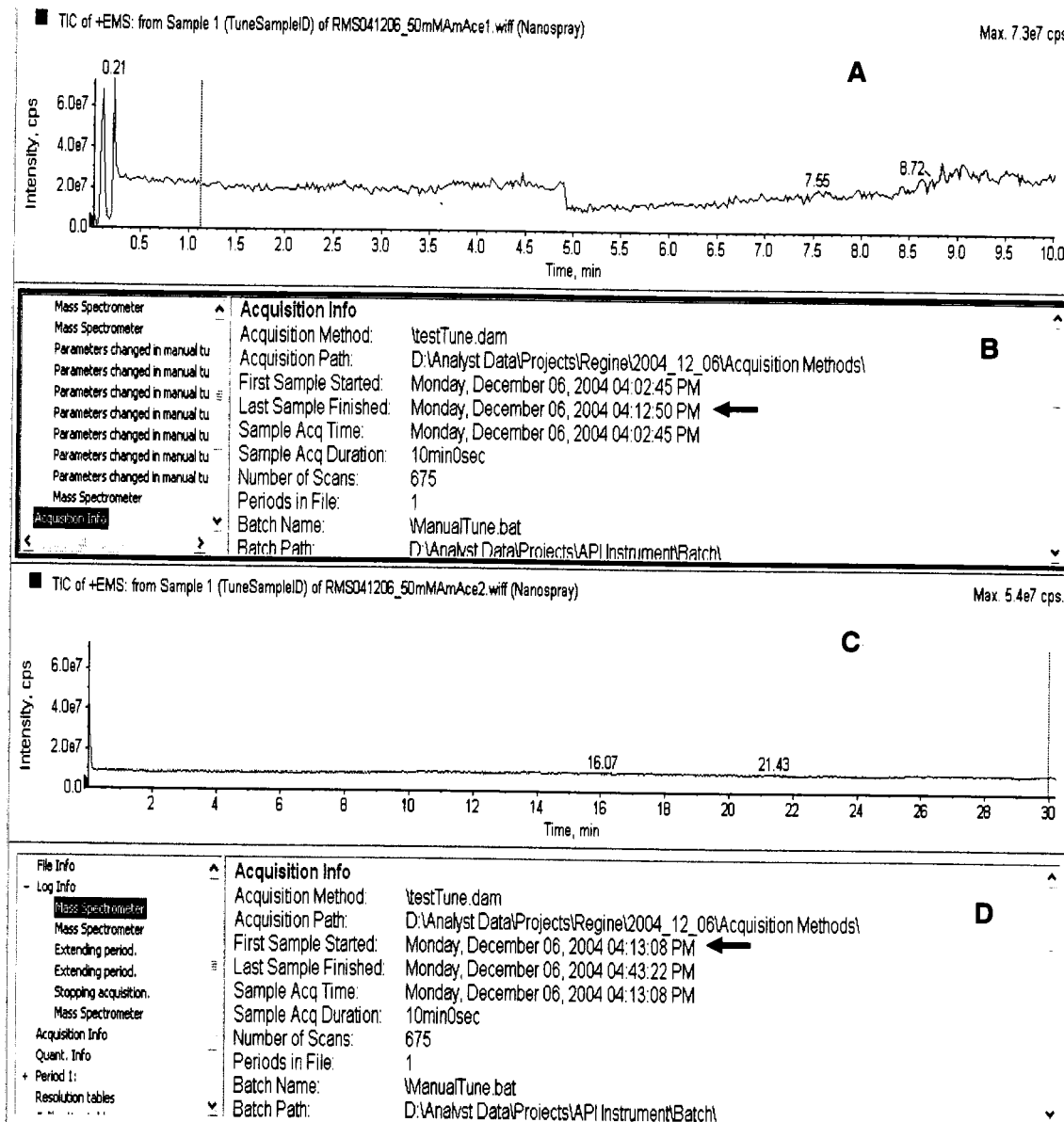
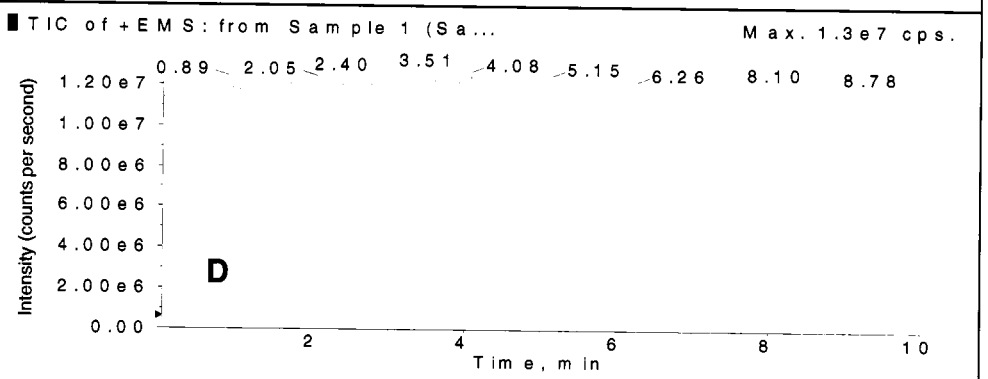
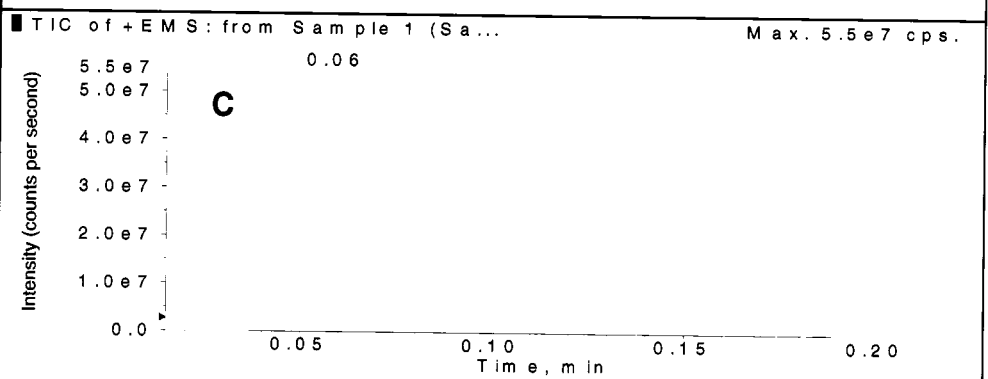
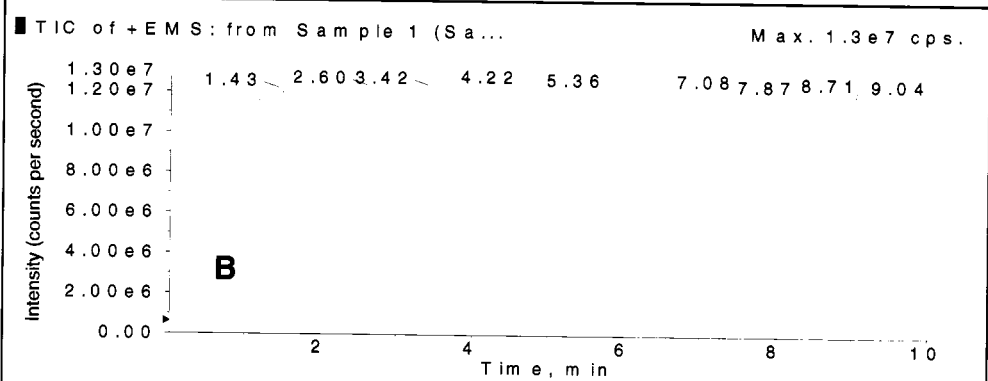
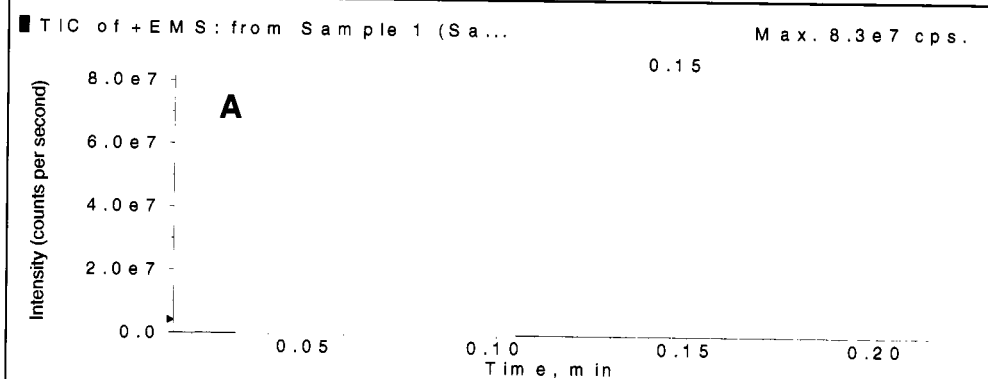


Figure 2-18. Baselines obtained with running buffer before (A) and after (C) data acquisition had stopped and a new data acquisition had begun. B and D show the acquisition information panes for both acquisitions and the arrows indicate their stop and start times. Neither the CE voltage nor the NFM flow had been stopped.

Figure 2-19. Electropherograms for two consecutive blank experiments using batch acquisition in the Analyst software. **A** and **C** illustrate the TIEs of the 0.2 min preruns; **B** and **D** illustrate the baselines of the runs that were automatically started after the preruns using the acquisition batch feature of Analyst.



(MATRIX)
(SCIENCE)

Mascot Search Results

User : Regine Schoenherr
 Email : reginems@u.washington.edu
 Search title : D:\Analyst Data\Projects\Regine\2004_12_14\Data\RMS041214_cytCdigPep1.f
 MS data file : C:\DOCUME~1\MSUser\LOCALS~1\Temp\mas3.tmp
 Database : SwissProt 45.3 (212217 sequences; 96518935 residues)
 Taxonomy : Mammalia (mammals) (73018 sequences)
 Timestamp : 16 Dec 2004 at 20:45:06 GMT
 Significant hits: P00008 (CYC_RABIT) Cytochrome c Cytochrome c
 F62894 (CYC_BOVIN) Cytochrome c Cytochrome c ←

Probability Based Mowse Score

Ions score is $-10 \cdot \log(P)$, where P is the probability that the observed match is a random event.
 Individual ions scores > 3.4 indicate identity or extensive homology ($p < 0.05$).
 Protein scores are derived from ions scores as a non-probabilistic basis for ranking protein hits.

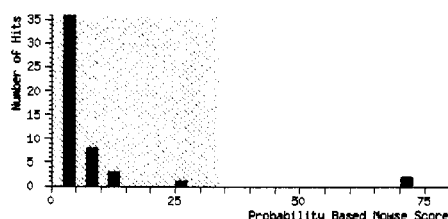


Figure 2-20. Screen capture of Mascot Search Results for trypsin bulk-digested cytochrome C. Data were collected with the Information Dependent Acquisition feature of the Analyst software.

CE parameters: buffer: 50 mM (ammonium) acetate (pH 4.0); capillary: PVA-coated, 48 μ m ID, 142 μ m OD, 41.8 cm; injection: +10.0 kV (240 V/cm) (5 sec); the IS voltage was off during injection; running voltage: +13.8 kV (278 V/cm); sheath liquid: 90% MeOH at 1000 nL/min.

MS parameters: for survey scans: IS voltage: 2200V; CUR: 15.0; GS1: 0.0; m/z range: 400-1200 amu; scan rate: 4000 amu/sec. For enhanced resolution scans: same as for survey scan, except m/z range was set based on the m/z peak selected, and scan rate: 250 amu/sec. For enhanced product ion scans: same as for survey scan, except m/z range: 100-1700 amu; scan rate: 1000 amu/sec. IDA criteria: the 2 most intense mass peaks (with intensities $> 50,000$ counts per second) were selected in the 400-1200 amu range of the survey scans; ions with 2+ to 5+, or unknown, charge states were submitted for fragmentation; ions that had been fragmented twice were excluded from fragmentation for 60 sec. For all scans, two m/z range scans were collected and summed before going on to the next scan. One cycle lasted 8.1182 sec.

Sample: 60 μ M cytochrome C, bulk digested with pepsin, in 2% ACN-0.1% TFA; The arrow indicates the bovine cytochrome C identification.

Mascot search parameters: PepsinA chosen as enzyme; database searched: SwissProt; allow up to 1 missed cleavages; peptide mass tolerance: ± 0.5 Da; MS/MS mass tolerance: ± 0.3 Da; monoisotopic mass; instrument used: ESI-QUAD.

Peptide Summary Report

Peptide Summary

Significance threshold $p < 0.05$ Max. number of hits AUTO

Standard scoring ☒ MudPIT scoring ☐ Ions score cut-off 0 Show sub-sets ☐

Show pop-ups ☒ Suppress pop-ups ☐ Sort unassigned Decreasing Score Require bold red ☐

☐ Error tolerant

- P00008** Mass: 11553 Score: 71 Queries matched: 2
 (CYC_RABIT) Cytochrome c Cytochrome c
☐ Check to include this hit in error tolerant search

Query	Observed	Mr(expt)	Mr(calc)	Delta	Miss	Score	Expect	Rank	Peptide
<input checked="" type="checkbox"/> 19	575.98	1149.95	1149.64	0.32	1	36	0.056	1	IAYLKKATNE
<input checked="" type="checkbox"/> 29	672.59	1343.17	1342.76	0.41	0	35	0.084	1	AGIKKKDERADL
- P62894** Mass: 11565 Score: 71 Queries matched: 2
 (CYC_BOVIN) Cytochrome c Cytochrome c
☐ Check to include this hit in error tolerant search

Query	Observed	Mr(expt)	Mr(calc)	Delta	Miss	Score	Expect	Rank	Peptide
<input checked="" type="checkbox"/> 19	575.98	1149.95	1149.64	0.32	1	36	0.056	1	IAYLKKATNE
<input checked="" type="checkbox"/> 29	672.59	1343.17	1342.76	0.41	0	35	0.084	1	AGIKKKGEREDL

Proteins matching the same set of peptides:
P62895 Mass: 11565 Score: 71 Queries matched: 2
 (CYC_PIG) Cytochrome c Cytochrome c
P62896 Mass: 11565 Score: 71 Queries matched: 2
 (CYC_SHEEP) Cytochrome c Cytochrome c

Figure 2-21. Screen capture of the Mascot Search Results listing the protein identifications and the peptides upon which the identifications were made.

{MATRIX}
{SCIENCE}

Mascot Search Results

Peptide View

MS/MS Fragmentation of IAYLK~~K~~ATNE

Found in P62894, (CYC_BOVIN) Cytochrome c Cytochrome c

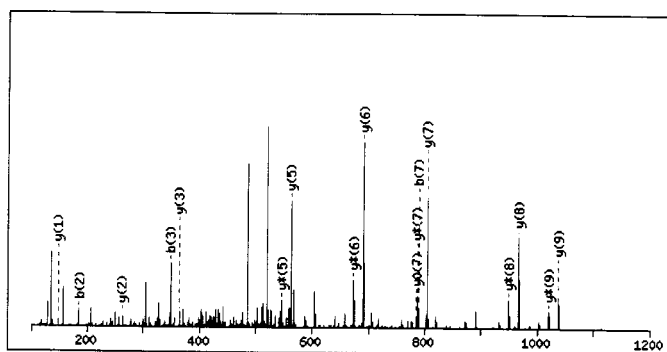
Match to Query 19: 1149.954799 from(575.984675,2+)

Elution from: 7.8 to 7.8 period: 0 experiment: 2 cycles: 1

From data file C:\DOCUME~1\MSUser\LOCALS~1\Temp\mas3.tmp

Click mouse within plot area to zoom in by factor of two about that point

Or, 100 to 1200 Da



Monoisotopic mass of neutral peptide $M_r(\text{calc})$: 1149.6393

Ions Score: 36 Expect: 0.056

Matches (Bold Red): 17/84 fragment ions using 53 most intense peaks



Figure 2-22. Screen capture of the individual fragment mass spectrum when selecting Query # 19 (circled in **Figure 2-21**) of the IAYLK~~K~~ATNE peptide. 17 of the experimental fragment ion masses were matched with 84 theoretical fragment ion masses.

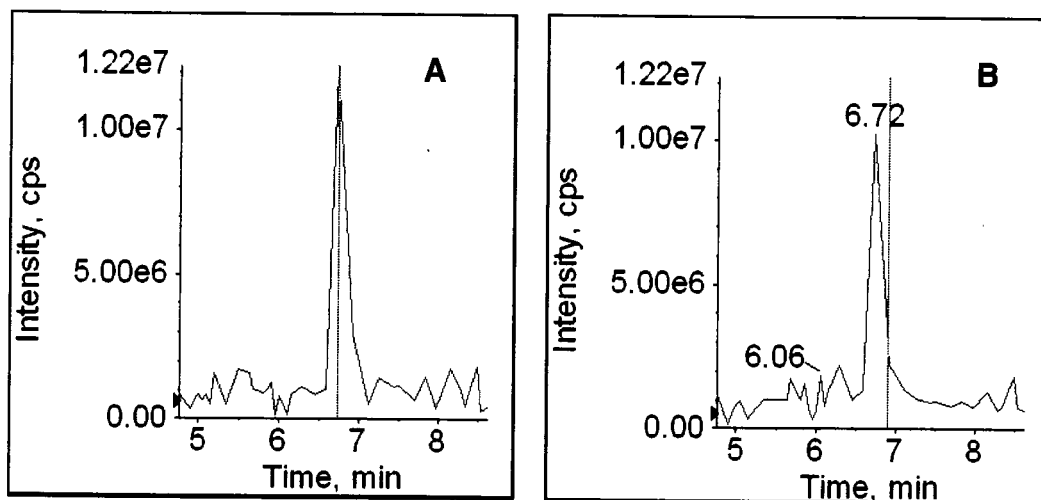


Figure 2-23. Illustration that obtaining high peak efficiencies in CE-MS-MS is not crucial. Two XIEs of ~ 672 amu obtained during an IDA run of pepsin bulk-digested cytochrome *C*. The black line in **A** indicates at which time this m/z had been selected for an enhanced resolution scan. The black line in **B** indicates at which time the spectrum of the enhanced product ion scan was recorded after the m/z passed the IDA criteria; most of the peak had already eluted from the CE capillary. The product ion mass spectra are thus of rather poor quality because of low intensities. This can hinder the matching of experimental product ion spectra to theoretical spectra of the databases (illustrated in **Figure 2-22**), and hence can make identification difficult.

Table 2-1. Pin assignments for the 50-pin ribbon cable between the National Instruments data acquisition board and the hardware wiring for 1D CE-UV-MS experiments.

Hardware Assignment	50-Pin Connector Pin Numbers	MIO-16 Series Signal Names	MIO-16E Series Signal Names
PMT Signal (+)	3	ACH0	ACH0
PMT Signal (-)	4	ACH8	ACH8
CE Current (+)	13	ACH5	ACH5
CE Current (-)	14	ACH13	ACH13
CE Voltage Control	20	DAC0	DAC0OUT
PMT Control	21	DAC1	DAC1OUT
Analog Output Ground	23	AOGND	AOGND

Table 2-2. 19 and 20 extracted ion electropherogram (XIE) masses that yielded the most intense peaks for the trypsin- and pepsin-digested cytochrome *C* peptides, respectively.

19 XIEs for Trypsin-digested Cytochrome <i>C</i>						
400-499 amu	500-599 amu	600-699 amu	700-799 amu	800-899 amu	900-999 amu	1000-1099 amu
434-435	521-522	607.5-608.5	729-730	799.5-800.5	964.5-	1005.5-
483-484	535-536	628.5-629.5	779-780		965.5	1006.5
489-490	585-586	634-635	793-794			
494-495		648-649				
		678-679				
		685.5-686.5				
20 XIEs for Pepsin-digested Cytochrome <i>C</i>						
400-499 amu	500-599 amu	600-699 amu	700-799 amu	800-899 amu	900-999 amu	1000-1099 amu
449-450	511.5-512.5	620-621	700.5-701.5	803-804	972-973	1037.5-
485-486	536-537	648.5-649.5	736.5-737.5	842.5-843.5		1038.5
495.5-496.5	554-555	672.5-673.5	765.5-766.5	891-892		
	576.5-577.5					
	582.5-583.5					
	594.5-595.5					

2.V. Notes to Chapter 2

- (1) Olivares, J. A.; Nguyen, N. T.; Yonker, C. R.; Smith, R. D. *Anal Chem* **1987**, *59*, 1230-1232.
- (2) Moini, M. *Anal Bioanal Chem* **2002**, *373*, 466-480.
- (3) Gelpi, E. *J Mass Spectrom* **2002**, *37*, 241-253.
- (4) Oda, R. P.; Landers, J. P. In *Handbook of Capillary Electrophoresis*, Second ed.; Landers, J. P., Ed.; CRC Press: Boca Raton, 1997, pp 1-47.
- (5) Wu, C. H.; Scampavia, L.; Ruzicka, J. *Analyst* **2002**, *127*, 898-905.
- (6) Belder, D.; Deege, A.; Husmann, H.; Koehler, F.; Ludwig, M. *Electrophoresis* **2001**, *22*, 3813-3818.
- (7) Fogarty, K.; Van Orden, A. *Anal Chem* **2003**, *75*, 6634-6641.
- (8) In *Q TRAP LC/MS/MS System Instrument Tutorials*; Applied Biosystems/MDS Sciex, 2004.
- (9) Anson, M. L. *J Gen Physiol* **1938**, *22*, 79-89.
- (10) Liu, C. S. *Development and application of capillary electrophoresis-electrospray mass spectrometry*; University of Alberta: Canada, 2001.
- (11) Hager, J. W. *Rapid Commun Mass Spectrom* **2002**, *16*, 512-526.
- (12) Nakashima, T.; Higa, H.; Matsubara, H.; Benson, A. M.; Yasunobu, K. T. *J Biol Chem* **1966**, *241*, 1166-1177.
- (13) Ye, M.; Hu, S.; Schoenherr, R. M.; Dovichi, N. J. *Electrophoresis* **2004**, *25*, 1319-1326.
- (14) <http://www.promega.com/tbs/9piv511/9piv511.pdf>, (Promega product information sheet on trypsin).
- (15) Hernández-Borges, J.; Neusüß, C.; Cifuentes, A.; Pelzing, M. *Electrophoresis*, **2004**, *25*, 2257-2281.
- (16) Schlamowitz, M.; Peterson, L. U. *J Biol Chem* **1959**, *234*, 3137-3145.
- (17) Christensen, L. K. *Arch Biochem Biophys* **1955**, *57*, 163-173.

Chapter 3 – Microreactor Experiments Off- and On-line With CE-MS

3.I. Introduction

Various types of enzymatic microreactors have been developed, as was discussed in section 1.V. of chapter 1. Our group has used a trypsin monolithic microreactor in the past for digesting α -lactalbumin, cytochrome *C*, and β -casein.¹ The monolith consisted of a poly(glycidyl methacrylate-co-ethylene dimethacrylate) polymer. Digestions as short as 9 seconds were possible, and the microreactor was coupled on-line to CZE. The peptides were post-column fluorescently labeled and detected with laser induced fluorescence detection. It was pointed out that the CE system would have to be connected to MS to identify the peptides. This has been accomplished in work that is detailed in this chapter, although pepsin was immobilized instead of trypsin. Pepsin is most active at low pHs (pH 1-3.5)^{2, 3} and analyte protonation in MS is facilitated at low pHs.

Chapter 2 described how the peptide separation of the CE-microreactor-CE-MS instrument was interfaced with MS, and how peptide separations were improved. This chapter describes the preparation of the pepsin-immobilized poly(glycidyl methacrylate-co-ethylene dimethacrylate) monolith, testing of the microreactors in off-line experiments, and finally their coupling on-line to the peptide separation capillary and MS.

In the off-line testing, separations of bulk solution cytochrome *C* digests were compared to microreactor digests and the repeatability of digestion using different

microreactors was investigated. Digestions with different protein concentrations were also performed to determine what concentrations could still be detected with CE-ESI-MS.

The CE-ESI-MS instrumentation was then modified for on-line microreactor-CE-ESI-MS experiments. On-line experiments were performed using different digestion times, and the experimental conditions were optimized. Hydroquinone (HQ) was added to the running buffer to stabilize the CE current. HQ and *p*-benzoquinone had been successfully used by Moini *et al.*^{4, 5} with sheathless CE-ESI-MS to suppress oxygen and hydrogen gas formation. Finally, a myoglobin sample was on-line digested in preparation for 2D experiments that would use both cytochrome *C* and myoglobin.

3.II. Experimental

3.II.A. Chemicals and Materials

Cytochrome *C* from bovine heart (C-3131), pepsin from porcine stomach mucosa (P-6887), myoglobin from horse heart (M-1882), 2,2'-azobisisobutyronitrile (AIBN) solid (98%), cyclohexanol (99%), dodecanol (98%), ethylene glycol dimethacrylate (EDMA) liquid (98%), γ -methacryloxypropyltrimethoxysilane liquid (also called 3-(trimethoxysilyl)propylmethacrylate or γ -MAPS) (98%), glycidyl methacrylate (GMA) liquid (97%), glycine ethyl ester hydrochloride solid (99%), hydroquinone solid (99+%), sodium hydroxide solid (98%), sodium periodate solid (99%), and trifluoroacetic acid solution (99%) were from Sigma (St. Louis, MO). Acetonitrile (HPLC grade) and formic acid solutions (88%) were from Fisher Scientific (Fair Lawn, NJ). Ammonium acetate solid (puriss. p.a. for mass spectroscopy) and sodium cyanoborohydride ($\geq 95\%$) were

from Fluka (Buchs, Germany). Methanol solution (HPLC grade) was from EMD Chemicals (Gibbstown, NJ), hydrochloric acid solution (38%) was from J.T. Baker (Phillipsburg, NJ), and helium gas (99.99%) was from Airgas (Radnor, PA). Water was distilled and deionized by a Nanopure (Barnstead, Dubuque, IA) system.

Buffers and sheath liquids were filtered with 0.22 μm Stericup ExpressTM PLUS filters (Millipore, Billerica, MA) until no particles were seen in the liquids in their clear glass storage flasks when observed against a dark background. Amber flasks were used for buffers containing hydroquinone (HQ) since HQ is light sensitive. Since the HQ buffers could not be checked for particles in the dark amber flasks, the buffers were filtered 5x before use to avoid particles in the buffer. The liquids were not stored in plastic flasks to avoid contamination by plasticizers that might be detected in mass spectra. Fresh HQ buffers were prepared every 1-2 weeks because of HQ degradation (the solutions turned slightly brown). Buffers and sheath liquids were He sparged for 5-10 min before use.

0.6 and 1.6 mL Eppendorf tubes and PCR tubes were from Island Scientific (Bainbridge Island, WA). 1 mL (309602) and 5 mL (309603) plastic syringes were from Becton Dickinson (Franklin Lakes, NJ). Long-wavelength UV glue (KOA 300) was from Kemxert Corp. (York, PA). All fused silica capillaries were from Polymicro Technologies (Phoenix, AZ). PEEK unions (P-704), the PEEK right-angle flow 4-way valve (V-100L), Teflon tubing, and the various Teflon sleeves were from Upchurch Scientific (Oak Harbor, WA). The electronic syringe pump (sp210iw) was from World Precision Instruments (Sarasota, FL).

3.II.B. Microreactor Preparation

Two types of microreactors were prepared; one in which whole capillaries were filled with monolith and short sections of those capillaries were used in either on- or off-line experiments, and one in which only parts of capillaries were filled with monolith. The former will be referred to as whole capillary microreactors, the latter as integrated capillary microreactors.

48 μm ID, 142 μm OD capillaries were used for both whole and integrated microreactors. The switch to smaller OD capillaries (as compared with the ones used in chapter 2) was necessary because the interface that coupled a microreactor to a peptide separation capillary used a 150 μm ID capillary sleeve. A larger, 523 μm ID, 695 μm OD capillary was also modified as a whole microreactor and used for some off-line experiments.

3.II.B.1. Whole Capillary Microreactors

3.II.B.1.a. 48 μm ID, 142 μm OD

Microreactor preparation took ~ 1 week, and hence two whole capillary microreactors, each ~ 8 -10 cm, were prepared at one time. The microreactor capillaries could be stored at 4°C for a couple of months and still exhibit activity, although the degree of decrease in activity was not studied. Microreactor sections as short as 2 cm were used in experimental set-ups, so that one 8-10 cm length could provide microreactor sections for several experimental set-ups.

A few practical notes are given here before describing the coating procedure.

Whenever silicon rubber pieces were taken off capillaries in the following procedures, 1-2 mm of the capillary ends was cut off since sometimes silicon rubber plugged the capillaries.

For convenience, initial coating steps were performed on one ~ 20 cm capillary with a gas purging device. A 4 psi He gas pressure (unless otherwise noted) was applied when using the gas purging device for either flushing liquid or gas through the capillary.

After the monolith was polymerized, the capillary was cut in half since the back pressure of the 20 cm monolith was too great to flush liquids through it efficiently. The back pressure also made the use of syringe purging devices necessary as the gas purging device did not suffice. During early microreactor preparations, a syringe purging device was used that consisted of a 5 mL plastic syringe with a Luer lock, a blunt (filed off) metal syringe needle (23 gauge), a PEEK union (P-704, Upchurch Scientific, Oak Harbor, WA), Teflon sleeves (a yellow sleeve with 685 μm ID, 1/16" OD for the syringe needle, a clear sleeve with ~ 180 μm ID for the capillaries, Upchurch Scientific), and two pieces of Plexiglas between which the syringe could be placed and that could be squeezed together with two screws to apply pressure to the syringe piston, see **Figure 3-1 A**.

However, the device often leaked at the Luer lock, especially when the microreactor was flushed in the cold room at 4°C because the plastic syringes contracted to a different extent than the metal needles. Using an electronic syringe pump in the cold room with a 1 mL glass syringe was also problematic because liquid started to leak between the plunger and the inside of the syringe.

It was found that 1 mL plastic syringes, see **Figure 3-1 B**, were easier to use and did not leak as much or not at all. The 1 mL syringes had a flame-pulled glass melting tube capillary at their outlet, with the tapered end pointed toward the body of the syringe. The syringe nozzle was melted and fused around the glass capillary to provide a liquid-proof seal, and a microreactor capillary could be inserted into the glass capillary and stopped at the tapering, also with a good seal. The 1 mL syringes were placed in between the two Plexiglas pieces that had been used with the 5 mL syringes to enable continuous flushing. The screws only needed to be tightened every ~ 30 min. Different syringes were used for each different solution, and all syringes were flushed with ddH₂O after each use and stored.

At the beginning of a microreactor preparation, the capillary was cleaned by flowing 1 M NaOH through it for 1 h, followed by 10 min each with ddH₂O and MeOH. The capillary was dried by a 30 min He gas flush, filled with a freshly prepared 50% γ -MAPS in MeOH solution, then stoppered with silicon rubber pieces, and stored at room temperature for one day. The γ -MAPS provided a vinyl coating to which the monolith could be attached. The capillary was then successively flushed for 10 min each with MeOH, ddH₂O, and MeOH, and dried for 30 min with He gas.

A monomer reaction solution was prepared fresh each time microreactor capillaries were prepared. The solution consisted of 4 mg of AIBN (the reaction initiator), 0.3 mL of glycidyl methacrylate, 0.1 mL of ethylene glycol dimethacrylate, 1.1 mL of cyclohexanol, and 0.1 mL of dodecanol. The latter two components acted as porogenic solvents to provide the void volume of the monolith. The reaction solution was stored at 4°C until use.

200 μ L of the reaction solution was sparged with He for 15 min in a 0.6 mL Eppendorf tube immediately before filling the capillary with the solution. Because the monomer solution was slightly viscous, a 10 psi He gas pressure was used for filling the capillary. Both ends of the capillary were stoppered and it was placed in a 50°C water bath. The polymerization reaction was allowed to proceed for 12 hours.

After the 20 cm capillary was taken out of the water bath, it was cut in half and the two capillaries were flushed with MeOH until the MeOH was visible at the other end (two syringe purging devices were used at the same time). The MeOH flush was continued for another 20 min, followed by ddH₂O for another ~ 20 min. Even though the preparation procedure had been carefully followed, the monoliths were not homogeneous. Inhomogeneities could be observed under a microscope when the monoliths were flushed with MeOH because some areas of the monoliths were darker than others. When cutting whole capillary pieces for experiments, fairly homogeneous sections were chosen as much as possible.

The reaction scheme for pepsin immobilization is shown in **Figure 3-2**. The epoxide groups on the monoliths were first reduced by HCl (pH 0.6). The HCl solution was flushed through the columns for 20 min and the ends were sealed with silicon rubber. The capillaries were then stored at room temperature for 48 hours. The HCl was flushed out of the monoliths with ddH₂O, and next a freshly prepared 2% (w/v) NaIO₄ solution was purged for 60 min to oxidize the monolith. The monolith was then rinsed with ddH₂O and 0.1 M (ammonium) acetate (pH 4.0) buffer.

A freshly prepared 3 mg/mL pepsin in 0.1 M (ammonium) acetate (pH 4.0) solution was purged through the microreactors for 10 hours in the cold room at 4°C,

followed by a 0.1 M (ammonium) acetate (pH 4.0) rinse. A solution of freshly prepared 25 mM sodium cyanoborohydride + 10 mM glycine ethyl ester hydrochloride in 0.1 M (ammonium) acetate (pH 4.0) was then pumped through the capillaries for 4 hours, followed again by a 0.1 M (ammonium) acetate (pH 4.0) rinse. The microreactors were stored at 4°C with their ends stoppered by silicon rubber until use.

3.II.B.1.b. 523 μ m ID, 695 μ m OD

The same chemicals and general procedure were used to prepare the 523 μ m ID microreactors as for the 48 μ m ID microreactors. The gas purging unit was not used, however, since the flow through the large ID capillaries was too fast. Therefore, the large capillary was connected to either 1 or 5 mL plastic syringes with a PEEK union and Teflon sleeves. The syringes were attached to the union with blunt metal needles (23 gauge).

A 523 μ m ID, 695 μ m OD, 32 cm fused silica capillary was vinylized with γ -MAPS as described earlier. After the monolith polymerization, the capillary was cut in half because the back pressure was quite high and the 16 cm capillaries were more easily flushed. When purging with the NaIO_4 and subsequent solutions, the 5 mL plastic syringes were attached to the two Plexiglas pieces as shown in **Figure 3-1 A**.

3.II.B.2. Integrated Capillary Microreactors

There were only few differences between coating whole and integrated 48 μ m ID, 142 μ m OD capillary microreactors. For the integrated microreactors, it was convenient

to coat 4 capillaries at one time and store them at 4°C until use. Capillaries were cut to ~ 45 cm length and each capillary was cleaned and filled with γ -MAPS as above.

After drying the capillaries with He gas, the capillaries were marked at one end with a permanent marker ~ 5 cm from the end. Taking one capillary at a time, the ends were filled with the monomer reaction solution *via* capillary action by laying the capillaries flat on a microscope stand and inserting the ends into an Eppendorf tube that contained the sparged monomer reaction solution. The tube was withdrawn once the solution reached the ~ 5 cm mark as observed under the microscope. Both ends of the capillaries were stoppered and the capillaries were placed in a 50°C water bath, making sure that the filled ends were positioned below the rest of the capillary to avoid flowing of the solution. The polymerization reaction that resulted in a ~ 5 cm monolithic column was allowed to proceed for 12 hours.

The capillaries were unstoppered and flushed from the monolith-filled ends with MeOH until the MeOH was visible at the other ends. The capillaries were flushed from the filled ends because those ends could be easily cut off by ~ 1-2 mm in case they became clogged. This would not have been possible the other way around, especially since backflushing a clog out of the microreactors was not always successful. The MeOH flush was continued for another 20 min. The reaction procedure was heretofore identical as the one for whole microreactors.

3.II.C. Instrumental Set-up

3.II.C.1. Off-line Microreactor Experiments

The same sheath flow interface and 1D CE-ESI-MS instrumental set-up was used as for experiments in chapter 2, see section 2.II.B.2..

3.II.C.2. On-line Microreactor Experiments

The 1D CE-ESI-MS set-up had to be modified for on-line microreactor experiments, see **Figure 3-3**. The on-line set-up included a Plexiglas-glass interface cross, a Plexiglas injection block, and a 4-way valve. Care was taken to adjust all liquid levels to the same height to avoid siphoning.

3.II.C.2.a. Plexiglas-glass Interface Cross

The Plexiglas-glass interface cross is shown in **Figure 3-4** and a close-up picture of the interface center is shown in **Figure 3-3**. Perpendicular channels were milled into a ¼” thick Plexiglas piece, and glass microcaps (0.037 inch OD, # 1-000-0040, VWR, West Chester, PA) and glass pipets (0.046 inch OD, # 2-000-001, VWR) were glued into the channels with UV glue. The channels’ depths corresponded to the glass microcaps’ and pipets’ outer diameters.

Either whole or integrated microreactors were glued into the interface. If an ~ 2 cm piece of whole microreactor was used, the Plexiglas piece was cut so that the channel for the microreactor was only ~ 0.7 cm long to leave enough room for the microreactor to protrude from the side, see **Figure 3-4**. This was necessary since that end of the microreactor was inserted into Teflon tubing to connect it to a sample transfer capillary.

If an integrated microreactor was used, no such restrictions were necessary, and the microreactor side of the Plexiglas piece was broader to allow easier handling of the interface.

150 μm ID, 360 μm OD fused silica capillary sleeves were glued into the pair of microcaps. The separation capillary and the microreactor would be glued into these sleeves later. The sleeve for a whole microreactor (~ 2 cm) piece could only be ~ 1.5 cm long.

A piece of glass microscope slide was then glued on top of the Plexiglas piece. The glue migrated between the Plexiglas piece and the microscope slide by capillary action and it was allowed to move to the edges of the center of the cross without having it spill excessively into the center. The center space of the interface where liquid would be during experiments was to be completely sealed off so that the only openings were through the glass capillaries.

Next, high purity Teflon tubing (# 1507, Upchurch Scientific, Oak Harbor, WA) was carefully twisted over, and glued to, the glass pipets for connections to the buffer reservoir that had the Pt electrode inserted in it (or to a waste container) and to the 4-way valve. 70% EtOH was flushed through the interface for a few min to dissolve and flush out any uncured UV glue. This was followed by ddH₂O and air, and the interface was allowed to dry overnight. The UV glue would not have cured correctly had the interface been wet when the separation and microreactor capillaries were glued into the capillary sleeves.

When using whole microreactors, an ~ 2 cm piece of microreactor was cut square on the end that would go into the interface, and ~ 1 -2 mm of polyimide was shaved off

that end. The other end was then twisted into an ~ 5 cm piece of Teflon tubing. The tubing had been pulled to a size that fit very snugly over the microreactor capillary. A 48 μm ID, 142 μm OD PVA-coated fused silica capillary was twisted into the other end of the pulled Teflon tubing; this capillary was the transfer capillary through which protein samples were delivered to the microreactor. When using integrated microreactors, the end of the capillary that contained the microreactor was cut square to give a desired microreactor length (e.g. 1.1 cm), and the other end was cut to obtain the desired whole length of capillary (e.g. 31.2 cm).

Before a microreactor was glued into the interface, the microreactor was flushed with buffer for 30 min by attaching either the transfer capillary, or the un-polymerized end of the integrated microreactor, to a 1 mL flushing syringe (see **Figure 3-1 B**) that was attached to a Plexiglas purging device shown in **Figure 3-1 A**. It had been observed in early experiments that pieces of white monolith polymer would flush out of the microreactor in the interface and get stuck either in the space between the two capillaries or even clog the separation capillary. This was not observed after flushing the microreactor before inserting it into the interface.

Next, a 48 μm ID, 142 μm OD PVA-coated capillary (lengths varied) was cut square on both ends and ~ 1 -2 mm of polyimide was shaved off the squarer end. This end was inserted into the interface. Since neither the PVA-coated capillary nor the microreactor were to dry out, 1 mL flushing syringes with ddH₂O or 0.1 M (ammonium) acetate (pH 4.0), respectively, were attached to their other ends. However, no pressure was applied to flush the liquids through, because the interface and the capillary outsides had to be dry for the UV glue to cure correctly.

The gap between the two capillaries in the interface was adjusted to $\sim 30\text{-}40\text{ }\mu\text{m}$ under a microscope. The capillaries were secured into the interface one-by-one by placing drops of UV glue at the ends of the $150\text{ }\mu\text{m}$ ID, $360\text{ }\mu\text{m}$ OD sleeve capillaries where the PVA capillary and the microreactor had been inserted. The alignment of the capillaries was checked before gluing the second capillary. The interface was flushed with ddH₂O and the glue points were checked for leaks before attaching the interface to the rest of the instrument set-up. If a leak occurred during an experiment, the MS signal became erratic and the leak had to be fixed before experiments could continue. Care was taken to flush air bubbles out of the interface and the Teflon tubing before running experiments. A camera that came with the Q TRAP was positioned above the Plexiglas-glass interface to monitor whether any bubbles had inadvertently gotten into the interface.

3.II.C.2.b. Plexiglas Injection Block

The Plexiglas injection block (see **Figure 3-5**) was fabricated by the Department of Chemistry machine shop at the University of Washington and consisted of 4 pieces of Plexiglas that were layered on top of each other and the 3 top pieces were held together by screws. The bottom piece was easily attached with metal clips. A cut-off PCR tube could be inserted into a well in the bottom piece and served as a buffer or sample reservoir ($50\text{ }\mu\text{L}$). A fresh PCR tube was used every time the liquid was changed. Different bottom pieces were used for the sample and the buffer, so that switching from sample to buffer after injection was fast and easy.

Several channels allowed the insertion of the transfer capillary, a power supply electrode cable, and Teflon tubing connected to the He gas supply. The electrode cable

did not have a Pt electrode soldered to it for experiments in this chapter, but it was only inserted to be able to pressurize the space above the liquid reservoir for purging purposes.

It was found that higher gas pressures could be applied without having liquid splash out of the reservoir if the screws were tightened very snugly. Using high gas pressures saved time when liquid was purged through the transfer capillary and microreactor. A solenoid valve with a button-controlled timer was in-line connected to the He gas tubing to be able to apply gas flow reproducibly, for example during sample injections.

3.II.C.2.c. 4-way Valve

A right-angle flow 4-way valve was used in two different configurations, see **Figure 3-6**; one during the day when performing experiments, and one when flushing ddH₂O through the PVA capillary overnight to prevent the capillary from drying out (setting up the PVA capillary in the MicroIonSpray head, see section 2.II.B.2., and positioning the head in front of the MS orifice was time-consuming, and therefore the PVA capillary was not taken out of the head and e.g. inserted into a vial with ddH₂O). The same Teflon tubing was used for both the waste and the syringe pump connections, only its attachment was changed. When flushing overnight, the waste line of the Plexiglas-glass interface was partially plugged and the transfer capillary was left in buffer in the injection block.

3.II.D. Off-line Microreactor Digestion and CE-ESI-MS Separations

Protein samples were flushed through the microreactors with a syringe pump (sp210iw, World Precision Instruments, Sarasota, FL) and the effluents were collected from the microreactors. The samples were either diluted or injected as they were. Off-line digestions were either performed in 48 μm ID, 142 μm OD, or 523 μm ID, 695 μm OD whole capillary microreactors. The larger microreactors allowed faster effluent collection when digestion repeatability and kinetic studies were done. Initial off-line experiments to test whether the microreactors worked at all were done with a 48 μm ID microreactor, however.

3.II.D.1 Off-line Microreactor Digestion Using a 48 μm ID Microreactor and CE-ESI-MS Separation Conditions

A previously prepared and frozen (at -80°C) 50 μL sample of 0.18 μM cytochrome *C* in ddH₂O was lyophilized and reconstituted with 10 μL formic acid (pH 2.5) (new cytochrome *C* concentration 0.90 μM). A 10 μL glass syringe was filled with the sample and attached to a PEEK union with a Teflon sleeve (F-246x, Upchurch Scientific).

A 48 μm ID pepsin microreactor was cut to 7.2 cm and was also attached to the union *via* a Teflon sleeve (F-239x, Upchurch Scientific). The sample was flushed through the microreactor with a syringe pump set at 0.02 $\mu\text{L}/\text{min}$, and the effluent was collected on ice in a 0.6 mL Eppendorf tube. 9 μL of the effluent was lyophilized and reconstituted in 135 μL of fresh 2% acetonitrile (ACN) + 0.1% trifluoroacetic acid (TFA)

(v/v). The final cytochrome *C* digest concentration was calculated to be $6 \times 10^1 \mu\text{M}$. The sample was used the same day in CE-ESI-MS experiments.

Three controls were analyzed as well. One control consisted of pepsin bulk-digested cytochrome *C* ($60 \mu\text{M}$ in 2% ACN-0.1% TFA) that was prepared as described in section 2.II.D.2.. A second control was a blank sample; formic acid (pH 2.5) was flushed through the microreactor at $0.035 \mu\text{L}/\text{min}$ and $9 \mu\text{L}$ of the effluent was lyophilized and reconstituted with $135 \mu\text{L}$ of fresh 2% ACN-0.1% TFA. The fourth control consisted of undigested cytochrome *C*. A $50 \mu\text{L}$ aliquot of 0.18 mM cytochrome *C*, from the same batch that was used for the microreactor digested sample, was treated the same way as described above, except it was not run through the microreactor.

The 1D CE-ESI-MS set-up included a $48 \mu\text{m}$ ID, $142 \mu\text{m}$ OD, 41.8 cm PVA-coated capillary. The running buffer was 50 mM (ammonium) acetate (pH 4.0). An injection voltage of $+10.0 \text{ kV}$ ($239 \text{ V}/\text{cm}$) was applied for 5 sec while the Q TRAP's ion spray (IS) voltage was turned off. The separation voltage was $+13.8 \text{ kV}$ with the IS voltage at $+2250 \text{ V}$; the electric field was $276 \text{ V}/\text{cm}$. The Q TRAP was run in linear ion trap (LIT) scan mode. The m/z range was from 300-1100 amu, and the curtain (CUR) and nebulizer gases (GS1) were set to 15.0 and 0.0 during the run, respectively. GS1 was set to 10.0 during the 0.2 min prerun of the acquisition batch (see section 2.III.B.5.). The sheath liquid was 90% MeOH and its flow rate was $1000 \text{ nL}/\text{min}$. The declustering and entrance potentials were 30 V and 10 V , respectively. The ion detector was set to 2300 V . Each sample was run twice.

3.II.D.2. Off-line Microreactor Digestion Using 523 μm ID Microreactors and CE-ESI-MS Separation Conditions

Two sets of cytochrome *C* digestion samples were prepared using the 523 μm ID microreactors. One set probed the microreactor homogeneity, the other aimed to establish a calibration curve to find the lowest sample concentration that could be digested and still be detected with MS.

For the homogeneity experiments, the two ~ 16 cm pieces of the 523 μm ID whole microreactors were cut into ~ 4.5 cm pieces and 60 μM cytochrome *C* samples in 10 mM (ammonium) formate (pH 2.5) were flushed through the pieces using the syringe pump (sp210iw, World Precision Instruments, Sarasota, FL). The flow rates were chosen to yield 5.0 min residence times of the samples in the microreactors. For the flow rate calculations, the void volume of the microreactor was assumed to be 75% based on the volume ratio of porogenic solvents (dodecanol and cyclohexanol) to that of the monomers (EDMA and GMA). Flow rates had to be adjusted for each microreactor because sometimes small, white pieces of monolith came loose when the flows were first started and the pieces fell out of the capillary ends. 50 μL of each of the effluents was collected in 0.6 mL Eppendorf tubes and stored in the -80°C freezer until use.

For the calibration curve, concentrations of 10, 20, 30, 40, 50, 60, 70, 80, and 120 μM cytochrome *C* in 10 mM (ammonium) formate (pH 2.5) were prepared by serial dilution. These samples were flushed through one of the microreactor pieces that had been used for the homogeneity experiments, again with a 5.0 min residence time. The effluents were collected and stored as above.

The samples were run with the CE-ESI-MS set-up. The set-up included a 48 μm ID, 142 μm OD, 42.1 cm PVA-coated capillary and the running buffer was 100 mM (ammonium) acetate (pH 4.0). An injection voltage of +15.0 kV (356 V/cm) was applied for 5 sec while the Q TRAP's ion spray (IS) voltage was off. The separation voltage was +16.0 kV with the IS voltage at 2250 V; hence, the electric field was 327 V/cm. The Q TRAP was run in linear ion trap (LIT) scan mode. The m/z range was from 300-1100 amu, and the curtain (CUR) and nebulizer gases (GS1) were set to 15.0 and 0.0 during the run, respectively. GS1 was set to 10.0 during the 0.2 min prerun of the acquisition batch (see section 2.III.B.5.). The sheath liquid was 90% MeOH and its flow rate was 1000 nL/min. The declustering and entrance potentials were 30 V and 10 V, respectively, and the ion detector was set to 2300 V.

3.II.E. On-line Microreactor Digestion and Microreactor-CE-ESI-MS Separations

3.II.E.1. Protein Sample Preparation

Solid cytochrome *C* was dissolved in either (ammonium) formate (pH 2.5) or (ammonium) acetate (pH 2.7) stock solutions to yield 200 μM concentrations of the protein in 10 mM buffer. Solid myoglobin was dissolved in (ammonium) acetate (pH 2.7) to final concentrations of 200 μM protein and 10 mM buffer.

Aliquots of the samples were stored in 0.6 mL Eppendorf tubes at -80°C until use. A sample was then thawed in the refrigerator and mixed by pipetting before being transferred to a cut-off PCR tube in a Plexiglas injection block bottom. In later experiments, the sample was also centrifuged at 8,000 rpm for 5 min before being

transferred to the PCR tube. 5-10 μ L of sample at the bottom of the Eppendorf tube was not used to avoid transferring particles that might clog the microreactor.

3.II.E.2. Experimental Procedure

3.II.E.2.a. General Procedure

The instrumental set-up for on-line microreactor experiments was given in section 3.II.C.2. and is shown in **Figure 3-3**. The general procedure for experiments was that sample was gas-purged from the injection block through the transfer capillary to the microreactor until the sample reached into the interface. A preliminary experiment (explained in section 3.II.E.2.b.) had been performed to determine how long the gas-purge needed to be done. After starting a timer for digestions, buffer was gently flushed through the interface to the waste to remove protein and peptides from the interface center, but without causing buffer from the center to move into the microreactor. It was found that the CE current was unstable if there had been no flow through the PVA capillary for more than ~ 3 min. Running voltages were therefore applied across the peptide separation capillary during the digestion time to keep buffer moving to the outlet of the PVA capillary.

Once the sample had digested, the running voltages were turned off and the Q TRAP was put into standby. A plug of sample was injected into the peptide separation capillary by applying a voltage at the interface buffer reservoir while at the same time applying pressure at the injection block. The run was then started by applying the Q TRAP and CE voltages. Acquisition batches as explained in section 2.III.B.5. were used.

The specific parameter values for each experiment will be given in the figure captions or in the text.

3.II.E.2.b. Preliminary Purging Experiments to Determine the Time Needed to Purge Sample to the Interface

It turned out that not all microreactors created the same back pressure, so that a purging experiment was performed before beginning experiments with protein samples whenever a new microreactor was glued into an interface. The purging experiment determined how long it took for liquid to travel from the injection block to the interface.

A food dye could have been used whose arrival at the interface could have been seen with the Q TRAP camera, but it was unclear what effect the dye might have on the pepsin. An experiment was thus devised in which a CE current drop indicated when liquid had reached the interface. For this purpose, all capillaries and tubing were filled with a high ionic strength buffer (e.g. 100 mM (ammonium) acetate (pH 4.0)) and the injection block bottom was filled with a low ionic strength buffer (e.g. 10 mM (ammonium) formate (pH 2.5)). CE and MS voltages were then applied and the low ionic strength buffer was gas purged from the injection block to the interface. A timer was started when the purging began. The CE current was monitored and the timer was stopped once a slow decrease in CE current was observed (see **Figure 3-7**). The decrease in CE current was due to the low ionic strength buffer mixing with the high ionic strength buffer in the interface.

3.III. Results and Discussion

3.III.A. Off-line Microreactor Digestion

3.III.A.1. Validation of the Pepsin Microreactor's Digestion Capability

To test whether the pepsin microreactor worked, an off-line experiment was performed as described in section 3.II.D.1.. **Figure 3-8** shows the reconstructed ion electropherograms (RIEs) of pepsin bulk solution digested and microreactor digested cytochrome *C*. The same 20 XIEs were used as listed in **Table 2-2**. This demonstrated that the cytochrome *C* was indeed digested in the microreactor.

One control experiment was performed with undigested cytochrome *C*. Another control was a blank consisting of sample matrix that had been flushed through the microreactor just as the cytochrome *C* had been, see section 3.II.D.1.. The RIEs of the controls are shown in **Figure 3-8**, with the RIEs again consisting of the 20 XIEs as before. No peaks were observed above the background. The absence of peaks in the blank indicated that none of the 20 XIEs were due to pepsin autodigestion products.

The data of the undigested sample were also analyzed using XIEs that had been determined as belonging to cytochrome *C* in previous infusion experiments (XIEs of 620-624, 680-684, 720-724, 764-768, and 816-820 amu). However, no peaks were observed with these XIEs. The reason for this is unclear because the protein should have migrated to the MS considering the pH of the buffer, the isoelectric point of cytochrome *C* (~ 10), and the applied voltages.

3.III.A.2. Repeatability of Injection Using the 1D CE-ESI-MS Set-up

To be able to perform quantitative analyses to characterize the microreactor performance, the repeatability of injection was tested first. Five consecutive experiments were performed using a bulk-digested cytochrome *C* sample (60 μ M in 2% ACN-0.1% TFA; bulk-digested cytochrome *C* sample was more readily available than microreactor-digested sample). The peak areas and heights of the most intense XIE (576.5-577.5 amu) were calculated using a Gaussian curve-fitting Matlab program written by Professor Dovichi. The percent relative standard deviations (%RSDs) of the peak areas and heights were 18% and 15%, respectively.

3.III.A.3. Microreactor Homogeneity

As mentioned in section 3.II.B.1.a., the microreactors were not homogeneous over the whole capillary lengths. Therefore, sections of the microreactors that appeared fairly homogeneous were used for experiments. It was investigated how much the digestions would vary when different sections were used. Microreactors with 523 μ m IDs were prepared since it would take much less time to collect a suitable amount of effluent (50 μ L) from these microreactors than when using 48 μ m ID microreactors.

The digestions were performed as described in section 3.II.D.2.. The cytochrome *C* samples for these experiments were prepared in 10 mM (ammonium) formate (pH 2.5). To mimic conditions that would maybe be used in future two-dimensional experiments, the effluents were not lyophilized and reconstituted in 2% ACN-0.1% TFA after collecting them from the microreactors. For stacking purposes (on-capillary concentration, see section 1.II.C.1.), a 100 mM (ammonium) acetate (pH 4.0) running

buffer was used. To still obtain fast separations with this high ionic strength buffer, the electric field strength was increased compared to the experiments using 50 mM (ammonium) acetate (pH 4.0).

Figure 3-9 shows the RIEs of five cytochrome *C* digests that were obtained with 5 different microreactor pieces. The %RSDs of the peak areas and heights for the 891.0-892.0 amu XIE were calculated, which showed clean and Gaussian shaped peaks. The XIE for run **A** in **Figure 3-9** was not included in the calculations since no peak was discernable. The %RSDs were 39% and 10% for the peak areas and heights, respectively. The former was worse than the 18% injection %RSD calculated in section 3.III.A.2., while the latter was better. Considering the overall appearance of the RIEs in **Figure 3-9**, the digestion efficiency between microreactors varied widely.

3.III.A.4. Concentration Limit of Microreactor Digestion Detectable with the 1D CE-ESI-MS Instrument

A 4.5 cm piece of 523 μm ID microreactor that visually appeared most homogeneous was chosen for these experiments. The same microreactor had been used to obtain the data in **Figure 3-9 D**. **Figure 3-10** illustrates the RIEs for cytochrome *C* digest concentrations of 70, 80, and 120 μM . The same 20 XIEs as listed in **Table 2-2** were overlaid and summed.

The 70 μM concentration showed no discernable peaks above the background in the RIE, even though peaks were observed in **Figure 3-9 D** with only a 60 μM sample concentration. Sample handling might have played a role in the inconsistency.

These last data shed some light on the kinetics of the microreactor. Initial experiments in section 3.III.A.1. showed peak intensities that were clearly above the background for the microreactor digest, see **Figure 3-8**. The sample concentration that was analyzed with 1D CE-ESI-MS was $\sim 60 \mu\text{M}$. But, the concentration of cytochrome *C* that was flushed through the microreactor had been 0.9 mM, and only after the effluent was collected was the sample diluted to $60 \mu\text{M}$. For experiments in this section, dilute samples were flushed through the microreactor, and no XIE peaks were seen for a $60 \mu\text{M}$ digest sample. The peak intensities for the $120 \mu\text{M}$ cytochrome *C* sample were also rather low compared with **Figure 3-8**. Based on these results, a $200 \mu\text{M}$ cytochrome *C* concentration was used in later on-line experiments to obtain data well above the detection limit of the system.

3.III.B. On-line Microreactor Digestion

3.III.B.1. Instrumental Set-up and Experiment-related

It was found in earlier experiments that certain plastic tubing and buffer containers leached plasticizers into the buffers that could contribute to the noise in mass spectra. The materials for the instrumental set-up therefore had to be carefully chosen. To determine which materials would be suitable, experiments were performed in which potential tubing and epoxy and UV glue were soaked in 80 mM (ammonium) acetate (pH 4.0) buffer in glassware for 5 days. A drop of epoxy had been allowed to harden, and a drop of UV glue had been cured under UV light before adding the buffer. After 5 days, 900 μL of MeOH was added to 200 μL of the soaking solutions to add volatility, and the

diluted solutions were infused using a syringe pump and the TurboIonSpray ion source of the Q TRAP. The TurboIonSpray source allowed easy and fast infusion of liquids.

The epoxy glue solution turned milky white after only 1 day of soaking, so that this solution was not further analyzed to prevent MS contamination. The tubing consisted of high purity Teflon and its soaking solution did not show extra mass spectral peaks when compared to a control.

The mass spectra of the UV solution and a control are shown in **Figure 3-11**. The two most dominant peaks (355 and 371 amu) of the control were suppressed in the UV solution mass spectrum, and instead a 477 amu peak was dominant. Even if the 477 amu peak might be observed in mass spectra, UV glue was deemed a better choice for gluing interfaces in light of the adverse reaction of epoxy with the (ammonium) acetate buffer. Fortuitously, if the interfaces were flushed thoroughly enough with 70% EtOH before use, any uncured UV glue was washed out, and the 477 amu peak was usually not seen. At one time, the 477 amu peak was observed after setting up the microreactor-CE-ESI-MS system, but once the 70% EtOH flush had been repeated, the 477 amu peak was not seen in subsequent mass spectra. UV glue was also preferred over epoxy because the former could be cured on demand when placing the interface under a long-wavelength UV lamp, whereas the use of 5 min epoxy would not have been as convenient.

As mentioned in section 3.II.E.2.b., purging experiments were performed each time a new microreactor was put on-line with the interface. The times it took for the 10 mM (ammonium) formate (pH 2.5) to be purged to the interface with a 22 psi He gas pressure ranged from ~ 2 min to ~ 9 min. Unfortunately, this was not surprising given the homogeneity experiments in section 3.III.A.3.. This meant that no quantitative data

between different on-line microreactor set-ups could be compared since samples were pressure injected (along with electrokinetic injection).

3.III.B.2. Repeatability of Digestion and Injection Using the Microreactor-CE-MS Set-up

The repeatability of injection and digestion was tested with the on-line system using 200 μ M cytochrome *C*. A digestion time of 5 min was chosen since preliminary experiments had shown that this time was sufficient for cytochrome *C* digestion. Four consecutive on-line experiments were performed. The areas and peak heights of 3 XIEs (449-50, 511.5-12.5, and 554-5 amu) were analyzed with the Matlab Gaussian peak fit program, and the %RSD values are given in **Table 3-1**. Respectively, these XIEs had low, medium, and high peak intensities, and all were fairly well Gaussian shaped. The lower the peak intensity, the worse was the %RSD. Peak area %RSDs were also poorer than peak height %RSDs.

3.III.B.3. Digestion Efficiency

Even though the data of the previous sections showed that quantification is rather poor with this microreactor-CE-ESI-MS system, on-line experiments were performed that probed the digestion efficiency with different digestion times. It was investigated how fast digestions could be accomplished, and whether a trend of peak area or peak height versus digestion time might be discerned and to maybe find an optimum digestion time. Digestion times of 2, 6, 7, 10, 13, 16, and 21 min were chosen, but the order of analysis was randomized and was 10, 6, 21, 2, 7, 16, and 13 min.

The instrumental set-up for these experiments included a 48 μm ID, 142 μm OD, 42.1 cm PVA-coated capillary. The running buffer was 100 mM (ammonium) acetate (pH 4.0). An injection voltage of +13.0 kV (309 V/cm) was applied for 10 sec while the Q TRAP's ion spray (IS) voltage was turned off. A pressure of 22 psi was applied for 5 sec during the injection as well. The separation voltage was +16.0 kV with the IS voltage at 2250 V; hence, the electric field was 327 V/cm. The m/z range was from 300-1100 amu, and the curtain (CUR) and nebulizer gases (GS1) were set to 15.0 and 0.0 during the run, respectively. GS1 was set to 10.0 during the 0.2 min prerun of the acquisition batch (see section 2.III.B.5.). The ion detector was set to 2300 V. 90% MeOH was used as the sheath liquid at a flow rate of 1000 nL/min.

The peak areas and heights of three XIEs (485-6, 511.5-12.5, and 554-5 amu) were analyzed with the Matlab Gaussian peak fit program. The 485-6 amu XIE was chosen instead of the 449-50 amu XIE that had been used before because the %RSDs with the latter had been very poor. The 485 amu XIE had peak intensities similar to the 511.5 amu XIE. Peak areas and heights were plotted against digestion times with Excel, see **Figure 3-12**. The peak area and height of the 554-5 amu XIE for the 13 min digestion were omitted from the plots as those points were outliers with very high values.

The R^2 correlation values that are shown on the plots indicated very little correlation. This was again not surprising based on the %RSD data given in previous sections.

It was investigated whether an m/z corresponding to a peptide with several missed cleavages might show decreased intensities with longer digestion times, and whether its products might show increased intensities. For this, a theoretical peptide mass list was

obtained with the MSDigest function of the Protein Prospector website.⁶ The theoretical digest was performed on bovine cytochrome *C* with accession number P62894 based on the SwissProt protein database. The enzyme was pepsin (porcine gastric), and up to 3 missed cleavages were allowed. The minimum and maximum fragment masses were set to 400 to 1100 m/z, the minimum fragment length was 0, and the instrument was chosen as ESI-3Q. Peptides with multiple charges were included in the report.

No experimental peptide mass, however, could be related to exclusively one theoretical peptide mass that would at the same time yield one product ion with an exclusive mass. For example, it was found that the ~ 555 amu peak could be potentially based on three different theoretical peptides, 555.2^{+1} (65-68), 556.0^{+3} (69-82), and 556.2^{+1} (47-51), where the superscripted numbers indicate charge states, and the amino acid sequence numbers of the peptides are given in parentheses. One theoretical product of the 556.0^{+3} (69-82) peptide has a m/z value of 891.5^{+1} (69-75), but two other theoretical peptides with 890.8^{+3} (11-35) and 891.5^{+1} (68-74) were also possible. Hence, no correlations between parent and product ions could be made.

Another factor that might be related to the low correlations is a change in ion suppression based on changes in sample compositions with differing digestion times. If a peptide's concentration increased with longer digestion times, it might have suppressed other peptides' ionization to a greater extent, hence making accurate quantification difficult.

One other reason for the poor correlation could have been that peptides might have been partially adsorbed and retained in the microreactor and that later runs were affected by these peptides. A control run had been performed at the end of the digestion

efficiency experiments in which the transfer capillary and microreactor had been flushed with ~ 1.3 capillary volumes of sample buffer (10 mM (ammonium) acetate (pH 2.7)). A plug of sample buffer had then been injected and run as had been done for the cytochrome *C* digest samples. The 554-5 amu XIE was observed with a peak intensity that was 5% of the average intensity of the 554-5 amu sample peaks (omitting the 13 min data point again). No other XIEs showed peaks for the control. Hence, a slight memory effect was observed.

These experiments did show that digestion was very fast. Digestion products were observed with ~ 2 minutes.

3.III.B.4. Use of Hydroquinone and *p*-benzoquinone as Buffer Additives

3.III.B.4.a. Obtaining Stable CE Currents with Hydroquinone and *p*-benzoquinone as Buffer Additives

Instabilities of the CE current were observed during the digestion efficiency experiments. These were eventually traced back to apparent hydrogen gas formation at the electrospray tip, the cathode of the CE system. The addition of the redox reagent hydroquinone to the buffer eventually lessened the instabilities, but initially it was not clear what caused them.

Because the CE and MS voltages were off for a few minutes while sample was purged to the microreactor, the CE current had to get back up to its steady state level during the prerun while the protein was digested. The CE current would start at $\sim 0 \mu\text{A}$ and then sometimes take up to one minute to get up to a $\sim 10 \mu\text{A}$ level when using 100 mM (ammonium) acetate (pH 4.0) and an electric field of 327 V/cm. In subsequent

peptide separations, the CE current would sometimes drop down to $\sim 0\text{-}4\ \mu\text{A}$ and not recover. Experiments had to be terminated when this happened.

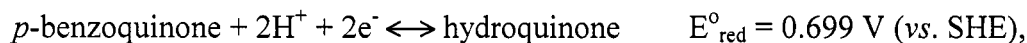
It was thought that siphoning from the electrospray tip caused the buffer in the PVA-coated capillary to move back from the spray tip outlet and therefore cause the CE current instabilities. All liquid levels were checked (see section 2.II.B.2.), and this possibility was ruled out. Also, the sheath flow had been left running when sample was purged to the interface to prevent the tip from drying out by excessive evaporation, and the sheath liquid flow rate was increased from 1000 to 1300 nL/min to decrease this possibility even further. This did not eliminate the instabilities, neither.

The current instabilities could have also been caused by Joule heating. To test this, an Ohm's plot of current vs. applied electric field was made, but no deviation from linearity was observed with the applied electric fields.

It was also observed that the CE current drops became more frequent once they had started to happen. This could have been due to the PVA coating deteriorating, especially since other group members had observed that their data became less reproducible if air had somehow gotten into their coated (although not with PVA) capillaries. Currents were more stable if PVA-coated capillaries were used that were not older than one month, but even with freshly coated capillaries, the CE currents could not always be stabilized. At one point, the whole interface and capillaries and tubing were exchanged, and initially the CE current seemed to behave more reliably, but eventually the instabilities returned.

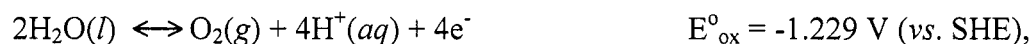
The problem was finally mostly resolved based on work done by Moini *et al.*,^{4,5} who had added hydroquinone or *p*-benzoquinone to buffers to suppress oxygen and

hydrogen gas formation. *p*-benzoquinone has a standard reduction potential of 0.699 V vs. a standard hydrogen electrode (SHE)⁷



and hydroquinone in turn has a standard oxidation potential of -0.699 V vs. SHE.

The oxidation of water to oxygen gas has a standard oxidation potential of -1.229 V vs. SHE



and the reduction of water to hydrogen gas has a standard reduction potential of -0.828 V vs. SHE



Hydroquinone is more easily oxidized to *p*-benzoquinone than water is to oxygen gas, and *p*-benzoquinone is more easily reduced back to hydroquinone than water is to hydrogen gas. Hence, Moini *et al.* were able to drastically reduce bubble formation in their sheathless CE-ESI-MS system. In their 2001 paper, they added *p*-benzoquinone to their buffers, and the reduction of *p*-benzoquinone provided hydroquinone in the buffer as well. For the experiments with the sheath flow set-up discussed in this thesis work, hydroquinone was used as the buffer additive to provide a source for *p*-benzoquinone (hydroquinone was already available in the lab).

The hydroquinone buffers had to be made fresh every 1-2 weeks, however, because hydroquinone degraded and the solutions turned slightly brown after ~ one week. CE currents became more frequently unstable again if older buffers were used.

3.III.B.4.b. Optimizing Experimental Conditions when Using Hydroquinone (and *p*-benzoquinone) as Buffer Additives

Once stable CE currents were obtained, experiments were performed to optimize the peptide separations for later two-dimensional (2D) experiments. The peptide separation forms the second dimension of the 2D system, and chapter 4 will describe in detail how 2D experiments are performed. For now, it should be mentioned that the separation window in the second dimension determines to a great extent how long 2D experiments take, with the separation window consisting of the time between the first and last migrating peaks; the shorter the separation window, the faster the 2D analysis. Migration times can be shortened by increasing the applied electric field or by decreasing the buffer ionic strength. Both of these options were tried. Beforehand, experiments were done to determine whether and how hydroquinone might alter the peptide separation.

Experiments with and without hydroquinone in the running buffers were performed with 60 μM of pepsin bulk-digested cytochrome *C* using a 1D CE-ESI-MS set-up for simplicity. Cytochrome *C* was digested as in section 2.II.D.2.. **Figures 3-13 A** and **B** illustrate results without hydroquinone in the running buffer (**A**), and with hydroquinone (**B**). No significant differences were observed. The data are shown as overlaid but not summed XIEs (and not smoothed) to provide a better comparison than would be obtained with RIEs. The same 20 XIEs were used as before (see section 2.II.F. and **Table 2-2**).

Further experiments were performed using the on-line microreactor-CE-ESI-MS set-up to mimic 2D conditions. 200 μM cytochrome *C* was digested for 5 min with the

microreactor. **Figures 3-13 C and D** show experiments using the same hydroquinone-containing running buffer but different applied electric fields (346 V/cm vs. 485 V/cm, respectively). The peak migration times with the higher electric field were shorter than with the lower electric field, but the total separation window was not changed significantly. The peak efficiencies in **D** are greater than in **C**, although that might not be beneficial because the mass spectrometer might not be fast enough to obtain adequate tandem mass spectra of very sharp peaks during information dependent acquisition (IDA) experiments (see section 2.III.B.6. and **Figure 2-23**). Unfortunately, the CE current was not stable at 485 V/cm even with hydroquinone in the running buffer. For other experiments, a 346 V/cm electric field was thus used.

Decreased buffer ionic strengths were tried next. **Figures 3-13 E and F** give the overlaid XIEs with 20 mM (ammonium) acetate + 10 mM hydroquinone (pH 3.9) and 30 mM (ammonium) acetate + 20 mM hydroquinone (pH 3.9), respectively, whereas 50 mM (ammonium) acetate + 20 mM HQ (pH 3.9) had been used before. The migration times became shorter compared with the higher ionic strength buffer, but the resolution deteriorated. It is not clear why the peak intensities decreased with decreasing ionic strengths. The CE currents also became less stable, especially with the lowest ionic strength buffer. It was thought that a 10 mM hydroquinone concentration might suffice to stabilize the CE current because electrolysis might be decreased with the lower ionic strength, but this was not the case. A 50 mM (ammonium) acetate + 20 mM HQ (pH 3.9) buffer was chosen for future experiments based on these results.

It should be noted that peak profile differences existed between the bulk solution and microreactor digested cytochrome *C* samples, see **Figures 3-13 A, B, and C**. These differences were consistently observed, but it is not clear what caused them.

3.III.B.5. On-line Microreactor Digestion Using Myoglobin

The purpose of the 2D CE-microreactor-CE-MS-MS system is to be able to separate proteins in the first dimension and then separate their peptides in the second dimension. As a proof-of-concept experiment, a two-protein sample was initially used in chapter 4. To be able to analyze 2D data more easily, horse heart myoglobin was digested with the 1D on-line microreactor-CE-MS set-up (using an integrated microreactor) to establish a list of XIEs as had been done for cytochrome *C*, see section 2.II.F.. **Table 3-2** lists the 20 XIEs that yielded the most intense peaks.

An RIE and the corresponding 20 overlaid XIEs are shown in **Figure 3-14**. A better separation was obtained than with cytochrome *C*. Fortuitously, the separation window was similar in length to the cytochrome *C* window, so that no further optimization of conditions was performed.

3.IV. Conclusions

Pepsin-immobilized monolithic microreactors were prepared and coupled on-line with the one-dimensional CE-ESI-MS instrument that was developed in chapter 2. The digestion capability of the microreactors was first tested in off-line experiments. The microreactors successfully digested cytochrome *C* although the digestion efficiency varied between microreactors and high cytochrome *C* concentrations had to be used.

The CE-ESI-MS instrument was then modified to enable the on-line coupling of the microreactors to the peptide separation capillaries. The on-line digestion efficiency of the microreactors was probed using different digestion times. No correlation between increasing peak areas or heights and digestion times was observed, and quantification was hampered by poor injection and digestion repeatabilities. A 2 minute digestion was sufficient, however, to detect cytochrome *C* digestion products with MS.

CE current instabilities due to apparent hydrogen gas formation were alleviated by adding hydroquinone (and also *p*-benzoquinone) to the running buffers because *p*-benzoquinone, instead of water, was reduced at the capillary outlet inside the electrospray needle. The experimental conditions were optimized and a moderate electric field and a 50 mM (ammonium) acetate + 20 mM hydroquinone buffer were found to give satisfactory and stable separations.

In preparation for two-dimensional experiments, myoglobin was also on-line digested. The experimental conditions that were used for cytochrome *C* also worked well for myoglobin. A list of myoglobin peptide masses was compiled to make the initial interpretation of two-dimensional data easier.

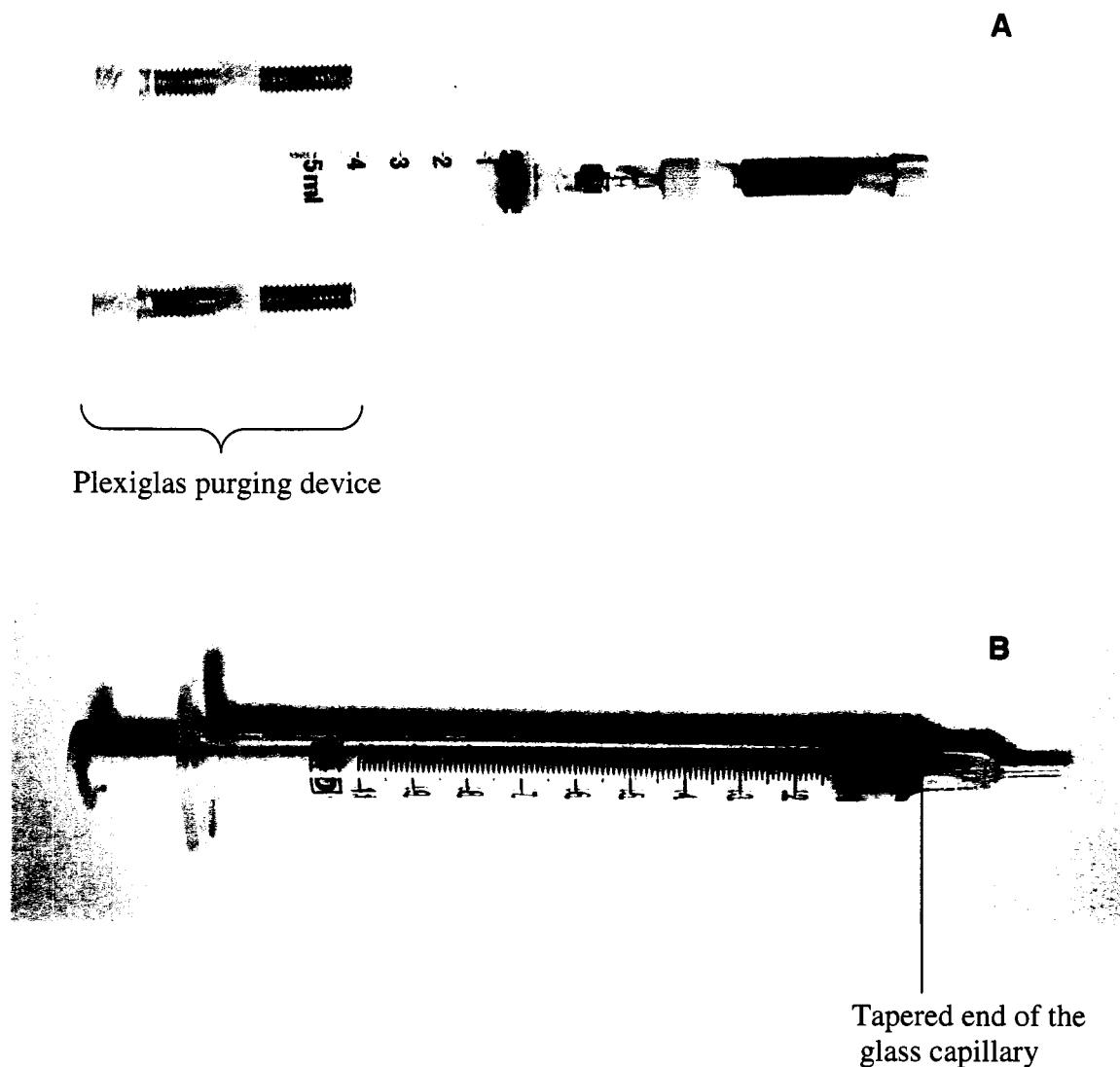


Figure 3-1. A) Syringe purging device for the 5 mL syringe with a capillary connected to the 5 mL syringe *via* a PEEK union. B) The 1 mL flushing syringe. A flame-pulled glass capillary was inserted tapered-end first into the front of the syringe, and the plastic at the front end of the syringe was melted around the pulled glass capillary to give a seal around the capillary. A fused silica capillary was inserted into the glass capillary for flushing the former. The syringe could be attached to the Plexiglas purging device shown in A to be able to purge continuously. The screws were tightened $\sim 1/4$ turn every ~ 30 min as needed.

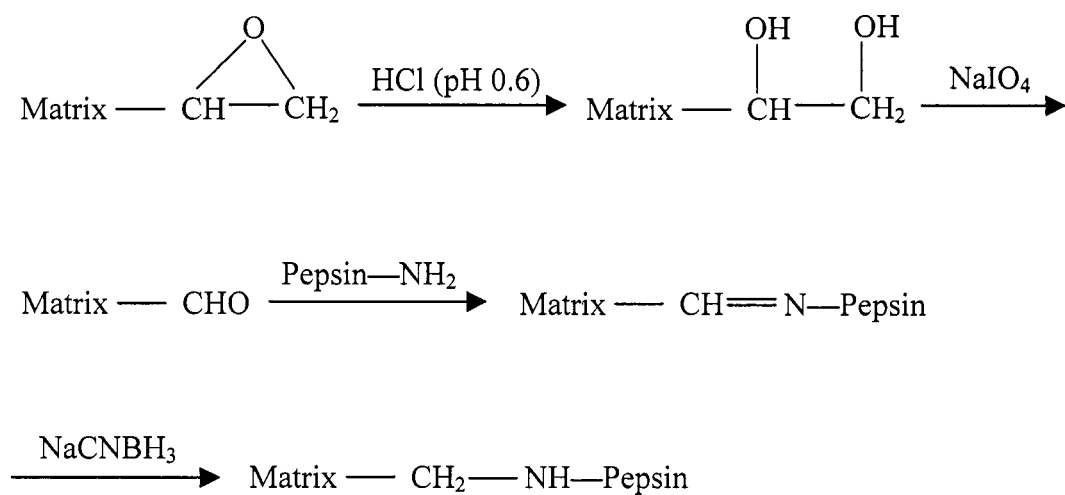


Figure 3-2. Reaction scheme for pepsin immobilization (adapted from ⁸).

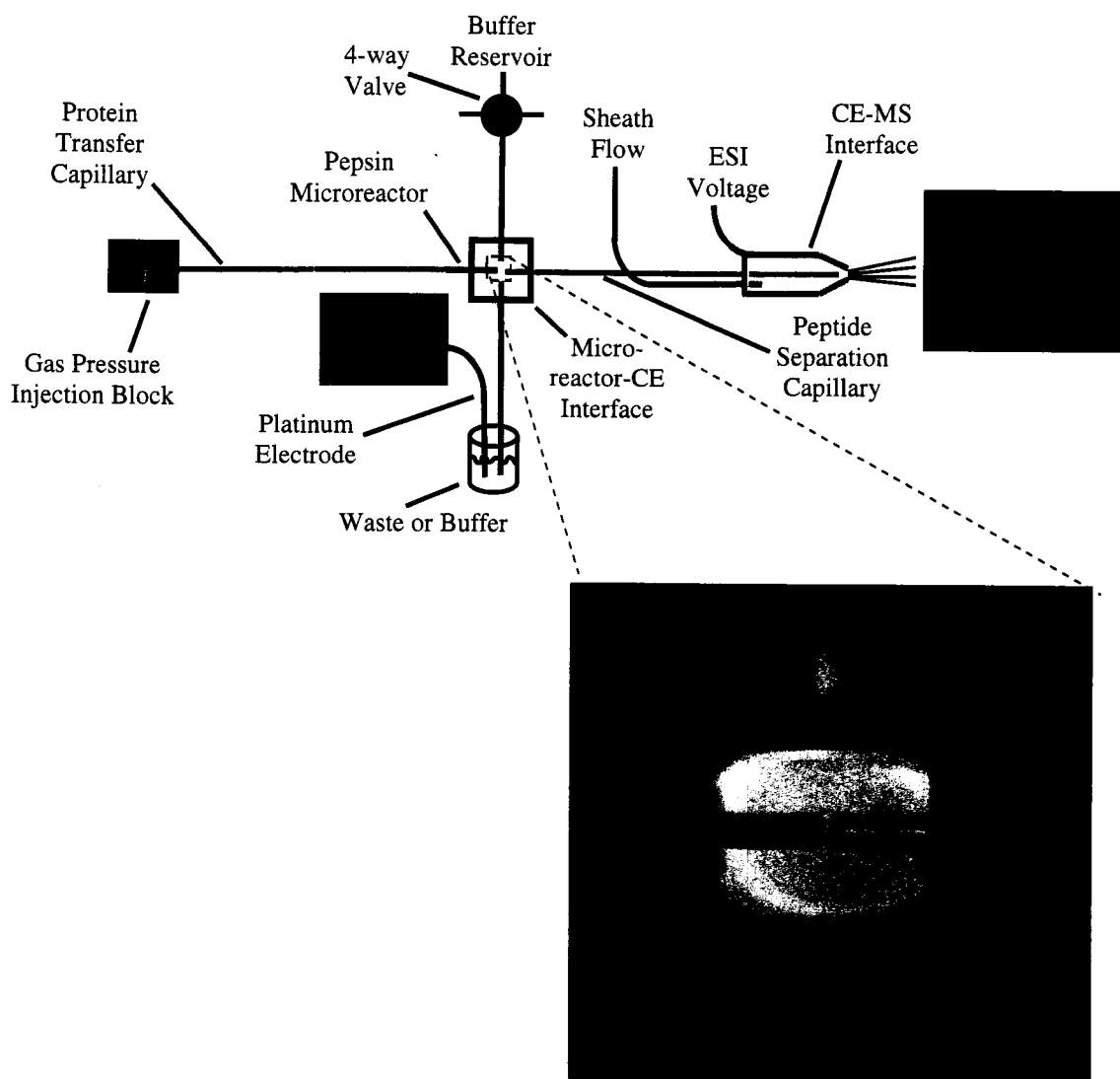
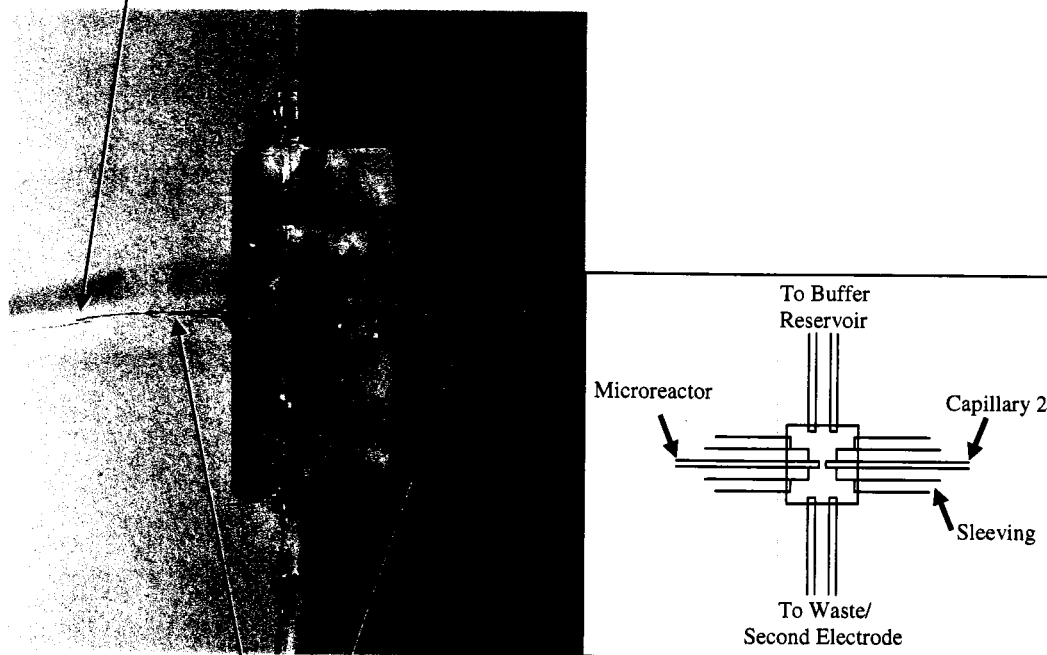


Figure 3-3. The modified CE-MS set-up for on-line microreactor-CE-ESI-MS experiments. The picture shows a detailed view of the Plexiglas-glass interface center; the microreactor's dark monolith can be seen inside the left, horizontal capillary.

Pepsin microreactor inserted into pulled Teflon tubing

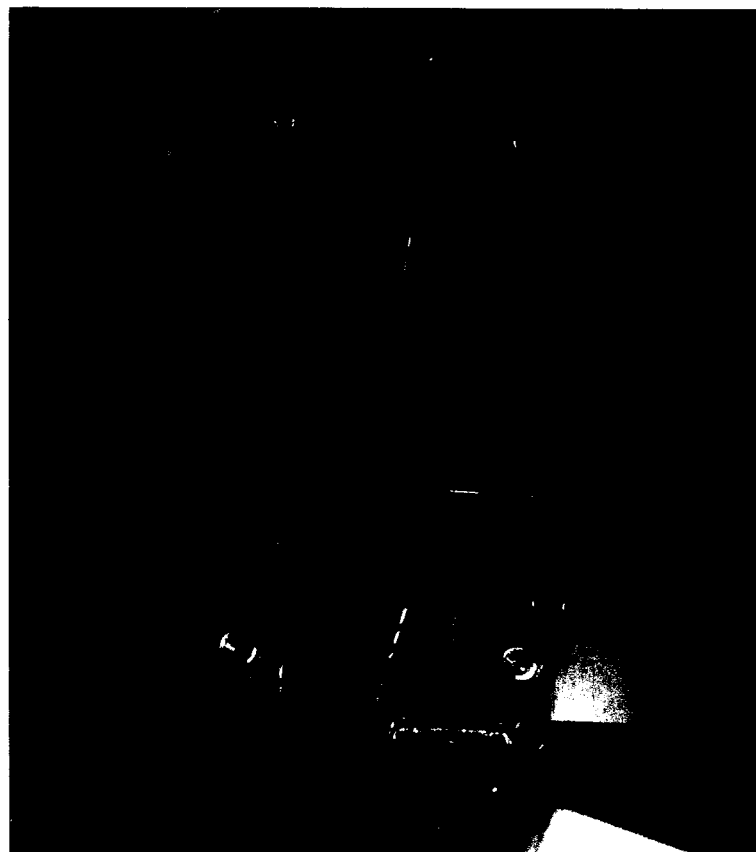
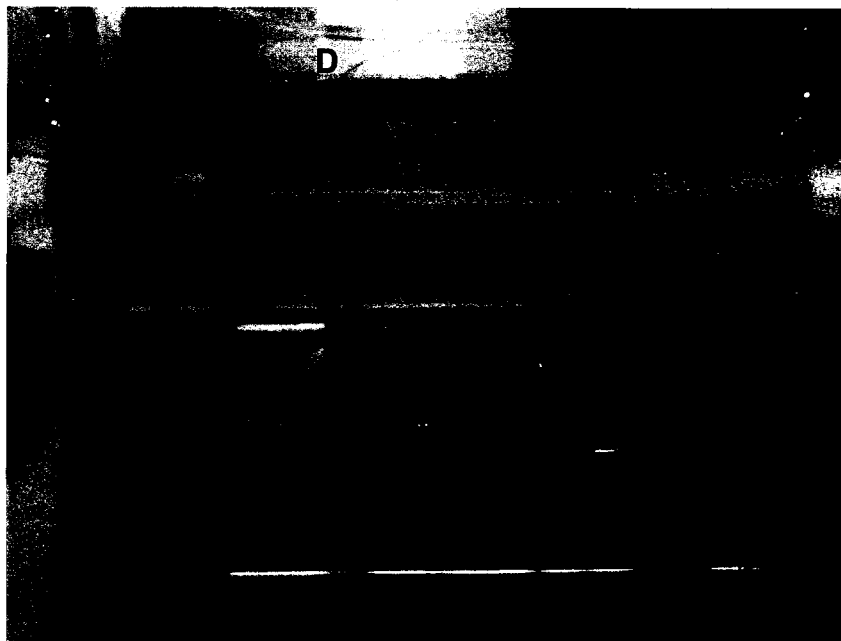


150 μm ID, 360 μm OD
fused silica capillary sleeves

48 μm ID, 148 μm OD PVA-coated
peptide separation capillary

Figure 3-4. The Plexiglas-glass interface for coupling the microreactor to the PVA-coated peptide separation capillary. A close-up of the interface center (dashed black rectangle in the left picture) is shown in the right diagram and in the picture in **Figure 3-3**.

Figure 3-5. Side and top views of the Plexiglas injection block. **A)** Well into which a cut-off PCR tube could be inserted to hold sample or buffer. **B)** The Teflon tubing for He gas was attached to the back of the injection block with a nut and ferrule. **C)** The pink power supply electrode cable was sandwiched between the top and one of the middle pieces of the injection block. A channel had been drilled to fit the electrode cable's outer diameter. **D)** The transfer capillary (that was attached to the microreactor *via* the pulled Teflon tubing) was inserted into the top of the injection block. **E)** Metal clips to fasten the bottom Plexiglas piece to the rest of the injection block.



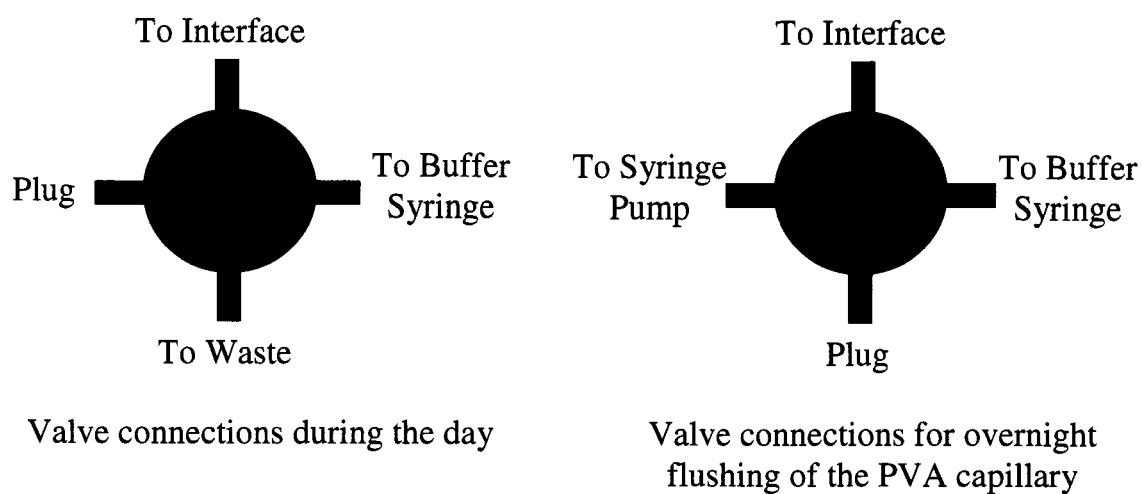


Figure 3-6. The two configurations of the 4-way valve. The right-angle flow position is not shown on the left because this position varied when performing experiments.

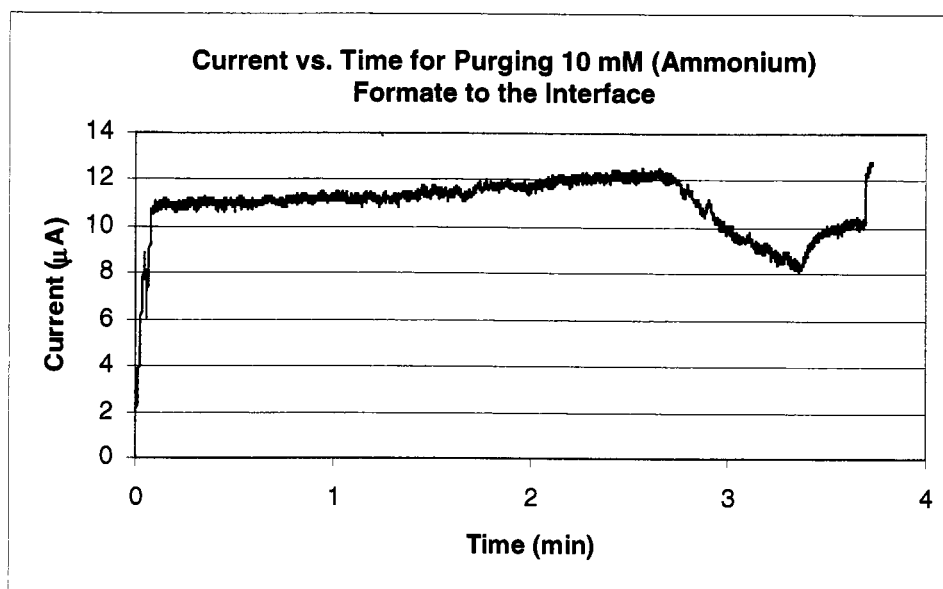


Figure 3-7. Preliminary purging experiment to determine the time needed to purge buffer (or sample) to the interface. See section 3.II.E.2.b. for explanation. The increase in current at ~ 3.3 min was due to the purging of 10 mM (ammonium) acetate (pH 2.7) being stopped. The jump at ~ 3.8 min was observed because the MS was put into standby (which turned off the ion spray voltage) before the CE voltage was stopped, hence the electric field across the PVA capillary was higher than before.

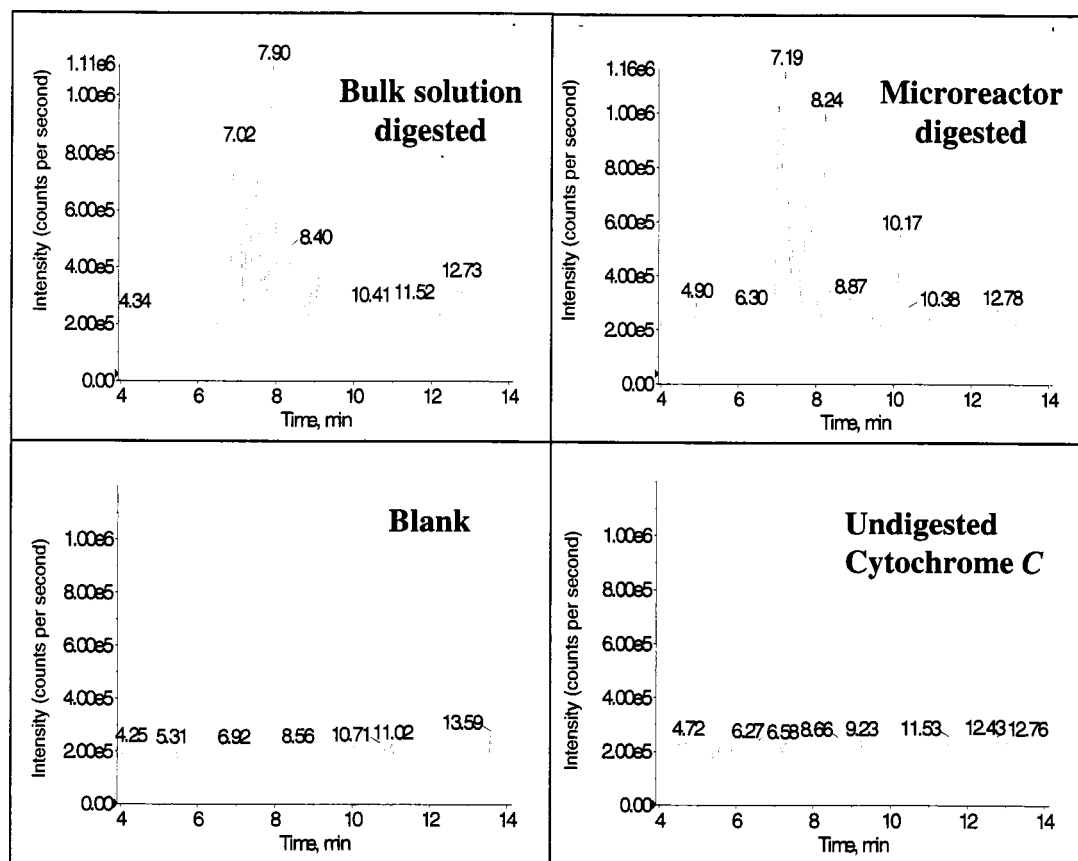


Figure 3-8. Reconstructed ion electropherograms (RIEs) of pepsin bulk-solution digested and microreactor-digested 60 μM cytochrome *C*, and two controls. A 48 μm ID microreactor was used to digest the sample off-line with a 5 min residence time in the microreactor. Experiments were performed with the 1D CE-ESI-MS set-up. One control was a blank consisting of sample matrix that was prepared like the cytochrome *C* sample that had been flushed through the microreactor. The other control was undigested cytochrome *C*. The RIEs were 1x Gaussian smoothed. For details, see sections 3.II.D.1. and 3.III.A.1.

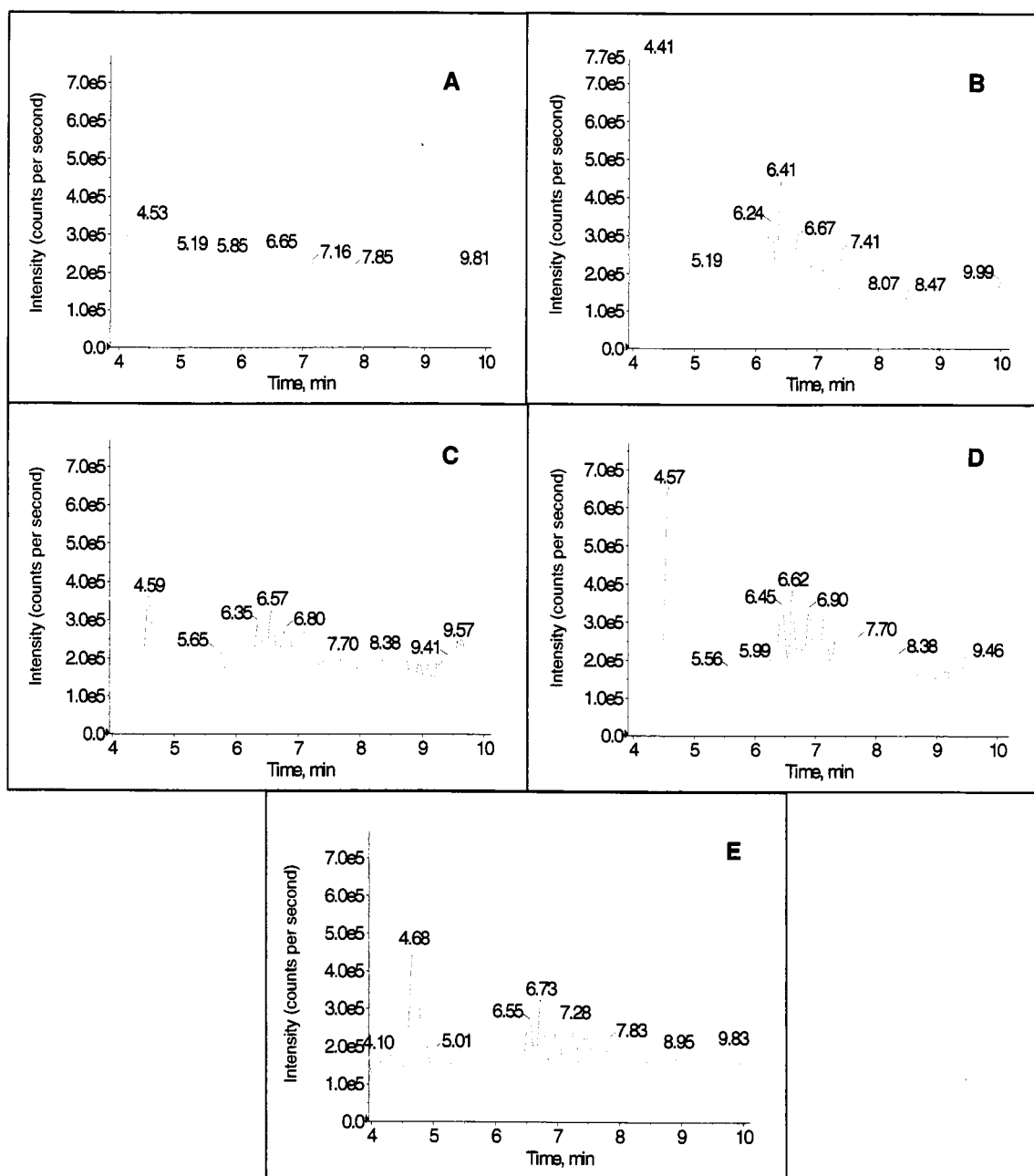


Figure 3-9. Reconstructed ion electropherograms (RIEs) of microreactor homogeneity (off-line) experiments using five different ~ 4.5 cm pieces of the $523 \mu\text{m}$ ID microreactors. $60 \mu\text{M}$ cytochrome C was flushed through the microreactors with a 5 min residence time, and the effluents were collected and run with the 1D CE-ESI-MS set-up. All RIEs were 1x Gaussian smoothed. See sections 3.II.D.2. and 3.III.A.3. for details.

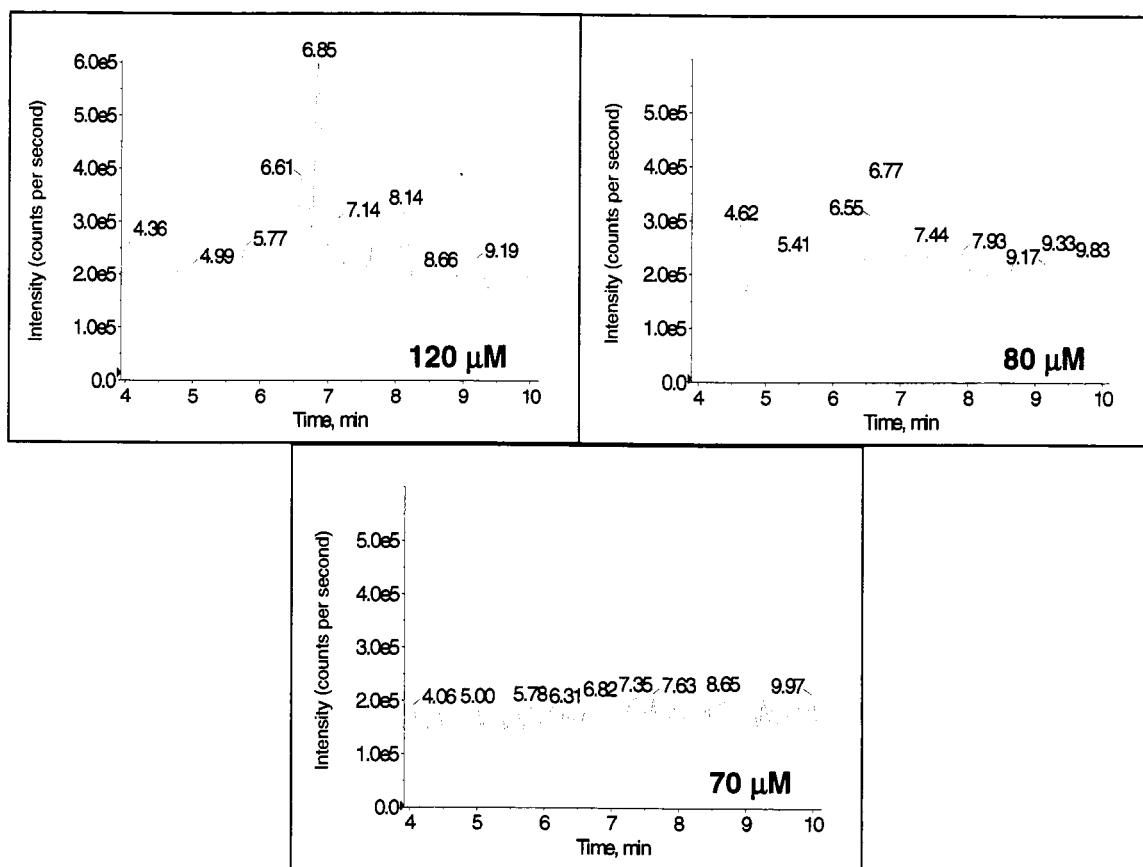


Figure 3-10. Different concentrations of cytochrome *C* digested off-line with the microreactor that was used for data in **Figure 3-9 D**. The residence time was 5 min. All RIEs were 1x Gaussian smoothed. See sections 3.II.D.2. and 3.III.A.4. for details.

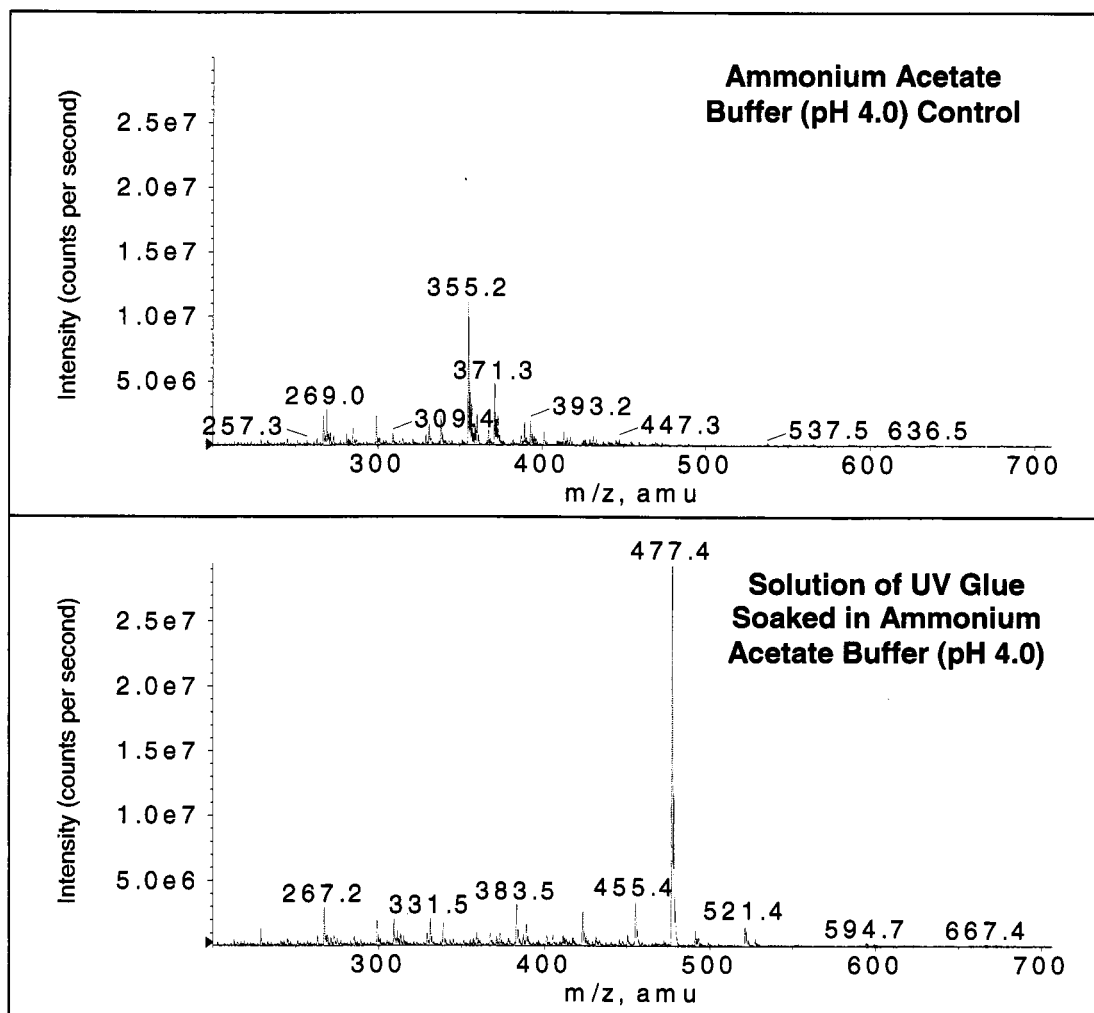


Figure 3-11. Mass spectra of an ammonium acetate (pH 4.0) control solution and a solution of UV glue soaked in ammonium acetate. The UV glue was used when constructing Plexiglas-glass interfaces. See section 3.III.B.1. for explanation.
MS parameters: LIT scan mode; IS voltage: +5500 V; CUR: 20.0; GS1: 20.0; m/z range: 200-1700 amu (although only 200-700 shown for a detailed view); scan rate: 1000 amu/sec; declustering potential: 30 V; entrance potential: 10 V. Solutions were infused with a syringe pump at 2.0 μ L/min.

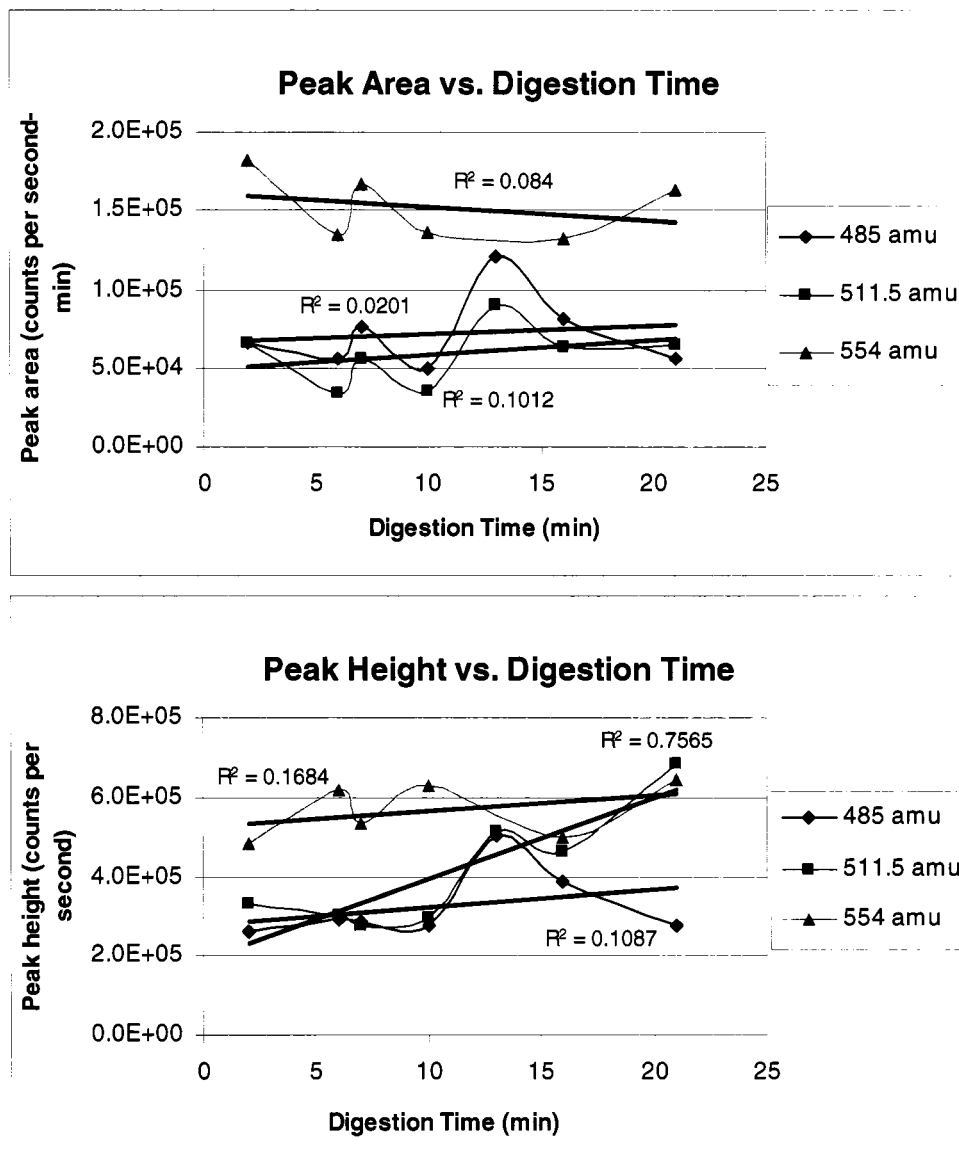


Figure 3-12. Peak areas and heights of selected XIEs vs. varying digestion times. See section 3.III.B.3. for explanation. Smooth curves are a guide for the eye.

Figure 3-13. A) 60 μ M of pepsin bulk-solution digested cytochrome *C* analyzed with 50 mM (ammonium) acetate (pH 4.0) with the 1D CE-ESI-MS set-up; 346 V/cm electric field; 42.4 cm PVA-coated capillary.

B) Same as in A, except with 50 mM (ammonium) acetate + 20 mM hydroquinone (pH 3.9).

C) 200 μ M cytochrome *C* on-line microreactor-digested for 5 min and analyzed with 50 mM (ammonium) acetate + 20 mM hydroquinone (pH 3.9); 346 V/cm electric field; 32.5 cm PVA-coated capillary.

D) Same as in C, except with a 485 V/cm electric field.

E) Same as in C, except with 20 mM (ammonium) acetate + 10 mM hydroquinone (pH 3.9).

F) Same as in C, except with 30 mM (ammonium) acetate + 20 mM hydroquinone (pH 3.9).

A and B can be compared to determine whether hydroquinone has any effect on the peptide separation.

C and D can be compared to determine whether a higher electric field is advantageous.

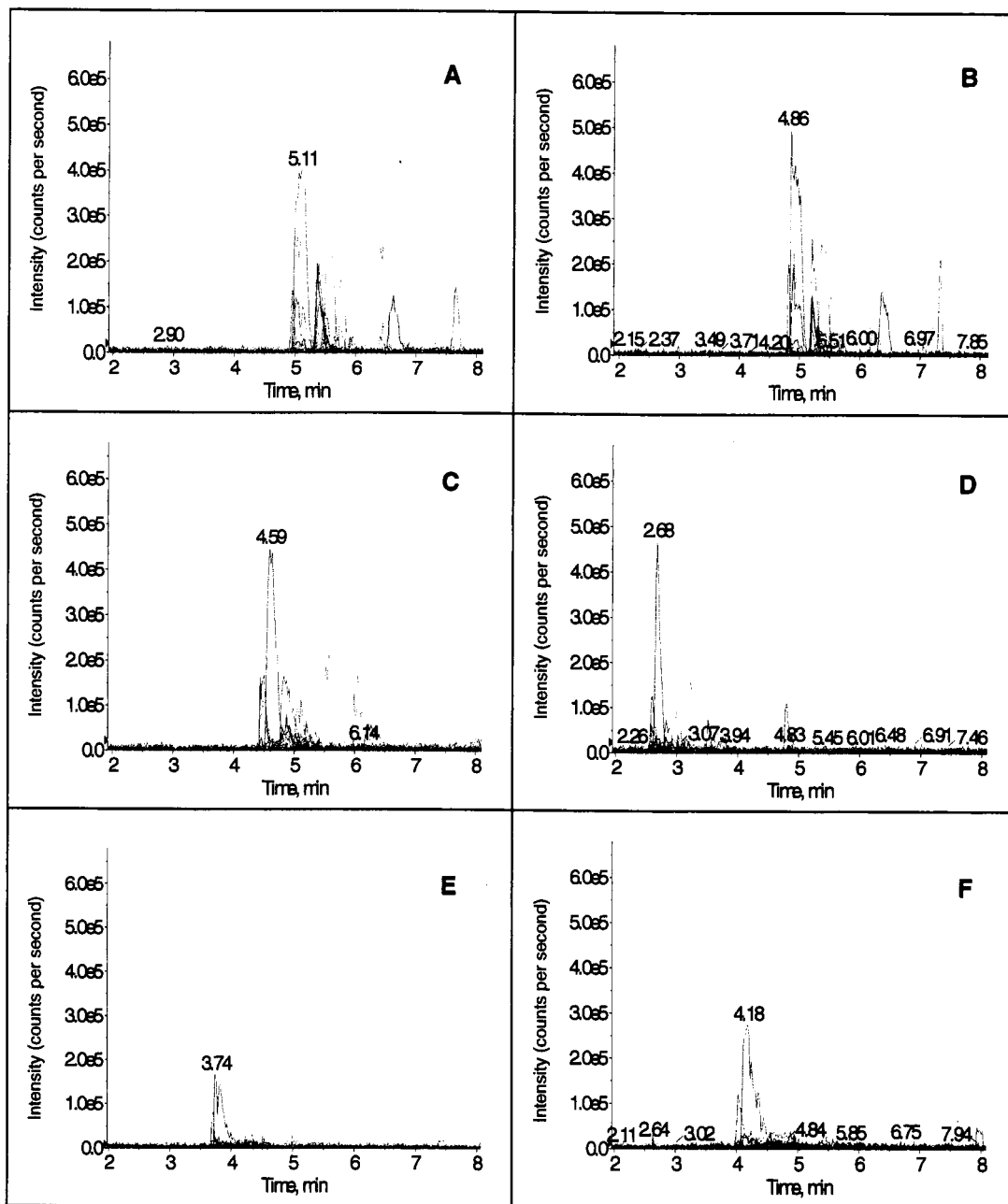
C, E, and F can be compared with respect to the different buffers used.

B and C can be compared with respect to using bulk digestion vs. on-line microreactor digestion, although the sample concentrations are different.

Experimental parameters for A and B: Capillary: 48 μ m ID, 142 μ m OD, 42.4 cm, PVA-coated; sheath liquid: 90% MeOH (1300 nL/min); CE parameters: Injection voltage: +11.5 kV (271 V/cm) (5 sec); the Q TRAP's ion spray (IS) voltage was turned off during injection; separation voltage: +16.9 kV (346 V/cm); MS parameters: LIT scan mode; IS voltage: +2250 V; CUR: 15.0; GS1: 0.0; GS1 was set to 10.0 during the 0.2 min prerun of the acquisition batch (see section 2.III.B.5.); m/z range from 300-1100 amu; scan rate: 1000 amu/sec; declustering potential: 30 V; entrance potential: 10 V.

Experimental parameters for C through F: Whole microreactor (48 μ m ID, 142 μ m OD, 2.0 cm) coupled to the transfer capillary (24.4 cm) *via* ~ 5 cm pulled Teflon tubing; separation capillary: 48 μ m ID, 142 μ m OD, 32.5 cm, PVA-coated; sheath liquid: 90% MeOH (1300 nL/min); CE parameters: Injection voltage: +8.8 kV (271 V/cm) (5 sec) and pressure injection: 22 psi (5 sec); the Q TRAP's ion spray (IS) voltage was turned off during injection; separation voltage: +13.5 kV (346 V/cm); MS parameters: LIT scan mode; IS voltage: +2250 V; CUR: 15.0; GS1: 0.0; GS1 was set to 10.0 during the 0.2 min prerun of the acquisition batch (see section 2.III.B.5.); m/z range from 300-1100 amu; scan rate: 1000 amu/sec; declustering potential: 30 V; entrance potential: 10 V.

None of the XIEs were individually Gaussian smoothed.



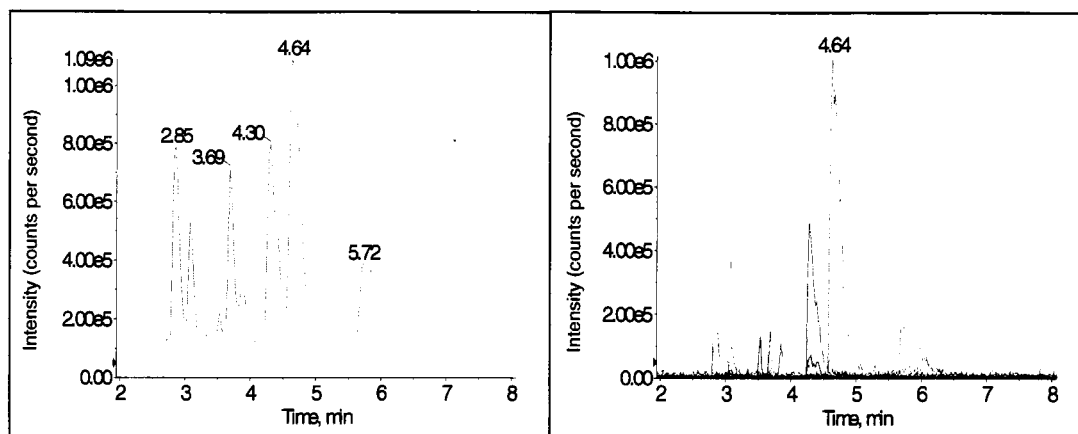


Figure 3-14. On-line 5 min microreactor digestion of 200 μM myoglobin in 10 mM (ammonium) acetate (pH 2.7). The left electropherogram consists of an RIE, 1x Gaussian smoothed, the right shows the 20 overlaid but not smoothed XIEs.

Integrated microreactor: 48 μm ID, 142 μm OD, 32.3 cm total length, 1.1 cm microreactor length; **separation capillary:** 48 μm ID, 142 μm OD, 32.9 cm, PVA-coated; **buffer:** 50 mM (ammonium) acetate + 20 mM hydroquinone (pH 3.9); **sheath liquid:** 90% MeOH (1300 nL/min); **CE parameters:** Injection voltage: +8.9 kV (271 V/cm) (5 sec) and pressure injection: 22 psi (5 sec); the Q TRAP's ion spray (IS) voltage was turned off during injection; separation voltage: +13.7 kV (347 V/cm); **MS parameters:** LIT scan mode; IS voltage: +2250 V; CUR: 15.0; GS1: 0.0; GS1 was set to 10.0 during the 0.2 min prerun of the acquisition batch (see section 2.III.B.5.); m/z range from 300-1100 amu; scan rate: 1000 amu/sec; declustering potential: 30 V; entrance potential: 10 V.

Table 3-1. Percent relative standard deviations (%RSDs) for three extracted ion electropherogram (XIE) masses of four consecutive on-line microreactor-CE-ESI-MS experiments with 200 μ M cytochrome *C*.

	XIE masses (amu)		
	449-450	511.5-512.5	554-555
Peak area %RSD	60	27	25
Peak height %RSD	33	15	7

Table 3-2. 20 extracted ion electropherogram (XIE) masses that yielded the most intense peaks for the myoglobin peptides.

400-499 amu	500-599 amu	600-699 amu	700-799 amu	800-899 amu	900-999 amu
401.5-402.5 492-493	510-511 531.5-532.5 550-551 589.5-590.5	602-603 620-621 623.5-624.5 628.5-629.5 654.5-655.5 675.5-676.5	711-712 763-764 769-770 774.5-775.5 786-787	855-856	902-903 930-931

3.V. Notes to Chapter 3

- (1) Ye, M.; Hu, S.; Schoenherr, R. M.; Dovichi, N. J. *Electrophoresis* **2004**, *25*, 1319-1326.
- (2) Schlamowitz, M.; Peterson, L. U. *J Biol Chem* **1959**, *234*, 3137-3145.
- (3) Christensen, L. K. *Arch Biochem Biophys* **1955**, *57*, 163-173.
- (4) Moini, M.; Cao, P.; Bard, A. J. *Anal Chem* **1999**, *71*, 1658-1661.
- (5) Smith, A. D.; Moini, M. *Anal Chem* **2001**, *73*, 240-246.
- (6) <http://prospector.ucsf.edu>.
- (7) <http://www.hbcpnetbase.com> *CRC Handbook of Chemistry and Physics*, 85th ed., 2004-5.
- (8) Pan, Z.; Zou, H.; Mo, W.; Huang, X.; Wu, R. *Anal Chim Acta* **2002**, *466*, 141-150.

Chapter 4 – 2D CE-UV-microreactor-CE-MS-MS

4.I. Introduction

The complexity of many proteomic samples makes two-dimensional (2D) separations necessary to be able to analyze and detect a large number of components. The two dimensions should be as orthogonal as possible and separate analytes based on different physical and chemical properties to allow better resolution.

As was described in chapter 1, many different 2D configurations have been developed based on liquid chromatography (LC) and/or capillary electrophoresis (CE). CE is fast, fairly easily automated, requires only small sample volumes, and is fairly inexpensive. Unfortunately, CE is not as concentration sensitive as LC because of the lower loading capacity of CE, although this can be improved by pre-capillary or on-capillary concentration.

2D analyses are most often done with protein digests to obtain more easily interpretable MS data. The sample handling required for digestion and other sample preparation can be extensive, and systems are being developed that minimize sample handling steps. For example, Kato *et al.*¹ developed a one-dimensional microreactor-CE-MS system that used a sol-gel based pepsin microreactor to analyze insulin chain β and lysozyme. Simpson and Smith² pointed out that adding a first protein separation dimension in front of the microreactor might be used to analyze proteins with post-translational modifications.

Such two-dimensional CE-microreactor-CE-MS-MS systems could be called orthogonal even if the two separation mechanisms are similar (such as for CZE-CZE), because the two dimensions separate different analytes. The work in this chapter describes initial proof-of-concept experiments with such a CZE-microreactor-CZE-MS-MS system. The one-dimensional (1D) microreactor-CE-ESI-MS system developed in the previous chapter was further modified to accommodate the integrated microreactor capillary as the first dimension for protein separations. UV detection was added in the first dimension to monitor protein migration, which simplified the optimization of 2D experiments. A mixture of cytochrome *C* and myoglobin, and another mixture of 6 proteins, were analyzed with this 2D system, and cytochrome *C* and myoglobin were identified based on tandem mass spectra. There were periodic dropouts of the electrospray, however, which will need to be eliminated in the future.

4.II. Experimental

4.II.A. Chemicals

Bovine pancreas α -chymotrypsinogen (C-4879), bovine heart cytochrome *C* (C-3131), bovine milk β -lactoglobulin (L-4756), chicken egg white lysozyme (L-7651), horse heart myoglobin (M-1882), bovine pancreas ribonuclease A (R-5500), and hydroquinone solid (99+%) were purchased from Sigma (St. Louis, MO). Acetonitrile solution (HPLC grade) was from Fisher Scientific (Fair Lawn, NJ). Ammonium acetate solid (puriss. p.a. for mass spectroscopy) was from Fluka (Buchs, Germany). Methanol solution (HPLC grade) was from EMD Chemicals (Gibbstown, NJ). Water was distilled

and deionized by a Nanopure (Barnstead, Dubuque, IA) system. Helium gas (99.99%) was from Airgas (Radnor, PA).

Buffers and sheath liquids were treated as given in chapter 3, except that 1 mL of the 30 mM (ammonium) acetate (pH 2.7) buffer for the first dimension was centrifuged for 5 min at 15,000 rpm in a 1.6 mL Eppendorf tube. 50 μ L of the solution at the top was transferred to cut-off PCR tubes inside injection block bottoms. This prevented particles from clogging the microreactor. Fresh buffers were used in each experiment.

4.II.B. Sample Preparation

Individual concentrated stock solutions of each of the proteins were prepared in ddH₂O and frozen at -80°C until use. From these, mixtures of either 200 μ M or 300 μ M of each protein in 10 mM ammonium (ammonium) acetate (pH 2.7) were prepared. A stock solution of 85 mM (ammonium) acetate (pH 2.7) was used.

50 μ L aliquots of the mixtures were frozen in 0.6 mL Eppendorf tubes at -80°C until use. An aliquot was then thawed in the refrigerator, briefly mixed by pipetting, and spun down at either 8,000 rpm (for 200 μ M samples) or 3,000 rpm (for 300 μ M samples) for 5 min. Lower speeds were used for more concentrated samples to avoid protein precipitation. Next, 40 μ L of the top of the sample solution was transferred to a cut-off PCR tube inside an injection block bottom. 10 μ L was left behind in case it contained particles that might clog the microreactor. The sample in the injection block was covered with a piece of clean parafilm and stored in the refrigerator between injections. A fresh aliquot was thawed each day.

4.II.C. Instrumental Set-up

The 2D instrumental set-up is shown in **Figures 4-1** and **4-2**. The parts that were added to the 1D instrument were the UV detection system and a power supply for applying voltages at the Plexiglas injection block. A different LabView program was used that was written for 2D analyses by Dr. Mingliang Ye, a former Dovichi group member (see Pocket Material). Some electronics of the instrument were changed as well. Details of these components will be given in the following sections.

4.II.C.1. UV Detection System

A description of the UV detection system has already been given in section 2.II.B.1.. In the 2D set-up, only integrated microreactor capillaries were used for electrophoresis purposes. The procedure for attaching the microreactor capillary to the Plexiglas-glass interface was the same as described in section 3.II.C.2.a.. However, because ~ 2 mm of the polyimide was shaved off with a razor ~ 7-8 cm from the monolith-containing end of the capillary, the microreactor capillary had to be handled very delicately to not break it at the exposed fused silica section.

The following steps for attaching the microreactor capillary to both the UV cross and the interface were found to work well to minimize breakage. The microreactor end was cut square first, and then the microreactor was flushed for 30 min from the monolith-void end to purge any loose monolith particles out of the capillary that might get into the interface space. Some polyimide was then shaved off to make the UV detection window. After that, the capillary was carefully inserted into a 158 μm ID, 360 μm OD, ~ 2-3 cm

capillary and the latter was slid over the detection window for protection. The microreactor capillary was then glued into the Plexiglas-glass interface as previously described.

Before the capillary was inserted into the UV cross, the 158 μm ID sleeve was slid off and the interface was sandwiched in between two Plexiglas pieces that secured the interface and enabled its attachment to the Plexiglas box ceiling, see **Figure 4-2**. The bottom Plexiglas piece had been cut so that the UV cross could rest on it and allow the distance between interface and cross to be quite short. The closer the UV detection was to the interface, the more time was allowed for protein separation before UV detection. Care was taken again when inserting the capillary into the UV cross. The UV fibers were inserted into the cross before the whole sandwich assembly was attached to the Plexiglas box ceiling. The UV fibers were connected to the UV light source and the photomultiplier (PMT) detector.

The UV detection window of the microreactor capillary was then aligned with the UV fibers while monitoring the UV signal with LabView. For this, the cross was carefully moved back and forth on the Plexiglas piece without being taped down so that the capillary could slide inside the cross. The Teflon sleeves and nuts of the cross did not clamp very tightly on the capillary because the tapped holes of the cross were easily stripped, and thus the nuts and sleeves were utilized mostly to hold the capillary and to keep ambient light out of the cross. Once an optimum detection position of the window was found, the microreactor capillary was glued to the sleeve (on the side that went to the injection block) with epoxy. After curing, the UV cross was taped to the bottom piece of the Plexiglas sandwich.

4.II.C.2. Second Power Supply and Related Electronics Modifications

The use of two power supplies and UV detection required three output channels for LabView control. The PCI-6035E data acquisition (DAQ) boards (National Instruments, Austin, TX) that were used in this work had only two output channels each, and hence a second board and ribbon cable (E57891, National Instruments) needed to be added for the 2D set-up. The new pin assignments for the 50 pin cables are given in **Table 4-1**. The wiring in the aluminum box between the hardware and software also had to be changed. The signal from the safety interlock at the Plexiglas box was split with BNC cables between the two power supplies so that no second interlock was needed. A grounding wire was attached between the new power supply and the back of the Q TRAP as had been done for the other power supply. A Pt wire was glued to the electrode cable of the new power supply with silver epoxy (CW2400, Chemtronics, Kennesaw, GA) and inserted into the injection block.

4.II.D. Experimental Procedures

4.II.D.1. CE-UV-microreactor-CE-MS Analyses

Figure 4-3 illustrates how 2D experiments were performed. The UV detection is omitted for clarity. Sample was injected and a prerun (e.g. 3 min) was performed that separated proteins in the first capillary. The applied voltages were then changed to allow for cycles between protein digestions and CZE peptide separations, and fraction transfers. In a fraction transfer, a small plug of digest was injected from the microreactor into the second dimension capillary. The peptides in this plug were then separated in the second

dimension while more protein was digested in the microreactor. The voltages across the first dimension capillary were applied to minimize movement of the components in the first dimension. The transfer-peptide separation cycles were then repeated until all proteins had migrated from the first dimension. As was mentioned in section 3.III.B.4.b., the overall experimental time could be shortened if the second dimension separation was fast.

The voltages shown in **Figure 4-3** were used for only some 2D experiments and were later adjusted. The specific values for each 2D experiment are given in the respective figure captions.

The procedure described in the next paragraphs was performed between runs to set up a new experiment. Some general comments should be made beforehand. First, the second dimension buffer (50 mM (ammonium) acetate + 20 mM hydroquinone (pH 3.9)) was flushed through the 4-way valve and interface to the second dimension (PVA-coated) capillary with a 20 mL glass syringe every ~ minute to not let the capillary dry out. Slight pressure was usually enough to see buffer come out at the electrospray tip. Second, the sheath liquid was kept at 250 nL/min between experiments to avoid having the MicroIonSpray head CE-MS interface dry out. Third, the flushing times for the integrated microreactor capillary depended on the particular microreactor that was used, since they were not completely homogeneous. Fourth, even though the 2D LabView program had a Pre-Run feature (see **Figure 4-4**), neither the UV signal nor the CE currents could be monitored when using it. All voltages were therefore applied using the 2-D Run Cycles feature of the program. The CE voltages had to be briefly turned off after a prerun and a new file had to be opened to start the 2D cycles. Fifth, the program

also did not allow for voltages to be changed to transfer and second dimension separation settings on-the-fly, but this turned out to be advantageous because voltage settings could be changed while a prerun was still being performed. This allowed the time between switching from the prerun to the cycles to be minimized.

At first, the first dimension buffer (30 mM (ammonium) acetate (pH 2.7)) in the injection block bottom was exchanged with fresh buffer. The same was done with the 50 mM (ammonium) acetate + 20 mM hydroquinone (pH 3.9) buffer in the 1.6 mL Eppendorf tube for the second dimension (see **Figure 4-2 B**). The nanofluidic module (NFM) sheath liquid pump (Scivex, Inc., Oak Harbor, WA, see also section 2.II.B.2.) was refilled with freshly sparged sheath liquid since the pump had a capacity of only 250 μ L.

The integrated microreactor capillary was next flushed with 30 mM (ammonium) acetate (pH 2.7) using a 1 mL plastic flushing syringe (see **Figure 3-1 B**). The 30 mM (ammonium) acetate was briefly rinsed from the interface to waste with 50 mM (ammonium) acetate + 20 mM hydroquinone (pH 3.9) from the 20 mL glass syringe. Second dimension buffer was then purged through the PVA-coated capillary for 5 min while the waste line of the interface was plugged. During this time, the density and back pressure of the monolith mostly prevented second dimension buffer from entering the first dimension, but a brief flush was still performed again after the second dimension flush to fill the microreactor capillary completely with first dimension buffer.

A 5 min pre-prerun was then performed with CE and MS voltages set as during protein digestion and peptide separation times (see **Figure 4-3** steps 3 or 5) to equilibrate the CE currents (although they were usually stable within \sim 20 sec). The Q TRAP was put into standby mode after the pre-prerun to inject sample. For some experiments, the

samples were both pressure (with He gas) and electrokinetically injected; for others, only electrokinetic injections were performed. The Q TRAP and CE voltages were reapplied after injection and a prerun was performed to separate the proteins. Analyst data were acquired using batch acquisition, see section 2.III.B.5.. After the prerun, the voltages were changed to the transfer and peptide separation voltages and the 2D cycles were started.

The runs could last as long as 2 hours. Liquid drops were sometimes formed at the spray tip that caused the MS signal to drop. When this happened the liquid was blown off with a brief spurt of Dust-Off®.

4.II.D.2. Preliminary 1D CE-UV Separations of Proteins

Before performing 2D experiments with samples whose protein migration patterns were not yet known, preliminary 1D experiments were performed to determine when the first proteins would be detected with UV and to obtain a UV trace of the complete protein profile. The procedure for preliminary 1D experiments differed from the one shown in **Figure 4-3** in that no voltages for 2D cycles of transfers and peptide separations were applied for the 1D experiments. Instead, only prerun voltages were applied after injection.

4.II.D.3. CE-UV-microreactor-CE-MS-MS Analyses

CE-ESI-MS-MS analyses using the Q TRAP's information dependent acquisition (IDA) capability were described in section 2.III.B.6.. The parameter values were slightly modified for the 2D IDA experiment in this chapter, and they will be given in the figure

caption for the IDA run. The 2D IDA data file was too large to be submitted to the Mascot search engine as a whole, and thus the data were submitted in 20 min sections.

4.II.E. 2D Data Analysis

4.II.E.1. 2D Data Analysis with Analyst

2D data were initially analyzed using the 40 extracted ion electropherograms (XIEs) for pepsin-digested cytochrome *C* and myoglobin that were given in **Tables 2-2** and **3-2**. However, only 13 XIEs of myoglobin and 10 XIEs of cytochrome *C* showed peaks in the 2D data, and these are listed in **Table 4-2**. These XIEs were overlaid and summed to give reconstructed ion electropherograms (RIEs). It should be noted that the 510-511 amu XIE was common to both proteins; to not skew the RIEs, only one XIE of this mass was included in the RIEs.

4.II.E.2. 2D Data Analysis with Matlab

A “Wiff to Matlab.dll” script was obtained from MDS Sciex to convert Analyst files with wiff extensions to the Matlab format. A copy of the script is attached in the Pocket Material of this thesis. The Matlab files were quite large and needed to be burned to CD to be able to transfer them between computers. Professor Dovichi wrote a Matlab program that allowed the data to be plotted in two or three dimensions. For the data given in this chapter, the mass dimension was compressed by a factor of six by successively averaging two adjacent mass data points three times. The scan dimension was not compressed. The scan dimension was related to the time axis in Analyst data; one scan took 0.8 sec at a rate of 1000 amu/sec with a m/z range of 300-1100 amu. The

data were plotted in two dimensions as scan number vs. m/z , and in three dimensions as intensity vs. scan number vs. time of the peptide separation in the second dimension. Unfortunately, the latter two axes' numbers of 3D data were difficult to adjust to real values, so that the given numbers in 3D plots are arbitrary. There were periodic dropouts of the electrospray during which no ions were detected with MS. These data dropouts were replaced in Matlab with average MS intensities of the whole run. The dropouts are discernable in the two-dimensional images as thick horizontal lines.

4.III. Results and Discussion

4.III.A. Sample Preparation

Only standard proteins were used in this proof-of-concept work. Cytochrome *C* and myoglobin were chosen because Dr. Mingliang Ye, a former member of the Dovichi group, used those in his work with a pepsin microreactor (unpublished results). A 6 protein mixture was also used that consisted of cytochrome *C*, myoglobin, α -chymotrypsinogen, β -lactoglobulin, ribonuclease A, and lysozyme. The proteins were available in the laboratory. The latter four proteins have disulfide bonds and are not easily digested by pepsin, but it was explored how well the pepsin microreactor would be able to digest them. For simplicity, no reducing agents were used in this work.

Unfortunately, two other proteins (α -lactalbumin and β -casein) that were tried precipitated when 10 mM (ammonium) acetate (pH 2.7) was added to aqueous solutions of them. This protein characteristic has been noted in the literature,² and it limits this system's universality.

4.III.B. Determination of Prerun Times with Preliminary 1D CE-UV Experiments

Having UV detection as part of the first dimension proved to be advantageous because the time for a prerun could be determined fairly easily based on preliminary 1D CE-UV protein separations. For these experiments, the voltages were applied as during a prerun, see e.g. step 2 in **Figure 4-3**. The experiments were run until all components had migrated past the UV detection window.

Figure 4-5 shows such a prerun UV electropherogram for a cytochrome *C* and myoglobin sample. It should first be noted that the y-axes are inverted because the LabView program did not display data as absorbance but as the signal directly recorded by the photomultiplier tube (PMT). The upper graph shows a baseline shift after 3 min, which was determined to be due to hydroquinone-related buffer components that migrated from the interface into the first dimension capillary. A baseline as between 0-3 min in **Figure 4-5** was obtained when flushing 50 mM (ammonium) acetate (pH 4.0) without hydroquinone through the first dimension.

The zoomed-in graph at the bottom of **Figure 4-5** shows the protein profile in more detail. Based on later MS detection, cytochrome *C* was probably detected at ~ 4-4.8 min, and the peak at ~ 7 min corresponded to myoglobin. Considering that the UV detection was 6.9 cm from the start of the microreactor, the proteins would not have reached the microreactor at ~ 3 min if the 2D cycles were started then. Choosing a shorter prerun time would ensure that the cycles were not started after a protein had already reached the microreactor. Other group members who had performed 2D

experiments with laser induced fluorescence detection also advised that it would be good to include a few cycles of void volume to give the system time to equilibrate to the 2D cycles before the first sample fractions would be transferred into the second dimension capillary. The prerun times could be optimized later based on 2D experiments to shorten the initial void time in 2D experiments, but these UV data gave at least a rough estimate of when 2D cycles could be started.

It should be noted that the non-monolithic part of the first dimension capillary had been coated with γ -MAPS as part of the capillary wall modifications before polymerization of the monolith. Even with the coating, however, the protein peaks were somewhat tailed.

4.III.C. Stability of First Dimension Contents During Second Dimension Separation Times

The proteins in the first dimension should experience as little electrophoretic movement as possible while the peptides are separated in the second dimension. To achieve this, an appropriate electric field needed to be applied across the first dimension capillary, and it was found that the use of the UV detection was again advantageous when optimizing the applied voltages.

Unlike what is shown in **Figure 4-3** for steps 3 and 5, the voltages on power supplies 1 and 2 in initial 2D experiments were both set to 13.0 kV during the protein digestion and peptide separation times. However, it was observed that the contents in the first dimension capillary apparently migrated. This was concluded based on drifts in the

UV signal during the peptide separation times, see the circled part in **Figure 4-6 A**. The absorbance of the hydroquinone-related components was fortuitous in this case.

The migration was due to a voltage drop across the Teflon tubing between the Plexiglas-glass interface and the electrode of power supply 2 in the second dimension buffer reservoir. This caused the voltage at the interface to be less than the voltage at the electrode. To limit the migration in the first dimension, the voltage of power supply 1 was varied and the UV signal was observed in 2D test experiments that did not use sample. **Figures 4-6 B** and **C** show the UV traces when power supply 1 was set to +12.9 kV and +12.95 kV, respectively. In **B**, the adjustment had been too much and the drift was opposite that observed in **A**. In **C**, however, hardly any drift was seen. Power supply 1 was therefore set to +12.95 kV during the protein digestion and peptide separation times of the 2D cycles.

Even with this adjustment, however, some drift of the first dimension contents was observed in later experiments using samples, see the UV trace circled between ~ 22-25 min in **Figure 4-6 D**. But the drifts were not observed during all cycles (see ~ 7-9 min in **Figure 4-6 D**), and hence no further improvements were attempted.

4.III.D. 2D Experiments with a Cytochrome C and Myoglobin Mixture

4.III.D.1. CE-UV-microreactor-CE-MS

10 mM (ammonium) acetate (pH 2.7), 30 mM (ammonium) acetate (pH 2.7), and 50 mM (ammonium) acetate + 20 mM hydroquinone (pH 3.9) were used as the sample, first, and second dimension buffers, respectively. The differences in ionic strength were chosen to achieve on-line stacking of the sample both after injection into the first

capillary and after the transfers into the second capillary. The low pH of the first dimension buffer was chosen because pepsin's activity is highest at low pHs.^{3,4}

Unfortunately, cytochrome *C* was not always observed in 2D experiments. At first it was thought that the cytochrome *C* stock solution that was used to make the cytochrome *C* and myoglobin mixture had been too old, but the protein was not always observed even with a mixture containing fresh cytochrome *C*. It is not clear why this was the case because prerun times had been chosen to ensure that cytochrome *C* had not inadvertently already passed through the microreactor before the 2D cycles were started.

The voltage program that was used for the experiments that are described in this section and the next is given in **Table 4-3 A**. **Figure 4-7 A** shows the total ion electropherogram (TIE) of a 2D run in which both proteins were detected. **Figures 4-7 B, C, and D** show a background mass spectrum, a mass spectrum with m/z values corresponding to cytochrome *C*, and a mass spectrum with m/z values corresponding to myoglobin, respectively. The blue highlighted areas in **Figure 4-7 A** indicate the time spans over which these spectra were summed. As mentioned in section 4.II.E.1., only 10 XIEs were found for cytochrome *C* and only 13 XIEs for myoglobin out of the 40 XIEs that were used in chapters 2 and 3. The 23 XIEs are listed in **Table 4-2**. Since the ~ 511 amu mass showed peaks for both cytochrome *C* and myoglobin, only one XIE (510-511 amu) of this mass was used for RIEs to not skew the data.

Figure 4-8 A shows the complete RIE of the data in **Figure 4-7**. Two broad envelopes are seen that indicate the separation of the proteins in the first dimension. The broad envelopes are broken down into smaller peaks, which correspond to individual transfers of digested proteins into the second dimension. **Figure 4-8 B** shows a detailed

view of the data. Some resolution of peptides in the second dimension can be seen in later peaks for myoglobin (e.g. at ~ 62, 65, and 68 min). The peak efficiency of the proteins in the first dimension might be improved in the future.

Figure 4-9 illustrates the same data as a two-dimensional gel image analyzed with Matlab, see section 4.II.E.2.. The spots from scan numbers ~ 1400-2000 are cytochrome C spots, and the spots from ~ 2000 and later are myoglobin spots. The zoomed area shows some details of the gel image. The two masses in the zoomed area appear at later scan numbers than the other spots corresponding to myoglobin, but no explanation for this has been found yet.

The data could also be presented as 3D images after Matlab processing, see **Figure 4-10**. The vertical axis represents MS signal intensity, the left horizontal axis represents the first dimension separation, and the right horizontal axis represents the second dimension separation. Unfortunately, it was difficult to convert the axes numbers to the correct values, so that they were left as arbitrary numbers. The peak for 930 amu happened to be split upon Matlab processing. The masses for the 3D plots were chosen to show peaks with different intensities and locations in the horizontal plane.

Figure 4-11 shows the RIEs of a second experiment that was performed on the same day and with the same conditions as the experiment shown in **Figures 4-7 to 4-10**. The dropout of the MS signal between ~ 19-32 min was due to a large liquid drop that had accumulated at the spray tip. This drop was blown off with Dust-Off®. The nebulizer gas (GS1) could not be used for this because its setting could not be changed on-the-fly during a run acquired with an acquisition batch. The data are also shown as a gel image in **Figure 4-12**, and as 3D images in **Figure 4-13**. This experiment was

stopped fairly early after the myoglobin peaks had eluted, whereas the earlier experiment had been run for a longer time. The gel images look therefore slightly different. The peaks are also more intense in the later run.

Overall, the peaks of 2D data were not as intense as with 1D data, but this was expected because in previous 1D analyses, a large plug of protein digest was hydrodynamically and electrokinetically injected from the microreactor into the PVA peptide separation capillary. In 2D experiments, the plugs of digest that were transferred to the second dimension were relatively small because they were transferred only electrokinetically.

4.III.D.2. CE-UV-microreactor-CE-MS-MS

An information dependent acquisition (IDA) experiment was performed with the same sample. Some of the IDA parameter values had been changed compared to the values used in chapter 2, see **Figure 2-20**. For example, the ion intensity threshold was lowered from 50,000 counts per second (cps) to 10,000 cps based on what was noted in the last paragraph. If a mass spectral peak did not exceed this threshold, it was not chosen for tandem mass spectral fragmentation. Also, the IS voltage was now 50 V higher at 2250 V because better spray stability was observed with this voltage than the earlier one. The enhanced product ion scan m/z range was shortened from 100-1700 amu to 100-1300 amu because hardly any mass spectral peaks were detected in the higher range. This reduced the IDA cycle times from 8.1182 to 6.5182 sec.

Both proteins were identified, see **Figures 4-14 to 4-17**. Cytochrome *C* was identified based on 4 different peptides, and myoglobin based on 2. The Mascot

parameters were also slightly different from the ones used in chapter 2. Up to 3 missed cleavages were allowed, instead of just 1. The peptide mass tolerance was increased from ± 0.5 Da to ± 0.8 Da, and the MS/MS mass tolerance from ± 0.3 Da to ± 0.6 Da. The identifications were based on average mass values instead of monoisotopic ones. Better identification results were obtained using these parameter values.

4.III.E. 2D Experiments with a 6 Protein Mixture

A slightly more complex mixture of proteins was also used that consisted of 300 μ M each of cytochrome *C*, myoglobin, α -chymotrypsinogen, β -lactoglobulin, ribonuclease A, and lysozyme in 10 mM (ammonium) acetate (pH 2.7). The latter four were available in the laboratory, but unfortunately these proteins either had disulfide bonds or were not easily digested by pepsin. They were still used to see how well the microreactor might digest them. A 200 μ M concentration had been previously tried but very weak protein signals were observed for myoglobin, and none for the other proteins. The voltage program was changed from the cytochrome *C* and myoglobin experiments to maybe increase the peak efficiencies and get a faster separation. The new voltage program is given in **Table 4-3 B**. No pressure injection was applied because the injection voltage had also been increased.

The UV electropherogram of a preliminary experiment is shown in **Figure 4-18**. The myoglobin peak, which is estimated to have been part of the doublet at ~ 3.2 min, was not as intense as in **Figure 4-5**. It is assumed that cytochrome *C* was part of the first peak, and that the three peaks consisted of two proteins each. All peaks were quite broad even with the increased electric field across the first dimension capillary.

Since no previous 1D CE-MS experiments had been performed with the 4 new proteins, no lists of XIEs were available with which to interrogate the data. Usually, the elution of e.g. myoglobin could be monitored in real time by displaying the 401.5-402.5 amu XIE in Analyst, but this was not possible here with the other four proteins. The 2D experiments were thus run for 2 h to ensure getting data for all 6 proteins. Unfortunately, no proteins other than myoglobin were observed, and not even all 13 XIEs of myoglobin yielded peaks. The 4 new proteins were apparently too resistant to pepsin cleavage, but it is still unclear why cytochrome *C* was not detected.

For the data analysis, one run's gel image was analyzed to give approximate m/z values, see **Figure 4-19**. Finding m/z values with the gel image was easier than using the Analyst software and the method described in section 2.II.F.. A subsequent analysis of the mass spectral data in Analyst yielded a list of six m/z values with which peaks were seen:

401.5-402.5, 510-511, 620-621, 763-764, 930-931, 985-986 amu.

The first 5 masses matched with the 20 XIEs of myoglobin peptides given in **Table 3-2**. An analysis of the previous 1D experiments with myoglobin determined that the 985-986 amu peak could also be attributed to myoglobin, although this mass showed only a very weak peak in the 1D data.

Two RIEs based on the 6 XIEs given above are shown in **Figures 4-20 A and B**. **Figure 4-20 A** represents the complete run, while **4-20 B** shows the time where myoglobin peaks were detected. An electropherogram of the overlaid but not summed XIEs is shown in **Figure 4-20 C**, and some peak assignments are given. The RIEs were 1x Gaussian smoothed, whereas the XIEs were not individually smoothed.

The peak efficiencies in the second dimension were very high and often peaks were only a few seconds wide. One factor for this might be that a PVA-coated capillary was used that had been prepared only a few days before the experiment. For the previous 2D experiments, the PVA capillary had been coated a month before and had been connected to the interface and the MS for ~ 1 week before the data in the previous sections were obtained.

The data are also presented as 3D plots, see **Figure 4-21**. The numbers on the horizontal axes are again arbitrary. Some trailing peaks are seen for masses 401.5 and 763 amu, which indicate that the protein content from the first dimension was transferred to the second dimension over several transfers. Some spatial resolution in the horizontal plane of first dimension vs. second dimension separation time is evident between the XIEs.

An information dependent acquisition experiment was performed using the same experimental conditions. No protein identifications were made with Mascot, however, possibly because the peak widths were so narrow (see also section 2.III.B.6.).

4.III.F. Periodic MS Signal Dropouts

Periodic absences of the electrospray and MS signal were briefly mentioned in section 4.II.E.2. on Matlab data analysis. These signal dropouts are evident when the data are presented with Analyst, see **Figures 4-7, 4-8, 4-11, and 4-20**. They were also observed in shorter 1D experiments, but their periodicity was not detected until longer 2D experiments were performed. Unsuccessful attempts were made to eliminate these

dropouts, but it is hypothesized that they might be related to the liquid compositions of the running buffers and/or the sheath liquid.

Since the Q TRAP was equipped with a camera, the liquid spray at the stainless steel tip could be somewhat observed. Before the dropouts occurred, there was usually a sudden liquid build-up at the tip and a concurrent MS signal jump (see **Figure 4-7**), but immediately afterwards no liquid spray was seen. After ~ 1-2 min, a large amount of liquid suddenly spurted out of the tip and splashed onto the MS orifice inlet plate. The liquid quickly evaporated and the MS signal usually went back to its previous baseline level.

Experiments were performed with either increased nebulizer gas (GS1) settings, increased or decreased sheath liquid flow rates, or with different sheath liquid compositions. An increase in GS1 to e.g. 2 consistently caused more liquid to accumulate at the spray tip than with a GS1 setting of 0. An increase or decrease of the sheath liquid flow rate from 1300 nL/min to 1500 nL/min or 1000 nL/min also did not alleviate the dropouts.

Changing the sheath liquid composition did have some effect on the periodicity of the dropouts. A more volatile sheath liquid of 90% MeOH, 5% ACN, and 5% ddH₂O was tried. However, the signal dropouts were even more frequent than with 90% MeOH and 10% ddH₂O, see **Figure 4-22**. There were also many shifts of the baseline, but that had sometimes been observed with the 90% MeOH sheath liquid as well. A sheath flow composition of 75% MeOH, 5% ACN, and 20% ddH₂O proved to be not volatile enough and much liquid accumulated at the electrospray tip. That experiment had to be terminated.

Based on these experiments, it is believed that the dropouts are related to the liquid compositions of the system and maybe also the composition of the running buffer. It could be possible that the concentrations of the ammonium acetate and hydroquinone are too high and that somehow evaporation at the spray tip causes solid to build up and temporarily clog the tip. The tip certainly seems to become clogged considering the sudden liquid spurt from the tip at the end of the dropouts. Further experiments will need to be performed to resolve this problem.

4.IV. Conclusions

The one-dimensional instrument developed in previous chapters was reconfigured to a CE-UV-microreactor-CE-MS-MS system. The workflow for 2D experiments consisted of an initial protein separation prerun in the first dimension, which was followed by cycles of fraction transfers (from the first to the second dimension) and peptide separations in the second dimension. The proteins in the first dimension were digested in the microreactor while the peptides were separated. Preliminary 1D experiments in the first dimension used UV detection to determine when the first proteins of a sample would elute, and thus when to start the 2D cycles after a prerun.

Two protein mixtures were analyzed; one contained cytochrome *C* and myoglobin, the other contained the same but also α -chymotrypsinogen, β -lactoglobulin, lysozyme, and ribonuclease A. Both cytochrome *C* and myoglobin and their peptides were separated and identified when using the 2 protein mixture in 2D experiments, although fewer masses were observed than in one-dimensional experiments. Only

myoglobin masses were observed in the 6 protein mixture experiments. Disulfide bonds and general resistance to pepsin cleavage probably prevented the latter four proteins from being detected. Unfortunately, cytochrome *C* was also not detected in the experiments with the 6 protein sample, and the same was true in some experiments with the 2 protein sample.

The data were analyzed with the Q TRAP's Analyst software and with Matlab. The latter allowed the data to be represented as gel images and in three dimensions. Periodic dropouts of the mass spectrometry signal and electrospray were observed, but they could not be eliminated with different experimental conditions.

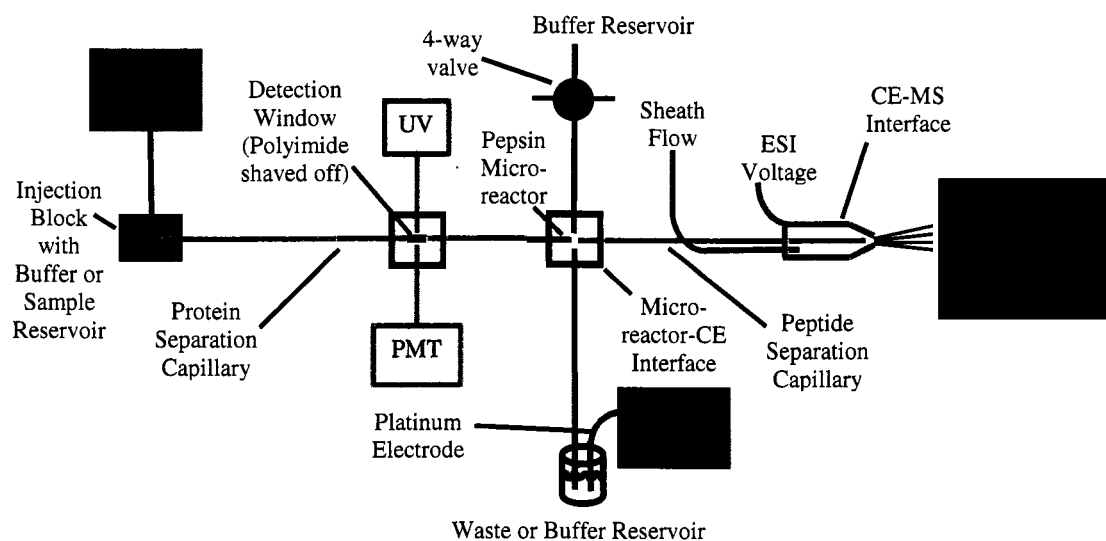


Figure 4-1. Schematic diagram of the 2D CE-UV-microreactor-CE-MS-MS instrument.

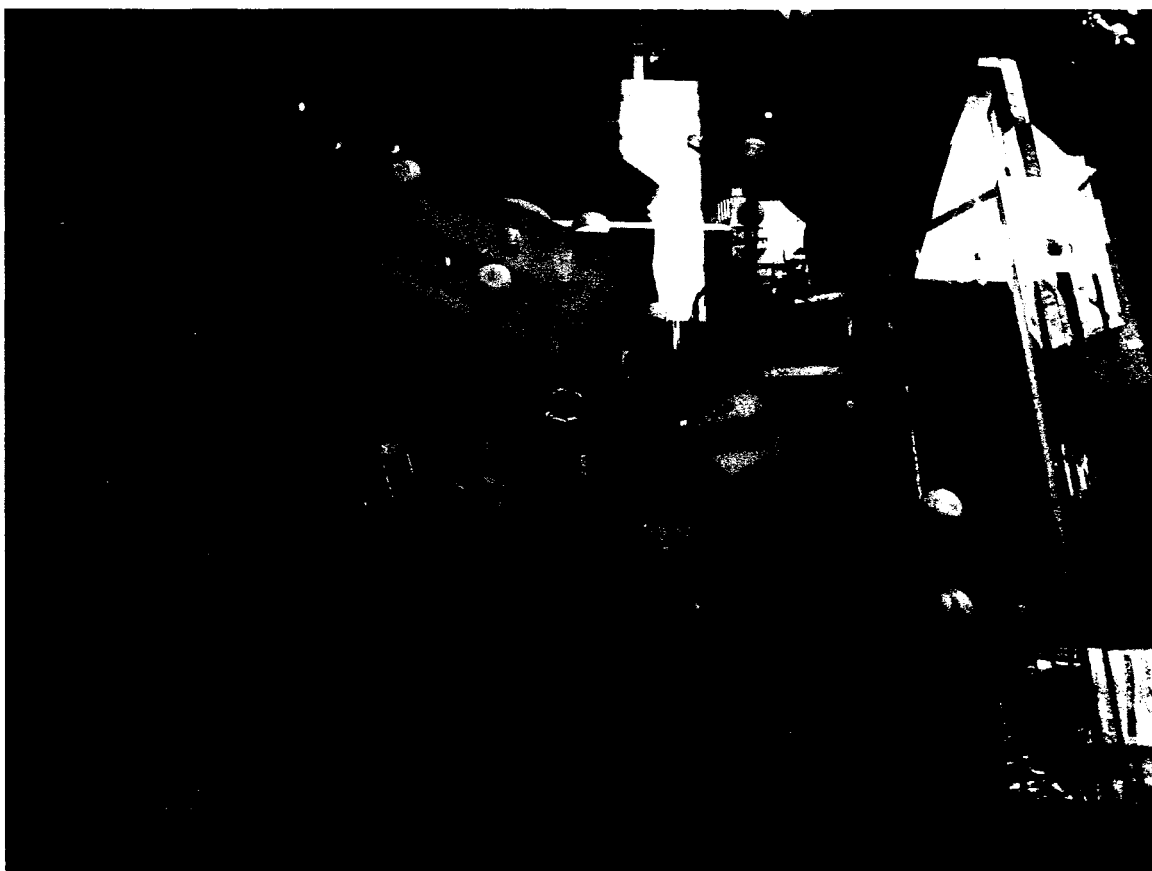


Figure 4-2. Picture of the 2D instrumentation. **A)** Plexiglas injection block with buffer or sample reservoir. The pink cable is the electrode cable from power supply 1. **B)** Holder for the Eppendorf tube that contains the second dimension buffer. **C)** Teflon cross for UV detection. **D)** Plexiglas-glass interface cross and its holder. **E)** Holder for the electrode cable from power supply 2. **F)** 4-way valve.

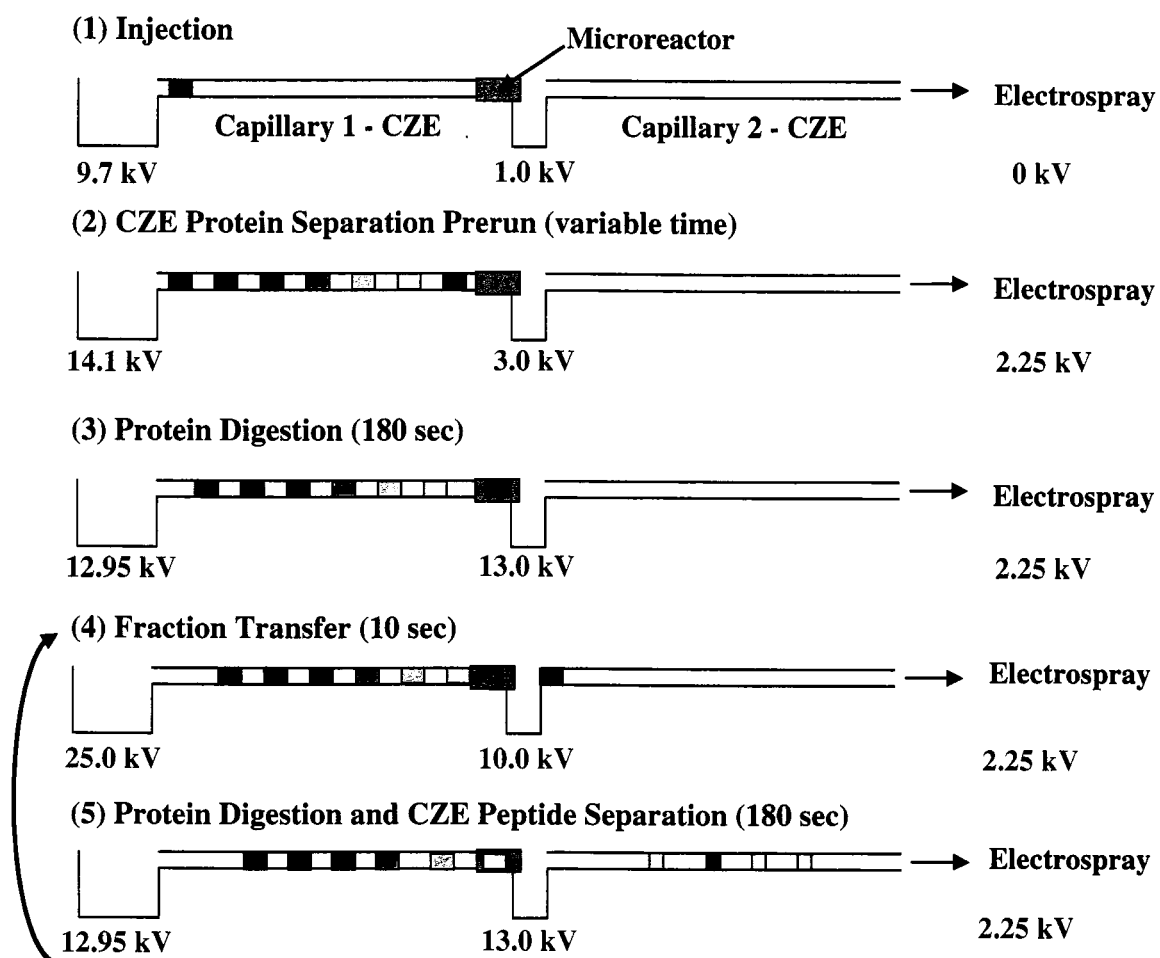


Figure 4-3. Experimental procedure for 2D experiments. The voltages shown are examples, and not every experiment used these same voltages. Please see the figure captions of each experiment for specific values.

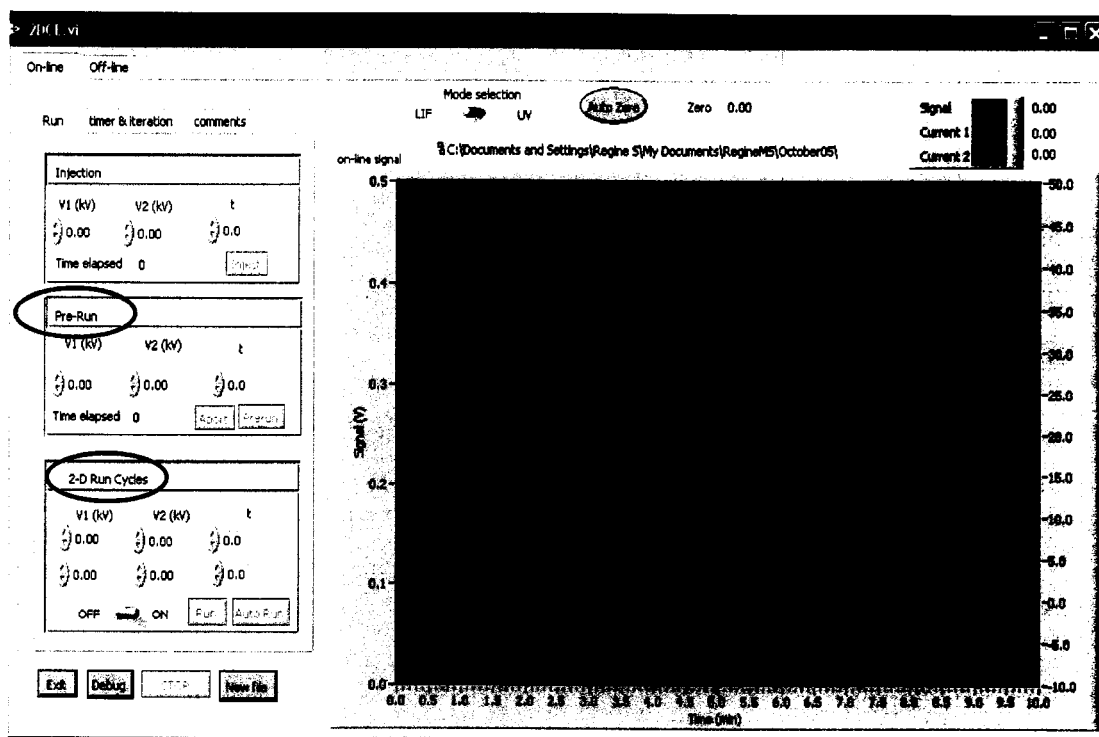


Figure 4-4. Front panel of the 2D LabView program.

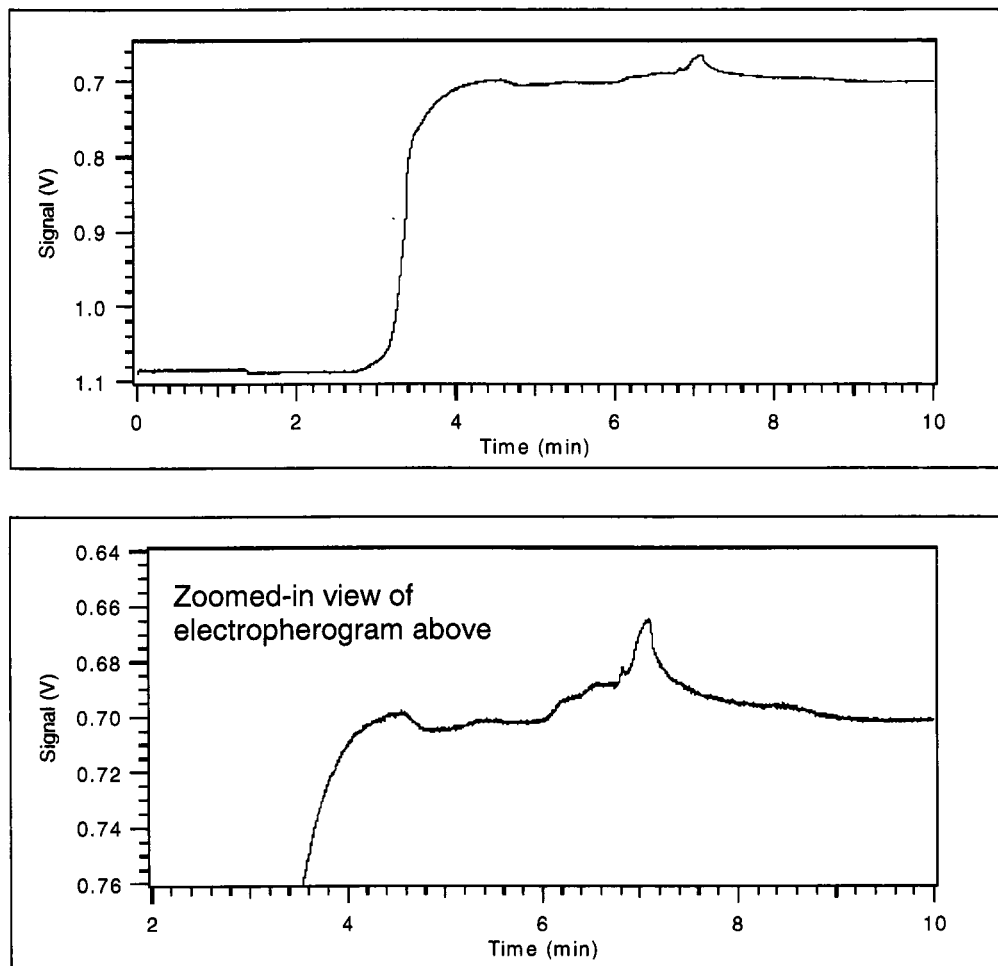


Figure 4-5. UV detection traces of the same preliminary 1D CE-UV experiment with 200 μ M cytochrome *C* and 200 μ M myoglobin in 10 mM (ammonium) acetate (pH 2.7). The baseline differences in the top electropherogram are due to hydroquinone-related components migrating from the Plexiglas-glass interface into the first dimension capillary.

Experimental conditions: **Integrated microreactor:** 48 μ m ID, 142 μ m OD, 32.2 cm total length, 1.1 cm microreactor length, 24.2 cm from inlet to UV detection window; **PVA-coated capillary:** 48 μ m ID, 142 μ m OD, 31.2 cm; **1st dimension buffer:** 30 mM (ammonium) acetate (pH 2.7); **2nd dimension buffer:** 50 mM (ammonium) acetate + 20 mM hydroquinone (pH 3.9); **sheath liquid:** 90% MeOH (1300 nL/min); **CE parameters:** Injection: power supply 1 = +9.7 kV (270 V/cm); power supply 2 = +1.0 kV (10 sec) and pressure injection: 22 psi (10 sec); the Q TRAP's ion spray (IS) voltage was turned off during injection; 1st dimension separation voltage: power supply 1 = +14.1 kV (346 V/cm); power supply 2 = +3.0 kV; PMT bias = +0.5 kV; **MS parameters:** LIT scan mode; IS voltage: +2250 V; CUR: 15.0; GS1: 0.0; m/z range from 300-1100 amu; scan rate: 1000 amu/sec; declustering potential: 30 V; entrance potential: 10 V.

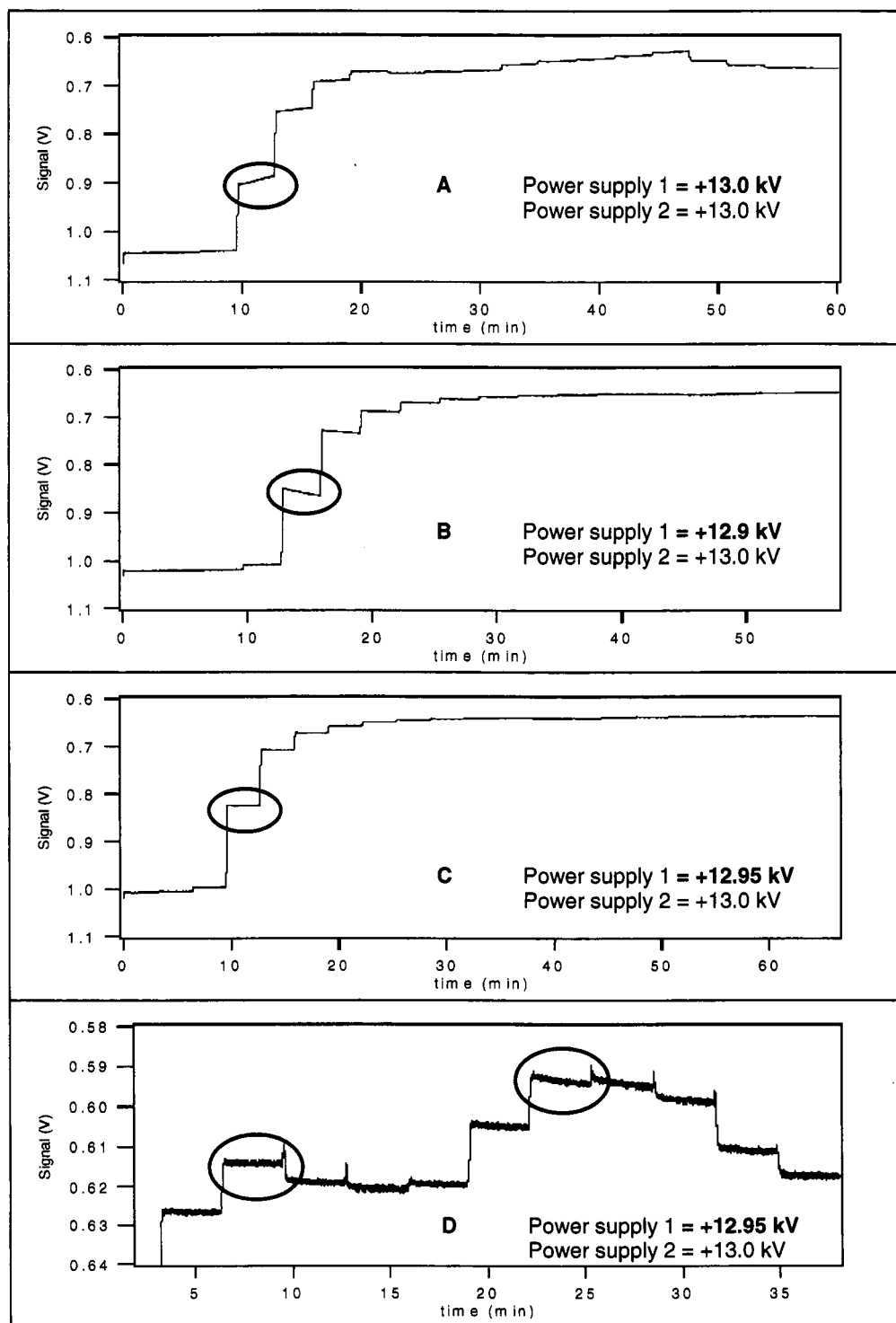


Figure 4-6. Optimization of applied voltages during protein digestion and peptide separation times in 2D cycles. See section 4.III.C. for explanation.

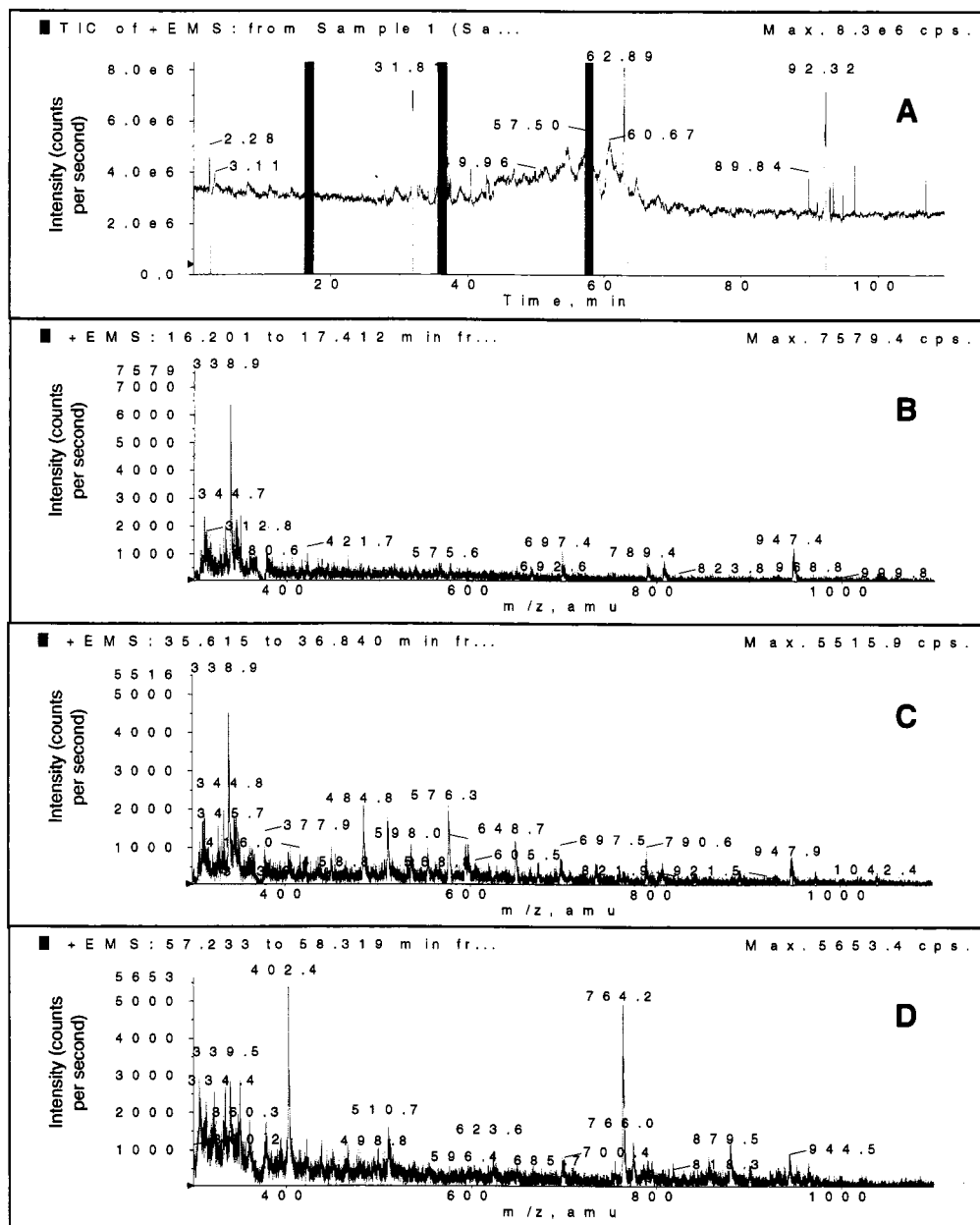


Figure 4-7. A) Total ion electropherogram of a 2D experiment with 200 μ M each of cytochrome C and myoglobin in 10 mM (ammonium) acetate (pH 2.7). B) Mass spectrum of background. C) Mass spectrum of a cytochrome C peak. D) Mass spectrum of a myoglobin peak. Experimental details are given in **Figure 4-8**.

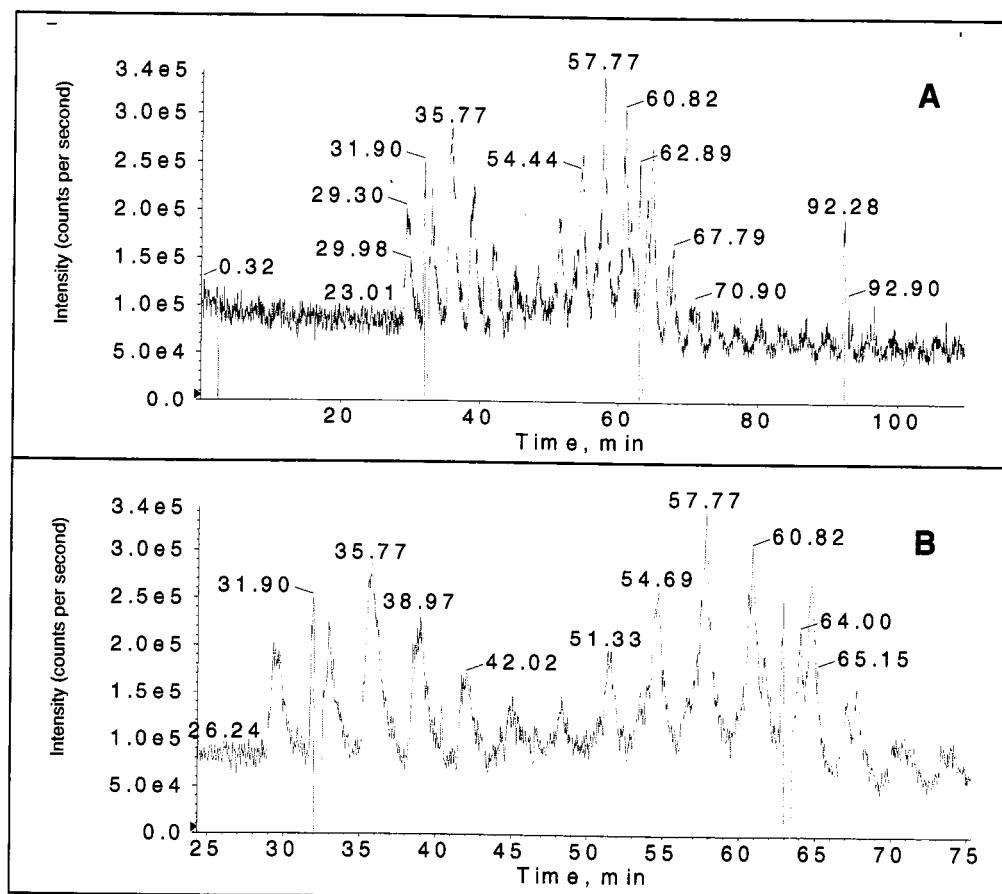


Figure 4-8. 2D experiment data (same experiment as in **Figure 4-7**) analyzed with the Q TRAP's Analyst software. **A)** RIE of 9 XIEs of cytochrome *C* and 13 XIEs of myoglobin. **B)** Detailed view of **A**.

Experimental conditions: **Integrated microreactor:** 48 μm ID, 142 μm OD, 30.7 cm total length, 1.1 cm microreactor length, 22.7 cm from inlet to UV detection window; **PVA-coated capillary:** 48 μm ID, 142 μm OD, 31.2 cm; **1st dimension buffer:** 30 mM (ammonium) acetate (pH 2.7); **2nd dimension buffer:** 50 mM (ammonium) acetate + 20 mM hydroquinone (pH 3.9); **sheath liquid:** 90% MeOH (1300 nL/min); **CE parameters:** PMT bias = +0.5 kV; **Injection:** power supply (PS) 1 = +9.7 kV (283 V/cm); PS 2 = +1.0 kV; (10 sec) and pressure injection: 22 psi (10 sec); the Q TRAP's ion spray (IS) voltage was turned off during injection; **Prerun:** PS 1 = +14.1 kV (362 V/cm); PS 2 = +3.0 kV; (180 sec); **Transfers:** PS 1 = +25.0 kV (490 V/cm); PS 2 = +10.0 kV; (10 sec); **Separations:** PS 1 = +12.95 kV; PS 2 = +13.0 kV (345 V/cm); (180 sec); **MS parameters:** LIT scan mode; IS voltage: +2250 V; CUR: 15.0; GS1: 0.0; GS1 was set to 10.0 during the 0.2 min prerun of the acquisition batch (see section 2.III.B.5.); m/z range from 300-1100 amu; scan rate: 1000 amu/sec; declustering potential: 30 V; entrance potential: 10 V.

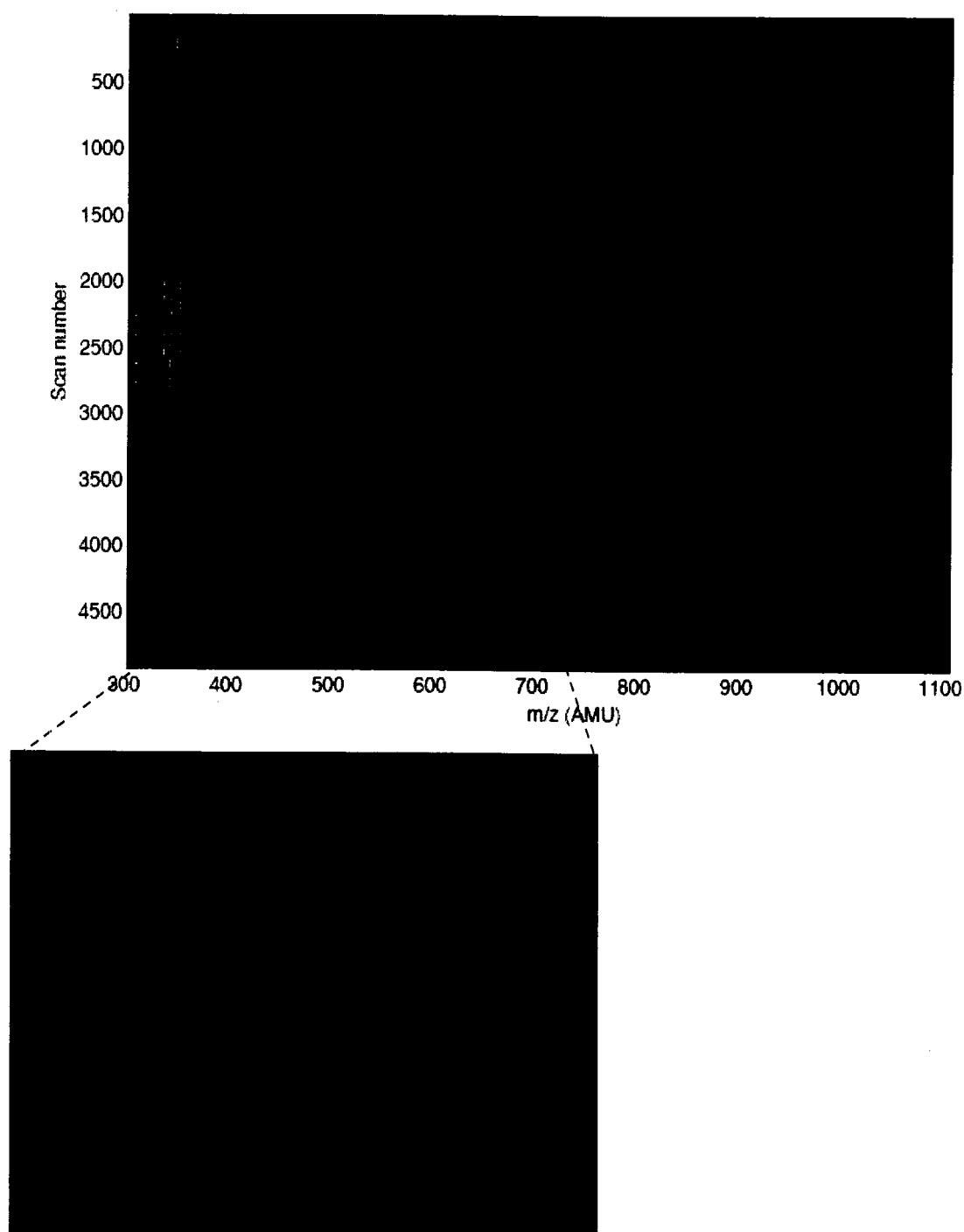
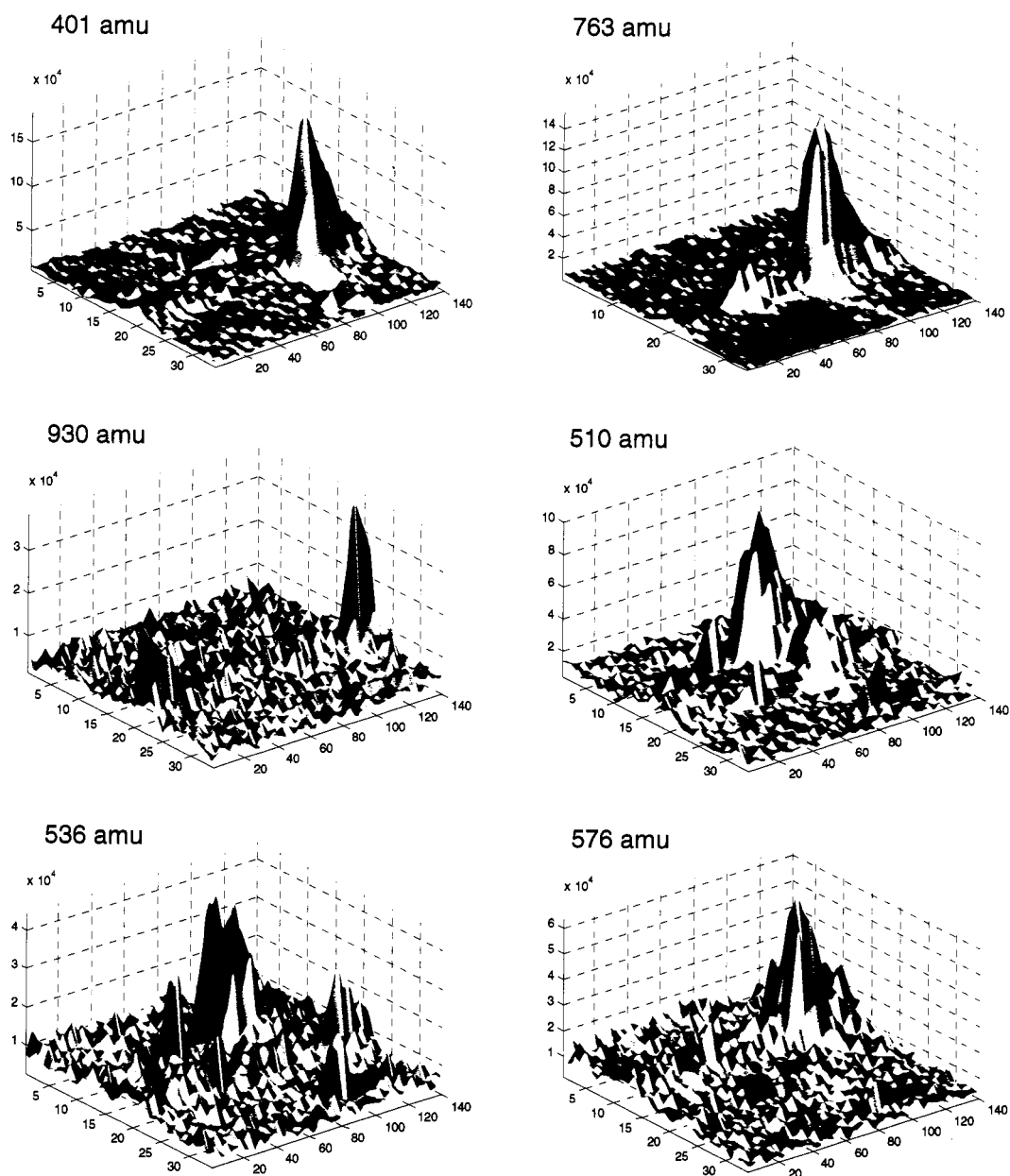


Figure 4-9. Two-dimensional gel image representation of the data shown in **Figures 4-7** and **4-8**. The data were analyzed in Matlab as described in section 4.II.E.2.. The scan number is related to the time axis in **Figures 4-7** and **4-8**.



For axes descriptions, see the figure caption.

Figure 4-10. Three-dimensional Matlab representation of selected XIEs of the experiment shown in **Figures 4-7 to 4-9**. The m/z values are approximate values ± 1 amu. The vertical axis represents MS signal intensity (counts per second), the left horizontal axis represents the first dimension separation (arbitrary numbers), and the right horizontal axis represents the second dimension separation (arbitrary numbers).

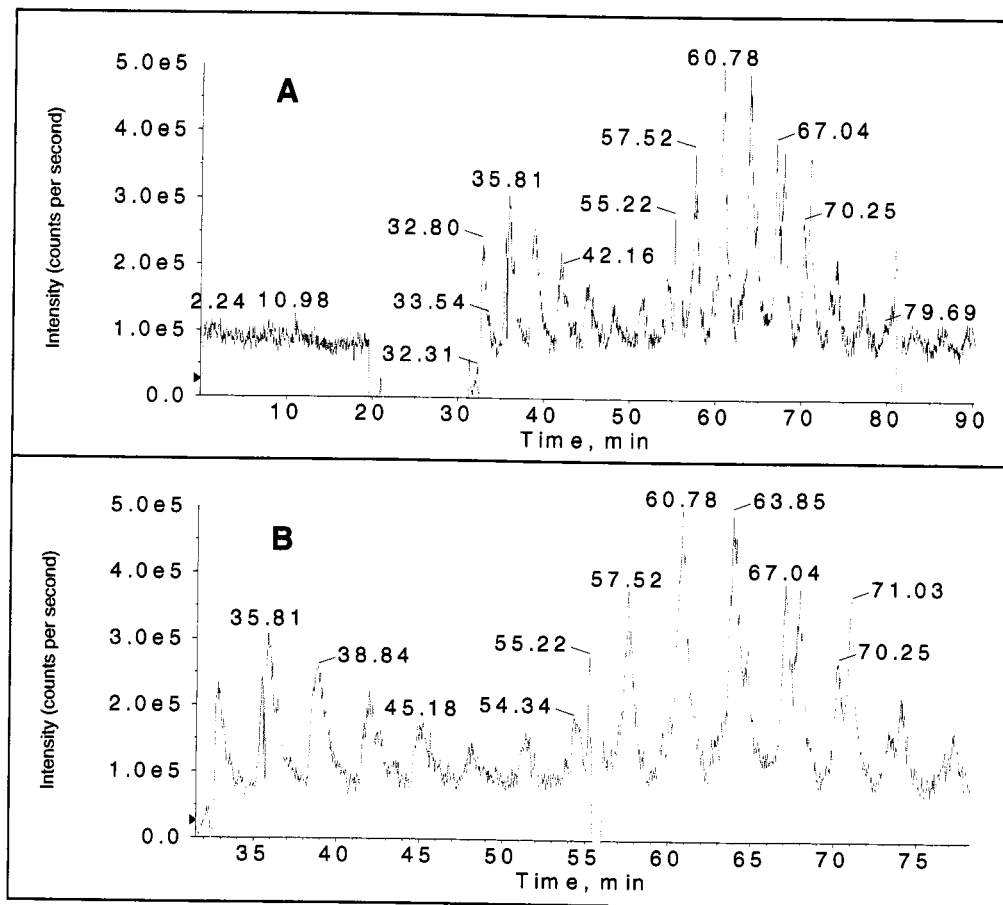


Figure 4-11. 2D experiment data of 200 μM each of cytochrome C and myoglobin in 10 mM (ammonium) acetate (pH 2.7) analyzed with the Q TRAP's Analyst software. **A)** RIE of 9 XIEs of cytochrome C and 13 XIEs of myoglobin. **B)** Detailed view of A. The data was acquired on the same day as the 2D experiment shown in **Figures 4-7 to 4-10** with the same sample and conditions as given in **Figure 4-8**.

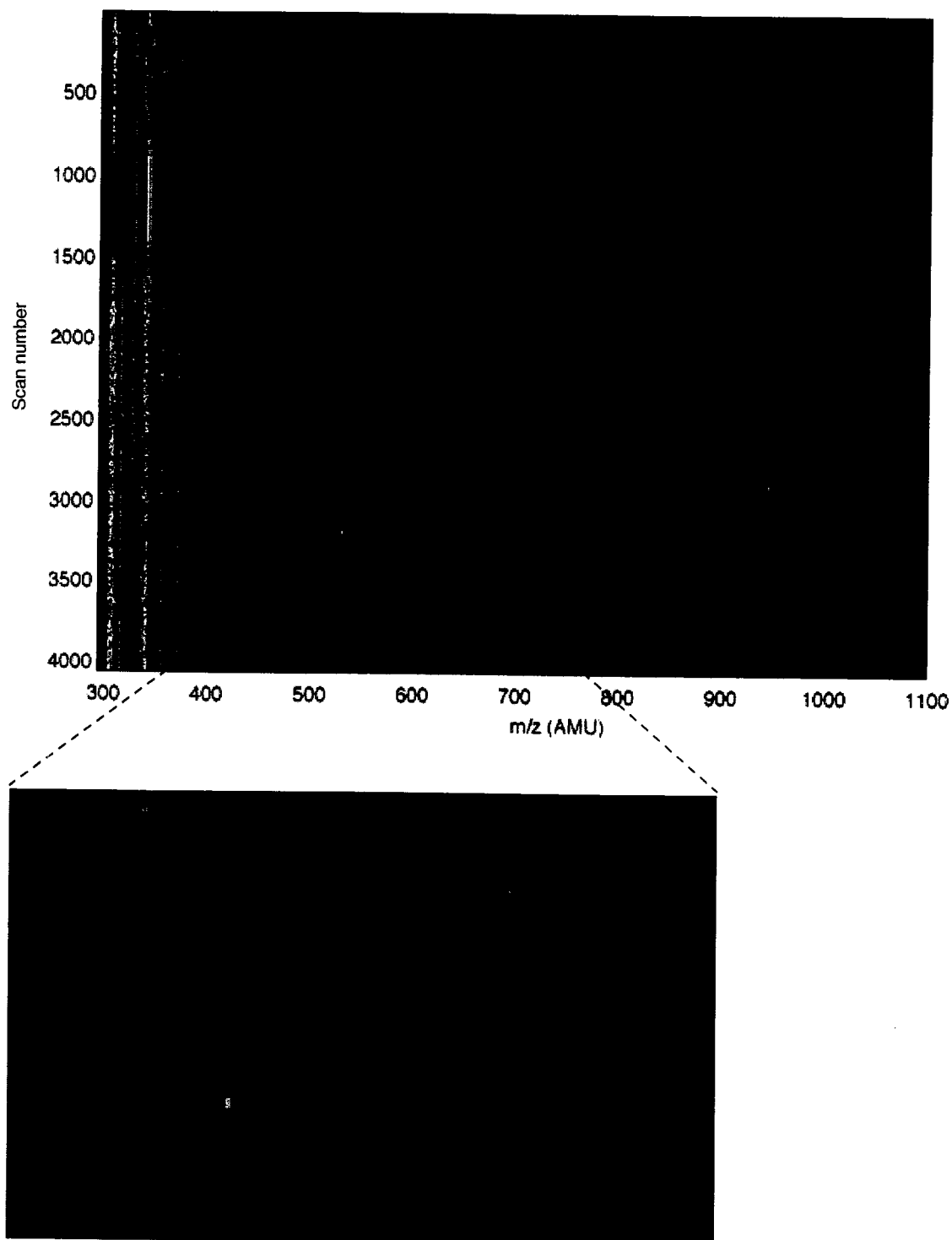
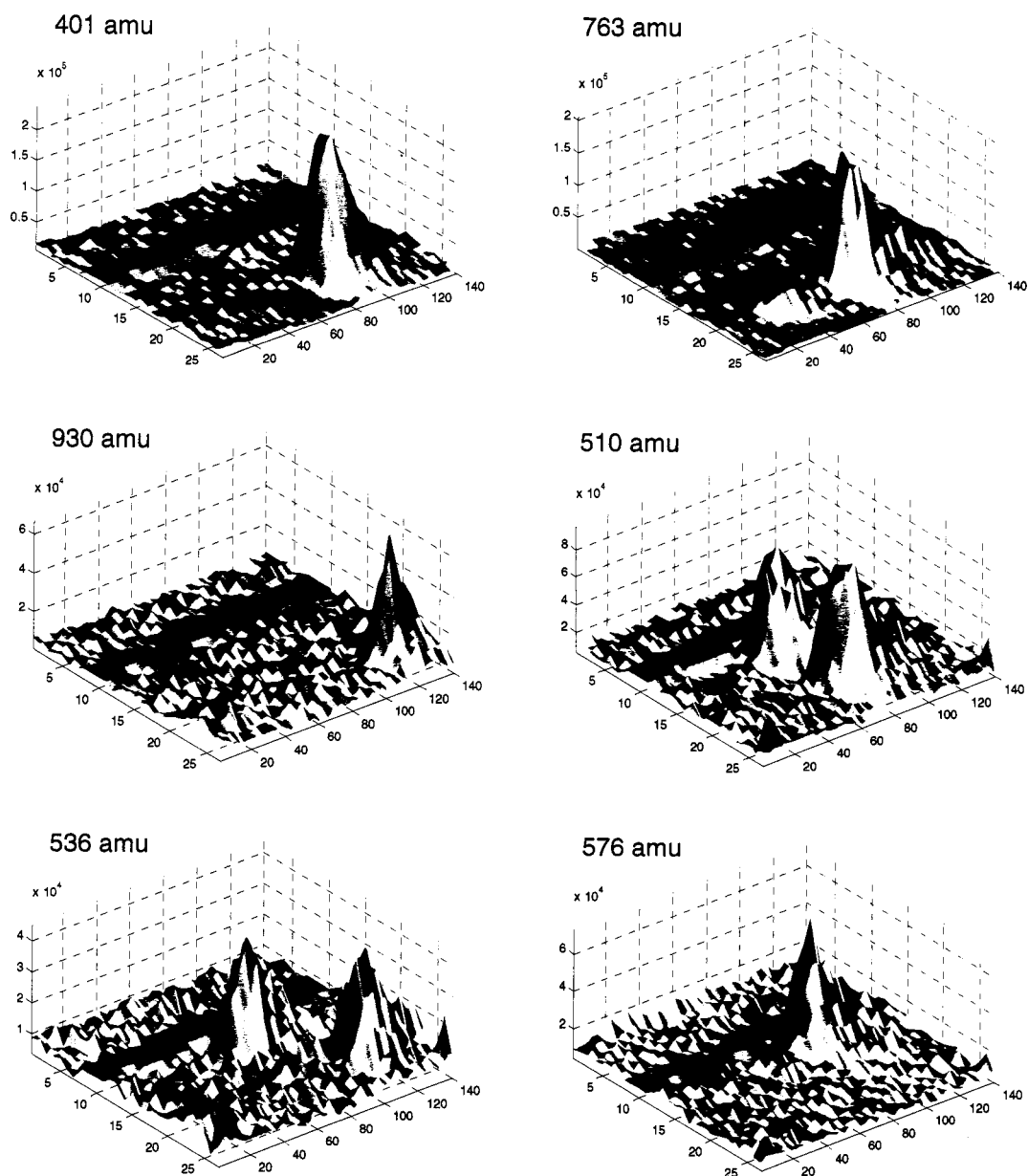


Figure 4-12. Two-dimensional gel image of a 2D experiment (the same as in **Figure 4-11**) with cytochrome *C* and myoglobin run on the same day as the experiment shown in **Figures 4-7 to 4-9**.



For axes descriptions, see the figure caption.

Figure 4-13. Three-dimensional Matlab representation of selected XIEs of the experiment shown in **Figures 4-11** and **4-12**. The m/z values are approximate values ± 1 amu. The vertical axis represents MS signal intensity (counts per second), the left horizontal axis represents the first dimension separation (arbitrary numbers), and the right horizontal axis represents the second dimension separation (arbitrary numbers).

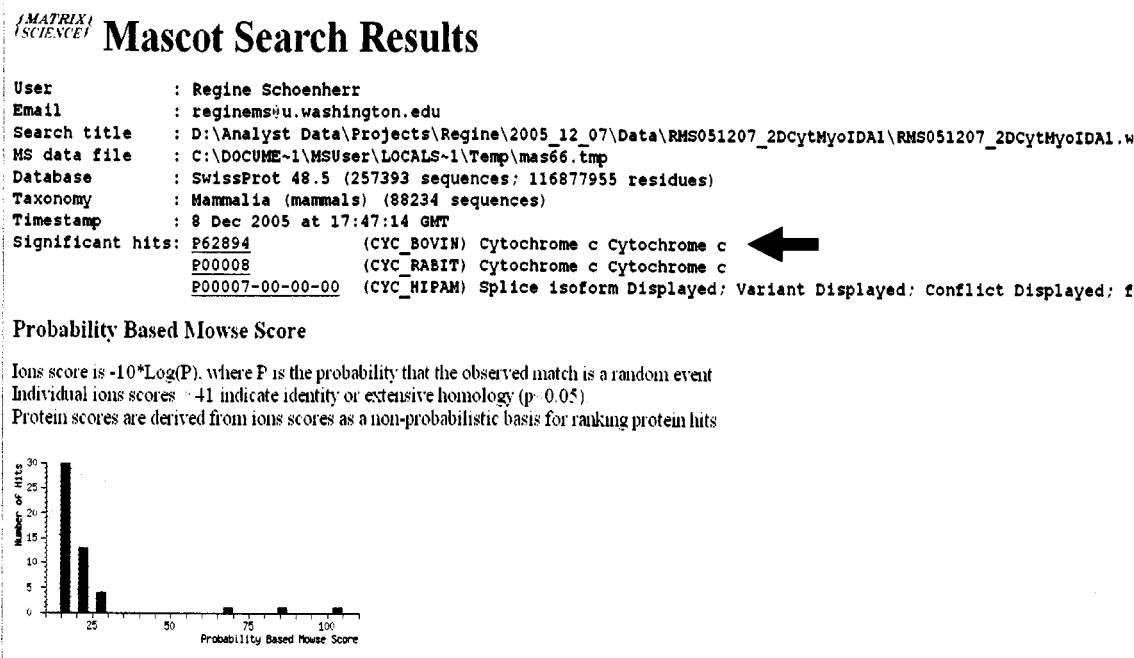


Figure 4-14. Screen capture of Mascot Search Results for microreactor-digested cytochrome C during a 2D experiment. Data were collected with the Information Dependent Acquisition feature of the Analyst software.

The CE experimental parameters were the same as given in **Figure 4-8**.

MS parameters: for survey scans: IS voltage: 2250V; CUR: 15.0; GS1: 0.0; m/z range: 400-1200 amu; scan rate: 4000 amu/sec. For enhanced resolution scans: same as for survey scans, except m/z range was set based on the m/z peak selected, and scan rate: 250 amu/sec. For enhanced product ion scans: same as for survey scans, except m/z range: 100-1300 amu; scan rate: 1000 amu/sec. IDA criteria: the 2 most intense mass peaks (with intensities $> 10,000$ counts per second) were selected in the 400-1200 amu range of the survey scans; ions with 2+ to 5+, or unknown charge states were submitted for fragmentation; ions that had been fragmented twice were excluded from fragmentation for 60 sec. For all scans, two m/z range scans were collected and summed before going on to the next scan. One cycle lasted 6.5182 sec.

Sample: 200 μ M cytochrome C + 200 μ M myoglobin in 10 mM (ammonium) acetate (pH 2.7).

The arrow indicates the bovine cytochrome C identification.

Mascot search parameters: PepsinA chosen as enzyme; database searched: SwissProt; allow up to 3 missed cleavages; peptide mass tolerance: ± 0.8 Da; MS/MS mass tolerance: ± 0.6 Da; average mass; instrument used: ESI-QUAD.

Peptide Summary Report

Format As Peptide Summary [Help](#)

Significance threshold p: 0.05 Max number of hits: AUTO

Standard scoring: MudPIT scoring Ions score cut-off: 0 Show sub-sets: ☐

Show pop-ups: ☐ Suppress pop-ups: ☐ Sort unassigned: Decreasing Score Require bold red: ☐

Select All Select None Search Selected ☐ Error tolerant

1. **P62894** Mass: 11572 Score: 103 Queries matched: 13
 (CYC_BOVIN) Cytochrome c Cytochrome c
☐ Check to include this hit in error tolerant search

Query	Observed	Mr(expt)	Mr(calc)	Delta	Miss	Score	Expect	Rank	Peptide
<input checked="" type="checkbox"/> 7	509.9432	1017.8704	1018.1273	-0.2568	0	14	43	1	F.GRKTGQAPGF.S
<input checked="" type="checkbox"/> 8	509.9435	1017.8710	1018.1273	-0.2562	0	(5)	2.8e+02	9	F.GRKTGQAPGF.S
<input checked="" type="checkbox"/> 9	509.9707	1017.9255	1018.1273	-0.2018	0	(7)	1.9e+02	2	F.GRKTGQAPGF.S
<input checked="" type="checkbox"/> 10	509.9893	1017.9626	1018.1273	-0.1646	0	(8)	1.2e+02	7	F.GRKTGQAPGF.S
<input checked="" type="checkbox"/> 11	576.0227	1150.0295	1150.3246	-0.2951	1	(9)	1.2e+02	2	L.IAYLKKATNE.-
<input checked="" type="checkbox"/> 12	576.0292	1150.0425	1150.3246	-0.2821	1	42	0.053	1	L.IAYLKKATNE.-
<input checked="" type="checkbox"/> 13	576.0522	1150.0886	1150.3246	-0.2360	1	(22)	4.9	1	L.IAYLKKATNE.-
<input checked="" type="checkbox"/> 14	576.0786	1150.1413	1150.3246	-0.1834	1	(17)	12	1	L.IAYLKKATNE.-
<input checked="" type="checkbox"/> 15	576.0933	1150.1707	1150.3246	-0.1539	1	(23)	3.3	1	L.IAYLKKATNE.-
<input checked="" type="checkbox"/> 16	448.7614	1343.2603	1343.5289	-0.2686	0	19	13	1	F.AGIKKKKGERDL.I
<input checked="" type="checkbox"/> 17	448.7680	1343.2803	1343.5289	-0.2487	0	(17)	17	1	F.AGIKKKKGERDL.I
<input checked="" type="checkbox"/> 18	448.7880	1343.3401	1343.5289	-0.1888	0	(16)	20	1	F.AGIKKKKGERDL.I
<input checked="" type="checkbox"/> 19	735.3067	2202.8962	2202.6339	0.2624	1	29	0.94	1	L.MEYLENPKKYPGTMIF.A

Proteins matching the same set of peptides:

P62895 Mass: 11572 Score: 103 Queries matched: 13
 (CYC_PIG) Cytochrome c Cytochrome c
P62896 Mass: 11572 Score: 103 Queries matched: 13
 (CYC_SHEEP) Cytochrome c Cytochrome c

Mascot Search Results

Peptide View

MS MS Fragmentation of GRKTGQAPGF

Found in P62894. (CYC_BOVIN) Cytochrome c Cytochrome c

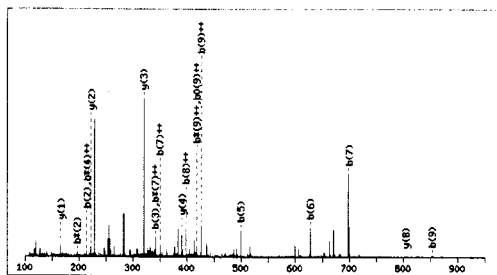
Match to Query: 1017.870442 from(509.943161.2+)

Elution from: 38.37 to 38.54 period: 0 experiment: 2 cycles: 2

From data file: C:\DOCUMENT1\MSUser\LOCALS-1\Temp\mas66.tmp

Click mouse within plot area to zoom in by factor of two about that point

Or: Platform 100 to 950 Da



Average mass of neutral peptide Mr(calc): 1018.1273

Ions Score: 14 Expect: 43

Matches (Bold Red): 19/60 fragment ions using 75 most intense peaks

Figure 4-15. Top: Screen capture of the Mascot Search Results for the cytochrome C identification listing the protein identifications and the peptides upon which the identifications were made. **Bottom:** Screen capture of the individual fragment mass spectrum when selecting Query # 7 (circled red in the top screen capture) of the GRKTGQAPGF peptide. 19 experimental fragment ion masses were matched with 80 theoretical fragment ion masses.

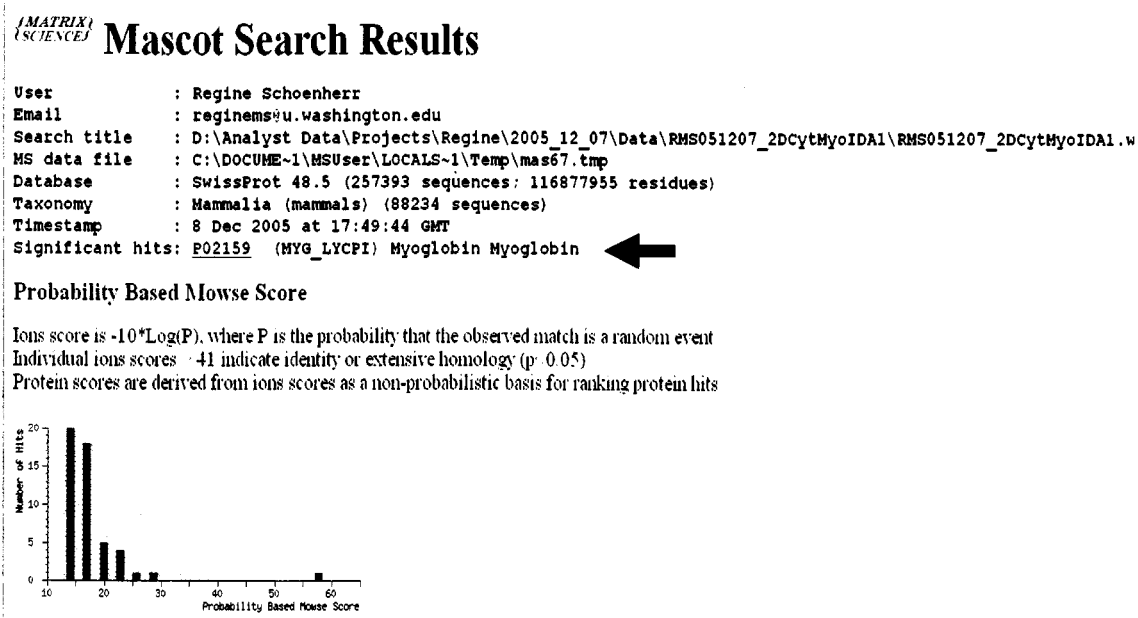


Figure 4-16. Screen capture of Mascot Search Results for microreactor digested myoglobin during the same 2D experiment as in **Figure 4-14**. Data were collected with the Information Dependent Acquisition feature of the Analyst software. The arrow indicates the myoglobin identification, and the arrow in the top part of **Figure 4-17** shows that more specifically horse heart myoglobin was identified.

Peptide Summary Report

Format As: **Peptide Summary** [Help](#)
Significance threshold p: 0.05 Max number of hits: AUTO
Standard scoring: + MudPIT scoring Ions score cut-off: 0 Show sub-sets: ☐
Show pop-ups: + Suppress pop-ups Sort unassigned: Decreasing Score Require bold red: ☐
 ☐ Error tolerant

1. **P02159** Mass: 17233 Score: 58 Queries matched: 5
(MYG_LYCPI) Myoglobin Myoglobin
☐ Check to include this hit in error tolerant search

Query	Observed	Mr(expt)	Mr(calc)	Delta	Miss	Score	Expect	Rank	Peptide
<input checked="" type="checkbox"/> 55	601.6445	1801.9096	1802.0827	-0.1731	2	37	0.093	1	L.TALGGILKKKGHNEAEL.K
<input checked="" type="checkbox"/> 57	619.8513	1856.5300	1857.0734	-0.5434	3	(17)	17	1	L.FRNDIAAKYKELGFQG.-
<input checked="" type="checkbox"/> 58	619.8596	1856.5550	1857.0734	-0.5185	3	(12)	54	1	L.FRNDIAAKYKELGFQG.-
<input checked="" type="checkbox"/> 59	619.8674	1856.5782	1857.0734	-0.4952	3	20	8.1	1	L.FRNDIAAKYKELGFQG.-
<input checked="" type="checkbox"/> 60	619.8714	1856.5905	1857.0734	-0.4829	3	(14)	32	1	L.FRNDIAAKYKELGFQG.-

Proteins matching the same set of peptides:

P02160	Mass: 17206	Score: 58	Queries matched: 5
(MYG_VULCH) Myoglobin Myoglobin			
P63113	Mass: 17206	Score: 58	Queries matched: 5
(MYG_CANFA) Myoglobin Myoglobin			
P63114	Mass: 17206	Score: 58	Queries matched: 5
(MYG_OTOME) Myoglobin Myoglobin			
P68082	Mass: 16951	Score: 58	Queries matched: 5
(MYG_HORSE) Myoglobin Myoglobin			
P68083	Mass: 16951	Score: 58	Queries matched: 5
(MYG_EQUBU) Myoglobin Myoglobin			

(MATRIX)
(SCIENCE)

Mascot Search Results

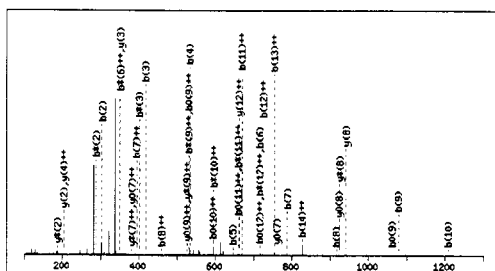
Peptide View

MS/MS Fragmentation of FRNDIAAKYKELGFQG
Found in P02159. (MYG_LYCPI) Myoglobin Myoglobin

Match to Query 59. 1856.578239 from (619.867353.3+)
Elution from: 67.87 to 68.3 period: 0 experiment: 2 cycles: 2
From data file C:\DOCUMENT-1\MSUser\LOCALS-1\Temp\mas67.tmp

Click mouse within plot area to zoom in by factor of two about that point

Or: 100 to 1300 Da



Average mass of neutral peptide Mr(calc): 1857.0734

Ions Score: 20 Expect: 8.1

Matches (Bold Red): 40/160 fragment ions using 99 most intense peaks

Figure 4-17. Top: Screen capture of the Mascot Search Results identifying horse heart myoglobin. **Bottom:** Screen capture of the individual fragment mass spectrum when selecting Query # 59 (circled red in the top screen capture) of the FRNDIAAKYKELGFQG peptide. 40 experimental fragment ion masses were matched with 160 theoretical fragment ion masses.

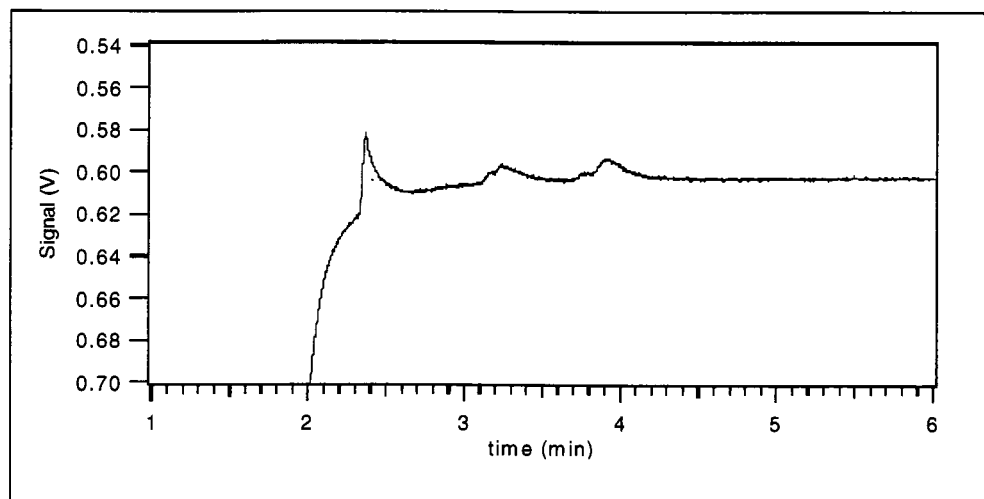
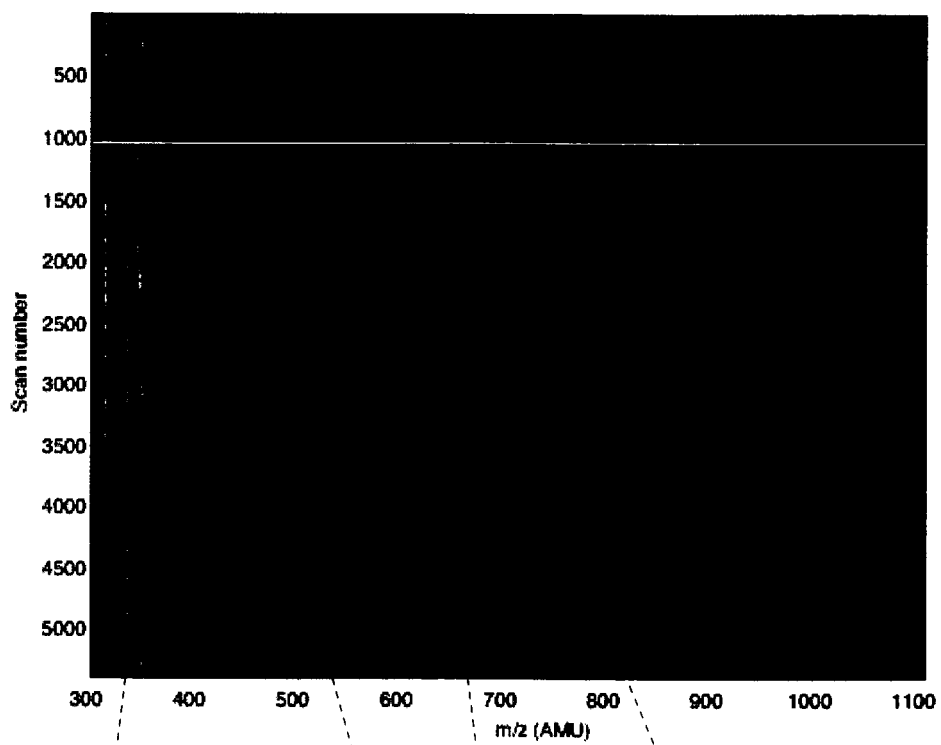
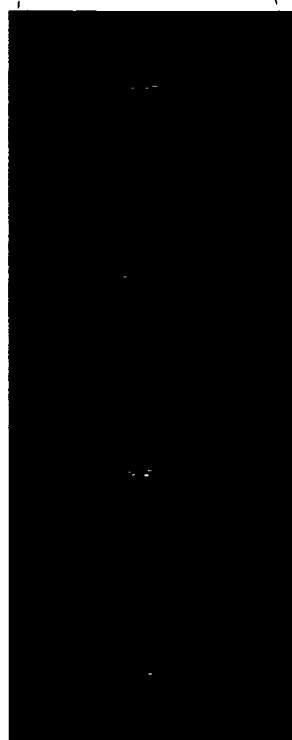


Figure 4-18. UV electropherogram of a preliminary 1D CE-UV experiment using the 6 protein mixture. It is believed that all three peaks consist of two proteins each, with the first and second peaks containing the cytochrome *C* and myoglobin proteins, respectively, based on previous data.

Figure 4-19. Two-dimensional gel image representation of data acquired with the 6 protein sample. The data were analyzed in Matlab as described in section 4.II.E.2.. The scan number is related to the time axis in **Figures 4-18**. The red squares in the top image show approximately the locations of the zoomed-in images on the left. The white line at scan number ~ 1000 is an artifact of copying and pasting the image and was not part of the original data.



~ scan number 1100-1600



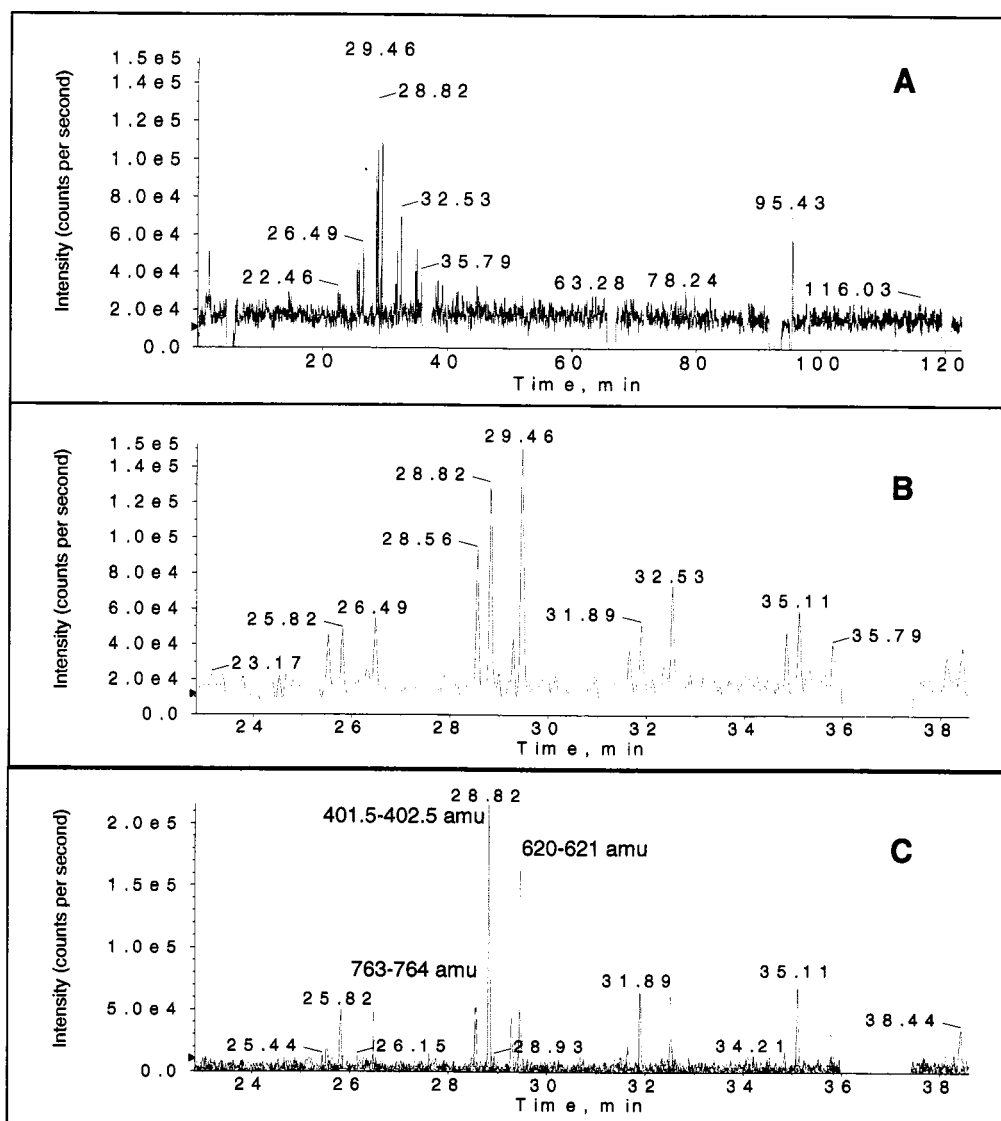
~ 401-402 amu

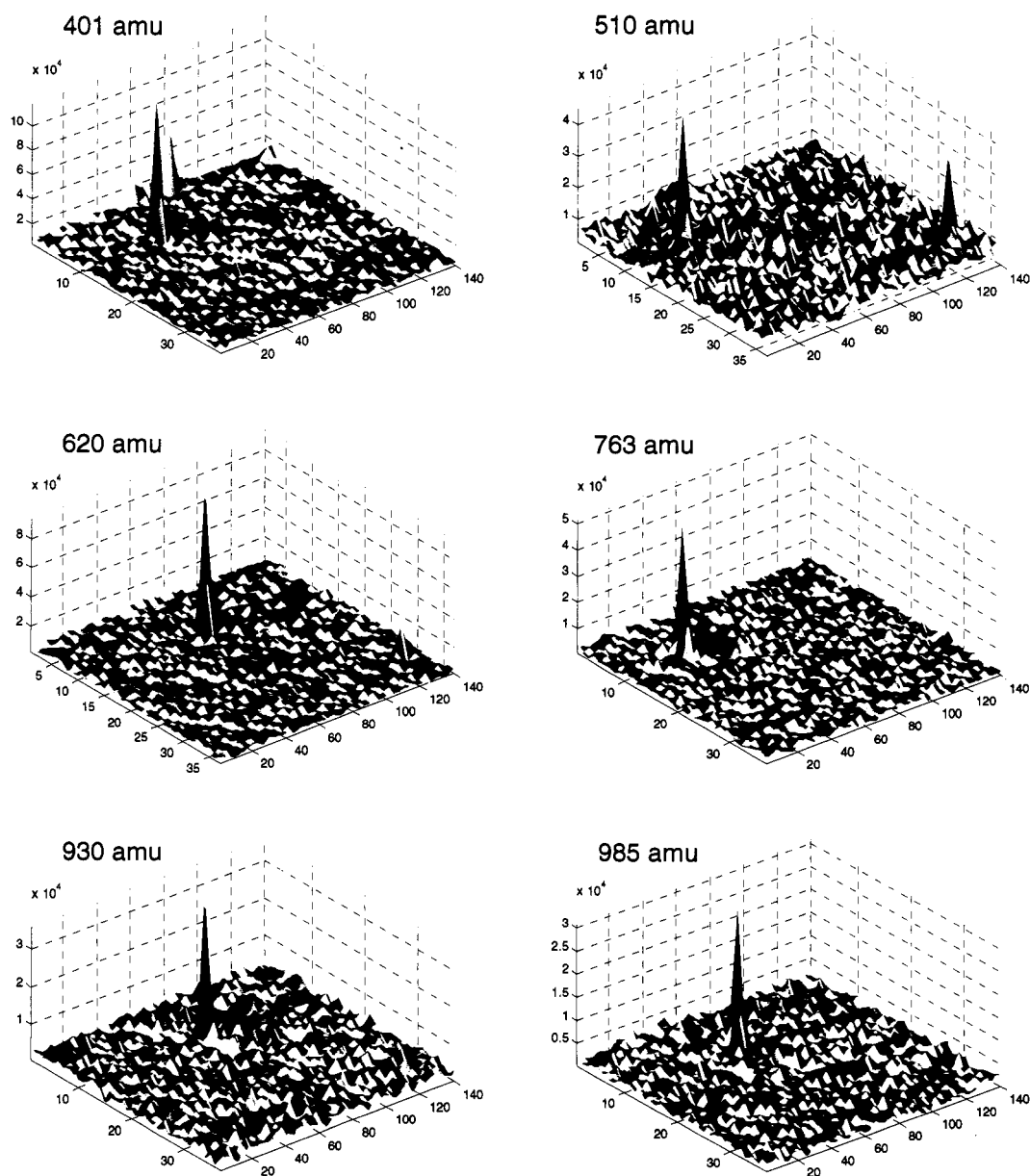


~ 620-621 amu

Figure 4-20. A) and B) RIEs of 2D experiment shown in **Figure 4-19** of a six protein mixture (300 μ M each of cytochrome C, myoglobin, α -chymotrypsinogen, β -lactoglobulin, ribonuclease A, and lysozyme in 10 mM ammonium acetate (pH 2.7)). Only 6 XIEs (overlaid but not summed in C) that could be related to myoglobin were observed. The RIEs were 1x Gaussian smoothed, the XIEs were not smoothed.

Experimental conditions: **Integrated microreactor:** 48 μ m ID, 142 μ m OD, 31.2 cm total length, 1.1 cm microreactor length, 24.0 cm from inlet to UV detection window; **PVA-coated capillary:** 48 μ m ID, 142 μ m OD, 31.5 cm; **1st dimension buffer:** 30 mM ammonium acetate (pH 2.7); **2nd dimension buffer:** 50 mM ammonium acetate + 20 mM hydroquinone (pH 3.9); **sheath liquid:** 90% MeOH (1300 nL/min); **CE parameters:** PMT bias = +0.5 kV; **Injection:** power supply (PS) 1 = +16.0 kV (481 V/cm); PS 2 = +1.0 kV; (10 sec); the Q TRAP's ion spray (IS) voltage was turned off during injection; **Prerun:** PS 1 = +18.0 kV (481 V/cm); PS 2 = +3.0 kV; (180 sec); **Transfers:** PS 1 = +25.0 kV (481 V/cm); PS 2 = +10.0 kV; (10 sec); **Separations:** PS 1 = +12.95 kV; PS 2 = +13.0 kV (341 V/cm); (180 sec); **MS parameters:** LIT scan mode; IS voltage: +2250 V; CUR: 15.0; GS1: 0.0; GS1 was set to 10.0 during the 0.2 min prerun of the acquisition batch (see section 2.III.B.5.); m/z range from 300-1100 amu; scan rate: 1000 amu/sec; declustering potential: 30 V; entrance potential: 10 V.





For axes descriptions, see the figure caption.

Figure 4-21. Three-dimensional Matlab representation of six XIEs of the 6 protein experiment shown in **Figures 4-19** and **4-20**. The m/z values are approximate values ± 1 amu. The vertical axis represents MS signal intensity (counts per second), the left horizontal axis represents the first dimension separation (arbitrary numbers), and the right horizontal axis represents the second dimension separation (arbitrary numbers).

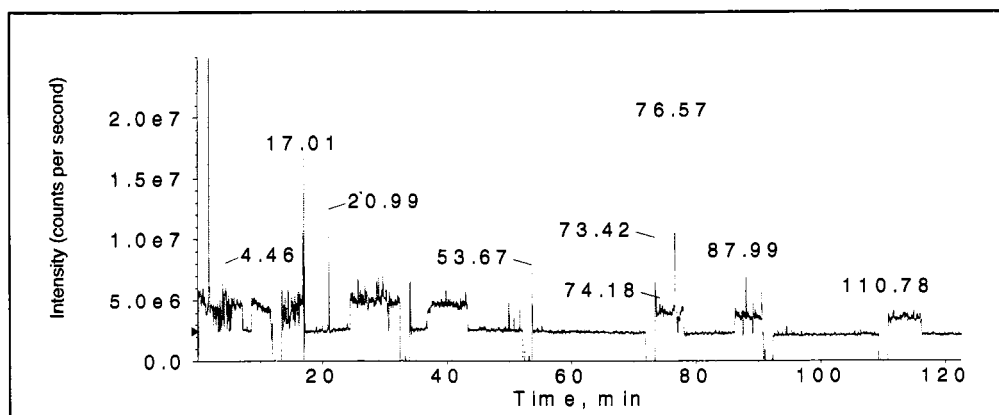


Figure 4-22. Total ion electropherogram of a 2D experiment using 90% MeOH + 5% ACN + 5% ddH₂O. The periodic MS signal dropouts were more frequent with this sheath liquid composition than with just 90% MeOH + 10% ddH₂O, see **Figures 4-7, 4-8, 4-11, and 4-20**. Except for the sheath flow composition, the same experimental parameters were applied as in **Figure 4-20**.

Table 4-1. Pin assignments for the 50-pin ribbon cable between the National Instruments data acquisition (DAQ) boards and the hardware wiring for 2D CE-UV-microreactor-CE-MS experiments.

Device (DAQ board) 1:

Hardware Assignment	50-Pin Connector Pin Numbers	MIO-16 Series Signal Names	MIO-16E Series Signal Names
PMT ^a Control	20	DAC0	DAC0OUT
Analog Output Ground	23	AOGND	AODGND

Device (DAQ board) 2:

Hardware Assignment	50-Pin Connector Pin Numbers	MIO-16 Series Signal Names	MIO-16E Series Signal Names
Current for PS ^b (CE Voltage) 2 (+)	3	ACH0	ACH0
Current for PS (CE Voltage) 2 (-)	4	ACH8	ACH8
Current for PS (CE Voltage) 1 (+)	5	ACH1	ACH1
Current for PS (CE Voltage) 1 (-)	6	ACH9	ACH9
PMT Signal (+)	7	ACH2	ACH2
PMT Signal (-)	8	ACH10	ACH10
PS (CE Voltage) 1 Control	20	DAC0	DAC0OUT
PS (CE Voltage) 2 Control	21	DAC1	DAC1OUT
Analog Output Ground	23	AOGND	AOGND

^aPMT: photomultiplier tube; ^bPS: power supply

Table 4-2. 13 and 10 extracted ion electropherogram (XIE) masses that yielded peaks for myoglobin and cytochrome C peptides in 2D experiments, respectively.

13 XIEs for Myoglobin					
400-499 amu	500-599 amu	600-699 amu	700-799 amu	800-899 amu	900-999 amu
401.5-402.5	510-511 550-551	602-603 620-621 623.5-624.5 628.5-629.5 654.5-655.5	763-764 774.5-775.5 786-787	855-856	930-931
9 XIEs for Cytochrome C					
400-499 amu	500-599 amu	600-699 amu	700-799 amu	800-899 amu	900-999 amu
449-450 484-485	511.5-512.5 536-537 554-555 576.5-577.5 594.5-595.5	648.5-649.5 672.5-673.5	736.5-737.5		

Table 4-3. Voltage programs for 2D experiments. **A)** Voltage program for experiments described in sections 4.III.D.1. and 4.III.D.2. **B)** Voltage program for experiment described in section 4.III.E. Relevant electric fields are given in parentheses. For other experimental parameters, see **Figures 4-8** and **4-20**.

A	Power supply 1 (kV)	Power supply 2 (kV)	IS voltage (kV)	Time (sec)
Injection	9.7 (283 V/cm)	1.0	0.0	10
1 st dimension prerun	14.1 (362 V/cm)	3.0	2.25	180
Transfer	25.0 (490 V/cm)	10.0	2.25	10
2 nd dimension separation	12.95	13.0 (345 V/cm)	2.25	180

B	Power supply 1 (kV)	Power supply 2 (kV)	IS voltage (kV)	Time (sec)
Injection	16.0 (481 V/cm)	1.0	0.0	10
1 st dimension prerun	18.0 (481 V/cm)	3.0	2.25	180
Transfer	25.0 (481 V/cm)	10.0	2.25	10
2 nd dimension separation	12.95	13.0 (341 V/cm)	2.25	180

4.V. Notes to Chapter 4

- (1) Kato, M.; Sakai-Kato, K.; Jin, H.; Kubota, K.; Miyano, H.; Toyo'oka, T.; Dulay Maria, T.; Zare Richard, N. *Anal Chem* **2004**, 76, 1896-1902.
- (2) Simpson, D. C.; Smith, R. D. *Electrophoresis* **2005**, 26, 1291-1305.
- (3) Schlamowitz, M.; Peterson, L. U. *J Biol Chem* **1959**, 234, 3137-3145.
- (4) Christensen, L. K. *Arch Biochem Biophys* **1955**, 57, 163-173.

Chapter 5 – Conclusions and Future Directions

5.I. Conclusions

An on-line CE-microreactor-CE-MS-MS instrument was developed for separating proteins in a first dimension, digesting them inside a pepsin-immobilized microreactor, separating peptides in a second dimension, and detecting the peptides with mass spectrometry. The development began from the MS end by coupling CE to a triple quadrupole-linear ion trap hybrid mass spectrometer with a sheath flow interface, and worked its way forward to the protein separation.

5.I.A. CE-ESI-MS Interface

Capillary electrophoresis was coupled to electrospray ionization (ESI) mass spectrometry using a sheathless and a sheath flow interface. The sheathless interface was not robust enough to establish stable electrosprays, and CE separations were hampered by bubbles due to electrolysis at the Pt electrode in the interface. Another drawback of this interface was that its dead volume caused peak tailing.

The sheath flow interface was more reliable because it provided a steady liquid flow to the electrospray tip. The sheath liquid also added volatility to the aqueous buffer, which simplified the buffer optimization for CE separations of peptides. Hardly any band broadening was observed with the sheath flow interface. All subsequent work was performed using this sheath flow interface.

5.I.B. 1D CE-ESI-MS and CE-ESI-MS-MS Experiments Using Bulk-digested Cytochrome *C*

Trypsin and pepsin bulk-digested cytochrome *C* samples were used to optimize the peptide separation in what would later become the second dimension of the two-dimensional system. Coating capillaries with poly(vinyl alcohol) and using high ionic strength buffers alleviated peptide-capillary wall interactions that could cause severe band broadening.

The mass spectrometry data acquisitions were optimized by using the MS software's batch acquisition capability. It was found that using acquisition batches with short preruns allowed the software to start, stop, and start data acquisitions, and that this yielded stable baselines in following longer runs during which peptides were separated and detected.

Tandem mass spectrometry experiments using the linear ion trap mass spectrometer's information dependent acquisition (IDA) capability were performed to obtain fragmentation data of cytochrome *C* peptides. Cytochrome *C* was successfully identified when these data were submitted to the protein database search engine Mascot.

5.I.C. Protein Digestion with a Pepsin Microreactor and 1D On-line Microreactor-CE-ESI-MS Experiments

Pepsin-immobilized monolithic capillary microreactors were prepared and used off- and on-line with the 1D CE-ESI-MS system. Pepsin was chosen because its enzymatic activity is highest at low pHs, and analyte protonation in MS is favored at low pHs as well. Initial off-line experiments established that the monoliths were unfortunately quite heterogeneous and that high concentrations of proteins had to be used

in order to detect peptides in subsequent CE-MS experiments. Quantification was difficult because of poor injection repeatability.

Poor quantification data were also obtained with on-line microreactor-CE-MS experiments that probed the efficiency of the microreactors. However, the on-line experiments showed that cytochrome *C* was successfully digested within only 2 minutes.

It was further found that the addition of hydroquinone (and *p*-benzoquinone) to the separation buffers aided the CE current stability because the additives, instead of water, were oxidized or reduced. Further optimization of separation conditions showed that the best peptide separations were obtained with relatively high concentrations of hydroquinone and moderate electric fields.

5.I.D. 2D CE-UV-microreactor-CE-MS and -MS-MS

The one-dimensional instrument was further modified to accommodate a first dimension protein separation capillary that also contained the pepsin microreactor. A Plexiglas-glass interface was used to couple the microreactor capillary to the second dimension PVA-coated capillary.

Two-dimensional experiments were performed by separating the proteins in the first dimension and then starting cycles of fraction transfers and peptide separations in the second dimension. Protein migration in the first dimension was minimized during second dimension separation times by applying appropriate voltages at the injection end and at the CE-CE interface. Fractions of proteins were digested in the microreactor while peptides were separated in the second dimension.

Two different protein mixtures were tried with the two-dimensional system. One contained cytochrome *C* and myoglobin, the other a six protein mixture that included cytochrome *C*, myoglobin, α -chymotrypsinogen, β -lactoglobulin, ribonuclease A, and lysozyme. Cytochrome *C* and myoglobin were successfully separated and identified using the two protein mixture, but only myoglobin was observed when using the six protein mixture. The other four proteins were known to be resistant to pepsin cleavage and/or had disulfide bonds.

5.II. Future Directions

5.II.A. Improving Sensitivity and Detection Limits

One common limitation of CZE-MS systems is their low loading capacities and thus poor concentration limits of detection. Band broadening restricts the amount of sample that can be injected into capillaries for CZE. One solution to this problem would be to use capillary isoelectric focusing (CIEF) in the first dimension of the 2D system since the whole capillary can be filled with sample. The different analytes are focused into tight bands according to their isoelectric points when an electric field is applied across the capillary, thus concentrating the analytes. Although the ampholytes that are used in CIEF cause ion suppression in MS analyses, the successful use of low concentrations of ampholytes has been reported in the literature.¹

Another way of improving the system's figures of merit would be to use electrospray tips with smaller outlet inner diameters (IDs). The system described here used a stainless steel electrospray tip with a 150 μm ID outlet, which is rather large.

Smaller ID tips enable more analytes to be ionized because smaller droplets are formed, and solvent evaporation is much more efficient from these smaller droplets than from larger ones. Dr. Chun-Sheng Liu, a former member of the Dovichi group, used a tapered fused silica capillary with a 30 μm ID orifice when coupling CE to ESI-MS,² and his work could be adapted to this 2D system.

In addition, this system could be coupled to other, more sensitive, mass spectrometers. For example, a newer version of the Q TRAP, a 4000 Q TRAP, is about 50 times more sensitive than the Q TRAP used in this work.

5.II.B. Analyzing More Complex Samples

The proof-of-concept work performed so far has shown that the 2D system can separate and identify standard proteins and their peptides. The next steps would be to analyze more complex, and preferably non-standard, samples. Treating proteins that contain disulfide bonds with reducing agents, such as dithiothreitol (DTT), would facilitate their digestion in the pepsin microreactor. The pH in the first dimension might also be increased to a level that enables better protein solubilization yet does not render pepsin inactive.

Finally, as Simpson and Smith noted,³ this system could be used to study post-translationally modified proteins. The functions and subcellular locations of proteins are often determined by the absence or presence of post-translational modifications (PTMs), which makes PTM analysis important.

5.III. Notes to Chapter 5

- (1) Storms, H. F.; van der Heijden, R.; Tjaden, U. R.; van der Greef, J. *Electrophoresis* **2004**, 25, 3461-3467.
- (2) Liu, C. S. *Development and application of capillary electrophoresis-electrospray mass spectrometry*; University of Alberta: Canada, 2001.
- (3) Simpson, D. C.; Smith, R. D. *Electrophoresis* **2005**, 26, 1291-1305.

BIBLIOGRAPHY

- (1) Albin, M.; Weinberger, R.; Sapp, E.; Moring, S. *Anal Chem* **1991**, *63*, 417-422.
- (2) Amankwa, L. N.; Harder, K.; Jirik, F.; Aebersold, R. *Protein Sci* **1995**, *4*, 113-125.
- (3) Amankwa, L. N.; Kuhr, W. G. *Anal Chem* **1992**, *64*, 1610-1613.
- (4) Amankwa, L. N.; Kuhr, W. G. *Anal Chem* **1993**, *65*, 2693-2697.
- (5) Anson, M. L. *J Gen Physiol* **1938**, *22*, 79-89.
- (6) Baldacci, A.; Prost, F.; Thormann, W. *Electrophoresis* **2004**, *25*, 1607-1614.
- (7) Banks, J. F., Jr. *J Chromatogr A* **1995**, *712*, 245-252.
- (8) Banks, J. F., Jr. *J Chromatogr A* **1996**, *743*, 99-104.
- (9) Banks, J. F., Jr.; Dresch, T. *Anal Chem* **1996**, *68*, 1480-1485.
- (10) Bao, J. J.; Fujima, J. M.; Danielson, N. D. *J Chromatogr B* **1997**, *699*, 481-497.
- (11) Bateman, K. P.; White, R. L.; Thibault, P. *Rapid Commun Mass Spectrom* **1997**, *11*, 307-315.
- (12) Beale, S. C.; Savage, J. C.; Wiesler, D.; Wietstock, S. M.; Novotny, M. *Anal Chem* **1988**, *60*, 1765-1769.
- (13) Beattie, J. H.; Richards, M. P. *J Chromatogr* **1994**, *664*, 129-134.
- (14) Belder, D.; Deege, A.; Husmann, H.; Koehler, F.; Ludwig, M. *Electrophoresis* **2001**, *22*, 3813-3818.
- (15) Bonneil, E.; Mercier, M.; Waldron, K. C. *Anal Chim Acta* **2000**, *404*, 29-45.
- (16) Bonneil, E.; Waldron, K. C. *Talanta* **2000**, *53*, 687-699.
- (17) Bruin, G. J.; Huisden, R.; Kraak, J. C.; Poppe, H. *J Chromatogr* **1989**, *480*, 339-349.
- (18) Burgi, D. S.; Chien, R.-L. In *Handbook of Capillary Electrophoresis*, Second ed.; Landers, J. P., Ed.; CRC Press: Boca Raton, 1997, pp 479-493.

- (19) Bushey, M. M.; Jorgenson, J. W. *J Chromatogr* **1989**, *480*, 301-310.
- (20) Bushey, M. M.; Jorgenson, J. W. *Anal Chem* **1990**, *62*, 161-167.
- (21) Bushey, M. M.; Jorgenson, J. W. *Anal Chem* **1990**, *62*, 978-984.
- (22) Caprioli, R. M.; Moore, W. T.; Martin, M.; DaGue, B. B.; Wilson, K.; Moring, S. *J Chromatogr* **1989**, *480*, 247-257.
- (23) Carter, S. J.; Li, X. F.; Mackey, J. R.; Modi, S.; Hanson, J.; Dovichi, N. J. *Electrophoresis* **2001**, *22*, 2730-2736.
- (24) Chang, W. W.; Hobson, C.; Bomberger, D. C.; Schneider, L. V. *Electrophoresis* **2005**, *26*, 2179-2186.
- (25) Chartogne, A.; Gaspari, M.; Jespersen, S.; Buscher, B.; Verheij, E.; Heijden Rv, R.; Tjaden, U.; van der Greef, J. *Rapid Commun Mass Spectrom* **2002**, *16*, 201-207.
- (26) Chen, D.; Dovichi, N. J. *Anal Chem* **1996**, *68*, 690-696.
- (27) Chen, J.; Lee, C. S.; Shen, Y.; Smith, R. D.; Baehrecke, E. H. *Electrophoresis* **2002**, *23*, 3143-3148.
- (28) Chen, Y.-R.; Her, G.-R. *Rapid Commun Mass Spectrom* **2003**, *17*, 437-441.
- (29) Cheng, Y. F.; Dovichi, N. J. *Science* **1988**, *242*, 562-564.
- (30) Chowdhury, S. K.; Chait, B. T. *Anal Chem* **1991**, *63*, 1660-1664.
- (31) Chu, Y.-H.; Dunayevskiy, Y. M.; Kirby, D. P.; Vouros, P.; Karger, B. L. *J Am Chem Soc* **1996**, *118*.
- (32) Cobb, K. A.; Novotny, M. *Anal Chem* **1989**, *61*, 2226-2231.
- (33) Cohen, A. S.; Karger, B. L. *J Chromatogr* **1987**, *397*, 409-417.
- (34) Cole, R. B.; Varghese, J.; McCormick, R. M.; Kadlecsek, D. *J Chromatogr A* **1994**, *680*, 363-373.
- (35) Cooper, J. W.; Chen, J.; Li, Y.; Lee, C. S. *Anal Chem* **2003**, *75*, 1067-1074.
- (36) Corradini, D.; Cogliandro, E.; D'Alessandro, L.; Nicoletti, I. *J Chromatogr A* **2003**, *1013*, 221-232.

- (37) Crabtree, H. J.; Bay, S. J.; Lewis, D. F.; Zhang, J.; Coulson, L. D.; Fitzpatrick, G. A.; Delinger, S. L.; Harrison, D. J.; Dovichi, N. J. *Electrophoresis* **2000**, *21*, 1329-1335.
- (38) Craig, D. B.; Arriaga, E.; Wong, J. C. Y.; Lu, H.; Dovichi, N. J. *Anal Chem* **1998**, *70*, 39A - 43A.
- (39) Demelbauer, U. M.; Plematl, A.; Kremser, L.; Allmaier, G.; Josic, D.; Rizzi, A. *Electrophoresis* **2004**, *25*, 2026-2032.
- (40) Dittman, M. M.; Rozing, G. P. In *Handbook of Capillary Electrophoresis*, Second ed.; Landers, J. P., Ed.; CRC Press: Boca Raton, 1997, pp 139-153.
- (41) Doherty, E. A. S.; Meagher, R. J.; Albarghouthi, M. N.; Barron, A. E. *Electrophoresis* **2003**, *24*, 34-54.
- (42) Dougherty, A. M.; Cooke, N.; Shieh, P. In *Handbook of Capillary Electrophoresis*, Second ed.; Landers, J. P., Ed.; CRC Press: Boca Raton, 1997, pp 675-715.
- (43) Dulay, M. T.; Quirino, J. P.; Bennett, B. D.; Kato, M.; Zare, R. N. *Anal Chem* **2001**, *73*, 3921-3926.
- (44) Emmett, M. R.; Caprioli, R. M. *J. Am. Soc. Mass Spectrom.* **1994**, *5*, 605-613.
- (45) Fang, L.; Zhang, R.; Williams, E. R.; Zare, R. N. *Anal Chem* **1994**, *66*, 3696-3701.
- (46) Fenn, J. B.; Mann, M.; Meng, C. K.; Wong, S. F.; Whitehouse, C. M. *Science* **1989**, *246*, 64-71.
- (47) Flory, M. R.; Griffin, T. J.; Martin, D.; Aebersold, R. *Trends Biotechnol* **2002**, *20*, S23-29.
- (48) Fogarty, K.; Van Orden, A. *Anal Chem* **2003**, *75*, 6634-6641.
- (49) Foret, F.; Kirby, D. P.; Vouros, P.; Karger, B. L. *Electrophoresis* **1996**, *17*, 1829-1832.
- (50) Foret, F.; Thompson, T. J.; Vouros, P.; Karger, B. L.; Gebauer, P.; Bocek, P. *Anal Chem* **1994**, *66*, 4450-4458.
- (51) Fujiwara, S.; Honda, S. *Anal Chem* **1987**, *59*, 487-490.
- (52) Galvani, M.; Hamdan, M. *Rapid Commun Mass Spectrom* **2000**, *14*, 721-723.

- (53) Gaskell, S. J. *J Mass Spectrom* **1997**, 32, 677-688.
- (54) Gassmann, E.; Kuo, J. E.; Zare, R. N. *Science* **1985**, 230, 813-814.
- (55) Gelpi, E. *J Mass Spectrom* **2002**, 37, 241-253.
- (56) Giddings, J. C. *Unified Separation Science*; Wiley Interscience: New York, 1991.
- (57) Gucek, M.; Gaspari, M.; Walhagen, K.; Vreeken, R. J.; Verheij, E. R.; van der Greef, J. *Rapid Commun Mass Spectrom* **2000**, 14, 1448-1454.
- (58) Gucek, M.; Vreeken, R. J.; Verheij, E. R. *Rapid Commun Mass Spectrom* **1999**, 13, 612-619.
- (59) Guo, Z.; Xu, S.; Lei, Z.; Zou, H.; Guo, B. *Electrophoresis* **2003**, 24, 3633-3639.
- (60) Guttman, A. *LCGC North America* **2004**, 22, 896-904.
- (61) Guzman, N. A.; Park, S. S.; Schaufelberger, D.; Hernandez, L.; Paez, X.; Rada, P.; Tomlinson, A. J.; Naylor, S. *J Chromatogr B* **1997**, 697, 37-66.
- (62) Gygi, S. P.; Corthals, G. L.; Zhang, Y.; Rochon, Y.; Aebersold, R. *Proc Natl Acad Sci U S A* **2000**, 97, 9390-9395.
- (63) Gygi, S. P.; Rist, B.; Gerber, S. A.; Turecek, F.; Gelb, M. H.; Aebersold, R. *Nat Biotechnol* **1999**, 17, 994-999.
- (64) Gygi, S. P.; Rochon, Y.; Franza, B. R.; Aebersold, R. *Mol Cell Biol* **1999**, 19, 1720-1730.
- (65) Hager, J. W. *Rapid Commun Mass Spectrom* **2002**, 16, 512-526.
- (66) Hayati, I.; Bailey, A. I.; Tadros, T. F. *Nature* **1986**, 319, 41-43.
- (67) Heiger, D. *High Performance Capillary Electrophoresis, An Introduction*; Agilent Technologies: Germany, 2000.
- (68) Herbert, B. *Electrophoresis* **1999**, 20, 660-663.
- (69) Hernández-Borges, J.; Neusüß, C.; Cifuentes, A.; Pelzing, M. *Electrophoresis* **2004**, 25, 2257-2281.
- (70) Hernández-Borges, J.; Rodríguez-Delgado, M. Á.; García-Montelongo, F. J.; Cifuentes, A. *Electrophoresis* **2004**, 25, 2065-2076.

- (71) Hilder, E. F.; Klampfl, C. W.; Buchberger, W.; Haddad, P. R. *Electrophoresis* **2002**, *23*, 414-420.
- (72) Hilder, E. F.; Svec, F.; Frechet, J. M. *Anal Chem* **2004**, *76*, 3887-3892.
- (73) Hjertén, S. *Chromatogr. Rev.* **1967**, *9*, 122-219.
- (74) Hjertén, S. *J Chromatogr* **1983**, *270*, 1-6.
- (75) Hjertén, S.; Zhu, M. D. *J Chromatogr* **1985**, *346*, 265-270.
- (76) Hooker, T. F.; Jorgenson, J. W. *Anal Chem* **1997**, *69*, 4134-4142.
- (77) Hsieh, F.; Baronas, E.; Muir, C.; Martin, S. A. *Rapid Commun Mass Spectrom* **1999**, *13*, 67-72.
- (78) Hu, S.; Dovichi, N. J. *Anal Chem* **2002**, *74*, 2833-2850.
- (79) Hu, S.; Michels, D. A.; Fazal, M. A.; Ratisoontorn, C.; Cunningham, M. L.; Dovichi, N. J. *Anal Chem* **2004**, *76*, 4044-4049.
- (80) Hu, S.; Ye, M.; Surh, G.; Clark, J. I.; Dovichi, N. J. *LC-GC Europe* **2002**, *15*, 166,168,170-171.
- (81) Hu, S.; Zhang, L.; Cook, L. M.; Dovichi, N. J. *Electrophoresis* **2001**, *22*, 3677-3682.
- (82) Hutterer, K.; Dolnik, V. *Electrophoresis* **2003**, *24*, 3998-4012.
- (83) Ishihama, Y.; Katayama, H.; Asakawa, N.; Oda, Y. *Rapid Commun Mass Spectrom* **2002**, *16*, 913-918.
- (84) Janini, G. M.; Chan, K. C.; Conrads, T. P.; Issaq, H. J.; Veenstra, T. D. *Electrophoresis* **2004**, *25*, 1973-1980.
- (85) Jensen, P. K.; Pasa-Tolic, L.; Anderson, G. A.; Horner, J. A.; Lipton, M. S.; Bruce, J. E.; Smith, R. D. *Anal Chem* **1999**, *71*, 2076-2084.
- (86) Jiang, H.; Zou, H.; Wang, H.; Ni, J.; Zhang, Q.; Zhang, Y. *J Chromatogr A* **2000**, *903*, 77-84.
- (87) Johnson, T.; Bergquist, J.; Ekman, R.; Nordhoff, E.; Schurenberg, M.; Kloppel, K. D.; Muller, M.; Lehrach, H.; Gobom, J. *Anal Chem* **2001**, *73*, 1670-1675.

- (88) Jorgenson, J. W. *Anal Chem* **1986**, 58, 743A-760A.
- (89) Jorgenson, J. W.; DeArman Lukacs, K. *J Chromatogr* **1981**, 218, 209-216.
- (90) Jorgenson, J. W.; Lukacs, K. D. *Anal Chem* **1981**, 53, 1298-1302.
- (91) Jorgenson, J. W.; Lukacs, K. D. *Science* **1983**, 222, 266-272.
- (92) Kaiser, T.; Wittke, S.; Just, I.; Krebs, R.; Bartel, S.; Fliser, D.; Mischak, H.; Weissinger, E. M. *Electrophoresis* **2004**, 25, 2044-2055.
- (93) Kasicka, V. *Electrophoresis* **1999**, 20, 3084-3105.
- (94) Kato, M.; Sakai-Kato, K.; Jin, H.; Kubota, K.; Miyano, H.; Toyo'oka, T.; Dulay Maria, T.; Zare Richard, N. *Anal Chem* **2004**, 76, 1896-1902.
- (95) Kelleher, N. L. *Anal Chem* **2004**, 76, 197A-203A.
- (96) Kennedy, R. T.; Oates, M. D.; Cooper, B. R.; Nickerson, B.; Jorgenson, J. W. *Science* **1989**, 246, 57-63.
- (97) Kenseth, J. R.; He, Y.; Tallman, D.; Pang, H.-m.; Coldiron, S. J. *Curr Opin Chem Biol* **2004**, 8, 327-333.
- (98) Khmel'nitsky, Y. L.; Mozhaev, V. V.; Belova, A. B.; Sergeeva, M. V.; Martinek, K. *Eur J Biochem* **1991**, 198, 31-41.
- (99) Kinter, M.; Sherman, N. E. *Protein Sequencing and Identification Using Tandem Mass Spectrometry*; Wiley Interscience: New York, 2000.
- (100) Kirby, D. P.; Thorne, J. M.; Gotzinger, W. K.; Karger, B. L. *Anal Chem* **1996**, 68, 4451-4457.
- (101) Klose, J.; Kobalz, U. *Electrophoresis* **1995**, 16, 1034-1059.
- (102) Knox, J. H.; Grant, I. H. *Chromatographia* **1991**, 32, 317-328.
- (103) Krenkova, J.; Foret, F. *Electrophoresis* **2004**, 25, 3550-3563.
- (104) Kriger, M. S.; Cook, K. D.; Ramsey, R. S. *Anal Chem* **1995**, 67, 385-389.
- (105) Krylov, S. N.; Dovichi, N. J. *Electrophoresis* **2000**, 21, 767-773.
- (106) Krylov, S. N.; Zhang, Z.; Chan, N. W.; Arriaga, E.; Palcic, M. M.; Dovichi, N. J. *Cytometry* **1999**, 37, 14-20.

- (107) Lander, E. S.; Linton, L. M.; Birren, B.; Nusbaum, C.; Zody, M. C.; Baldwin, J.; Devon, K.; Dewar, K.; Doyle, M.; FitzHugh, W.; Funke, R.; Gage, D.; Harris, K.; Heaford, A.; Howland, J.; Kann, L.; Lehoczky, J.; LeVine, R.; McEwan, P.; McKernan, K.; Meldrim, J.; Mesirov, J. P.; Miranda, C.; Morris, W.; Naylor, J.; Raymond, C.; Rosetti, M.; Santos, R.; Sheridan, A.; Sougnez, C.; Stange-Thomann, N.; Stojanovic, N.; Subramanian, A.; Wyman, D.; Rogers, J.; Sulston, J.; Ainscough, R.; Beck, S.; Bentley, D.; Burton, J.; Clee, C.; Carter, N.; Coulson, A.; Deadman, R.; Deloukas, P.; Dunham, A.; Dunham, I.; Durbin, R.; French, L.; Grafham, D.; Gregory, S.; Hubbard, T.; Humphray, S.; Hunt, A.; Jones, M.; Lloyd, C.; McMurray, A.; Matthews, L.; Mercer, S.; Milne, S.; Mullikin, J. C.; Mungall, A.; Plumb, R.; Ross, M.; Shownkeen, R.; Sims, S.; Waterston, R. H.; Wilson, R. K.; Hillier, L. W.; McPherson, J. D.; Marra, M. A.; Mardis, E. R.; Fulton, L. A.; Chinwalla, A. T.; Pepin, K. H.; Gish, W. R.; Chissoe, S. L.; Wendl, M. C.; Delehaunty, K. D.; Miner, T. L.; Delehaunty, A.; Kramer, J. B.; Cook, L. L.; Fulton, R. S.; Johnson, D. L.; Minx, P. J.; Clifton, S. W.; Hawkins, T.; Branscomb, E.; Predki, P.; Richardson, P.; Wenning, S.; Slezak, T.; Doggett, N.; Cheng, J. F.; Olsen, A.; Lucas, S.; Elkin, C.; Uberbacher, E.; Frazier, M.; Gibbs, R. A.; Muzny, D. M.; Scherer, S. E.; Bouck, J. B.; Sodergren, E. J.; Worley, K. C.; Rives, C. M.; Gorrell, J. H.; Metzker, M. L.; Naylor, S. L.; Kucherlapati, R. S.; Nelson, D. L.; Weinstock, G. M.; Sakaki, Y.; Fujiyama, A.; Hattori, M.; Yada, T.; Toyoda, A.; Itoh, T.; Kawagoe, C.; Watanabe, H.; Totoki, Y.; Taylor, T.; Weissenbach, J.; Heilig, R.; Saurin, W.; Artiguenave, F.; Brottier, P.; Bruls, T.; Pelletier, E.; Robert, C.; Wincker, P.; Smith, D. R.; Doucette-Stamm, L.; Rubenfield, M.; Weinstock, K.; Lee, H. M.; Dubois, J.; Rosenthal, A.; Platzer, M.; Nyakatura, G.; Taudien, S.; Rump, A.; Yang, H.; Yu, J.; Wang, J.; Huang, G.; Gu, J.; Hood, L.; Rowen, L.; Madan, A.; Qin, S.; Davis, R. W.; Federspiel, N. A.; Abola, A. P.; Proctor, M. J.; Myers, R. M.; Schmutz, J.; Dickson, M.; Grimwood, J.; Cox, D. R.; Olson, M. V.; Kaul, R.; Shimizu, N.; Kawasaki, K.; Minoshima, S.; Evans, G. A.; Athanasiou, M.; Schultz, R.; Roe, B. A.; Chen, F.; Pan, H.; Ramser, J.; Lehrach, H.; Reinhardt, R.; McCombie, W. R.; de la Bastide, M.; Dedhia, N.; Blocker, H.; Hornischer, K.; Nordsiek, G.; Agarwala, R.; Aravind, L.; Bailey, J. A.; Bateman, A.; Batzoglu, S.; Birney, E.; Bork, P.; Brown, D. G.; Burge, C. B.; Cerutti, L.; Chen, H. C.; Church, D.; Clamp, M.; Copley, R. R.; Doerks, T.; Eddy, S. R.; Eichler, E. E.; Furey, T. S.; Galagan, J.; Gilbert, J. G.; Harmon, C.; Hayashizaki, Y.; Haussler, D.; Hermjakob, H.; Hokamp, K.; Jang, W.; Johnson, L. S.; Jones, T. A.; Kasif, S.; Kasprzyk, A.; Kennedy, S.; Kent, W. J.; Kitts, P.; Koonin, E. V.; Korf, I.; Kulp, D.; Lancet, D.; Lowe, T. M.; McLysaght, A.; Mikkelsen, T.; Moran, J. V.; Mulder, N.; Pollara, V. J.; Ponting, C. P.; Schuler, G.; Schultz, J.; Slater, G.; Smit, A. F.; Stupka, E.; Szustakowski, J.; Thierry-Mieg, D.; Thierry-Mieg, J.; Wagner, L.; Wallis, J.; Wheeler, R.; Williams, A.; Wolf, Y. I.; Wolfe, K. H.; Yang, S. P.; Yeh, R. F.; Collins, F.; Guyer, M. S.; Peterson, J.; Felsenfeld, A.; Wetterstrand, K. A.; Patrinos, A.; Morgan, M. J.; de Jong, P.; Catanese, J. J.; Osoegawa, K.; Shizuya, H.; Choi, S.; Chen, Y. J. *Nature* **2001**, *409*, 860-921.

- (109) Landers, J. P. *Handbook of Capillary Electrophoresis*, 2nd ed.; CRC Press: Boca Raton, 1997.
- (110) Lazar, I. M.; Ramsey, R. S.; Ramsey, J. M. *Anal Chem* **2001**, *73*, 1733-1739.
- (111) Lee, E. D.; Muck, W.; Henion, J. D.; Covey, T. R. *J Chromatogr* **1988**, *458*, 313-321.
- (112) Lee, T. T.; Yeung, E. S. *Anal Chem* **1992**, *64*, 3045-3051.
- (113) Lee, Y.-H.; Maus, R. G.; Smith, B. W.; Winefordner, J. D. *Anal Chem* **1994**, *66*, 4142-4149.
- (114) Lewis, K. C.; Opiteck, G. J.; Jorgenson, J. W.; Sheeley, D. M. *J Am Soc Mass Spectrom* **1997**, *8*, 495-500.
- (115) Lewis, R. V.; Stern, A. S. In *Handbook of HPLC for the Separation of Amino Acids, Peptides, and Proteins*; Hancock, W. S., Ed.; CRC Press: Boca Raton, 1985; Vol. II, pp 313-325.
- (116) Licklider, L.; Kuhr, W. G. *Anal Chem* **1994**, *66*, 4400-4407.
- (117) Licklider, L.; Kuhr, W. G. *Anal Chem* **1998**, *70*, 1902-1908.
- (118) Licklider, L.; Kuhr, W. G.; Lacey, M. P.; Keough, T.; Purdon, M. P.; Takigiku, R. *Anal Chem* **1995**, *67*, 4170-4177.
- (119) Link, A. J. *Trends Biotechnol* **2002**, *20*, S8-13.
- (120) Link, A. J.; Eng, J.; Schieltz, D. M.; Carmack, E.; Mize, G. J.; Morris, D. R.; Garvik, B. M.; Yates, J. R., 3rd *Nat Biotechnol* **1999**, *17*, 676-682.
- (121) Lipton, M. S.; Pasa-Tolic, L.; Anderson, G. A.; Anderson, D. J.; Auberry, D. L.; Battista, J. R.; Daly, M. J.; Fredrickson, J.; Hixson, K. K.; Kostandarithes, H.; Masselon, C.; Markillie, L. M.; Moore, R. J.; Romine, M. F.; Shen, Y.; Stritmatter, E.; Tolic, N.; Udseth, H. R.; Venkateswaran, A.; Wong, K. K.; Zhao, R.; Smith, R. D. *Proc Natl Acad Sci U S A* **2002**, *99*, 11049-11054.
- (122) Liu, C. C.; Alary, J.-F.; Vollmerhaus, P.; Kadkhodayan, M. *Electrophoresis* **2005**, *26*, 1366-1375.
- (123) Liu, C. C.; Huang Jyy, S.; Tyrrell David, L. J.; Dovichi Norman, J. *Electrophoresis* **2005**, *26*, 1424-1431.

- (124) Liu, C. C.; Jong, R.; Covey, T. *J Chromatogr A* **2003**, *1013*, 9-18.
- (125) Liu, C. C.; Zhang, J.; Dovichi, N. J. *Rapid Commun Mass Spectrom* **2005**, *19*, 187-192.
- (126) Liu, C. S. *Development and application of capillary electrophoresis-electrospray mass spectrometry*; University of Alberta, Canada, 2001.
- (127) Liu, C. S.; Li, X. F.; Pinto, D.; Hansen, E. B., Jr.; Cerniglia, C. E.; Dovichi, N. J. *Electrophoresis* **1998**, *19*, 3183-3189.
- (128) Liu, H.; Yang, C.; Yang, Q.; Zhang, W.; Zhang, Y. *J Chromatogr B Analyt Technol Biomed Life Sci* **2005**, *817*, 119-126.
- (129) Liu, H.; Zhang, L.; Zhu, G.; Zhang, W.; Zhang, Y. *Anal Chem* **2004**, *76*, 6506-6512.
- (130) Liu, J.; Cobb, K. A.; Novotny, M. *J Chromatogr* **1990**, *519*, 189-197.
- (131) Liu, T.; Shao, X.-X.; Zeng, R.; Xia, Q.-C. *J Chromatogr A* **1999**, *855*, 695-707.
- (132) Long, G. L.; Winefordner, J. D. *Anal Chem* **1983**, *55*, 712A - 724A.
- (133) Loo, J. A.; Udseth, H. R.; Smith, R. D. *Anal Biochem* **1989**, *179*, 404-412.
- (134) Lu, J. J.; Liu, S.; Pu, Q. *J Proteome Res* **2005**, *4*, 1012-1016.
- (135) Lu, Y.; Bottari, P.; Turecek, F.; Aebersold, R.; Gelb, M. H. *Anal Chem* **2004**, *76*, 4104-4111.
- (136) Lubman, D. M.; Kachman, M. T.; Wang, H.; Gong, S.; Yan, F.; Hamler, R. L.; O'Neil, K. A.; Zhu, K.; Buchanan, N. S.; Barder, T. J. *J Chromatogr B Analyt Technol Biomed Life Sci* **2002**, *782*, 183- 196.
- (137) Luo, Q.; Mao, X.; Kong, L.; Huang, X.; Zou, H. *J Chromatogr B Analyt Technol Biomed Life Sci* **2002**, *776*, 139-147.
- (138) MacCoss, M. J.; McDonald, W. H.; Saraf, A.; Sadygov, R.; Clark, J. M.; Tasto, J. J.; Gould, K. L.; Wolters, D.; Washburn, M.; Weiss, A.; Clark, J. I.; Yates, J. R., 3rd *Proc Natl Acad Sci U S A* **2002**, *99*, 7900-7905.
- (139) Martin, M.; Guiochon, G.; Walbroehl, Y.; Jorgenson, J. W. *Anal Chem* **1985**, *57*, 559-561.
- (140) Massolini, G.; Calleri, E. *J Sep Sci* **2005**, *28*, 7-21.

- (141) Matysik, F. M. *Electrophoresis* **2002**, *23*, 400-407.
- (142) Mazereeuw, M.; Hofte, A. J. P.; Tjaden, U.; van der Greef, J. *Rapid Commun Mass Spectrom* **1997**, *11*, 981-986.
- (143) McCormick, R. M. *Anal Chemistry* **1988**, *60*, 2322-2328.
- (144) Meng, F.; Du, Y.; Miller, L. M.; Patrie, S. M.; Robinson, D. E.; Kelleher, N. L. *Anal Chem* **2004**, *76*, 2852-2858.
- (145) Michels, D. A.; Hu, S.; Dambrowitz, K. A.; Eggertson, M. J.; Lauterbach, K.; Dovichi, N. J. *Electrophoresis* **2004**, *25*, 3098-3105.
- (146) Michels, D. A.; Hu, S.; Schoenherr, R. M.; Eggertson, M. J.; Dovichi, N. J. *Mol Cell Proteomics* **2002**, *1*, 69-74.
- (147) Mikes, O. *High-Performance Liquid Chromatography of Biopolymers and Biooligomers; Part B: Separation of Individual Compound Classes*; Elsevier: Amsterdam, 1988.
- (148) Mikkers, F. E. P.; Everaerts, F. M.; Verheggen, T. P. E. M. *J Chromatogr* **1979**, *169*, 11-20.
- (149) Mohan, D.; Lee, C. S. *Electrophoresis* **2002**, *23*, 3160-3167.
- (150) Moini, M. *Anal Chem* **2001**, *73*, 3497-3501.
- (151) Moini, M. *Anal Bioanal Chem* **2002**, *373*, 466-480.
- (152) Moini, M. *Methods Mol Biol* **2004**, *276*, 253-290.
- (153) Moini, M.; Cao, P.; Bard, A. J. *Anal Chem* **1999**, *71*, 1658-1661.
- (154) Moini, M.; Huang, H. *Electrophoresis* **2004**, *25*, 1981-1987.
- (155) Moore, A. W., Jr.; Jorgenson, J. W. *Anal Chem* **1995**, *67*, 3456-3463.
- (156) Moseley, M. A.; Deterding, L. J.; Tomer, K. B.; Jorgenson, J. W. *J Chromatogr* **1989**, *480*, 197-209.
- (157) Moseley, M. A.; Deterding, L. J.; Tomer, K. B.; Jorgenson, J. W. *J Chromatogr* **1990**, *516*, 167-173.
- (158) Muck, W. M.; Henion, J. D. *J Chromatogr* **1989**, *495*, 41-59.

- (159) Nakashima, T.; Higa, H.; Matsubara, H.; Benson, A. M.; Yasunobu, K. T. *J Biol Chem* **1966**, *241*, 1166-1177.
- (160) Neusüß, C.; Pelzing, M.; Macht, M. *Electrophoresis* **2002**, *23*, 3149-3159.
- (161) Nielsen, L. G.; Ash, K. O. *Am J Med Technol* **1978**, *44*, 30-37.
- (162) Nielsen, R. G.; Sittampalam, G. S.; Rickard, E. C. *Anal Biochem* **1989**, *177*, 20-26.
- (163) Oda, R. P.; Landers, J. P. In *Handbook of Capillary Electrophoresis*, Second ed.; Landers, J. P., Ed.; CRC Press: Boca Raton, 1997, pp 1-47.
- (164) Okanda, F. M.; El Rassi, Z. *Electrophoresis* **2005**, *26*, 1988-1995.
- (165) Olivares, J. A.; Nguyen, N. T.; Yonker, C. R.; Smith, R. D. *Anal Chem* **1987**, *59*, 1230-1232.
- (166) Pasa-Tolic, L.; Harkewicz, R.; Anderson, G. A.; Tolic, N.; Shen, Y.; Zhao, R.; Thrall, B.; Masselon, C.; Smith, R. D. *J Am Soc Mass Spectrom* **2002**, *13*, 954-963.
- (167) Pentoney, S. L., Jr.; Sweedler, J. V. In *Handbook of Capillary Electrophoresis*, Second ed.; Landers, J. P., Ed.; CRC Press: Boca Raton, 1997, pp 379-423.
- (168) Peterson, D. S.; Rohr, T.; Svec, F.; Fréchet, J. M. J. *Anal Chem* **2002**, *74*, 4081-4088.
- (169) Pinto, D.; Arriaga, E.; Craig, D.; Angelova, J.; Sharma, N.; Ahmadzadeh, H.; Dovichi, N. J. *Anal Chem* **1997**, *69*, 3015-3021.
- (170) Pleasance, S.; Thibault, P.; Kelly, J. *J Chromatogr* **1992**, *591*, 325-339.
- (171) Popa, T. V.; Mant, C. T.; Hodges, R. S. *Electrophoresis* **2004**, *25*, 94-107.
- (172) Quigley, W. W.; Dovichi, N. J. *Anal Chem* **2004**, *76*, 4645-4658.
- (173) Rabilloud, T. *Proteomics* **2002**, *2*, 3-10.
- (174) Ramsey, J. D.; Jacobson, S. C.; Culbertson, C. T.; Ramsey, J. M. *Anal Chem* **2003**, *75*, 3758-3764.
- (175) Ramstrom, M.; Bergquist, J. *FEBS Lett* **2004**, *567*, 92-95.

- (176) Rashkovetsky, L. G.; Lyubarskaya, Y. V.; Foret, F.; Hughes, D. E.; Karger, B. L. *J Chromatogr A* **1997**, *781*, 197-204.
- (177) Reinhoud, N. J.; Schroder, E.; Tjaden, U. R.; Niessen, W. M.; ten Noever de Brauw, M. C.; van der Greef, J. *J Chromatogr* **1990**, *516*, 147-155.
- (178) Riekkola, M.-L.; Joensson, J. A.; Smith, R. M.; Moore, D.; Ingman, F.; Powell, K. J.; Lobinski, R.; Gauglitz, G. G.; Kolotov, V. P.; Matsumoto, K.; Smith, R. M.; Umezawa, Y.; Vlasov, Y.; Fajgelj, A.; Gamsjaeger, H.; Hibbert, D. B.; Kutner, W.; Wang, K.; Zagatto, E. A. G.; Riekkola, M. L.; Kim, H.; Sanz-Medel, A.; Ast, T. *Pure and Applied Chemistry* **2004**, *76*, 443-451.
- (179) Rigaut, G.; Shevchenko, A.; Rutz, B.; Wilm, M.; Mann, M.; Seraphin, B. *Nat Biotechnol* **1999**, *17*, 1030-1032.
- (180) Rocklin, R. D.; Ramsey, R. S.; Ramsey, J. M. *Anal Chem* **2000**, *72*, 5244-5249.
- (181) Rodríguez-Díaz, R.; Wehr, T.; Zhu, M.; Levi, V. In *Handbook of Capillary Electrophoresis*, Second ed.; Landers, J. P., Ed.; CRC Press: Boca Raton, 1997, pp 101-138.
- (182) Ross, G. A. *LC-GC Europe* **2001**, *14*, 2-6.
- (183) Safarpour, H.; Asiaie, R.; Katz, S. *J Chromatogr A* **2004**, *1036*, 217-222.
- (184) Sakai-Kato, K.; Kato, M.; Toyo'oka, T. *Anal Chem* **2002**, *74*, 2943-2949.
- (185) Schlamowitz, M.; Peterson, L. U. *J Biol Chem* **1959**, *234*, 3137-3145.
- (186) Schmitt-Kopplin, P.; Englmann, M. *Electrophoresis* **2005**, *26*, 1209-1220.
- (187) Schneider, B. B.; Douglas, D. J.; Chen, D. D. Y. *Rapid Commun Mass Spectrom* **2001**, *15*, 2168-2175.
- (188) Schroeder, W. A.; Honnen, L.; Green, F. C. *Proc Natl Acad Sci U S A* **1953**, *39*, 23-30.
- (189) Senk, P.; Kozak, L.; Foret, F. *Electrophoresis* **2004**, *25*, 1447-1456.
- (190) Settlege, R. E.; Russo, P. S.; Shabanowitz, J.; Hunt, D. F. *J. Microcol. Sep.* **1998**, *10*, 281-285.
- (191) Severs, J. C.; Smith, R. D. *Anal Chem* **1997**, *69*, 2154-2158.

- (192) Shapiro, A. L.; Vinuela, E.; Maizel, J. V., Jr. *Biochem Biophys Res Commun* **1967**, 28, 815-820.
- (193) Shen, J.; Buko, A. *Anal Biochem* **2002**, 311, 80-83.
- (194) Shen, Y.; Berger, S. J.; Anderson, G. A.; Smith, R. D. *Anal Chem* **2000**, 72, 2154-2159.
- (195) Shen, Y.; Smith, R. D. *Electrophoresis* **2002**, 23, 3106-3124.
- (196) Shen, Y.; Tolic, N.; Zhao, R.; Pasa-Tolic, L.; Li, L.; Berger, S. J.; Harkewicz, R.; Anderson, G. A.; Belov, M. E.; Smith, R. D. *Anal Chem* **2001**, 73, 3011-3021.
- (197) Shen, Y.; Xiang, F.; Veenstra, T. D.; Fung, E. N.; Smith, R. D. *Anal Chem* **1999**, 71, 5348-5353.
- (198) Shihabi, Z. K. In *Handbook of Capillary Electrophoresis*, Second ed.; Landers, J. P., Ed.; CRC Press: Boca Raton, 1997, pp 457-477.
- (199) Siethoff, C.; Nigge, W.; Linscheid, M. *Anal Chem* **1998**, 70, 1357-1361.
- (200) Simo, C.; Elvira, C.; Gonzalez, N.; San Roman, J.; Barbas, C.; Cifuentes, A. *Electrophoresis* **2004**, 25, 2056-2064.
- (201) Simo, C.; Soto-Yarritu, P. L.; Cifuentes, A. *Electrophoresis* **2002**, 23, 2288-2295.
- (202) Simpson, D. C.; Smith, R. D. *Electrophoresis* **2005**, 26, 1291-1305.
- (203) Skoog, D. A.; Holler, F. J.; Nieman, T. A. *Principles of Instrumental Analysis*, 5th ed.; Saunders College Publishing: Philadelphia, 1998.
- (204) Sluszný, C.; Yeung, E. S. *Anal Chem* **2004**, 76, 1359-1365.
- (205) Slys, G. W.; Schriemer, D. C. *Rapid Commun Mass Spectrom* **2003**, 17, 1044-1050.
- (206) Slys, G. W.; Schriemer, D. C. *Anal Chem* **2005**, 77, 1572-1579.
- (207) Smith, A. D.; Moini, M. *Anal Chem* **2001**, 73, 240-246.
- (208) Smith, R. D. *Trends Biotechnol* **2002**, 20, S3-7.
- (209) Smith, R. D.; Anderson, G. A.; Lipton, M. S.; Pasa-Tolic, L.; Shen, Y.; Conrads, T. P.; Veenstra, T. D.; Udseth, H. R. *Proteomics* **2002**, 2, 513-523.

- (210) Smith, R. D.; Barinaga, C. J.; Udseth, H. R. *Anal Chem* **1988**, *60*, 1948-1952.
- (211) Smith, R. D.; Loo, J. A.; Barinaga, C. J.; Edmonds, C. G.; Udseth, H. R. *J Chromatogr* **1989**, *480*, 211-232.
- (212) Smith, R. D.; Loo, J. A.; Edmonds, C. G.; Barinaga, C. J.; Udseth, H. R. *Anal Chem* **1990**, *62*, 882-899.
- (213) Smith, R. D.; Loo, J. A.; Edmonds, C. G.; Barinaga, C. J.; Udseth, H. R. *J Chromatogr* **1990**, *516*, 157-165.
- (214) Smith, R. D.; Olivares, J. A.; Nguyen, N. T.; Udseth, H. R. *Anal Chem* **1988**, *60*, 436-441.
- (215) Smolka, M.; Zhou, H.; Aebersold, R. *Mol Cell Proteomics* **2002**, *1*, 19-29.
- (216) Soga, T.; Heiger, D. N. *Anal Chem* **2000**, *72*, 1236-1241.
- (217) Soga, T.; Kakazu, Y.; Robert, M.; Tomita, M.; Nishioka, T. *Electrophoresis* **2004**, *25*, 1964-1972.
- (218) Stein, P. E.; Leslie, A. G.; Finch, J. T.; Carrell, R. W. *J Mol Biol* **1991**, *221*, 941-959.
- (219) Storms, H. F.; van der Heijden, R.; Tjaden, U. R.; van der Greef, J. *Electrophoresis* **2004**, *25*, 3461-3467.
- (220) Storms, H. F.; van der Heijden, R.; Tjaden, U. R.; van der Greef, J. *J Chromatogr B Analyt Technol Biomed Life Sci* **2005**, *824*, 189-200.
- (221) Stroink, T.; Paarlberg, E.; Waterval, J. C. M.; Bult, A.; Underberg, W. J. M. *Electrophoresis* **2001**, *22*, 2374-2383.
- (222) Suter, M. J.; DaGue, B. B.; Moore, W. T.; Lin, S. N.; Caprioli, R. M. *J Chromatogr* **1991**, *553*, 101-116.
- (223) Swedberg, S. A. *J Chromatogr* **1993**, *503*, 449-452.
- (224) Terabe, S.; Otsuka, K.; Ando, T. *Anal Chem* **1985**, *57*, 834-841.
- (225) Terabe, S.; Otsuka, K.; Ichikawa, K.; Tsuchiya, A.; Ando, T. *Anal Chem* **1984**, *56*, 111-113.
- (226) Thibault, P.; Pleasance, S.; Laycock, M. V. *J Chromatogr* **1991**, *542*, 483-501.

- (227) Tiselius, A. *Trans. Faraday Soc.* **1937**, 33, 524-531.
- (228) Tomlinson, A. J.; Benson, L. M.; Guzman, N. A.; Naylor, S. *J Chromatogr A* **1996**, 744, 3-15.
- (229) Tseng, M.-C.; Chen, Y.-R.; Her, G.-R. *Electrophoresis* **2004**, 25, 2084-2089.
- (230) van de Goor, T.; Apffel, A.; Chakel, J.; Hancock, W. In *Handbook of Capillary Electrophoresis*, Second ed.; Landers, J. P., Ed.; CRC Press: Boca Raton, 1997, pp 213-258.
- (231) Venter, J. C.; Adams, M. D.; Myers, E. W.; Li, P. W.; Mural, R. J.; Sutton, G. G.; Smith, H. O.; Yandell, M.; Evans, C. A.; Holt, R. A.; Gocayne, J. D.; Amanatides, P.; Ballew, R. M.; Huson, D. H.; Wortman, J. R.; Zhang, Q.; Kodira, C. D.; Zheng, X. H.; Chen, L.; Skupski, M.; Subramanian, G.; Thomas, P. D.; Zhang, J.; Gabor Miklos, G. L.; Nelson, C.; Broder, S.; Clark, A. G.; Nadeau, J.; McKusick, V. A.; Zinder, N.; Levine, A. J.; Roberts, R. J.; Simon, M.; Slayman, C.; Hunkapiller, M.; Bolanos, R.; Delcher, A.; Dew, I.; Fasulo, D.; Flanigan, M.; Florea, L.; Halpern, A.; Hannenhalli, S.; Kravitz, S.; Levy, S.; Mobarry, C.; Reinert, K.; Remington, K.; Abu-Threideh, J.; Beasley, E.; Biddick, K.; Bonazzi, V.; Brandon, R.; Cargill, M.; Chandramouliswaran, I.; Charlab, R.; Chaturvedi, K.; Deng, Z.; Di Francesco, V.; Dunn, P.; Eilbeck, K.; Evangelista, C.; Gabrielian, A. E.; Gan, W.; Ge, W.; Gong, F.; Gu, Z.; Guan, P.; Heiman, T. J.; Higgins, M. E.; Ji, R. R.; Ke, Z.; Ketchum, K. A.; Lai, Z.; Lei, Y.; Li, Z.; Li, J.; Liang, Y.; Lin, X.; Lu, F.; Merkulov, G. V.; Milshina, N.; Moore, H. M.; Naik, A. K.; Narayan, V. A.; Neelam, B.; Nusskern, D.; Rusch, D. B.; Salzberg, S.; Shao, W.; Shue, B.; Sun, J.; Wang, Z.; Wang, A.; Wang, X.; Wang, J.; Wei, M.; Wides, R.; Xiao, C.; Yan, C.; Yao, A.; Ye, J.; Zhan, M.; Zhang, W.; Zhang, H.; Zhao, Q.; Zheng, L.; Zhong, F.; Zhong, W.; Zhu, S.; Zhao, S.; Gilbert, D.; Baumhueter, S.; Spier, G.; Carter, C.; Cravchik, A.; Woodage, T.; Ali, F.; An, H.; Awe, A.; Baldwin, D.; Baden, H.; Barnstead, M.; Barrow, I.; Beeson, K.; Busam, D.; Carver, A.; Center, A.; Cheng, M. L.; Curry, L.; Danaher, S.; Davenport, L.; Desilets, R.; Dietz, S.; Dodson, K.; Doup, L.; Ferreira, S.; Garg, N.; Gluecksmann, A.; Hart, B.; Haynes, J.; Haynes, C.; Heiner, C.; Hladun, S.; Hostin, D.; Houck, J.; Howland, T.; Ibegwam, C.; Johnson, J.; Kalush, F.; Kline, L.; Koduru, S.; Love, A.; Mann, F.; May, D.; McCawley, S.; McIntosh, T.; McMullen, I.; Moy, M.; Moy, L.; Murphy, B.; Nelson, K.; Pfannkoch, C.; Pratt, E.; Puri, V.; Qureshi, H.; Reardon, M.; Rodriguez, R.; Rogers, Y. H.; Romblad, D.; Ruhfel, B.; Scott, R.; Sitter, C.; Smallwood, M.; Stewart, E.; Strong, R.; Suh, E.; Thomas, R.; Tint, N. N.; Tse, S.; Vech, C.; Wang, G.; Wetter, J.; Williams, S.; Williams, M.; Windsor, S.; Winn-Deen, E.; Wolfe, K.; Zaveri, J.; Zaveri, K.; Abril, J. F.; Guigo, R.; Campbell, M. J.; Sjolander, K. V.; Karlak, B.; Kejariwal, A.; Mi, H.; Lazareva, B.; Hatton, T.; Narechania, A.; Diemer, K.; Muruganujan, A.; Guo, N.; Sato, S.; Bafna, V.; Istrail, S.; Lippert, R.; Schwartz, R.; Walenz, B.; Yooseph, S.; Allen, D.; Basu, A.; Baxendale, J.; Blick, L.; Caminha, M.; Carnes-

- Stine, J.; Caulk, P.; Chiang, Y. H.; Coyne, M.; Dahlke, C.; Mays, A.; Dombroski, M.; Donnelly, M.; Ely, D.; Esparham, S.; Fosler, C.; Gire, H.; Glanowski, S.; Glasser, K.; Glodek, A.; Gorokhov, M.; Graham, K.; Gropman, B.; Harris, M.; Heil, J.; Henderson, S.; Hoover, J.; Jennings, D.; Jordan, C.; Jordan, J.; Kasha, J.; Kagan, L.; Kraft, C.; Levitsky, A.; Lewis, M.; Liu, X.; Lopez, J.; Ma, D.; Majoros, W.; McDaniel, J.; Murphy, S.; Newman, M.; Nguyen, T.; Nguyen, N.; Nodell, M.; Pan, S.; Peck, J.; Peterson, M.; Rowe, W.; Sanders, R.; Scott, J.; Simpson, M.; Smith, T.; Sprague, A.; Stockwell, T.; Turner, R.; Venter, E.; Wang, M.; Wen, M.; Wu, D.; Wu, M.; Xia, A.; Zandieh, A.; Zhu, X. *Science* **2001**, *291*, 1304-1351.
- (232) Virtanen, R. *Acta Polytechnica Scand.* **1974**, *123*, 1-67.
- (233) von Brocke, A.; Nicholson, G.; Bayer, E. *Electrophoresis* **2001**, *22*, 1251-1266.
- (234) Voss, K. O.; Roos, H. P.; Dovichi, N. J. *Anal Chem* **2001**, *73*, 1345-1349.
- (235) Wachs, T.; Henion, J. *Anal Chem* **2001**, *73*, 632-638.
- (236) Wahl, J. H.; Gale, D. C.; Smith, R. D. *J Chromatogr A* **1994**, *659*, 217-222.
- (237) Wahl, J. H.; Goodlett, D. R.; Udseth, H. R.; Smith, R. D. *Electrophoresis* **1993**, *14*, 448-457.
- (238) Walhagen, K.; Unger, K. K.; Hearn, M. T. *Anal Chem* **2001**, *73*, 4924-4936.
- (239) Warriner, R. N.; Craze, A. S.; Games, D. E.; Lane, S. J. *Rapid Commun Mass Spectrom* **1998**, *12*, 1143-1149.
- (240) Washburn, M. P.; Ulaszek, R.; Deciu, C.; Schieltz, D. M.; Yates, J. R., 3rd *Anal Chem* **2002**, *74*, 1650-1657.
- (241) Washburn, M. P.; Ulaszek, R. R.; Yates, J. R., 3rd *Anal Chem* **2003**, *75*, 5054-5061.
- (242) Washburn, M. P.; Wolters, D.; Yates, J. R., 3rd *Nat Biotechnol* **2001**, *19*, 242-247.
- (243) Waterval, J. C.; Bestebreurtje, P.; Lingeman, H.; Versluis, C.; Heck, A. J.; Bult, A.; Underberg, W. J. *Electrophoresis* **2001**, *22*, 2701-2708.
- (244) Waterval, J. C.; Hommels, G.; Bestebreurtje, P.; Versluis, C.; Heck, A. J.; Bult, A.; Lingeman, H.; Underberg, W. J. *Electrophoresis* **2001**, *22*, 2709-2716.
- (245) Weber, K.; Osborn, M. *J Biol Chem* **1969**, *244*, 4406-4412.

- (246) Wei, W.; Ju, H. *Electrophoresis* **2005**, *26*, 586-592.
- (247) Weinmann, W.; Parker, C. E.; Baumeister, K.; Maier, C.; Tomer, K. B.; Przybylski, M. *Electrophoresis* **1994**, *15*, 228-233.
- (248) Weissinger Eva, M.; Wittke, S.; Kaiser, T.; Haller, H.; Bartel, S.; Krebs, R.; Golovko, I.; Rupprecht Harald, D.; Haubitz, M.; Hecker, H.; Mischak, H.; Fliser, D. *Kidney Int* **2004**, *65*, 2426-2434.
- (249) Wetterhall, M.; Nilsson, S.; Markides, K. E.; Bergquist, J. *Anal Chem* **2002**, *74*, 239-245.
- (250) Wheat, T. E.; Lilley, K. A.; Banks, F. J., Jr. *J Chromatogr A* **1997**, *781*, 99-105.
- (251) Wilm, M.; Mann, M. *Anal Chem* **1996**, *68*, 1-8.
- (252) Wittke, S.; Fliser, D.; Haubitz, M.; Bartel, S.; Krebs, R.; Hausadel, F.; Hillmann, M.; Golovko, I.; Koester, P.; Haller, H.; Kaiser, T.; Mischak, H.; Weissinger, E. M. *J Chromatogr A* **2003**, *1013*, 173-181.
- (253) Wittke, S.; Kaiser, T.; Mischak, H. *J Chromatogr B Analyt Technol Biomed Life Sci* **2004**, *803*, 17-26.
- (254) Wolf, S. M.; Vouros, P. *Anal Chem* **1995**, *67*, 891-900.
- (255) Wolters, D. A.; Washburn, M. P.; Yates, J. R., 3rd *Anal Chem* **2001**, *73*, 5683-5690.
- (256) Wu, C. H.; Scampavia, L.; Ruzicka, J. *Analyst* **2002**, *127*, 898-905.
- (257) Wu, H.; Zhai, J.; Tian, Y.; Lu, H.; Wang, X.; Jia, W.; Liu, B.; Yang, P.; Xu, Y.; Wang, H. *Lab Chip* **2004**, *4*, 588-597.
- (258) Wu, J. T.; Huang, P.; Li, M. X.; Qian, M. G.; Lubman, D. M. *Anal Chem* **1997**, *69*, 320-326.
- (259) Wu, R.; Zou, H.; Ye, M.; Lei, Z.; Ni, J. *Electrophoresis* **2001**, *22*, 544-551.
- (260) Wu, R. a.; Zou, H.; Ye, M.; Lei, Z.; Ni, J. *Anal Chem* **2001**, *73*, 4918-4923.
- (261) Wu, S.; Dovichi, N. J. *J Chromatogr* **1989**, *480*, 141-155.
- (262) Yang, C.; Liu, H.; Yang, Q.; Zhang, L.; Zhang, W.; Zhang, Y. *Anal Chem* **2003**, *75*, 215-218.

- (263) Yates, J. R., 3rd *Electrophoresis* **1998**, *19*, 893-900.
- (264) Ye, M.; Hu, S.; Schoenherr, R. M.; Dovichi, N. J. *Electrophoresis* **2004**, *25*, 1319-1326.
- (265) Yi, E. C.; Li, X. J.; Cooke, K.; Lee, H.; Raught, B.; Page, A.; Aneliunas, V.; Hieter, P.; Goodlett, D. R.; Aebersold, R. *Proteomics* **2005**, *5*, 380-387.
- (266) Zhang, J.; Hu, H.; Gao, M.; Yang, P.; Zhang, X. *Electrophoresis* **2004**, *25*, 2374-2383.
- (267) Zhang, J.; Yang, M.; Puyang, X.; Fang, Y.; Cook, L. M.; Dovichi, N. J. *Anal Chem* **2001**, *73*, 1234-1239.
- (268) Zhang, S.; Huang, X.; Zhang, J.; Horvath, C. *J Chromatogr A* **2000**, *887*, 465-477.
- (269) Zhao, D. S.; Gomez, F. A. *Chromatographia* **1997**, *44*, 514-520.
- (270) Zheng, J.; Jann, M. W.; Hon, Y. Y.; Shamsi, S. A. *Electrophoresis* **2004**, *25*, 2033-2043.
- (271) Zhou, F.; Johnston Murray, V. *Electrophoresis* **2005**, *26*, 1383-1388.
- (272) Zhou, F.; Johnston, M. V. *Anal Chem* **2004**, *76*, 2734-2740.
- (273) Zhou, H.; Ranish, J. A.; Watts, J. D.; Aebersold, R. *Nat Biotechnol* **2002**, *20*, 512-515.
- (274) Zou, H.; Huang, X.; Ye, M.; Luo, Q. *J Chromatogr A* **2002**, *954*, 5-32.

VITA

Regine Schoenherr was born in Nürnberg, Germany. She obtained an Associate in Science degree in Environmental Science in December 1996 from Central Texas College at Killeen, Texas. In December 1999, she graduated with a Bachelor of Science in Chemistry from Iowa State University at Ames, Iowa. She started her graduate studies in September of 2000 at the University of Washington under the supervision of Prof. Norman J. Dovichi. In 2006, Regine graduated from the University of Washington as a Doctor of Philosophy specialized in analytical chemistry.